Effects of calcitriol and fingolimod on remyelination in the cuprizone model

Agnes Elisabeth Nystad

Thesis for the degree of Philosophiae Doctor (PhD)
University of Bergen, Norway
2020

UNIVERSITY OF BERGEN

Effects of calcitriol and fingolimod on remyelination in the cuprizone model

Agnes Elisabeth Nystad

Thesis for the Degree of Philosophiae Doctor (PhD)

at the University of Bergen

Scientific environment

The work of this thesis has been carried out at the Norwegian Multiple Sclerosis Competence Centre, Department of Neurology, and at the Department of Clinical Medicine (K1), University of Bergen. Animal experiments were done at the Laboratory Animal Facility, Vivarium, at the Faculty of Medicine, University of Bergen, and other laboratory work was done at the Neurological Research Laboratory and the Department of Pathology at Haukeland University Hospital. The Proteomics Unit at the University of Bergen (PROBE) analyzed the proteomic data.

Main supervisor: Øivind F. Torkildsen
Norwegian Multiple Sclerosis Competence Centre, Department of Neurology, Haukeland University Hospital, Bergen, Norway.
Department of Clinical Medicine, University of Bergen, Bergen, Norway.

Co-supervisor: Stig Wergeland
Norwegian Multiple Sclerosis Competence Centre, Department of Neurology, Haukeland University Hospital, Bergen, Norway.
Department of Clinical Medicine, University of Bergen, Bergen, Norway.

Contents

Acknowledgements

The work on the present thesis started in 2011 at the Medical Research Program at the Faculty of Medicine, University of Bergen (UoB), and continued through the Ph.D. program at the UoB from 2017-2020. I am grateful that the Research Program gave me the opportunity to discover research at an early stage in my career; this has been invaluable.

I always loved spending time with my dear uncle Knutten. He was the one who initially triggered my interest in research on multiple sclerosis (MS). Knutten also showed me that despite serious illness, it's possible to truly enjoy life. When he passed away in 2016, he left me with a lasting impression: although severely affected by MS, he cherished life and still wanted to live. He has always been in my thoughts during my research, reminding me to be grateful for all the opportunities in life.

I am deeply indebted to my supervisors Øivind Torkildsen and Stig Wergeland, who have made it possible to carry out the work with this thesis relatively smoothly. Øivind, thank you for always being present, positive, and enthusiastic! Your office door is always open, and you never hesitate to share the wealth of your vast knowledge in the field. I appreciate your good ideas, that you are solution-oriented, and always respond quickly and promptly to my queries. Stig, you're always interested, helpful, and knowledgeable at an impressive level of detail. Your help, especially with the practical work throughout the experiments, has been fantastic! You always come up with excellent input that advances our work. I want to thank both of you for your genuine interest in the research field; you are a true inspiration. I couldn't have asked for better academic guidance and support; it's been crucial to me and our work.

I also want to express my gratitude to all the co-authors. Lars Bø and Kjell-Morten Myhr, your continuing contributions within the MS field are enormously impressive; it has been an honor working with you. Thanks to PROBE, under the leadership of Frode Berven. Ragnhild R. Lereim and Eystein Oveland, your expertise and insight

into proteomics have helped lift our research to new heights. It has been a pleasure cooperating with you, thank you! I am also grateful for the collaboration we had with Lage Aksnes on the serum vitamin D analyses in paper I. Maria Alme and Christian Vedeler, thank you for the excellent cooperation on paper III.

Thanks to Vivarium (The Laboratory Animal Facility, UoB), for excellent assistance with the animal experiments. And to Edith Fick for assistance and for teaching me immunohistochemistry staining techniques.

To all my colleagues at the MS Center, thank you for all your support, discussions, and enjoyable socializing. I am eternally grateful that everyone is so kind and contributes to such a great atmosphere! Thanks to the Neurological Research Laboratory, administrated by Hanne Linda Nakkestad, for help and support.

Håvard N. Henriksen and Hilde Marie Torgauten, thanks for being wonderful office mates! Thanks for everlasting procrastination, all the interesting (and less interesting) discussions, and that our licorice stock is always full. You have been generously supportive all the way! Special thanks to Håvard for teaching me all I know about the semicolon; your proofreading has been invaluable.

A big thanks to all my friends. Especially many thanks to my unconditionally kind friend Benedikte, who I will say more or less saved this thesis! Your generosity knows no bounds. I genuinely admire every single bit of you. Dear Karin, thank you for always providing your positive being, splendid company, and lunch (even when I tell you not to bring lunch). Magnus, Siri, Melody, "Kjekkejentene" and "Kvinneforum", thanks for making life more meaningful and fun! To my friends in Carte Blanche, who never give up trying to persuade me to join you dancing and never letting me forget the joy of dance, thanks! Special thanks to Ole Martin, who made his apartment available to us when we unexpectedly found ourselves homeless[1].

[1] It's a long story

Most importantly, my gratitude goes to my beloved family. To my dear mother and father, Merete and Einar, thank you for your unconditional love, support, and faith in me. I am forever grateful! I would also like to extend my appreciation to my dear stepfather, Lars, and my wonderful aunt, Kristin, and the rest of the family for all your support and the joy you bring to life. Thanks to my siblings, especially to Bjørn Magnus and Erlend, who live in Bergen, always support us, and make life here more fun and livable! To my extended family, Aste and Memeth, thanks for all the help and care in everyday life.

To my dear Svein, my companion and loved one. Thank you for always being by my side (regardless of my crazy ideas and endless stubbornness). I am grateful for your unconditional love and emotional support. I couldn't have done this without you!

Finally, a special thanks to my grandmother. My role model, who sadly passed away during the writing of this thesis. You meant, and still mean the world to me. Your unconditional kindness, wisdom, and strength will always guide me through life.

Bergen, February 2020

Agnes Elisabeth Nystad

Abbrevations

APP	Amyloid precursor protein
ARR	Annual relapse rate
ATP	Adenosine triphosphate
BBB	Blood-brain barrier
CCR7	Chemokine receptor seven
CIS	Clinically isolated syndrome
CNS	Central nervous system
CSF	Cerebrospinal fluid
Cu	Copper
DMT	Disease-modifying treatment
EBV	Epstein-Barr virus
EBNA	Epstein-Barr nuclear antigen
EDSS	Expanded Disability Status Scale
ER	Endoplasmic reticulum
Fingolimod-p	Fingolimod-phosphate
FTY720	Fingolimod
GFAP	Glial fibrillary acidic protein
GWAS	Genome-wide association studies
HC	Histochemistry
HLA	Human Leukocyte Antigen
IFN-β	Interferon β
IHC	Immunohistochemistry
ip.	Intraperitoneal
IU	International units
LFB	Luxol Fast Blue
LPC	Lysophosphatidylcholine
MAG	Myelin-associated glycoprotein
MAO	Monoamine oxidase
MBP	Myelin basic protein

MHC	Major histocompatibility complex
MOG	Myelin oligodendrocyte glycoprotein
MRI	Magnetic resonance imaging
MS	Multiple Sclerosis
NAGM	Normal-appearing grey matter
NAWM	Normal-appearing white matter
NFL	Neurofilament light
NFM	Neurofilament medium
NFH	Neurofilament heavy
NOGO-A	Neurite outgrowth Inhibitor Protein A
NSC	Neuronal stem cell
OLG	Oligodendrocyte
OPC	Oligodendrocyte precursor cell
OR	Odds ratio
PLP	Myelin proteolipid protein
PPMS	Primary progressive multiple sclerosis
PR	Progressive relapsing
RRMS	Relapsing-remitting multiple sclerosis
RXRγ	Retinoid X receptor gamma
SD	Standard deviation
SEM	Standard error of the mean
SMI-32	Sternberg Monoclonals Incorporated, product no. 32
SPMS	Secondary progressive multiple sclerosis
SphK	Sphingosine kinases
S1P	Sphingosine-1-phosphate
S1PR	Sphingosine-1-phosphate receptor
VDR	Vitamin D receptor
25(OH)D	25-hydroxyvitamin D, calcidiol
1.25$(OH)_2$D	1.25-dihydroksyvitamin D, calcitrol
1α-OHase	25-hydroxyvitamin D-1-αhydroxylase
24-OHase	1.25$(OH)_2$D-24-hydroxylase

Abstract

Multiple sclerosis (MS) is a chronic disease characterized by inflammation, demyelination, and neurodegeneration of the central nervous system (CNS). There is no cure. Current treatments target the autoimmune aspects of MS but do not directly improve CNS remyelination. Pro-remyelinating treatment might optimize the treatment of MS patients. In this project, we aimed to investigate different strategies to improve remyelination and mitigate axonal damage in the cuprizone model, an animal model for de- and remyelination. Our goal was to determine the effect of biologically active vitamin D (calcitriol) on remyelination (Paper I), and axonal damage (Paper II). Moreover, we investigated the effect of the MS-medication fingolimod on remyelination and axonal damage in the cerebellum (Paper III). Finally, we assessed the impact of fingolimod in the cerebrum (Paper IV).

C57Bl/6 mice were exposed to the neurotoxicant cuprizone. In the vitamin D experiment, high-dose calcitriol or placebo was given by intraperitoneal injections twice a week. In the fingolimod experiment, fingolimod or placebo was given by oral gavage daily. In both experiments, mice were investigated at several time points during remyelination. Histochemistry and immunohistochemistry were used to investigate remyelination, axonal damage, and loss. We analyzed the brain proteome by proteomic analysis to further determine the CNS effects of fingolimod exposure.

Treatment with high-dose calcitriol improved the remyelination process (paper I).
Vitamin D given before, but not after cuprizone-induced demyelination prevented acute axonal damage and axonal loss (paper II). Given after cuprizone-induced demyelination, fingolimod did not affect cerebellar remyelination, the number of oligodendrocytes, microglia or astrocyte activation, or acute axonal damage at any time point (paper III). Fingolimod was functionally active during remyelination, resulting in a downregulation of sphingosine-1-phosphate receptor 1 protein levels in the brain. We found, however, no difference in the degree of remyelination, oligodendrocyte numbers, nor the degree of axonal damage or loss in the corpus callosum (paper IV).

In the cuprizone model, high-dose calcitriol given during remyelination improved remyelination. However, axonal damage was only prevented if vitamin D was given before demyelination occurred. Fingolimod modulated the sphingosine-1-phosphate receptor 1 levels in the cerebrum but did not increase remyelination, nor protect against axonal injury or loss in the cerebellum or cerebrum when given after cuprizone-induced demyelination.

List of publications

I. Nystad AE, Wergeland S, Aksnes L, Myhr KM, Bø L, Torkildsen Ø.
Effect of high-dose 1.25 dihydroxyvitamin D_3 on remyelination in the cuprizone model.
APMIS. 2014 Dec;122(12):1178-86.

II. Nystad AE, Torkildsen Ø, Wergeland S.
Effects of vitamin D on axonal damage during de- and remyelination in the cuprizone model.
J Neuroimmunol. 2018 Aug 15;321:61-65.

III. Alme MN, Nystad AE, Bø L, Myhr KM, Vedeler CA, Wergeland S, Torkildsen Ø.
Fingolimod does not enhance cerebellar remyelination in the cuprizone model.
J Neuroimmunol. 2015 Aug 15;285:180-6.

IV. Nystad AE, Lereim RR, Wergeland S, Oveland E, Myhr KM, Bø L, Torkildsen Ø.
Fingolimod downregulates brain sphingosine-1-phosphate receptor 1 levels but does not promote remyelination or neuroprotection in the cuprizone model.
J Neuroimmunol. 2020 Feb 15;339:577091.

1 Introduction

1.1 Multiple sclerosis

Multiple sclerosis (MS) is an immune-mediated disease of the central nervous system (CNS), characterized by inflammation, demyelination, and neurodegeneration. Loss of myelin results in neurologic symptoms, e.g., reduced motor and sensory function, visual impairment, and cognitive dysfunction. The particular triggering event(s) remains unknown, but both genetic and environmental factors seem to be involved. MS mainly affects young adults and gives symptoms from the whole CNS (Compston and Coles 2002).

Already in 1838, the first portrayal of disseminated plaques in the CNS was published in the "Pathological Anatomy" by Robert Carswell. Later, in 1849, the German pathologist Friedrich von Frerichs described a disease with motor and visual symptoms. He believed that the disease was caused by sclerotic lesions disseminated throughout the CNS and became the first to diagnose living patients with "Hirnsklerose" (Murray 2009). However, it was during the three last decades of the 19th century that the studies of *la sclerose en plaques disseminées*, later called MS, started with the works of the French neurologist Jean-Martin Charcot (Compston, Lassmann et al. 2006).

There is no curative treatment, but there is a rapid development of new immune-modulating therapies. A challenge in the field of MS is to develop treatments that have the ability to prevent the progression of disability and to repair the damage that has already occurred. Remyelination is the brain's way to regenerate myelin after CNS damage and demyelination. Remyelination therapy may contribute to existing therapies to optimize MS treatment and halt disease progression in MS patients (Plemel, Liu et al. 2017).

1.1.1 Epidemiology

Norway has one of the highest prevalence of MS in the world. MS affects about 203/100 000, and it is estimated that 10 500 Norwegians have MS (Grytten, Torkildsen et al. 2015). However, the prevalence may be underestimated, and more than 12 000 individuals may be living with the disease (Aarseth, Smedal et al. 2018). Worldwide data show that over 22 million people are affected (Collaborators 2019), and the prevalence is increasing due to increasing incidence (Magyari and Sorensen 2019), reduced mortality, and earlier diagnosis (Rotstein, Chen et al. 2018).

There is a large geographical variance in the distribution of MS. MS seems to be most prevalent in temperate zones, typical in high-income countries and is not common in tropical areas and low-income countries (Koch-Henriksen and Sorensen 2010). Generally, the prevalence of MS is low around the equator. The variation in geographical distribution may reflect differences in environmental factors and genetic predisposition.

The onset of the disease is usually during the third or fourth decade; MS is rare in individuals before the age of 10 years. MS is one of the most common causes of neurological disability in young adults (Compston and Coles 2002), and the disease has a considerable economic impact both to the patients and society. The disease affects females more often than men in a 2-3:1 F: M ratio (Dobson and Giovannoni 2019).

1.1.2 Symptoms and classification

MS can present itself like a mono- or polysymptomatic disease. The clinical manifestations of MS depend on the areas affected, and the symptoms reflect the location of the lesions. The symptoms are extremely diverse, but the most common presenting symptoms are sensory symptoms, optic neuritis, and motor deficits (Weinshenker, Bass et al. 1989). Other clinical signs include diplopia, clumsiness, bladder, bowel, and sexual dysfunction, as well as cognitive and mood alterations, fatigue, and temperature sensitivity (Compston and Coles 2008).

In 1996, the National MS Society (USA) Advisory Committee on Clinical Trials in MS (Lublin and Reingold 1996) defined the course of MS by four clinical subtypes, relapsing-remitting, secondary progressive, primary progressive and progressive relapsing. The classification was revised in 2013 (Lublin, Reingold et al. 2014). Accordingly, MS is still divided into the two main groups, also called MS disease modifiers phenotypes, relapsing-remitting MS (RRMS) and primary progressive MS (PPMS). The RRMS group includes active or not active RRMS and clinically isolated syndrome (CIS). The PPMS group includes PPMS and secondary progressive MS (SPMS), active or not active, with or without progression (Figure 1 and 2). The previous progressive relapsing (PR) form was eliminated and is now a part of PPMS with activity.

1.1.2.1 Relapsing-remitting MS

Relapsing-remitting MS (RRMS) is the most common disease course and characterizes around 80-85%. RRMS is characterized by acute exacerbation (relapses) followed by complete or partial recovery (remission) as residual symptoms may persist. Relapses are clinical episodes where the patients have subjective and/or objective MS symptoms reflecting an inflammatory CNS lesion, lasting more than 24 hours, in the absence of fever and infection. Between relapses, the patients are clinically stable (Thompson, Banwell et al. 2018). The percentage of patients who convert from RR- to SPMS increases with disease duration. Untreated, around 90% of the patients are estimated to evolve into a secondary progressive phase after about 25 years (Weinshenker, Bass et al. 1989). However, the increase in treatment options, earlier treatment initiation, and more efficient therapies have resulted in a slower disease progression (Tedeholm, Lycke et al. 2013, Brown, Coles et al. 2019).

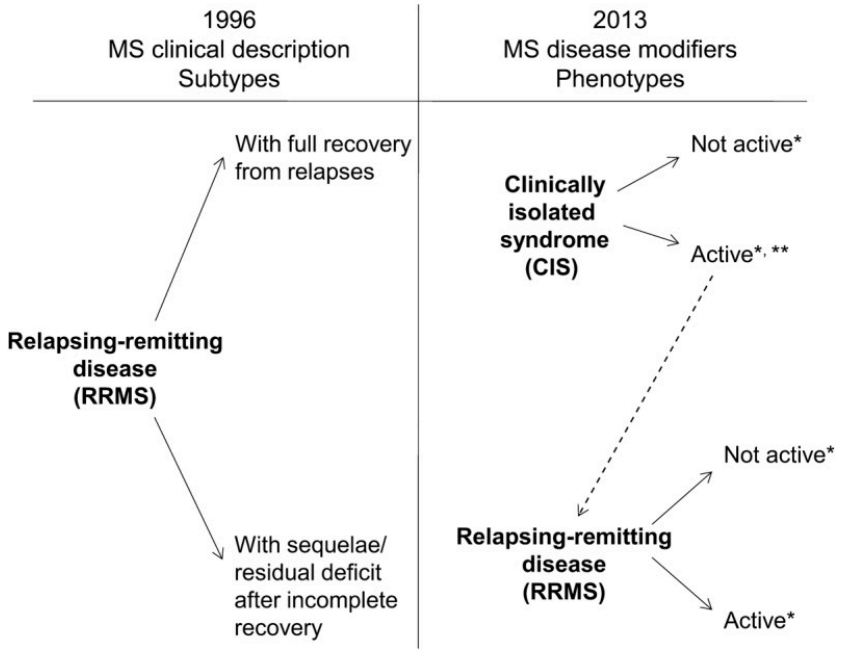

Figure 1

The 1996 vs 2013 multiple sclerosis phenotype descriptions for relapsing disease

**Activity determined by clinical relapses and/or MRI activity (contrast-enhancing lesions; new or unequivocally enlarging T2 lesions assessed at least annually); if assessments are not available, activity is "indeterminate." **CIS, if subsequently clinically active and fulfilling current multiple sclerosis (MS) diagnostic criteria, becomes relapsing-remitting MS (RRMS).*

1.1.2.2 Primary progressive MS

About 5-20% of MS patients have a clinical course compatible with PPMS (Lublin and Reingold 1996, Dobson and Giovannoni 2019). PPMS is characterized by disease progression from onset without clear relapses prior to clinical deterioration, with sporadic plateaus or minor fluctuations (Lublin and Reingold 1996, Thompson, Banwell et al. 2018). PPMS has a later onset than RRMS, typically in the 5th decade.

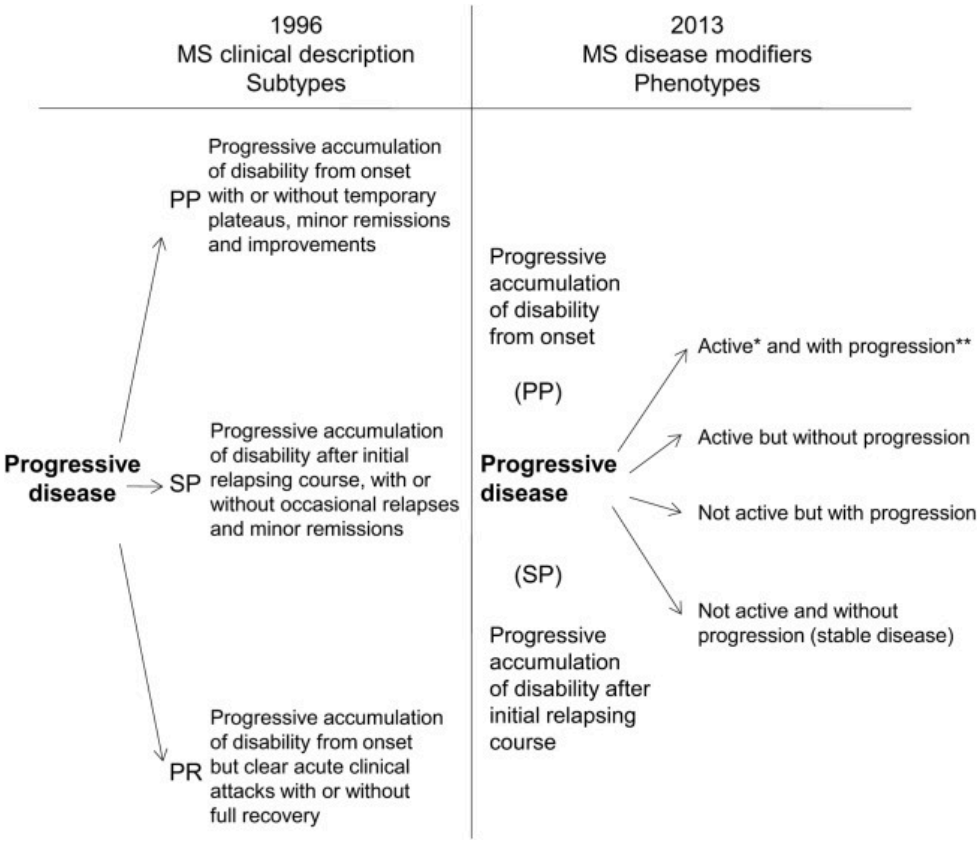

Figure 2

**Activity determined by clinical relapses assessed at least annually and/or MRI activity (contrast-enhancing lesions; new and unequivocally enlarging T2 lesions). **Progression measured by clinical evaluation, assessed at least annually. If assessments are not available, activity and progression are "indeterminate." MS 5 multiple sclerosis; PP 5 primary progressive; PR 5 progressive relapsing; SP 5 secondary progressive.*

1.1.3 Diagnosis

The current diagnosis of MS is based on diagnostic criteria, established by the International Panel on the Diagnosis of Multiple Sclerosis, known as the "McDonald Criteria" first in 2001, then revised in 2005, 2010, and finally by Polman et al., leading to the 2017 revision of the criteria by Thompson et al. (Thompson, Banwell et al. 2018). The diagnosis of MS can be based solely upon clinical grounds. Usually, the diagnosis is based on clinical history, neurological examination, magnetic resonance imaging (MRI), cerebrospinal fluid (CSF) examination, and exclusion of differential diagnosis. CSF oligoclonal bands confirm pathological inflammation (Compston and Coles 2002). The hallmark for the RRMS-diagnosis is disease dissemination in time and space within the CNS, while the PPMS diagnosis is made on the basis of disability progression independent of clinical relapses. In patients with CIS combined with clinical or MRI lesions with dissemination in space, the presence of CSF-specific oligoclonal bands may lead to the diagnosis of MS. Moreover, symptomatic lesions may demonstrate dissemination in space or time in patients with supratentorial, infratentorial, or spinal cord syndrome. Finally, cortical lesions can be used to demonstrate dissemination in space.

1.1.4 Treatment

During the last 25 years, there has been great progress in the development of new MS drugs resulting in a dramatic improvement in the prognosis of newly diagnosed MS patients (Tedeholm, Lycke et al. 2013). Despite this development, still, there is no curative treatment, and progressive MS has few available options.

There are four therapeutic target principles in MS treatment. First, to halt the severity and duration of an attack, patients are treated with high-dose of oral or intravenous glucocorticoid (methylprednisolone) (Miller, Weinstock-Guttman et al. 2000).
Second, treatments that aim to prevent MS activity (disease-modifying treatments (DMTs)). This may hamper and delay disability progression; however, it does not usually improve an already acquired disability. DMTs limit the availability and activity of immune cells. The first peroral treatment fingolimod (FTY720, Gilenya), showed a reduction in annual relapse rate (ARR) and MRI lesions compared to placebo (Kappos, Radue et al. 2010) and interferon (IFN)-β-1a (Cohen, Barkhof et al. 2010). Third, to treat symptoms, there are several symptomatic treatment options available, which can alleviate ailments, such as spasticity and fatigue (Newsome, Aliotta et al. 2017). Fourth, treatments that aim to regenerate the brain after damage. Remyelination is a complex process that occurs in varying degrees; treatments that enhance this endogenous regenerative mechanism could possibly reverse disease progression. As remyelinating therapies may be neuroprotective, they could benefit MS patients throughout the entire disease course. There are several promising pro-remyelinating agents; however, at the current moment, none are approved. In this thesis, we investigate two compounds, vitamin D and fingolimod, and their effect on remyelination.

1.1.5 Etiology

MS is believed to be caused by a complex interaction between several environmental factors and a genetic vulnerability (Compston and Coles 2002, Dobson and Giovannoni 2019).

1.1.5.1 Genetics

Both the incidence and the prevalence of MS are higher in family members of affected individuals compared to the general population, where the lifetime risk for developing MS is around 0.1-0.3%. The concordance rate for monozygotic twins is around 20-30% and high compared to dizygotic twins who have a rate of about 2-5%. Lifetime risk in siblings of an affected individual is about 3% (Compston and Coles 2008, Canto and Oksenberg 2018).

The major histocompatibility complex (MHC) gene complex is associated with MS susceptibility and dominates the genetic influences on MS risk (Canto and Oksenberg 2018). Human Leukocyte Antigen (HLA) genes are located within MHC and encode for cell surface glycoproteins on different cells. These are involved in immune regulation, through exposure to non-self proteins (class I) or extracellular proteins (class II). The HLA gene cluster on chromosome 6 is viewed as the strongest genetic locus for MS with HLA-DRB1*15:01 as the major candidate allele, with a moderate effect on causing the disease. The association has been confirmed by genome-wide association studies (GWAS); in addition, more than 200 genetic loci beyond the MHC region have been uncovered (Patsopoulos 2018).

1.1.5.2 Vitamin D

High latitudes, low sun exposure, and low levels of vitamin D were early associated with MS-risk (Acheson, Bachrach et al. 1960, Goldberg 2007). Munger and colleagues have investigated data from two prospective cohorts and found that vitamin D supplements reduced the risk of MS in women (Munger, Zhang et al. 2004). In another large, prospective, nested case-control study, the MS risk among whites decreased with increasing vitamin 25(OH)D levels, supporting a protective role of vitamin D in the risk of developing the disease. High vitamin D levels before the age of 20 had especially protective effects (Munger, Levin et al. 2006). More recently, Mendelian randomization studies have supported a causal role of vitamin D in MS susceptibility (Mokry, Ross et al. 2015, Rhead, Baarnhielm et al. 2016). A genetically dependent reduction of vitamin D levels increases the risk of MS. Yet, the studies do not tell us whether vitamin D also could modulate the disease course. Altogether, low vitamin D was strongly associated with an increased risk of developing MS; hence, vitamin D supplementation might also reduce MS in those at risk.

1.1.5.3 Epstein-Barr virus

Epstein-Barr virus (EBV) is the main infectious agent linked to MS risk (Belbasis, Bellou et al. 2015). The risk of developing MS is low in EBV-negative individuals but increases drastically after EVB infection with subsequent infectious mononucleosis (symptomatic infection) in the adolescents (Thacker, Mirzaei et al. 2006). Thus, especially infectious mononucleosis and Epstein-Barr nuclear antigen (EBNA) IgG seropositivity is associated with MS. Due to an increase in serum antibody titers to EBV antigens in the late teens to the mid-20s, before the clinical onset of MS, EBV is suggested to be involved in the early stages of MS pathogenesis (Levin, Munger et al. 2005, Munger, Levin et al. 2011).

Several studies have suggested a link between EBV and vitamin D (Holmoy 2008, Disanto, Meier et al. 2011, Wergeland, Myhr et al. 2016). The vitamin D receptor (VDR) is expressed on different cell types, including immune cells, and vitamin D regulates the immune response (Kamen and Tangpricha 2010). There is an association between low 25(OH)D levels and increased EBV antibody levels in MS patients (Salzer, Nystrom et al. 2013, Wergeland, Myhr et al. 2016) and vitamin D deficiency may influence the immune response to EBV (Disanto, Meier et al. 2011). EBV-infected B-cells are transformed into immortalized lymphoblasts, which grow as cell lines *in vitro* and, amongst others, express six nuclear proteins. One of these proteins, EBNA-3, have been shown to bind to the VDR and downregulate/block the activation of vitamin D regulated genes and thus protect lymphoblastoid cell lines from VDR-induced arrest growth/ apoptosis (Yenamandra, Hellman et al. 2010). Moreover, Røsjø and colleagues found that high-dose vitamin D_3 may have a transient effect on the humoral immune response against EBNA-1 in RRMS patients (Rosjo, Lossius et al. 2017). Altogether, data points towards a link between two of the most important risk factors of MS.

1.1.5.4 Smoking and obesity

Several reports have suggested that smoking increases the risk of MS and worsens MS symptoms and smoking has also been suggested to explain the increasing female/male gender ratio (Ascherio and Munger 2007, Rosso and Chitnis 2019). Obesity and high body mass index also seem to increase the risk of the disease (Wesnes, Riise et al. 2015).

1.1.6 Pathology

The pathologic hallmark of MS is focal, white matter, inflammatory, demyelinating lesions, that may become sclerotic plaques, hence the name multiple sclerosis (Compston and Coles 2002). Autoimmune inflammation has long been seen as the primary disease mechanism, where immune cells migrate across a compromised blood-brain barrier (BBB) (Compston and Coles 2008).

Active lesions are dominated by perivascular T-cell infiltration, where $CD8^+$ T-cells are highly represented from the start together with microglia cells. Microglia cells exert dual roles, as pro-inflammatory (M1) cells or anti-inflammatory (M2) cells, which clear myelin and contain remnants of myelin-sheaths. Further, a secondary T-cell mediated inflammation wave evolves, including $CD8^+$ and $CD4^+$ T-lymphocytes, B-lymphocytes, and plasma cells. Moreover, the lesions are characterized by oligodendrocyte (OLG) death, demyelination, and astrogliosis (Kutzelnigg and Lassmann 2014, Lassmann 2018). Acute axonal injury is highly variable and accompanies the inflammation (Trapp, Peterson et al. 1998). As the lesions develop into an inactive lesion, the inflammatory infiltrate decreases. At this stage, oligodendrocyte precursor cells (OPCs) have been/are recruited, differentiated, and remyelination may occur (Lassmann 2011). Remyelinated plaques are more susceptible to recurrent demyelinating events compared to normal-appearing white matter myelin (NAWM) (Bramow, Frischer et al. 2010). The end-stage of the formation of plaques is gliotic scars with ongoing axonal injury (Lassmann 2018). While active lesions are most prominent in the early phases of the disease, the progressive phase is dominated by the slow expansion of inactive lesions (smoldering plaques) (Frischer, Weigand et al. 2015). The disease progression is related to the accumulation of axonal degeneration (Compston and Coles 2008).

Demyelination in cortex was unrecognized for a long time until Trapp/Bø and colleges did systematic immunohistochemical analyses to show that cortical demyelination is extensive in MS patients (Peterson, Bo et al. 2001, Bø, Vedeler et al. 2003). Cortical demyelination is now established from early disease onset, but is more prominent in

progressive MS (Popescu and Lucchinetti 2012). The lesions show demyelination, OLG loss, and variable neurodegeneration. Chronic lesions show less permeability of the BBB, decreased inflammation and microglia activation, and the absence of macrophages and lymphocytes (Lassmann 2011). However, early cortical lesions have more features in common with white matter lesions (Popescu and Lucchinetti 2012). Data show that grey matter lesion load correlates better with disability in patients than white matter lesion load (Rahmanzadeh, Bruck et al. 2018). The demyelination process may be driven by meningeal inflammatory infiltrates (Lassmann 2011, Popescu and Lucchinetti 2012). Remyelination has been shown to be extensive in cortical lesions, with little failure in the recruitment of OPCs (Strijbis, Kooi et al. 2017). Moreover, neurodegeneration in the cerebral cortex seems to be, at least to a large extent, independent of cortical demyelination (Klaver, Popescu et al. 2015).

At the same time, diffuse alterations are present in the NAWM and normal-appearing grey matter (NAGM) (Frischer, Bramow et al. 2009, Beer, Biberacher et al. 2016). Thus, MS is a global CNS disease and lesions are disseminated throughout the CNS. Predilection sites are the optic nerves, periventricular white matter, juxtacortical, subpial spinal cord, brainstem, and cerebellum (Popescu, Pirko et al. 2013).

1.1.7 Myelination

Andreas Vesalius was the first to describe white and grey matter in the cerebrum in 1543, and myelinated fibers were first described by Antoni van Leeuwenhoek in the early 1700s. Myelin comes from Greek *myelos*; after bone marrow color and texture. In 1854, the pathologist Rudolf Virchow minted the word myelin. However, it was first in 1868, that the neurologist Jean-Martin Charcot used the word myelin in its modern meaning. Myelin was, for a long time, hypothesized to originate from the axon itself. Pío del Río-Hortega introduced the name oligodendroglia cell in 1921, yet it took some time before it was accepted that CNS-myelin is produced by mature OLGs (Boullerne 2016). Myelin consists mainly of different types of lipids and proteins. Myelination is the process of forming a myelin sheath around nerve fibers (Yamafuji and Matsuki 1989). The axon is wrapped by myelin several times, where the thickness is determined by the axon diameter. However, OLGs may form myelin sheaths in the absence of molecular axonal cues. Thus, the sheath length may not solely depend on the fiber but on the regional origin of the OLG. These regional properties are determined before OPC differentiation (Bechler, Byrne et al. 2015).

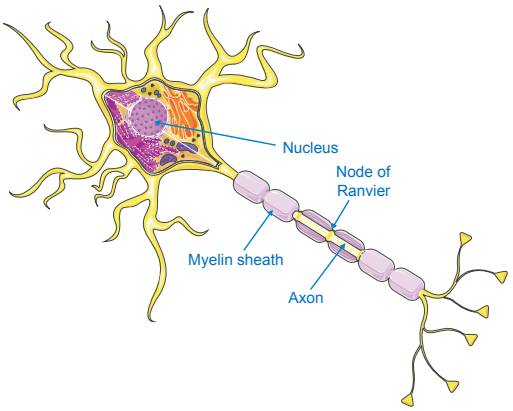

Figure 3

Normal neuron with an intact axonal myelin ensheathment (light purple). During demyelination, the myelin-sheath is destroyed. Image downloaded from https://smart.servier.com/image-set-download/. Servier Medical Art by Servier is licensed under a Creative Commons Attribution 3.0 Unported License.

The myelin sheaths (internodes) are separated by small gaps – the nodes of Ranvier (discovered by Louis-Antoine Ranvier in 1871). The myelin sheath increases the conduction velocity in axons as it lets the action potential jump from node to node; this is termed saltatory conduction. Myelin is essential for proper connections within the neural circuits and provides trophic support to the axon. Furthermore, myelin also has a role in brain plasticity and learning, as myelination may be triggered by activity including, reading and piano playing (Nave and Werner 2014).

Myelin may not be protective per se as axons can persist without myelin. This is probably due to neurotrophic factors produced by mature OLGs and astrocytes that could stimulate sprouting and survival of the axons (Smith, Cooksey et al. 2013). Moreover, axonal damage may occur although myelin is present, as shown in the cuprizone model for de- and remyelination (Manrique-Hoyos, Jurgens et al. 2012).

The myelination process is a complex process, which involves several steps (Nave and Werner 2014). First, there is an initiation of proliferation and migration of OPCs.

During migration OPCs extend, and retract processes (Yamafuji and Matsuki 1989). Excess OLGs are produced and subsequently eliminated, to make sure that the number of OLGs matches the number of axons ready for myelination (myelin-receptive axons) (Trapp, Nishiyama et al. 1997). Through glia signaling, target axons are located. After glia-axonal contact and retraction, the axon segment is selected, and the contact between the OPC and axon stabilized. OPCs may differentiate into pre-myelinating (immature) OLGs or myelinating (mature) OLGs. Differentiation is regulated by inhibitory axonal signals. Further, different signaling pathways are essential in driving the myelin formation. Moreover, the process of membrane outgrowth and axonal wrapping are followed by the trafficking of membrane components, before myelin compaction and formation of the nodes of Ranvier. Compacted myelin provides high electrical resistance and low capacitance, increasing the saltatory conduction velocity of the action potentials. The myelination process is controlled/influenced by a plethora of different inhibitory, growth, and survival factors (Yamafuji and Matsuki 1989).

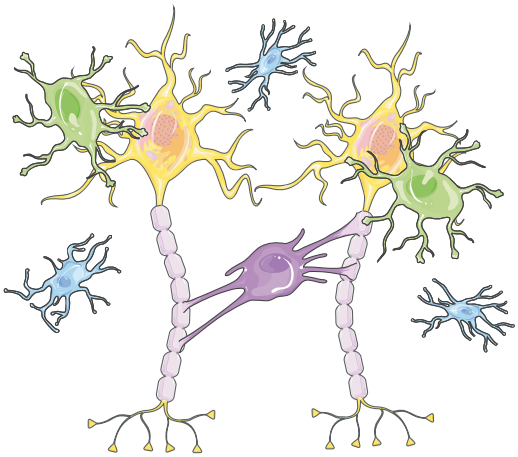

Figure 4

Two normal neurons, connected by a mature OLG (dark purple) maintaining the myelin-sheaths (light purple), surrounded by microglia (blue) and astrocytes (green). Image downloaded from https://smart.servier.com/image-set-download/. Servier Medical Art by Servier is licensed under a Creative Commons Attribution 3.0 Unported License.

1.1.8 Demyelination

Demyelination is the destruction of the myelin of axons. It is a pathological process and is usually a consequence of OLG injury (primary demyelination). Demyelination causes impaired function and is associated with axonal conduction block. Eventually, demyelination will cause neurodegeneration. The two major mechanisms that may lead to primary demyelination of the CNS are genetic abnormalities (leukodystrophies) and inflammatory damage that affects myelin and OLGs. In MS patients, demyelination is thought to be initiated by inflammation (Franklin and Ffrench-Constant 2008).

Lucchinetti and colleagues investigated active, demyelinating lesions in MS patients. They divided the lesions into four distinct patterns of demyelination based on type of infiltrate, complement activation, oligodendrocyte and myelin protein loss. Patterns I and II are described as autoimmune-mediated, while III and IV resemble a primary oligodendrogliapathy. All lesions had an inflammatory reaction dominated by T-lymphocytes and macrophages. In pattern I and II, demyelination was typically centered around veins/venules and sharply demarcated, with effective remyelination of the lesions. Pattern II had deposition of activated complement. In type III lesions, the inflammation was not centered around veins. Other features of this pattern were ill-defined lesion borders and preferential loss of myelin-associated glycoprotein (MAG), a profound OLG loss, and a lack of remyelination. The features of pattern IV were sharply demarcated perivenous lesions, and simultaneous loss of all myelin proteins, similar with type I and II lesions. However, type IV lesions were characterized by an extensive OLG loss and lack of remyelination (Lucchinetti, Bruck et al. 2000). More recently, Metz and colleagues investigated the immunopathological patterns in human tissue. Their findings supported the interindividual immunopathological heterogeneity in early, active MS lesions (Metz, Weigand et al. 2014).

Damaged myelin is engulfed and degraded by activated microglia and macrophages. Therefore, the MS lesion stage can be determined by the temporal development of degradation of myelin proteins and the pattern of immune cell infiltrate. Immunohistochemically, the minor myelin proteins (first degraded) may be stained by myelin oligodendrocyte glycoprotein (MOG) or MAG, while major (later degraded) myelin proteins are stained by myelin basic protein (MBP) or myelin proteolipid protein (PLP). An alternative histochemical stain is Luxol Fast Blue (LFB) staining, especially for shadow plaques (remyelinated plaques). Hematoxylin and eosin give an overview and indication of the degree of cell infiltration and inflammation. Preferably, in immunohistochemistry (IHC) stains, the nucleus should be counterstained with, for example, hematoxylin (Kuhlmann, Ludwin et al. 2017). Anti-Mac-3 (Lindner, Fokuhl et al. 2009) and anti-CD68 are reliable markers for microglia/macrophage cells. Further, mature OLGs can be stained by anti-Nogo-A (Neurite Outgrowth Inhibitor Protein A), astrocytes by anti-GFAP (Glial fibrillary acidic protein), T-cells by anti-CD3, axonal damage by anti-APP (Kuhlmann, Ludwin et al. 2017) and non-phosphorylated neurofilament heavy chain (anti-NFH) (Lindner, Fokuhl et al. 2009). Neurofilament light chain (NFL) is a major structural protein in neurons and a marker for axonal damage (Lycke, Karlsson et al. 1998); reduced NFL-immunoreactivity reflects increased axonal loss.

1.1.9 Remyelination

Remyelination is the creation of new myelin sheaths subsequent to demyelination. This regeneration of myelin by OLGs restores the cytoarchitecture and function of axons (Franklin and Ffrench-Constant 2008). Remyelination is extensive in MS patients (Patrikios, Stadelmann et al. 2006, Patani, Balaratnam et al. 2007), and the structure of and conduction in axons may be restored. Thus, protecting axons from further degeneration could prevent disability and disease progression in MS patients (Irvine and Blakemore 2008). There are two ways to improve remyelination: 1) exogenous remyelination by transplantation of cells or 2) promoting the present endogenous remyelination (Blakemore and Irvine 2008).

The remyelination process differs from developmental myelination as it follows demyelination and immune response (Plemel, Liu et al. 2017). The process is thought to involve the generation of new OLGs, mainly from CNS stem cells or OPCs widespread in the CNS. OPCs are activated from a quiescent state to a regenerative state; the activation is associated with injury and changes in astrocytes and microglia. After the recruitment phase (migration and proliferation of OPCs), the differentiation phase follows: OPCs are differentiated into pre-myelinating and mature (myelinating) OLGs. Axon contact is established, new myelin generated, wrapped and compacted (Franklin and Goldman 2015, Neumann, Segel et al. 2019). Differentiation is suggested to be the most vulnerable phase and the most likely time point for remyelination failure.

After remyelination, the myelin-sheaths are completely reconstructed (Franklin and Ffrench-Constant 2008), but thinner than compared to original, non-damaged myelin-sheaths. Myelin thickness is expressed by the *g* ratio*,* calculated as axon diameter/ axon diameter + myelin-sheath. Thus, remyelinated axons have a higher *g* ratio compared to normally myelinated axons. However, in areas such as the corpus callosum where we find axons with a smaller diameter with usually thinner myelin sheaths, the *g* ratio may remain unchanged after remyelination (Stidworthy, Genoud et al. 2003, Franklin and Ffrench-Constant 2017). As the reduction in thickness is mainly evident in lager axons, it may be difficult to distinguish remyelination and myelination in small axons by the

g ratio (Blakemore and Franklin 2008). The development of OLGs and remyelination is regulated by negative and positive factors such as growth factors, cytokines, and chemokines; however, the mechanisms behind how remyelination is controlled are not completely known (Plemel, Liu et al. 2017). Recent studies suggest that also old OLGs participate in remyelination in animal models and humans (Duncan, Radcliff et al. 2018, Yeung, Djelloul et al. 2019). Mature OLGs, from post-mortem brain tissue, were birth-dated to assess the dynamics of OLGs in MS patients. Surprisingly, the study found that OLGs in shadow plaques were old and not newly generated. Hence, the remyelination of lesions may be conducted by old, spared OLGs and not newly formed OLGs. Moreover, there might be principal differences in the dynamics of remyelination in rodents and humans (Yeung, Djelloul et al. 2019).

Furthermore, inflammation is necessary and has a key role in remyelination. Inflammatory cells express pro-inflammatory factors that may affect the regeneration of damaged tissue. The innate immune response is essential, and microglia/macrophage activation is associated with both damage and regeneration (Franklin and Goldman 2015). Resident macrophages (microglia) and monocyte-derived macrophages coordinate CNS myelin regeneration (Lloyd and Miron 2019). Myelin has an inhibitory effect on OPC differentiation. Therefore, myelin debris needs to be efficiently cleared to ensure subsequent remyelination after a demyelinating event. Both monocytes of the innate immune system and microglia can develop into macrophages and are crucial in the process of removing debris. Thus, microglia facilitate OPC recruitment, differentiation, and remyelination. Simplified, microglia activation can be divided into M1 microglia and M2 microglia, where M1 is pro-inflammatory and associated with OPC recruitment. M2 is anti-inflammatory/immune-regulatory and associated with myelin phagocytosis, secretion of regenerative factors, enhancing of OPC differentiation, and remyelination. Thus, both M1 and M2 are important for sufficient remyelination (Miron and Franklin 2014). The switch from M1 to M2 macrophages have been shown to be delayed by aging; activation, recruitment, and differentiation of OPCs declines with age, consequently, also remyelination.

Astrocytes are the most abundant cell in the CNS. They are believed to be supporting cells that adapt their functions to their environment and are involved in CNS development, homeostasis, and injury repair. However, astrocytes have roles beyond support, for example, during myelination and remyelination by secreting both regenerative and inhibiting factors that communicate with other cells (Nair, Frederick et al. 2008). As microglia, astrocytes have a simplified categorization, where A1 is pro-inflammatory and facilitate inflammation and damage, and A2 are more pro-repair and beneficial. In MS patients, astrocytes make glial scars, which may limit inflammation, but less beneficially inhibit OPCs migrating into the area. Astrocytes interact with microglia and regulate their function, including regulation of microglia activation, phagocytosis by microglia, and factors secreted by microglia. On the other side, microglia may also influence astrocytes (Molina-Gonzalez and Miron 2019). During cuprizone-induced demyelination, astrocyte ablation was shown to impair remyelination, probably due to reduced chemokine secretion with subsequently less microglia activation and less myelin debris phagocytosis (Skripuletz, Hackstette et al. 2013).

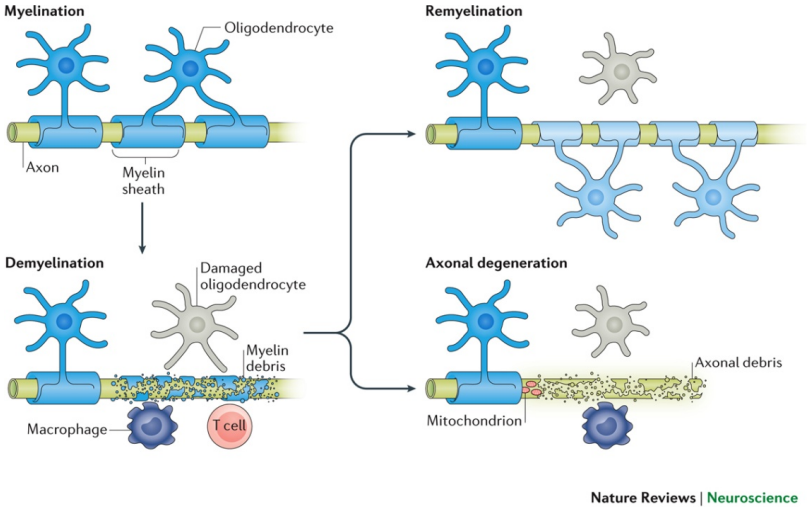

Figure 5

The figure illustrates myelination, demyelination, and subsequently remyelination by newly formed OLGs on an intact axon. Recent studies suggest that old OLGs may contribute to remyelination in animal models and humans. Of note, the remyelination process may differ in animal models and humans. Remyelination failure halt the axonal conduction and loss of the supportive myelin. Further leading to energy deficiency, perturbed axonal transport, and eventually axonal degeneration. Adapted from *Regenerating CNS myelin - from mechanisms to experimental medicines*, accessed Feb. 2., 2020 (Franklin and Ffrench-Constant 2017).

In MS patients, remyelination occurs in varying degrees, frequently at the border of lesions. However, repair may occur in the whole plaque in approximately 20% of MS lesions (Patrikios, Stadelmann et al. 2006, Patani, Balaratnam et al. 2007). Completely remyelinated areas are referred to as shadow plaques and show a lighter staining pattern compared to staining of normal white matter, owing to the fact that remyelinated axons are covered with thinner myelin sheaths and have shortened internodes compared to normal myelin sheaths (Blakemore 1974, Prineas and Connell 1979). Remyelination may occur during ongoing demyelination within the same lesion (Prineas, Kwon et al. 1984). Hence, remyelination starts shortly after or during demyelination (Kutzelnigg and Lassmann 2014). Remyelination occurs during the whole disease course, yet to a lesser extent in chronic/inactive lesions. The process is heterogeneous in and between patients and depends on the location of the lesion; remyelination is shown to be more pronounced in the subcortical area and deep white matter compared to periventricular plaques and cerebellum (Patrikios, Stadelmann et al. 2006, Goldschmidt, Antel et al. 2009). However, the number of myelin receptive axons have been shown to be higher in the corpus callosum than in the cerebral cortex (Trapp, Nishiyama et al. 1997). Factors such as the presence of OPCs, their potential to migrate and differentiate, the number of susceptible axons, and repetitive de- and remyelination could all play a role in the repair process (Lassmann 2018).

1.1.9.1 Causes of remyelination failure

Persisting demyelination results in axonal and neuronal loss. Despite adequate medication and an apparently stable, relapse-free disease, patients may experience increasing disability and progression, possibly due to remyelination failure. Remyelination efficiency is affected by general factors like gender, genetics, and age. However, regeneration failure could also be caused by more disease-specific factors. Factors as OPC deficiency, failure of recruitment, differentiation, repopulation, and maturation could impact remyelination efficiency. Older OPCs may be less efficient, and larger demyelinated areas need a higher number of functioning OPCs (Franklin and Ffrench-Constant 2008). The OPCs ability to remyelinate might differ according to the brain areas, as neuronal activity contributes to OPC proliferation, areas with higher neuronal activity might have more extensive repair (Goldschmidt, Antel et al. 2009). Failure in the differentiation and maturation of OPCs into OLGs has been suggested to be the most vulnerable stage regarding remyelination in MS patients. Moreover, failure can be caused by dysregulation of several events in a preset sequence (the dysregulation hypothesis). Demyelinated axons may also be less receptive to remyelination than healthy axons (Franklin and Ffrench-Constant 2008).

Naturally, regeneration becomes less efficient with aging; thus, age is suggested to be a primary reason for remyelination failure. Changes due to aging in the development of mature OLGs are especially important, as well as age-related changes to microglia/macrophages and their pro-myelination factors, and the removal of myelin debris. Although less investigated, changes in astrocytes would likely impact their ability to support the process (Neumann, Segel et al. 2019).

Delayed remyelination leaves the axon more exposed and vulnerable to degeneration. Although remyelination has been shown to be evident and efficient in some MS patients, it often fails during the disease course. However, robust remyelination exists in some patients; therefore, enhancing remyelination should be possible through therapeutic agents. There are a large number of ongoing experimental studies

investigating the effect of different compounds on remyelination. Several compounds have been tested out in clinical trials (Plemel, Liu et al. 2017). We have studied two compounds, calcitriol and fingolimod; both cross the BBB and have the ability to bind to receptors on CNS cells. Therefore they could affect the endogenous remyelination process and possibly mitigate axonal degeneration.

1.2 Vitamin D

1.2.1 Metabolism and sources

When the skin is exposed to solar UVB radiation (wavelength 290-315), photons are absorbed by 7-dehydrocholesterol, which is transformed into pre-vitamin D_3 and rapidly converted to vitamin D_3 (cholecalciferol). Excess vitamin D_3 is degraded to inactive photoproducts. Although the major source of vitamin D is the sun, vitamin D_2 (ergocalciferol) and D_3 from dietary sources as fish, egg yolk, and fortified food are important. Vitamin D is stored in adipocytes, bound to vitamin binding protein in the circulation, and converted to 25-hydroxyvitamin D (25(OH)D, calcidiol) by vitamin D-25-hydroxylase in the liver. 25(OH)D is the major circulating form; however, it is biologically inactive and must be further converted to biologically active 1.25-dihydroxyvitamin D ($1.25(OH)_2D$, calcitriol) by 25-hydroxyvitamin D-1-αhydroxylase (1-α-OHase) in the kidneys and other tissues. Excess calcitriol is degraded by $1.25(OH)_2D$-24-hydroxylase (24-OHase) to calcitroic acid and secreted through the bile (figure 6) (Holick 2007, Ascherio, Munger et al. 2010).

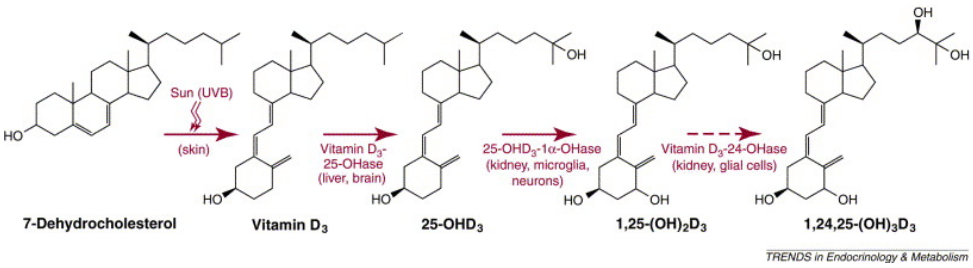

Figure 6

Vitamin D metabolism. The bold arrow indicates activation and the dash arrow inactivation of vitamin D. Reprinted from Trends in Endocrinology & Metabolism, Volume 13, Garcion, E. Wion-Barbot, N. Montero-Menei, C. N. Berger, F.Wion, D., New clues about vitamin D functions in the nervous system, Pages No. 100-5. Copyright (2002), with permission from Elsevier Science Ltd., (Garcion, Wion-Barbot et al. 2002).

1.2.2 Vitamin D mechanisms

The classical function of calcitriol is the regulation of calcium and phosphorus absorption, and calcitriol synthesis is regulated through the calcium-phosphate-parathyroid hormone (PTH) axis (Holick 2007). Vitamin D is lipid-soluble, and calcitriol has endocrine effects. Moreover, vitamin D also has key roles in the immune system and the brain (Garcion, Wion-Barbot et al. 2002, Christakos, Li et al. 2019). Vitamin D signaling is mainly mediated through the VDR. The VDR is expressed in almost every tissue (Bikle 2014), including brain-, and immune cells, supporting a role for vitamin D in immune modulation. VDR and 1α-OHase immunoreactivity was shown to be widely distributed in the brain and respectively located to the nucleus and cytoplasm in neurons and glia (Eyles, Smith et al. 2005). VDR forms a heterodimer together with the retinoid X receptor (RXR), interacting with DNA sequences causing up- or downregulation of transcription (Christakos, Li et al. 2019).

1.2.3 Measuring vitamin D

As the major circulating form in the blood, and due to the short half-life of calcitriol, 25(OH)D is usually measured to evaluate vitamin D status. The conversion of vitamin D to 25(OH)D is believed to be little influenced by feedback regulation by 25(OH)D or calcitriol. There is no consensus of what is the adequate level of 25(OH)D. The recommendations vary from country to country, and the results from the studies may not reflect the appropriate level for healthy groups and different patient groups (Christakos, Li et al. 2019). Of note, the interindividual variability of the vitamin D concentration is not only due to sun exposure, geographical latitude, and vitamin D intake. The individual genetic variations are suggested to increase the risk of vitamin D insufficiency (Wang, Zhang et al. 2010). The recommended daily supplemental dose for healthy people is around 600 international units (IU) (Christakos, Li et al. 2019). In MS patients, supplements of 1000-2000 IU daily may prevent low vitamin D levels associated with insufficient bone mineral density. Studies point towards target 25(OH)D levels around 100 nmol/L, which could be achieved with higher doses, depending on sun exposure, season, and home country (Smolders, Torkildsen et al. 2019).

1.2.4 Vitamin D and MS

1.2.4.1 Animal studies

Calcitriol administrated before, and during the immunization-phase prevents the development of EAE in rodents (Lemire and Archer 1991). Thus, suggesting an immunosuppressive role in the EAE model for MS. In a study by Cantorna and colleagues, calcitriol was reported to prevent the development of EAE and reverse EAE progression; and in addition, vitamin D deficiency accelerated EAE onset (Cantorna, Hayes et al. 1996). In our research group, several studies have been conducted using the cuprizone model. Mice receiving a salmon-based diet had reduced demyelination, microglia/macrophage infiltration, and MRI lesion load compared to cod liver and soybean diets (Torkildsen, Brunborg et al. 2009). High-dose cholecalciferol reduced demyelination and microglia/macrophage activation in cuprizone mice. More unexpectedly, two weeks after cuprizone discontinuation, mice fed low-dose cholecalciferol had improved remyelination compared to those fed high-dose cholecalciferol (Wergeland, Torkildsen et al. 2011). These studies mainly laid the foundation for investigating how high-dose vitamin D affects remyelination and axonal damage in the cuprizone model, which is addressed in papers I and II.

1.2.4.2 Clinical trials

The association between low vitamin D levels and increased MS risk, suggests that high-dose vitamin D could be beneficial for MS patients. Evidence up to date remains inconclusive in the answer of the effect of vitamin D on the course of MS. Goldberg and colleagues treated MS patients with cod liver oil, equivalent to 5000 IU daily, resulting in a significant decrease in the number of relapses (Goldberg, Fleming et al. 1986). A double-blind RCT compared high- versus low-dose D_2 for six months. There was no difference between the groups in the primary endpoint, brain MRI disease activity. Exit EDSS was higher in the high-dose group; however, after adjusting entry EDSS, there was only an insignificant trend towards higher exit EDSS following high-dose treatment. Further, there was no therapeutic advantage of high-dose vitamin D (Stein, Liu et al. 2011). In a 96-weeks long RCT with 68 participants, designed to study vitamin D's effect on bone and mass density in MS patients, 20 000 IU cholecalciferol weekly were compared to placebo. Based on results from ARR, EDSS, and other clinical measures, although not powered to address clinical outcomes, the study concluded with no beneficial effect of high-dose cholecalciferol. A prospective cohort study, including 145 patients, investigated if higher levels of 25(OH)D could reduce the relapse risk among MS patients. They reported an association between increasing levels of 25(OH)D and reduced hazard of relapse (Simpson, Taylor et al. 2010). In a Cochrane review from 2018, aiming to evaluate the benefit and safety of vitamin D in the treatment of MS patients, the authors conclude that evidence points towards no effect of vitamin D on the recurrence of relapses, EDSS or new MRI gadolinium-enhancing T1 lesions in MS patients. Due to few and small trials, short follow-up time, and high risk of bias, the evidence is of deficient quality; thus, the conclusion is vague (Jagannath, Filippini et al. 2018).

More recently, results from larger RCTs have been published. In the SOLAR (Hupperts, Smolders et al. 2019) and CHOLINE (Camu, Lehert et al. 2019) studies, high-dose cholecalciferol compared to placebo were investigated for respectively 48 and 96 weeks, in randomized MS patients treated with IFN-β-1a. Primary endpoints of

NEDA-3 (no evidence of disease activity) and ARR were not reached. However, the studies suggested an effect on secondary endpoints. The results from the SOLAR study suggested an effect of high-dose cholecalciferol on MRI lesion activity. In the CHOLINE study, there was a reduction in new T1 lesions and a decrease in the volume of hypointense T1-weighted MRI lesions and lower EDSS progression in those who received cholecalciferol compared to placebo. Moreover, the EVIDIMS study, comparing low- versus high-dose cholecalciferol, did not find differences in clinical or MRI parameters. The study did not disprove or support a favorable effect of high-dose cholecalciferol (Dorr, Backer-Koduah et al. 2020).

Vitamin D is affordable, easy to administrate, and safe (Kimball, Ursell et al. 2007). Therefore, vitamin D could potentially serve as add-on therapy to the standard therapies. That the findings are inconclusive could be due to vitamin Ds immunologic mechanisms (inhibition of monocytes, T-regulator cell differentiation, shifting from T_H2 to T_H1 cellular response), which overlaps the effect of different DMTs. Thus, the impact of vitamin D could be redundant when compared to DMTs (Rotstein, Healy et al. 2015).

1.2.4.3 Remyelination

Few studies have investigated the effect of vitamin D on remyelination. Goudarzvand and colleagues studied the effects of vitamin E and D_3 on de- and remyelination in the hippocampus of rats after ethidium bromide-induced damage. Both vitamins were suggested to exert a protective effect against apoptosis and demyelination and increase remyelination (Goudarzvand, Javan et al. 2010). Shirazi et al. demonstrated that neural stem cells (NSCs) express VDR and that calcitriol upregulated VDR expression. Further, calcitriol promoted proliferation of NSC and enhanced the differentiation into neurons and OLGs in vitro. The results indicated a direct effect of calcitriol on NSC development and differentiation. Thus, vitamin D might affect neurodegeneration and repair (Shirazi, Rasouli et al. 2015). In an in vivo study by the same group, calcitriol suppressed ongoing EAE, induced NSC proliferation, and differentiation into OPCs/OLGs and increased remyelination (Shirazi, Rasouli et al. 2017).

Retinoid X receptor gamma (RXRγ) signaling may improve OPC differentiation. RXRγ binds to several nuclear receptors, VDR is one of them. RXRγ forms a complex with the VDR receptor, and a study by de la Fuenta demonstrated that calcitriol promoted OPC differentiation through RXR-VDR complex signaling. The findings support that vitamin D could improve repair. Moreover, VDR was highly expressed in a broad specter of CNS cells, including OLGs, microglia, and astrocytes in MS plaques. The VDR expression was more pronounced in active than in chronic MS plaques (de la Fuente, Errea et al. 2015). Furthermore, injections of cholecalciferol compared to placebo was shown to increase the expression of the myelin proteins MOG and 2', 3'-cyclic nucleotide 3'-phosphodiesterase (CNPase) in the cortex of cuprizone mice (Mashayekhi and Salehi 2016). Treatment with cholecalciferol, in rats before and after lysolecithin injections, was suggested to improve proliferation and differentiation of NSCs. Moreover, the study showed increased differentiation of OPCs and enhanced MBP and PLP expression, indicating reduced myelin loss and improved remyelination (Gomez-Pinedo, Cuevas et al. 2020). Altogether, these studies indicate that vitamin D could have a decisive role in remyelination.

1.3 Fingolimod

1.3.1 Mechanisms of action

Fingolimod (2-amino-2-[2-(4-octylphenyl)ethyl]propane-1.3-diol) is the synthetic form of natural sphingosine-1-phosphate (S1P), a lipid mediator, included in the family of lysophospholipids. S1P regulates a variety of physiological processes in the body. In vivo, the pro-drug fingolimod is phosphorylated to the active metabolite fingolimod-phosphate (fingolimod-p) by sphingosine kinases (SphK 1 or 2). S1P and fingolimod-p bind to cell surface G-protein-coupled receptors, sphingosine-1-phosphate receptors (S1PRs). Five subtypes exist ($S1PR_{1-5}$), and fingolimod-p modulates four of them, $S1PR_1$ and $S1PR_{3-5}$. S1PRs are distributed and expressed on a wide range of cell types in the immune and central nervous system (Chun and Hartung 2010).

Lymphocytes express both S1PRs and chemokine receptor seven (CCR7), where the latter inhibits lymphocyte migration from the lymph node. When S1P interacts with its receptor (mainly $S1PR_1$) on the lymphocyte surface, this overcomes the inhibitory signals by CCR7, and the lymphocyte leaves the lymph node. When fingolimod-p binds to S1PRs, the product is internalized, and the receptor is degraded, which prevents further cell surface signaling. Initially, fingolimod-p is an agonist, but the irreversible receptor internalization leads to functional antagonism (Groves, Kihara et al. 2013). Thus, the lymphocytes are sequestered in the lymph node. As a result, the autoreactive lymphocytes are prevented from crossing the BBB and damaging the CNS (Chun and Hartung 2010, Subei and Cohen 2015). Of note, fingolimod causes redistribution rather than depletion of lymphocytes; when fingolimod is discontinued, the immune system will be restored. Moreover, S1P is synthesized from sphingomyelin, studies have found that MS patients have lower levels of sphingomyelin in white matter (Wheeler, Bandaru et al. 2008) and the levels of S1P are increased in CSF (Kulakowska, Zendzian-Piotrowska et al. 2010). Hence, S1P signaling may be interrupted in MS patients.

1.3.2 Treatment of MS

Several RCTs have assessed the effect and safety of fingolimod. In FREEDOMS I (FTY720 Research Evaluating Effects of Daily Oral Therapy in MS) (Kappos, Radue et al. 2010) and FREEDOMS II (Calabresi, Radue et al. 2014) fingolimod reduced the ARRs compared to placebo. Likewise, in TRANSFORMS (Trial Assessing injectable IFN versus FTY720 Oral in Relapsing-remitting MS) when compared to IFN-β1a (Cohen, Barkhof et al. 2010). All trials showed an effect on MRI lesion activity and brain volume loss. Only FREEDOMS I showed a reduced impact on disability worsening. Due to fingolimod's nonselective modulation of S1PRs, several adverse effects were reported, e.g., bradycardia, macular edema, and infections. Another RCT, INFORMS, assessing fingolimod's effect in PPMS, did not find differences in brain volume loss or disability progression compared to placebo (Lublin, Miller et al. 2016). More S1PR selective drugs have been developed, and the $S1P_1$ and $S1P_5$ modulator, siponimod (BAF312), have shown a modest reduction in disability progression and brain volume loss in SPMS patients compared to placebo, suggesting a neuroprotective effect (Kappos, Bar-Or et al. 2018). In March 2019, the Food and Drug Administration (FDA) approved siponimod in the treatment of SPMS. Several selective S1PR modulators have been/ are under investigation (Chaudhry, Cohen et al. 2017).

1.3.3 Fingolimod and remyelination

S1PRs are expressed by CNS cells like OLGs (Jaillard, Harrison et al. 2005), astrocytes (Pebay, Toutant et al. 2001) neurons, and microglia (Chun and Hartung 2010). Fingolimod is lipophilic and crosses the BBB (Foster, Howard et al. 2007, Hunter, Bowen et al. 2016). Binding of S1PRs results in the activation of several intracellular signaling pathways. Moreover, S1P signaling could mediate processes like astrogliosis and demyelination. Hence, fingolimod may exert a direct CNS effect and have an impact on neuropathological processes, thus promoting neuroprotection (Hunter, Bowen et al. 2016). As there might be undesired interactions between an immunomodulator and a pro-remyelinating substance, it would be a great advantage to find a compound that possesses both properties.

Several studies have tried to determine whether fingolimod has a positive impact on the remyelination process. Studies of organotypic cerebellar slices cultures have indicated that fingolimod increase remyelination, process extension in OPCs and OLGs, the number of microglia cells, and astrocyte activation after lysophosphatidylcholine (LPC)-induced demyelination. The effects on remyelination and astrocytes were mainly mediated through $S1P_3$ and $S1P_5$ (Miron, Ludwin et al. 2010). Jackson and colleagues used a reaggregate spheroid cell culture model combined with LPC-induced demyelination and investigated fingolimod during the following spontaneous remyelination. They found that fingolimod increased the levels of MBP in the remyelination phase, possibly through ameliorating pathological effects related to microglia activation (Jackson, Giovannoni et al. 2011).

In vivo, fingolimod given before LPC-induced demyelination decreased inflammation and demyelination. Additionally, the study reported increased OPC recruitment, oligodendrogenesis, and remyelination (Yazdi, Baharvand et al. 2015). Early intervention with fingolimod inhibits relapses in relapsing EAE, but long-term treatment initiated at a later time point does not slow the worsening, and secondary progression continues (Al-Izki, Pryce et al. 2011). Another study in the EAE model found that fingolimod treatment initiated post-onset of EAE symptoms, enhanced

remyelination, OPC proliferation and -differentiation (Zhang, Zhang et al. 2015). Fingolimod attenuated demyelination, acute axonal damage, astrocyte, and microglia activity and increased the number of OLGs during cuprizone induced demyelination when given from day one. However, when investigating the effect of rescue treatment on remyelination, they found no difference in remyelination, the number of OLGs, OPCs, or microglia compared to placebo. Moreover, there was an increased number of astrocytes (Kim, Miron et al. 2011). Rescue therapy with fingolimod has failed to improve remyelination in the cuprizone model, although fingolimod increased OPC proliferation and astrocyte activation (Hu, Lee et al. 2011). In a study of acute and chronic cuprizone-induced demyelination, Slowik et al. found that fingolimod did not affect remyelination, microglia or astrocytes in the corpus callosum and the cerebral cortex of mice. However, the study reported less acute axonal damage in fingolimod-treated mice compared to placebo in both acute and chronic lesions (Slowik, Schmidt et al. 2015). Early treatment with fingolimod was shown to suppress demyelination, OLG death, microglia, and astrocyte activation, possibly through $S1PR_1$ signaling. However, fingolimod, as rescue therapy, failed to increase remyelination (Kim, Bielawski et al. 2018).

2 Aims of the thesis

2.1 General aim:

The overall objective of the thesis was to investigate the effects of calcitriol and fingolimod on remyelination in the cuprizone model for de- and remyelination.

2.2 Specific aims:

1) To examine the effect of high-dose calcitriol on remyelination, axonal damage, and axonal loss in the cerebrum of cuprizone mice by applying IHC. This is addressed in papers I and II.

2) To investigate how fingolimod impacts remyelination, axonal damage, and axonal loss in the cerebrum and cerebellum of cuprizone mice by applying IHC and proteomics. This is addressed in papers III and IV.

3 Methodological considerations

3.1 Experimental models

There are several experimental MS-models that replicate different pathophysiological aspects of the disease. Since the availability of brain tissue research samples from MS patients is limited, especially from the early disease phases, experimental models are an essential contribution to MS research as they allow us to look at different pathological mechanisms and hypotheses under controlled conditions. The models illustrate demyelination, but some of them also allow us to investigate and achieve more insight into the process of remyelination, why it fails, and how compounds may enhance this process. However, all the models have limitations and reflect only part of the pathological spectrum. MS is a human disease, and none of the animal models entirely describes the pathophysiology underlying MS. The models are classified as autoimmune, viral, or toxin-induced demyelination (Blakemore and Franklin 2008).

3.1.1 Experimental autoimmune encephalomyelitis (EAE)

The experimental autoimmune encephalomyelitis (EAE) model was first studied by Rivers and Schwentker in monkeys (Rivers and Schwentker 1935). EAE is induced by immunization with CNS antigens emulsified in Freund's adjuvant (active EAE) or by adoptive transfer of lymph node cells, T-cells, and clones from immunized animals to naïve recipients (passive EAE). Spontaneous EAE develops in T cell receptor transgenic mice. The model works mainly through T-cell ($CD4^+$) driven autoimmunity towards CNS myelin proteins or peptides. The animals develop encephalomyelitis with pathologic changes in the BBB, T-cell infiltration, demyelination, and neuronal degeneration, resulting in neurologic episodes with paralysis (Kipp, van der Star et al. 2012). EAE has contributed to the comprehension of CNS autoimmunity and the development of new DMTs for MS patients. Even though EAE and MS have similarities regarding inflammation, demyelination and overlapping pathology, they differ in pathogenesis, clinical presentation, and therapy response (Lassmann 2019). The autoimmune destruction affects both myelin and axons unpredictably and in

different locations. Therefore this model, with its limitations, may not be the most reliable for studying the mechanisms of endogenous remyelination (Skripuletz, Gudi et al. 2011).

3.1.2 Viral models

In animals, natural infections with viruses can induce myelin damage in the CNS. Inoculation of a virus in susceptible animals leads to inflammation and demyelination. Some of the viruses used are measles, semliki forest virus, and mouse hepatitis virus (Kipp, van der Star et al. 2012). One of the most widely used models is Theiler's virus-induced encephalitis, where infection with the picornavirus leads to progressive demyelination due to T-lymphocyte infiltration (Theiler 1934, Kipp, van der Star et al. 2012).

3.1.3 Toxin models

Toxin models may be induced by focal injections or systemic administration. Among the most used toxins to induce focal demyelination is lysolecithin (LPC) (Hall 1972) and ethidium bromide (Yajima and Suzuki 1979). Remyelination and varying degrees of OPC, OLG, and astrocyte death occur in both models (Blakemore and Franklin 2008). These models require special equipment (Kipp, van der Star et al. 2012), for stereotaxic lesioning of white matter tracts in the rodent brain. Thus, the technique may be better suited for studies in larger animals, such as rats (Stidworthy, Genoud et al. 2003).

3.1.3.1 The cuprizone model for de- and remyelination

For this thesis, we used a model of the systemic toxin, cuprizone (bis-cyclohexanone oxaldihydrazone). This model is commonly used to study de- and remyelination (Skripuletz, Gudi et al. 2011). Gustav Nilsson was the first to describe cuprizone in the 1950s (Praet, Guglielmetti et al. 2014). However, cuprizone was established as a neurotoxin for mice first by W.W. Carlton and was originally described to cause spongy degeneration and hydrocephalus (Carlton 1966). Much of the early work by Ludwin, Blakemore, and colleagues created the basis for further work in the model (Blakemore 1973, Blakemore 1973, Ludwin 1978). Later, Matsushima and colleagues refined the model (Matsushima and Morell 2001).

Cellular effects of cuprizone exposure

The cuprizone model is a mechanism model that allows studying specific aspects of MS pathology, such as de- and remyelination. Cuprizone mainly affects OLGs, causing inflammation, OLG death, and demyelination; OPCs and astrocytes are spared (Blakemore and Franklin 2008). Microglia/macrophages are observed at week one of cuprizone exposure, the number usually peaks between weeks four and six (Hiremath, Saito et al. 1998). Astrocyte activation is evident after three weeks and peak around week five (Skripuletz, Gudi et al. 2011). In contrast to the more transient microglia activation, astrocytosis may persist for weeks (Gudi, Gingele et al. 2014). During week three of exposure, OPCs are recruited and start to differentiate in week five. Remyelination occurs already in week 5, during cuprizone exposure, and is evident in week six (Matsushima and Morell 2001). Microglia/macrophages phagocyte myelin debris and dead cells, recruit OPCs, give trophic support, and facilitate tissue remodeling (Praet, Guglielmetti et al. 2014). Moreover, astrocytes have been suggested to modulate the removal of myelin debris and facilitate remyelination by recruiting microglia/macrophages (Skripuletz, Hackstette et al. 2013). Astrocytes and microglia/macrophages co-operate, and both cells respond to and actively participate in de- and remyelination. Thus, a controlled inflammatory

response seems to be required for successful myelin regeneration (Gudi, Gingele et al. 2014).

In the cuprizone model, the BBB remains intact (Bakker and Ludwin 1987), in part explaining the lack of B and T lymphocytes. Only a few T lymphocytes are present (Wergeland, Torkildsen et al. 2012). Moreover, axonal damage is present, and remyelination may protect against axonal degeneration after cuprizone-induced demyelination (Irvine and Blakemore 2008). Although mice seem to recover completely, the axonal damage continues (Manrique-Hoyos, Jurgens et al. 2012), and prolonged cuprizone exposure results in increased axonal degeneration, despite remyelination (Lindner, Fokuhl et al. 2009).

Mechanisms of cuprizone

Copper (Cu) is a cofactor in several enzymatic processes, and disturbance in Cu homeostasis may be the reason for cuprizone pathology. Cuprizone has been suggested to entrap Cu within the cell or to induce Cu deficiency by Cu chelation, resulting in the pathologic effects of cuprizone (Rossi, Lombardo et al. 2004). Cu brain content decreased after cuprizone exposure (Venturini 1973); cuprizone does not cross the intestinal barrier and does not accumulate in the liver or the brain, supporting that the neurotoxic effect could be due to Cu chelation resulting in Cu deficiency (Benetti, Ventura et al. 2010). Other studies have speculated that cuprizone has to be present in the brain; the physicochemical behavior of cuprizone is reviewed by Praet and colleagues (Praet, Guglielmetti et al. 2014). Carlton et al. failed to antidote the effect of cuprizone by feeding Cu supplements (Carlton 1967), suggesting that cuprizone (or a metabolite of cuprizone) could be toxic per se regardless of Cu deficiency (Kipp, Clarner et al. 2009). Feeding a 0.5% cuprizone diet leads to status spongiosus (vacuolation) in the CNS and formation of megamitochondria in the liver (Suzuki and Kikkawa 1969). Moreover, Venturini and colleagues showed that cuprizone affects mitochondrial proteins by inhibiting monoamine oxidase (MAO), cytochrome oxidase (complex IV), and increasing the succinate dehydrogenase (complex II) activity. They concluded that the mechanism could be enzymatic inhibition affecting the cellular respiration. Inhibition of mitochondrial respiration might reduce the adenosine

triphosphate (ATP) synthesis, and status spongiosus could be a result of inhibition of active transport (Venturini 1973). In addition, to produce ATP, mitochondria play a key role in other processes, such as calcium homeostasis and apoptosis; thus, disturbance in mitochondria and the energy metabolism could induce cell death (Skripuletz, Gudi et al. 2011). Megamitochondria in the liver are not observed with a 0.2% diet (Hiremath, Saito et al. 1998).

Cuprizone seems to have selective toxicity to OLGs in vitro (Benardais, Kotsiari et al. 2013), and may elevate the production of ROS/RNS, resulting in increased oxidative stress in OLGs (Praet, Guglielmetti et al. 2014). Cuprizone especially inhibits complex IV activity (Acs, Selak et al. 2013). OLG death is extensive in the cuprizone model, and OLGs seem to be especially susceptible to cuprizone, Cu deficiency, or other alterations in the Cu homeostasis. Furthermore, oxidative stress could lead to stress on the ER, and ER stress reduce mRNA transcription/translation (preventing the accumulation of misfolded proteins) (Praet, Guglielmetti et al. 2014). Thus, downregulation of myelin protein is observed early after cuprizone exposure; however, re-expression occurs (Morell, Barrett et al. 1998, Lindner, Heine et al. 2008, Kipp, Clarner et al. 2009). Werner et al found proteomic analysis to be a useful tool to highlight effects during de- and remyelination in the cuprizone model. Mitochondrial function was shown to be the most altered cellular function subsequent to cuprizone exposure. Moreover, myelin-related and OLG-specific proteins decreased after cuprizone exposure and increased towards control levels during recovery (Werner, Saha et al. 2010). Proteomic analysis of the cortex, spleen, and skeletal muscle of cuprizone mice, revealed wider biochemical and cellular effects of cuprizone. Protein alterations in the cortex were related to axon growth, energy metabolism, and calcium signaling (Partridge, Gopinath et al. 2016). Cuprizone also affects the myelin lipid metabolism, shown by the decrease in the myelin-specific lipids cerebroside and cholesterol (Jurevics, Largent et al. 2002), in addition to phospholipids. These represent the largest portion of lipids in myelin.

The most well-known and plausible hypothesis is that maintenance of myelin causes a high metabolic demand in OLGs; when there is too little energy, these cells become especially vulnerable (Matsushima and Morell 2001, Kipp, van der Star et al. 2012). OPCs survive cuprizone exposure, this could be due to a less energy demanding metabolism, as OPCs become vulnerable when they differentiate into OLGs. Moreover, under continuous cuprizone exposure, newly differentiated OLGs die around week eight of exposure; and remyelination is limited. This is probably due to a depletion in available OPCs and, or increase in inhibitory or decrease in stimulation signals that result in halted OPC recruitment/differentiation (Praet, Guglielmetti et al. 2014). A critical time window for remyelination has been suggested as cuprizone exposure over one and a half week seems to drive axonal damage beyond repair (Crawford, Mangiardi et al. 2009). Axonal degeneration may continue on a low level, gradually accumulate and eventually become evident, despite initially completed remyelination (Manrique-Hoyos, Jurgens et al. 2012). Therefore, initiating early remyelination, before demyelination-induced axonal damage, may be crucial to improve axon recovery and inhibit disease progression. Nevertheless, it seems like once OLGs are disturbed by cuprizone, an irreversible sequence of cellular and inflammatory events starts that results in OLG death and demyelination. In recent years, the mechanism of the cuprizone model has become more elucidated, yet further work remains before the model is fully understood. Altogether, current knowledge indicates that Cu chelation by cuprizone leads to disturbances in the Cu homeostasis, alteration in mitochondria enzyme function, with further increase in oxidative stress. ER stress disrupts the myelin protein and lipid synthesis. Prolonged mitochondria stress and activation of the innate immune system result in OLG death and demyelination (Praet, Guglielmetti et al. 2014).

Cuprizone administration

The cuprizone toxin can be mixed into animal food and is easy to administrate. Although cuprizone easily induce demyelination, the effect depends on the specifics of the experiment. Cuprizone has been used in rats, guinea pigs (Carlton 1969), as well as several mice strains (Praet, Guglielmetti et al. 2014). The effect of cuprizone depends on the mice strain (Skripuletz, Lindner et al. 2008), and C57Bl/6 mice are usually used in cuprizone experiments (Skripuletz, Gudi et al. 2011, Gudi, Gingele et al. 2014). Early studies showed that a 0.5% cuprizone diet caused growth restriction, demyelination, and hydrocephalus (Carlton 1966). However, 0.2% cuprizone diet reduced the toxic effect of cuprizone (Carlton 1967). Thus, the dose has to be taken into concern according to the strain (Matsushima and Morell 2001, Skripuletz, Gudi et al. 2011).

Moreover, the duration of exposure is crucial. To mimic acute demyelination and subsequent remyelination, six weeks of exposure is common. However, it is also possible to mimic chronic demyelination, 12 weeks of exposure is common and without further detrimental effects. Age at the time of cuprizone exposure is also essential; 8-10 weeks old mice have shown reproducible demyelination and fewer unwanted side effects such as liver toxicity and death. Established by Hiremath and colleagues, the most common cuprizone protocol is to feed 8-week-old C57Bl/6 mice 0.2% cuprizone for six weeks. Demyelination is evident at the third week and completed during the fifth-sixth week of exposure, depending on the investigated area (Hiremath, Saito et al. 1998). Complete demyelination occurs in the corpus callosum after five weeks and in the cortex after six weeks (Gudi, Gingele et al. 2014). The model is also used in transgenic C57Bl/6 mice (Praet, Guglielmetti et al. 2014). Demyelination is anatomically localized, and the corpus callosum is the most investigated area. However, demyelination also occurs in several other areas. Later studies established that demyelination is evident and widespread in the grey matter (Skripuletz, Lindner et al. 2008, Skripuletz, Gudi et al. 2011, Goldberg, Clarner et al. 2015).

There is regional heterogeneity in the pathology between the corpus callosum and cortex (Wergeland, Torkildsen et al. 2012). Demyelination and remyelination of the cerebellum are well described in mice (Groebe, Clarner et al. 2009, Skripuletz, Bussmann et al. 2010), demyelination is possibly less pronounced in the cerebellar cortex (Groebe, Clarner et al. 2009).

Gender may affect the degree of demyelination. Nevertheless, both male and female C57Bl/6 mice showed a similar pattern of de- and remyelination (Taylor, Gilmore et al. 2010). Initial body weight is critical for the outcome of the experiment (Kipp, Clarner et al. 2009), and the weight is influenced by the dose of cuprizone, as diets above 0.2% cause extensive weight loss (Hiremath, Saito et al. 1998). Cuprizone causes subtle behavioral changes, and parameters such as motor, anxiety, fatigue, sleep, and pain, have been studied, and there are several standardized tests. Motor behavior is the most frequently studied parameter, and the RotaRod test is the most commonly used test (Sen, Mahns et al. 2019).

Cuprizone – value in MS research

Based on the heterogeneity within active MS lesions, the four distinct patterns of demyelination were described by Lucchinetti and colleagues. Patterns I and II are described as autoimmune-mediated, while III and IV resemble a primary oligodendrogliapathy (Lucchinetti, Bruck et al. 2000). Cuprizone-induced demyelination is more similar to pattern III, and to a lesser extent pattern IV pathology. This is due to OLG disturbance and apoptosis, and ill-defined demyelination lesion with many microglia/macrophages. Axonal swelling is observed both in pattern III and cuprizone lesions. The pattern does not correspond accurately; for example, the cuprizone demyelinated lesions lack perivenous distribution and inflammation, BBB breakdown, and infiltration of T-lymphocytes (Lucchinetti, Bruck et al. 2000, Kipp, Clarner et al. 2009). Thus, the cuprizone model only elucidates some of the mechanisms involved in MS. Nevertheless, in order to examine the direct CNS effects of compounds, especially during remyelination and independently of the adaptive immune system, a mechanistic model like the cuprizone model is a good option. The model is easy to administrate, requires little equipment, and is well characterized and reproducible (Skripuletz, Gudi et al. 2011, Zendedel, Beyer et al. 2013).

3.2 Design of the study on the effect of high-dose 1.25-dihydroxyvitamin D3 on remyelination and axonal damage in the cuprizone model (paper I and II)

In paper I, we investigated the effect of high-dose calcitriol on remyelination. Paper II assessed axonal damage in two different experiments; in the demyelinating experiment, the analysis was performed on mice obtained from an earlier study by Wergeland and colleagues. Mice were randomized into four different diets with supplements of cholecalciferol. The experiment showed that high-dose cholecalciferol did not improve the rate or degree of remyelination (Wergeland, Torkildsen et al. 2011) The remyelinating experiment (presented in paper I and II) was a follow-up study of the results of Wergeland et al., investigating the effects of calcitriol on remyelination and axonal damage.

3.2.1 Mouse strain

In the first experiment of the thesis (paper I and II), we used 48, female C57Bl/6 mice. The strain was chosen as de- and remyelination has been established in this strain (Hiremath, Saito et al. 1998). The strain is the most investigated (Skripuletz, Gudi et al. 2011), allowing comparison with other studies. The genetic background and phenotype of this strain is uniform. Therefore, genetic variation does not need to be taken into consideration in the planning of the study (Torkildsen, Brunborg et al. 2008). Male mice are more commonly used; however, the pattern of de- and remyelination is similar between genders in this strain (Taylor, Gilmore et al. 2010). As female mice have less aggressive behavior towards each other and humans than male mice, female mice were chosen for the experiment.

3.2.2 Study design of the remyelination experiment

In paper I, the results from three different time points during remyelination are presented. Due to a large amount of data and findings pointing in the same direction (data not published), we chose to only present data from three weeks of remyelination, in paper II.

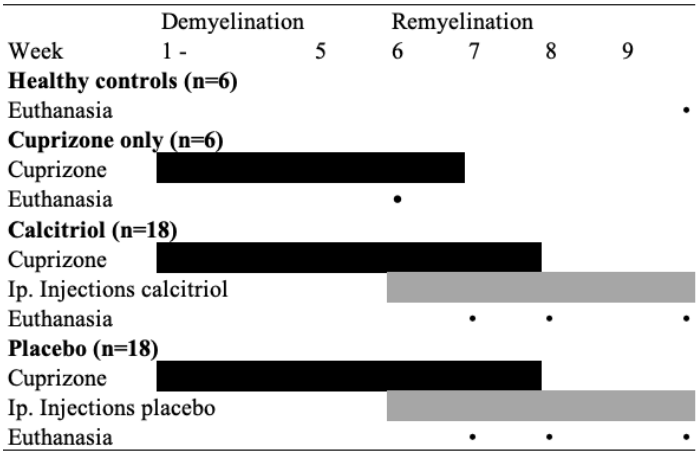

Figure 7

Overview of weeks, experimental groups, cuprizone exposure, intraperitoneal (ip.) injections and euthanasia for the remyelination experiment presented in papers I and II.

3.2.3 Administration of cuprizone, calcitriol, and cholecalciferol

Mice were randomized to ip. injections of either 0.2 µg calcitriol or placebo twice weekly from week six throughout week nine. The determination of the dose was based on a study in EAE mice, where daily ip. injections of 20 ng calcitriol prevented EAE. Further, injection of 300 ng calcitriol at EAE symptom onset halted EAE progression. The latter dose increased the calcium levels, yet the treatment was well tolerated (Cantorna, Hayes et al. 1996). To monitor adverse effects associated with calcitriol, we measured serum levels of calcium, 25(OH)-vitamin D_3, and 24.25$(OH)_2$-vitamin D_3. Due to the short half-life, it is not convenient to measure serum calcitriol.

Cantorna et al. used ip. injections, which might reduce variation in bioavailability. Based on this, we chose ip. injections, even though administration through diet, which is an easy and established method, could have been an option. Another reason for ip. injections were that the previous study by Wergeland and colleagues showed that it took several weeks to obtain steady-state serum levels of cholecalciferol when cholecalciferol was added to the diet. Calcitriol is the biologically active form of vitamin D and does not need to be enzymatically converted to achieve an effect. Avoiding the need for enzymatic conversion by using calcitriol and securing rapid uptake through ip. injections allowed us to study the limited time of regeneration after cuprizone termination, while calcitriol exerts its effect, in the best possible way.

Demyelination was induced by 0.2% cuprizone, as this is shown to give sufficient demyelination with subsequent spontaneous remyelination and a minimum of adverse side effects. Cuprizone was added to the milled mouse chow (Skripuletz, Gudi et al. 2011), which is easy to administrate and gives an adequate intake of cuprizone. The cuprizone exposure was continued for seven weeks to ensure a high serum level of calcitriol within and throughout the remyelination phase.

3.2.4 Investigated areas in the cerebrum

In papers I and II, we investigated the midline of the corpus callosum at the bregma ± 1mm. The level of bregma in a C57Bl/6 mouse brain is illustrated by zero in figure 8 and in a coronal section of the brain (figure 9).

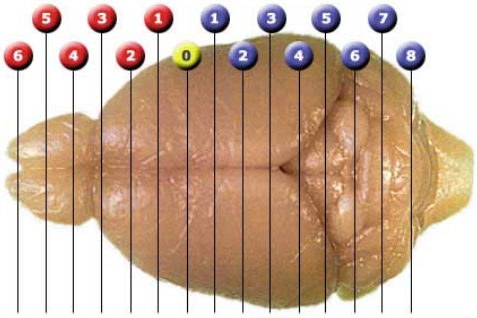

Figure 8

The mouse brain, bregma = 0 (http://www.mbl.org/atlas170/atlas170_frame.html).

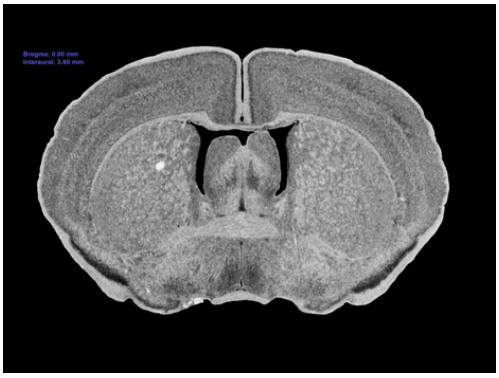

Figure 9

Coronal section of the mouse brain.

Neurogenetics at UT Health Science Center ©1999 RW Williams, design by AG Williams, atlas by T Capra (http://www.mbl.org/atlas170/atlas170_frame.html).

3.2.5 Histochemistry and immunohistochemistry

We investigated different features such as myelin loss, OLGs, astrogliosis, microglia/macrophage activation, T-lymphocytes, and axonal damage using histochemistry (HC) or IHC. Sections were evaluated in the midline area of the corpus callosum, from the bregma ± 1 mm. In paper II, three different immunohistochemical markers of axonal damage and loss were used. The primary antibodies for papers I and II are specified in table 1.

Antibody	**Host, isotype**	**Working dilution**	**Incubation time/ Temperature**	**Demasking**	**Provider**
Paper I					
Anti-GFAP	Rabbit, IgG1	1:2000	½h/RT	Tris-EDTA	Dako (Agilent)
Anti-NOGO-A	Rabbit, pAb	1:1000	1h/RT	Citrate	Chemicon
Anti-MAC-3	Rat, IgG1	1:200	24h/RT	Citrate	BD Biosciences
Anti- CD3	Rabbit, pAb	1:500	½h/RT	Tris-EDTA	Dako
Paper II					
Anti-NFL	Mouse mAb	1:1600	1h/ RT	Tris-EDTA	Millipore
Anti-NFH (non-p)	Mouse mAb	1:2000	1h/RT	Citrate	Millipore
Anti-APP	Mouse mAb	1:2000	24h/RT	Citrate	Millipore

Table 1

Papers I and II, antibodies used for immunohistochemistry specified.

pAb = polyclonal antibody, RT = room temperature, non-p = non-phosphorylated.

Semi-quantitative methods

To study remyelination, we chose an easy yet reliable semi-quantitative method. Based on studies by Lindner and colleagues, we used the histochemical staining with LFB where myelin loss is quantified by a semi-quantitative scoring system from completely myelinated (0) to completely demyelinated (3) (Hiremath, Saito et al. 1998, Lindner, Heine et al. 2008). Astrocytosis was assessed semi-quantitatively: no (0), minimal (1), moderate (2), or severe (3) reactive astrocytosis, as described before (Bruck, Pfortner et al. 2012, Wergeland, Torkildsen et al. 2012). Although GFAP staining is not specific and only labels a small fraction of astrocytes, this is the most widely used method (Molina-Gonzalez and Miron 2019).

Density of cells

To evaluate the density of cells, we used an ocular morphometric grid to count the number of immunoreactive cells in an area of 0.0625 mm^2 at 40x. Mature OLG density was quantified as the number of NOGO-A immunopositive cells in the area. This method has been earlier validated in the cuprizone model (Kuhlmann, Remington et al. 2007). No molecular marker differentiates between myelinated and remyelinated axons (Kuhlmann, Ludwin et al. 2017). However, $BCAS1^+$ cells have been suggested to represent early, myelinating OLGs, and might identify active re-/myelination. The marker was found in both active and inactive lesions (Fard, van der Meer et al. 2017). Thus, adding this marker could be of value in future experiments. Moreover, we chose to quantify microglia/macrophages, T-cells, and acute axonal damage by using the reliable and well-described markers Mac-3 (Lindner, Fokuhl et al. 2009), CD3 and APP (Kuhlmann, Ludwin et al. 2017).

Neurofilaments

The specialized intermediate filament of nerve cells, neurofilament, is a structural protein that consists of three subunits; heavy (NFH), medium (NFM), and light (NFL) in reference to their molecular mass. Neurofilaments have important functions in the development and maintenance of neurons. A disruption in neurofilament structure may result in axonal disorganization and in the end, axonal degeneration. SMI-32

recognizes the non-phosphorylated epitope of the heavy and medium neurofilament subunits (Ouda, Druga et al. 2012). The reaction is masked when the epitope is phosphorylated. Neurofilaments in healthy myelinated axons are phosphorylated, and therefore not stained by SMI-32. Thus, SMI-32 immunoreactivity, in normally myelinated regions of the brain, provides a sensitive marker for axonal injury (Trapp, Peterson et al. 1998). Previously, in the cuprizone model, SMI-32 staining has been observed after long-term demyelination (after eight weeks) as punctuations, ovoids, and continuous lines. The same study hypothesized that SMI-32 represents another pattern of axonal damage, detecting slow degeneration of axons, in contrast to APP staining, which is associated with acute axonal damage and transection (Lindner, Fokuhl et al. 2009). Moreover, we used anti-NFL to label axonal loss. Of note, a major advantage of the latter marker is that NFL may also be measured in CSF and blood (Disanto, Barro et al. 2017).

Quantifying immunoreactivity

An image-based technique for calculating immunoreactivity was used when analyzing phosphorylated NFL and non-phosphorylated NFH (SMI-32). By using the program Image J (Rasband 2012), an original image was converted into a greyscale image, before unspecific background staining was manually adjusted. Then the picture was again compared to the original image before calculating the area of the fraction of immunopositive staining. The image-based technique is an alternative to semi-quantitative calculation (Wergeland, Torkildsen et al. 2012). In paper II, only a few SMI-32 positive axons were detected after six weeks of cuprizone exposure, consistent with the observations of Lindner and colleagues. Therefore, at least in the cuprizone model, SMI-32 might be more suitable to show axonal damage after long-term demyelination.

3.2.6 Weight and RotaRod test

Weight measurements were conducted twice weekly. The initial mean weight was 19.6 g ± SD 1.5 (Nystad, Wergeland et al. 2014). One mouse weighed 15 g and died during week six; this was probably due to the low initial weight (Skripuletz, Gudi et al. 2011). Motor coordination was tested twice weekly throughout the experimental period using the RotaRod test. This test is one of the most frequently used motor behavior tests. The mice are placed on a rotating rod, where the rotation speed increases with constant acceleration. Mice with impaired motor/coordination skills will have reduced capacity to stay on the rod, thus, shorter time intervals (Sen, Mahns et al. 2019). We could not detect any differences between the groups during the remyelination process. Although the RotaRod test is the most commonly used motor performance test, it may be less sensitive and reliable compared to other tests, and we cannot exclude that other tests would have been better suited. However, as cuprizone mice show little reduction in motor performance, and the conduction of behavioral tests are time-consuming, additional tests would yield limited information. Other tests might be better suited to demonstrate a difference in behavior (Skripuletz, Gudi et al. 2011); however, this was beyond the scope of the study.

3.3 Design of the study of effects of and mechanisms of fingolimod on remyelination and axonal damage in the cuprizone model (papers III and IV)

3.3.1 Study design, cuprizone, and fingolimod/placebo administration

In paper III and IV, we investigated the effect of fingolimod on remyelination and axonal damage. We used 48, female C57Bl/6 mice. After 12 days of acclimatization, the mice (n=48) were randomized into four groups: healthy controls (n=6), cuprizone controls (n=6), cuprizone + fingolimod (n=18) and cuprizone + placebo (n=18). In this experiment, we followed a frequently used protocol adding 0.2% cuprizone to milled mouse chow for six weeks. Subsequently, mice were fed normal chow.

Based on earlier studies, fingolimod, 1 mg/kg (Hu, Lee et al. 2011, Kim, Miron et al. 2011, Deshmukh, Tardif et al. 2013), reconstituted in distilled water, or placebo (equivalent volume of water) was administered by oral gavage once daily from week five. Gavage administration is an alternative to ip. injections, gavage was chosen to resemble the normal daily intake of the drug. There was a one week overlap in cuprizone exposure and fingolimod treatment to ensure that fingolimod was taken up and phosphorylated to its active compound during the cuprizone exposure and the remyelination process.

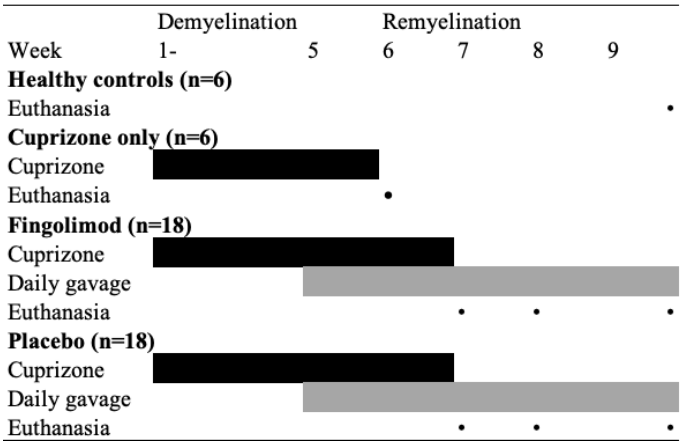

Figure 10

Overview of weeks, experimental groups, cuprizone exposure, daily gavage of fingolimod or placebo, and euthanasia for the remyelination experiment presented in papers III and IV.

3.3.2 Regional sampling sites for HC and IHC

The sampling sites for the cerebellum (paper III) are stated in the manuscript. Two areas in the subcortical region, the purkinje cell layer, and the internal granule layer were investigated. In paper IV, we expanded the number of areas investigated, shown in figure 11. However, due to the extensive amount of data pointing towards the same direction (data not published), we chose to present data mainly from the corpus callosum.

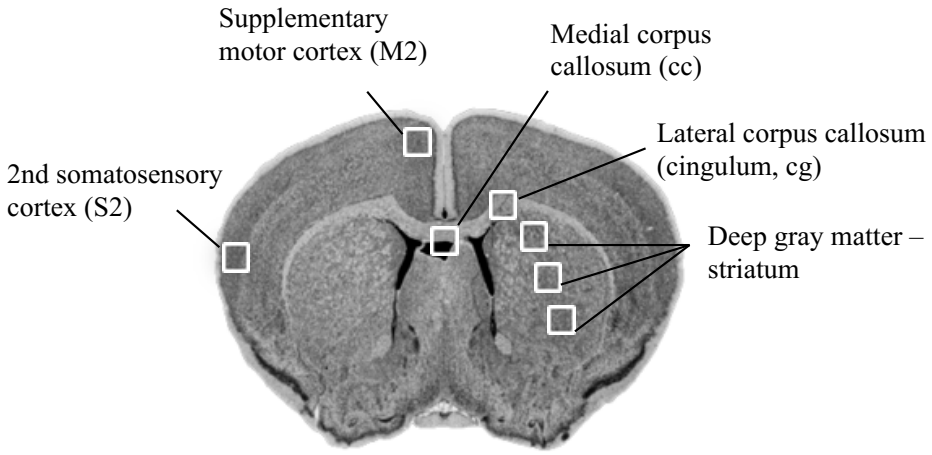

Figure 11

Overview of areas investigated in paper IV.

3.3.3 Histopathology and immunohistochemistry

For papers III and IV, we added several antibodies, elucidating remyelination, and axonal damage and loss. Although the time points for euthanasia are presented slightly differently in the two manuscripts, they correspond, and the analysis for cerebrum and cerebellum are, thus, comparable (1 wr = DM, 2wr = 1RM, 4wr = 3RM). However, to avoid confusion and increase comprehension, the manuscripts could have benefited from a more equal and precise presentation. Moreover, the use of identical markers in both tissues would have made it easier to compare the data directly. IHC for paper III was performed by Alme and colleagues, and are stated in paper III. Primary antibodies for paper IV are specified in table 2.

Antibody	**Host, isotype**	**Working dilution**	**Incubation time/ Temperature**	**Demasking**	**Provider**
Anti-PLP	Mouse, monoclonal	1:1000	24h/4°C	Citrate	Serotec
Anti-GFAP	Rabbit, monoclonal	1:2000	½h/RT	Tris-EDTA	Dako (Agilent)
Anti-NOGO-A	Rabbit, polyclonal	1:1000	1h/RT	Citrate	Chemicon
Anti-MAC-3	Rat, monoclonal	1:200	24h/RT	Citrate	BD Biosciences
Anti-CD3	Rabbit, polyclonal	1:500	½h/RT	Tris-EDTA	Dako
Anti-APP	Mouse, monoclonal	1:2000	24h/4°C	Citrate	Merck
Anti-NFL	Mouse, monoclonal	1:1600	1h/RT	Tris-EDTA	Merck

Table 2

Paper IV, antibodies used for immunohistochemistry specified.

3.3.4 Quantitative mass spectrometry-based proteomics

Through quantitative proteomics, it is possible to identify and quantify thousands of proteins simultaneously and compare them quantitatively between biological conditions. In this approach, the proteins are typically proteolytically cut into shorter sequences called peptides, e.g., by the sequence-specific protease trypsin. The resulting peptides are separated by high-performance liquid chromatography and analyzed by the mass spectrometer, e.g., by liquid-chromatography electrospray-ionization mass spectrometry system (LC-MS). Simply put, the mass spectrometer contains an ion source that provides molecules with charges, a mass analyzer that measure the mass-to-charge ratio *(m/z)* of the charged molecules, and a detector that records signal intensity. Following mass spectrometry analysis, the information is stored in spectra and used to identify and quantify peptides, and subsequently proteins, using software tools. The technique is sensitive and allows a high throughput of proteins as reviewed in (Aebersold and Mann 2003) and (Pappireddi, Martin et al. 2019).

In paper IV, the frontal right hemisphere of mice receiving fingolimod or placebo was dissected and prepared for analysis by quantitative proteomics. The six biological replicates in each condition were divided into three pools containing two biological replicates in each and, following the trypsinization, the samples were individually labeled with tandem mass tags (TMT-tags). TMT tags are stable isotopes that allow simultaneous analysis of up to 16 samples in one LC-MS/MS run, thereby reducing the number of runs and technical variation (Ragnhild Lereim, personal communication). Following labeling, the TMT experiments were fractionated to reduce the sample complexity and maximize the number of proteins identified and quantified by LC-MS/MS.

Werner et al. used proteomic analysis to identify altered brain proteins during de- and remyelination in the cuprizone model. The results suggested that whole-brain proteome analysis could be a useful method to elucidate de- and remyelination in this model (Werner, Saha et al. 2010). In the present proteomic analysis, we used tissue from the

right, frontal brain, including tissue from the corpus callosum for the proteomic analysis, meaning that the proteomic results show an overall average difference, where several cell types and signaling pathways may be included. Moreover, as we used pools for proteomic analysis, the results do not say anything about individual changes. We do not show in which specific region the proteomic changes occur. As cuprizone-induced demyelination are region specific (Skripuletz, Gudi et al. 2011), using specific regions for the proteomic analysis could be more optimal. However, analysis of particular areas, such as the corpus callosum, would require a large number of mice to obtain a sufficient amount of tissue. In addition, microdissection of the mouse brain is very demanding, both technically and time-wise. Another limitation is that we could not discern specific cell types. Thus, we can't show if there is an altered protein expression between different types of cells. This was, however, outside the scope of our study. All the proteomic analyses, statistical calculations, and interpretation were in collaboration with colleagues at PROBE.

3.4 Statistics

The calcitriol experiment was based on the results from previous results in our group (Wergeland, Torkildsen et al. 2011). The power calculation of the fingolimod experiment was based on the calcitriol experiment. Based on the difference in myelin content between calcitriol- and placebo-treated mice from (Nystad, Wergeland et al. 2014), a sample size of six animals per experimental group would give a power of 0.7 to detect a difference corresponding to an effect size δ of 1.67 (mean LFB-score of 2.0 ± SD 0.6 and 1.0 ± 0.6 after three weeks of remyelination). Due to some technical issues with slicing and staining, all animals could not be included for the analysis; thus, the power could be less than 0.7. To get more robust data, a higher sample size could have been included in the experiment to get more power.

We used the Kolmogorov-Smirnov test and/or Shapiro-Wilk test to assess the normal distribution of the data together with the assessment of descriptive data such as histograms, boxplots, and Q-Q plots. The boxplots were investigated for outliers, which were removed when applicable. Descriptive statistics were presented as mean or median with SD. In paper I, we presented the data with mean and SEM; however, a more common presentation would have been with SD. For parametric data t-test or one-way analysis of variance (ANOVA) with Fisher's least significant difference (LSD) for post hoc analysis was used. Non-parametric data were analyzed by using the Mann-Whitney *U* test or Kruskal-Wallis H-test. For non-parametric related data, Wilcoxon's signed-rank test was used. For all manuscripts, differences were considered significant at $p < .05$. The latest version of SPSS was at all times used to calculate the results.

3.5 Ethics

The cuprizone model provides isolated OLG death and demyelination, allowing us to study the remyelination process without the infiltration of T-cells. Examination of de- and remyelination is not possible in tissue cultures, and satisfactory in vitro models are not available (Franklin and Kotter 2008). There are currently no other models that can replace animal models for this type of experiment. Therefore, it is difficult to replace this experiment and find better options to investigate this issue.

Cuprizone given in the appropriate doses has previously not been reported to cause significant discomfort or pain to the animals. The mice do not get paralysis when the right amounts and duration of cuprizone is given. Unlike in other animal models, demyelination is almost completely reversible in the cuprizone model. Weight loss and decreased activity or hyperactivity have been observed during cuprizone administration. However, the mice seem not to be distressed, they regain weight and a normal activity level (Morell, Barrett et al. 1998).

We performed two animal experiments. During the trial period, the mice were inspected daily and assessed for weight loss, dehydration, and loss of motor skills. Mice experiencing signs of discomfort or major weight loss were sacrificed. At the end of the experiments, to minimize discomfort, the animals were anesthetized and killed by exsanguination (cardiac puncture). Aiming to reduce the number of animals in the experiment, we did an a priori statistical power analysis and reduced the number of control animals. Different species of animals react differently to cuprizone; C57Bl/6 mice are the most widely used mice strain in this model (Torkildsen, Brunborg et al. 2008). The experiments were carried out in accordance with the Federation for European Laboratory Animal Science Associations recommendations, and the protocols were approved by the Norwegian Animal Research Authority (permit # 2012-4421 and # 2013-5682).

4 Summary of the papers

4.1 "Effect of high-dose 1.25 dihydroxyvitamin D3 on remyelination in the cuprizone model"

Nystad AE, Wergeland S, Aksnes L, Myhr KM, Bø L, Torkildsen O.
APMIS. 2014 Dec;122(12):1178-86.

After six weeks of cuprizone exposure, there was a significant loss of myelin compared to healthy mice. Calcitriol-treated mice had less myelin compared to placebo-treated mice after seven weeks of cuprizone exposure. However, the myelin in the placebo group had an unstructured pattern, resembling damaged myelin. There was no difference between the groups after one week of remyelination. However, after three weeks of remyelination, calcitriol-treated mice had more myelin compared to placebo-treated mice. The number of mature OLGs were higher in the calcitriol-treated mice compared to placebo at all time points; the difference was significant after one week of remyelination. The calcitriol group had earlier astrocyte activation than the placebo group. The difference was significant after seven weeks of cuprizone exposure. We saw the same pattern for microglia/macrophage activation. Initially, the activation was increased in the calcitriol group, but the difference was only significant after one week of remyelination, where the placebo group had increased activation compared to the calcitriol group. The s-calcium levels were normal at all time points. There was no difference in motor performance between the groups.

4.2 "Effects of vitamin D on axonal damage during de- and remyelination in the cuprizone model"

Nystad AE, Torkildsen Ø, Wergeland S.
J Neuroimmunol. 2018 Aug 15;321:61-65.

We investigated the effects of high-dose versus low-dose cholecalciferol and high-dose calcitriol versus placebo, on axonal damage and loss in the cuprizone model. Two experiments in the cuprizone model were used. In the first experiment, mice were fed high-dose or low-dose cholecalciferol before and during cuprizone induced demyelination. In the second experiment, mice were injected with high-dose calcitriol or placebo, after cuprizone induced demyelination, and during remyelination. IHC was used to assess axonal damage and axonal loss in the corpus callosum. After six weeks of cuprizone exposure, mice treated with high-dose of cholecalciferol had less axonal loss as measured by NFL immunopositivity compared to mice treated with low-dose cholecalciferol. There was more acute axonal damage in the low-dose group, as measured by the density of APP immunopositive bulbs; however, the difference was not statistically significant. In the remyelination experiment, there was no difference in APP, SMI-32, or NFL immunoreactivity in calcitriol mice compared to placebo.

4.3 "Fingolimod does not enhance cerebellar remyelination in the cuprizone model"

Alme MN, Nystad AE, Bø L, Myhr KM, Vedeler CA, Wergeland S, Torkildsen Ø.
J Neuroimmunol. 2015 Aug 15;285:180-6.

Mice were exposed to cuprizone for six weeks; treatment with 1 mg fingolimod or placebo daily by gavage was initiated from week five. Mice were assessed and scored in the subcortex and two areas of the rostral parts of the cerebellum. De- and remyelination was evaluated by PLP1- and MBP-staining. Subcortical demyelination was robust in cuprizone controls. Cuprizone caused demyelination in the cortex of the cerebellum compared to healthy control mice. There was evident remyelination in both fingolimod- and placebo-treated mice. However, there were no differences between the groups at any time point in all areas investigated. In both subcortical and cortical cerebellum, there was a loss of mature OLGs, as measured by NOGO-A immunopositivity, after cuprizone exposure. During remyelination, the number of OLGs increased similarly in both fingolimod- and placebo-treated mice. Astrocytosis was measured by the number of GFAP immunopositive cells. In the subcortex, there was an increase in GFAP-immunopositivity in cuprizone-exposed mice. During the regeneration process, the immunopositivity remained high, without differences between fingolimod- and placebo-treated mice. Microglia/macrophages were stained by Iba1. Cuprizone caused a subcortical increase in Iba1-positive microglia/macrophages. The cerebellar cortex showed no significant changes in astrocytosis or microgliosis. Acute axonal damage was assessed by counting β-APP positive spheroids. Cuprizone control mice had increased axonal damage. Fingolimod caused no difference in subcortical acute axonal damage compared to placebo. There was no loss of axons after cuprizone exposure as measured by phosphorylated NFL at any time points. Fingolimod did not affect remyelination, mature OLG density, astrocytosis, microgliosis, or axonal damage.

4.4 "Fingolimod downregulates brain sphingosine-1-phosphate receptor 1 levels but does not promote remyelination or neuroprotection in the cuprizone model"

Nystad AE, Lereim RR, Wergeland S, Oveland E, Myhr KM, Bø L, Torkildsen Ø.
J Neuroimmunol. 2019 Oct 31;339:577091.

In the study of the effect of fingolimod on remyelination in the cerebrum, we used TMT-labeling and proteomic analysis and detected 7949 proteins, of which 7183 were quantified. Further, 6386 of these formed the basis for the statistical analysis. Two proteins ($S1PR_1$ and GNG5) in fingolimod-treated mice were downregulated at all time points compared to placebo-treated mice. However, only $S1PR_1$ remained significant after false discovery rate correction. Hence, fingolimod was functionally active by downregulating $S1PR_1$. LFB staining showed cuprizone induced demyelination in the corpus callosum after five weeks of exposure. There was no difference in myelin loss, as measured by LFB and PLP, in the corpus callosum or the cortex of mice fed fingolimod compared to placebo. Fingolimod-treated mice had increased density of mature OLG in the cortex after three weeks of remyelination, however, not at earlier time points, and there was no difference in the corpus callosum between the intervention groups. Supported by proteomic markers of myelination, the fingolimod-treated groups did not show an increased expression of myelin proteins or mature OLGs compared to the placebo group. Both groups had a time-dependent increase in myelin-associated proteins during the repair phase. Cuprizone caused increased microglia/macrophage and astrocyte activation after five weeks of exposure. Fingolimod did not affect microgliosis or astrocytosis in the corpus callosum or the cortex. The findings were supported by no difference in the proteomic markers between the intervention groups.

5 General discussion

Current MS treatment is primarily immunomodulating and affects the inflammatory feature of the disease. Nonetheless, neurodegeneration causes deterioration and disability progression in MS patients. Therefore, to treat the aspect of repair in the disease is of high importance. In this Ph.D. project, we investigated the effect of calcitriol and fingolimod on the remyelination process and axonal damage in the cuprizone model, and partly the mechanisms that would be behind this effect. The articles included in this thesis support that calcitriol might be beneficial for the remyelination process in a mice model, which is thought to illustrate some of the immunopathological mechanisms behind MS. We could not show that fingolimod had the same beneficial effect.

A major limitation of the results and implication of the studies is the choice of the cuprizone model. The exact mechanisms in this model are not fully known; this could affect the investigation of compounds in this model, especially during the demyelination process. However, in the experiments in this thesis, we investigated remyelination, which makes it less likely that cuprizone would affect the substances we studied. Moreover, the cuprizone model has been shown to be a reliable model to investigate remyelination (Skripuletz, Gudi et al. 2011). Cuprizone 0.2% diet, causes acute demyelination with subsequent remyelination. Although the repair process may begin in week five of cuprizone exposure, there is little overlap between de- and remyelination. The repair takes mainly place between two-three weeks after cuprizone withdrawal in week six. This allows investigation of remyelination relatively independent from the initial process of demyelination. In other models like EAE, it is difficult to separate the processes of de- and remyelination as they occur in parallel (Franklin and Kotter 2008). Supporting that the cuprizone model may be the most suitable animal model to investigate the repair process, although it could never perfectly mimic the repair process in MS patients.

5.1 Papers I and II

Several studies in the cuprizone model in our group formed the basis for choosing this model to study remyelination (Torkildsen, Brunborg et al. 2009, Wergeland, Torkildsen et al. 2011). We started calcitriol injections in week six of cuprizone exposure. To achieve a higher serum level of calcitriol during remyelination, we chose to continue the cuprizone exposure throughout week seven, which could make a delay in the remyelination process. In retrospect, we could ideally have started calcitriol injections in week five of cuprizone exposure and terminated cuprizone in week six, alternatively in week five, as suggested by Skripuletz and colleagues (Skripuletz, Gudi et al. 2011). One extra week of cuprizone possibly resulted in an initially slower remyelination process; it has been showed that prolonged cuprizone exposure extends the regeneration phase (Lindner, Fokuhl et al. 2009). However, while remyelination is detectable the first week after cuprizone withdrawal, it is probably most evident during week two-three of the repair process (Vega-Riquer, Mendez-Victoriano et al. 2019). Using our protocol for cuprizone exposure, we observed an increase in remyelination throughout the whole study period after ending cuprizone exposure.

As pointed out earlier in the thesis, several studies have found that vitamin D deficiency increases the susceptibility risk of MS. Vitamin D deficiency may adversely affect the course of illness and MS patients are recommended to take supplements of vitamin D. In paper I, we found that high-dose calcitriol might have a positive effect on remyelination, possibly through stimulating early OLG maturation, microglia, and astrocyte activation. The calcitriol-treatment led to less myelin in the early stages of remyelination, compared to the placebo group. Nevertheless, after three weeks of remyelination the calcitriol-treated mice had more myelin than the placebo group. Mice receiving calcitriol also showed an increase in myelin during the remyelination phase. To our knowledge, our study was the first to elucidate the effect of high-dose calcitriol on remyelination in the cuprizone model. Our results support that biologically active vitamin D affects myelin regeneration. Previously, it was found that rats injected with ethidium bromide and treated with cholecalciferol showed increased remyelination, as

measured by MBP expression, the authors suggested that the increase in remyelination could be due to a positive effect on proliferation, migration, and differentiation of OPCs into OLGs (Goudarzvand, Javan et al. 2010). Mature, myelin-producing OLGs, is a prerequisite for the regeneration of myelin. Corresponding to the increase in myelin in our study, the calcitriol group had more mature OLGs at all measured time points, and the difference was significant between the groups after one week of remyelination. Supporting our findings, Shirazi et al. found that calcitriol might affect the development and differentiation of NSC into OLGs in vitro (Shirazi, Rasouli et al. 2015). In vivo, calcitriol increased the proliferation and differentiation of NSC into OPCs/OLGs and was suggested to improve remyelination in the spinal cord of EAE mice (Shirazi, Rasouli et al. 2017). More recently, rats treated with cholecalciferol before and after LPC-induced demyelination, showed increased OPC proliferation and differentiation, in addition to increased levels of MBP and PLP (Gomez-Pinedo, Cuevas et al. 2020). The aforementioned studies support our findings in paper I, suggesting that vitamin D may have a favorable effect, improving remyelination through stimulation of OPCs and OLGs.

In paper I, we found that astrocytosis increased early in the calcitriol group and gradually decreased, while the placebo group had a slower astrocyte activation. Similar was the case for microglia activation as the placebo group showed delayed microglia activation compared to the placebo mice. As stated previously in this thesis, both astrocytes and microglia have supportive and detrimental functions in remyelination, and their interaction are thought to facilitate remyelination. Moreover, glia cells also communicate with OLGs (Lloyd and Miron 2019, Molina-Gonzalez and Miron 2019). As calcitriol mice had an earlier glia activation, this might have caused more efficient removal of damaged myelin and possibly improved cell communication; hence, earlier recruitment of mature OLGs and increased remyelination. Of note, the study by Gomes-Pinedo et al. did not confirm that cholecalciferol-treatment increased microglia activation as they found less marked microglia activation in rats receiving cholecalciferol (Gomez-Pinedo, Cuevas et al. 2020). There may be several reasons why

our findings are inconsistent, for example, the use of different animal models, and time and dose of cholecalciferol or calcitriol administration.

Few have investigated the mechanisms behind the effect of vitamin D in remyelination. Shirazi et al. found that several neurotrophic factors were upregulated during the presence of calcitriol, which could explain some of the mechanisms behind the effect of calcitriol on NSC proliferation and differentiation into OPCs and OLGs (Shirazi, Rasouli et al. 2015). As a follow-up study of paper I, not included in this thesis, we investigated the mechanisms by adding proteomics (Oveland, Nystad et al. 2018). Six myelin related proteins were found, and the levels of these proteins were generally higher in the calcitriol group, supporting our findings in paper I. We found that 125 proteins were regulated differently in the brain tissue of mice that received calcitriol compared to placebo. Among these were proteins involved in calcium homeostasis and mitochondrial function. More research needs to be done to elucidate the mechanisms further. Future studies should address how the modulation of vitamin D regulated proteins affects the remyelination process. Efforts should be made to find signaling pathways involved in the remyelination process.

It is conceivable that remyelination failure may contribute to axonal loss (Irvine and Blakemore 2008). However, axonal degeneration is proposed to continue at a low level despite remyelination (Manrique-Hoyos, Jurgens et al. 2012). Hence, it would be optimal if vitamin D not only improved remyelination but also prevented or at least reduced axonal damage. Therefore, in paper II, we examined how 1) cholecalciferol given before and during demyelination, and 2) how calcitriol given during remyelination, affected axonal damage in cuprizone mice. We found that high-dose cholecalciferol given before and during demyelination mitigated axonal loss in the corpus callosum. In EAE mice, calcitriol-treatment from peak clinical severity decreased the amount of axonal loss (Sloka, Zhornitsky et al. 2015). In an animal model of peripheral nerve trauma, rats fed high-dose cholecalciferol showed an increased number of preserved or new axons (Chabas, Stephan et al. 2013). The findings were confirmed in another study by the same group. Moreover, new findings suggested that

cholecalciferol had to be given promptly to promote efficient repair (Gueye, Marqueste et al. 2015). This supports our findings that high-dose calcitriol given after cuprizone-induced demyelination did not affect axonal damage and loss (paper II). Altogether, data indicates that vitamin D should be administrated before, or at least during, demyelination to diminish axonal damage.

5.2 Papers III and IV

Fingolimod could exert a direct CNS effect and promote neuroprotection (Hunter, Bowen et al. 2016). To find a substance that promotes neuroprotective strategies would be vital in the treatment of MS patients. Previous experimental studies show inconsistent results regarding fingolimod's effect on remyelination. In paper III and IV, we aimed to clarify if fingolimod could affect remyelination and axonal damage when given after cuprizone-induced demyelination.

We found no difference in remyelination between the fingolimod- and placebo-treated groups. Fingolimod-treated mice had not increased numbers of OLGs in the cerebellum or in the corpus callosum. After three weeks of remyelination, we found that fingolimod-treated mice had an increased number of OLGs in the secondary motor cortex. Nevertheless, it did not affect the degree of remyelination. The results were further supported by no difference in the levels of proteins involved in myelination between the groups (paper IV).

In vitro, fingolimod affected the membrane dynamics and survival of human, mature OLGs. The effects were dependent on the dose and treatment duration (Miron, Hall et al. 2008). Fingolimod exerted dose- and time-dependent effects on human OPC process extension, differentiation, and survival (Miron, Jung et al. 2008). Moreover, fingolimod enhanced remyelination in organotypic cerebellar slices after LPC-induced demyelination (Miron, Ludwin et al. 2010). In vivo, fingolimod given before LPC-induced demyelination resulted in increased OPC recruitment, oligodendrogenesis, and remyelination (Yazdi, Baharvand et al. 2015). Fingolimod given post-onset of EAE symptoms improved remyelination, OPC proliferation, and differentiation (Zhang, Zhang et al. 2015). However, most studies using rescue treatment with fingolimod did not show effect on remyelination (Hu, Lee et al. 2011, Kim, Miron et al. 2011, Slowik, Schmidt et al. 2015, Kim, Bielawski et al. 2018) or the number of OPCs and OLGs (Kim, Miron et al. 2011, Slowik, Schmidt et al. 2015).

In papers III and IV, the degree of acute axonal damage was not affected by fingolimod-treatment in the cerebellum of cuprizone mice. In the lateral corpus callosum, fingolimod-treated mice had more acute axonal damage after three weeks of remyelination. However, the proteomic results did not show an overall difference in axonal damage at any time point. Few studies have investigated the effect of fingolimod on axonal damage during remyelination. Kim et al. found that fingolimod given during cuprizone-induced demyelination exerted protective effects on myelin, OLGs, and axons. However, this was not the case when fingolimod was given from week four of demyelination. Axonal damage was not assessed during remyelination (Kim, Miron et al. 2011). In the study by Slowik et al., fingolimod did not affect remyelination; nonetheless, the study reported attenuated acute axonal damage in both acute and chronic lesions of fingolimod-treated mice (Slowik, Schmidt et al. 2015). The authors highlight that an absence of promyelinating effects of fingolimod does not necessarily exclude neuroprotective features. Although remyelination is not the cause of the neuroprotective effect, they point out that there may be other underlying mechanisms that are affected by fingolimod. We could not confirm that fingolimod mitigates acute axonal damage or axonal loss in the cerebellum or in the cerebrum. Our findings were further supported by no difference in the proteomic markers of axonal damage (paper IV).

While the treatment window and dose of 1mg/kg fingolimod daily were based on reports from earlier studies in the cuprizone and EAE model available while planning the experiment (Kataoka, Sugahara et al. 2005, Al-Izki, Pryce et al. 2011, Hu, Lee et al. 2011, Kim, Miron et al. 2011); later studies have used other doses, and we are aware of that this could have affected our result (discussed in paper IV). The dose of fingolimod and the time and duration of administration could be crucial to the remyelination process. Due to a possible dose-response effect, e.g., a lower dose of fingolimod could have shown a more beneficial effect. In a larger experiment, it would have been interesting to test lower doses of fingolimod as some studies using lower doses have found an effect on remyelination and axonal damage. Moreover, it would have been advantageous to use human-equivalent doses. This would, however, require

proper tools to convert and adjust the doses for use in mice. In addition, there are several other reasons for the discrepant findings between our study and other studies, such as the animal model, experimental settings, the different antibodies used, time points, and the brain regions investigated. Furthermore, blood samples could have been obtained and measured for fingolimod and fingolimod-p concentration to confirm adequate absorption. We could have included a control group receiving fingolimod; this would have given information about any changes caused by fingolimod in the normal mice brain proteome.

Next-generation selective S1PR modulators like siponimod have shown promising results (Kappos, Bar-Or et al. 2018). At the European Council for Treatment and Research in MS (ECTRIMS) 2019, Behrangi et al. presented that siponimod given during cuprizone-induced demyelination ameliorated demyelination, acute axonal damage, microglia and astrocyte activation (Behrangi and Kipp 2019), indicating a CNS-intrinsic mechanism of action. However, as siponimod were given during cuprizone administration, the positive effects might have been due to an initially anti-inflammatory effect and not necessarily a pro-regenerative effect. In a recent study, promising promyelinating therapeutics were tested in a *Xenopus* transgenic line. The findings indicated that siponimod was among the most efficient compounds possessing a promyelinating effect, probably induced through $S1PR_5$ modulation (Mannioui, Vauzanges et al. 2018). A non-classical dose-effect relationship has been suggested both for fingolimod (Yazdi, Ghasemi-Kasman et al. 2020) and siponimod (Martin 2019), and higher doses may reduce a pro-remyelinating effect; thus, this should be taken into account in future studies and finding the appropriate dose for an optimal pro-regenerative effect is of high importance.

In paper IV, both LFB and PLP showed a significant difference in demyelination between healthy controls and the cuprizone control group; however, at later time points, there was less remyelination than expected (compared to findings in paper I). This could be due to weak staining, which could have led to misinterpretation during the scoring of the brain sections. Another possibility is that there were too few individuals

in the group to show a difference. Electron microscopy (EM) is considered the gold standard for assessing remyelination, and LFB may not be equally suited to separate remyelination from normal myelin (Blakemore and Franklin 2008). Even though studies have demonstrated that EM correlates well with LFB staining (Lindner, Heine et al. 2008) and PLP staining detects early myelin-regeneration after cuprizone withdrawal (Wergeland, Torkildsen et al. 2012), EM could have added valuable information to the study. However, since HC- and IHC-staining methods are widely accepted, easier to perform, allows quantification of several brain regions, and is less time consuming (Skripuletz, Gudi et al. 2011), we chose this approach for the experiment.

IHC of S1PRs could have strengthened our results, although S1PRs are expressed in the CNS, IHC of S1PRs is not widely studied. We performed several unsuccessful attempts to stain for $S1PR_1$. The IHC stainings for $S1PR_1$ showed no clear staining of any particular cell type. At that time, there were few publications to give us support. However, one publication had detected $S1PR_1$ in human brain astrocytes (Nishimura, Akiyama et al. 2010). This was confirmed in another study by Brana and colleagues; in control and MS lesions, $S1PR_1$ expression was restricted to astrocytes and endothelial cells, while S1PR5 expression was limited to myelin and OLGs (Brana, Frossard et al. 2014). We conducted new tests with a monoclonal antibody, but the staining was not specific, and due to background staining, it was impossible to interpret the sections. Our and others' experiences show that, for unknown reasons, IHC staining of S1PRs seems to be difficult in rodent tissue.

6 Conclusions

I

Our results suggest that calcitriol may improve remyelination through oligodendrocyte maturation, microglia, and astrocyte activation. Functional studies may elucidate the mechanisms behind calcitriol and remyelination.

II

Our results indicate that high-dose cholecalciferol mitigates axonal loss if given before and during cuprizone exposure. Conversely, high-dose calcitriol, given after demyelination and during remyelination, did not affect axonal damage or loss.

III

Fingolimod did not affect remyelination, the number of mature OLGs, microgliosis, astrocytosis, axonal damage, or loss at any time point in the cerebellum. We conclude that fingolimod does not enhance remyelination in the cerebellum when given after cuprizone-induced demyelination.

IV

Fingolimod-treated mice showed downregulation of brain $S1PR_1$ levels at all time points compared to placebo. Fingolimod-treated mice had slightly more OLGs in the cortex after three weeks of remyelination. Nevertheless, fingolimod did not improve myelin density, axonal damage, or mitigate axonal loss compared to placebo, as measured by proteomics, histochemistry, and immunohistochemistry.

7 Future perspectives

In this thesis, we have contributed to the research field of remyelination by using a well-known animal model for de- and remyelination. Thereby, we have taken the research on remyelination a few steps forward. Our results add to the evidence that it is possible to enhance remyelination in vivo.

We have conducted two separate experiments testing two different compounds, calcitriol and fingolimod, where calcitriol seems to enhance remyelination, whereas fingolimod does not. Further, the results have been supported by proteomic analysis. Supported by our findings and earlier research, the cuprizone model, without the interference of the adaptive immune system, seems to be a suitable model to determine if a substance may affect the remyelination process. Although improvements can still be made, we have established a pipeline for testing the ability of compounds to enhance remyelination in the cuprizone model by adding HC, IHC, and proteomics analysis.

7.1 Papers I and II

Our findings of calcitriol improving remyelination in the cuprizone model are novel and suggest further research. Results should be replicated in the cuprizone model as well as in clinical trials on remyelination. Several clinical studies on remyelination have paved the way for how future remyelination studies may be conducted. Further investigation of the molecular mechanisms of how vitamin D affects remyelination could give us new opportunities in the development of regenerative medicines.

7.2 Papers III and IV

In this study, we add more knowledge to the ongoing debate on whether fingolimod may affect remyelination and neuroprotection. The study provides negative findings that complement some of the prior work of fingolimod on remyelination. The results in this thesis suggest further investigation of the effect of S1PR receptor modulators on remyelination and neuroprotection both in animal models and eventually in clinical trials. Fingolimod successors like siponimod, which is approved for the treatment of SPMS, are interesting candidates for new experiments. The cuprizone model, combined with quantitative proteomics, would be a suitable pipeline to test, for example, siponimod versus placebo. For comparison, fingolimod could be included in the same experiment. Due to the fact that there may be a dose-dependent effect, it will be appropriate to test various doses. In the present experiment, we tested 1 mg/kg fingolimod daily. In future experiments, it will be favorable to test lower doses; moreover, the doses should be equivalent to human doses.

8 References

Acheson, E. D., C. A. Bachrach and F. M. Wright (1960). "Some comments on the relationship of the distribution of multiple sclerosis to latitude, solar radiation, and other variables." Acta Psychiat. (Scand.) **35**(Suppl. 147): 132.

Acs, P., M. A. Selak, S. Komoly and B. Kalman (2013). "Distribution of oligodendrocyte loss and mitochondrial toxicity in the cuprizone-induced experimental demyelination model." J Neuroimmunol **262**(1-2): 128-131.

Aebersold, R. and M. Mann (2003). "Mass spectrometry-based proteomics." Nature **422**(6928): 198-207.

Al-Izki, S., G. Pryce, S. J. Jackson, G. Giovannoni and D. Baker (2011). "Immunosuppression with FTY720 is insufficient to prevent secondary progressive neurodegeneration in experimental autoimmune encephalomyelitis." Mult Scler **17**(8): 939-948.

Ascherio, A. and K. L. Munger (2007). "Environmental risk factors for multiple sclerosis. Part II: Noninfectious factors." Ann Neurol **61**(6): 504-513.

Ascherio, A., K. L. Munger and K. C. Simon (2010). "Vitamin D and multiple sclerosis." Lancet Neurol **9**(6): 599-612.

Bakker, D. A. and S. K. Ludwin (1987). "Blood-brain barrier permeability during Cuprizone-induced demyelination. Implications for the pathogenesis of immune-mediated demyelinating diseases." J Neurol Sci **78**(2): 125-137.

Bechler, M. E., L. Byrne and C. Ffrench-Constant (2015). "CNS Myelin Sheath Lengths Are an Intrinsic Property of Oligodendrocytes." Curr Biol **25**(18): 2411-2416.

Beer, A., V. Biberacher, P. Schmidt, R. Righart, D. Buck, A. Berthele, J. Kirschke, C. Zimmer, B. Hemmer and M. Muhlau (2016). "Tissue damage within normal appearing white matter in early multiple sclerosis: assessment by the ratio of T1- and T2-weighted MR image intensity." J Neurol **263**(8): 1495-1502.

Behrangi, N. A., D. and M. Kipp (2019). Siponimod ameliorates inflammation and axonal injury in a novel multiple sclerosis model. ECTRIMS 2019.

Belbasis, L., V. Bellou, E. Evangelou, J. P. Ioannidis and I. Tzoulaki (2015). "Environmental risk factors and multiple sclerosis: an umbrella review of systematic reviews and meta-analyses." Lancet Neurol **14**(3): 263-273.

Benardais, K., A. Kotsiari, J. Skuljec, P. N. Koutsoudaki, V. Gudi, V. Singh, F. Vulinovic, T. Skripuletz and M. Stangel (2013). "Cuprizone [bis(cyclohexylidenehydrazide)] is selectively toxic for mature oligodendrocytes." Neurotox Res **24**(2): 244-250.

Benetti, F., M. Ventura, B. Salmini, S. Ceola, D. Carbonera, S. Mammi, A. Zitolo, P. D'Angelo, E. Urso, M. Maffia, B. Salvato and E. Spisni (2010). "Cuprizone neurotoxicity, copper deficiency and neurodegeneration." Neurotoxicology **31**(5): 509-517.

Bikle, D. D. (2014). "Vitamin D metabolism, mechanism of action, and clinical applications." Chem Biol **21**(3): 319-329.

Blakemore, W. F. (1973). "Demyelination of the superior cerebellar peduncle in the mouse induced by cuprizone." J Neurol Sci **20**(1): 63-72.

Blakemore, W. F. (1973). "Remyelination of the superior cerebellar peduncle in the mouse following demyelination induced by feeding cuprizone." J Neurol Sci **20**(1): 73-83.

Blakemore, W. F. (1974). "Pattern of remyelination in the CNS." Nature **249**(457): 577-578.

Blakemore, W. F. and R. J. Franklin (2008). "Remyelination in experimental models of toxin-induced demyelination." Curr Top Microbiol Immunol **318**: 193-212.

Blakemore, W. F. and K. A. Irvine (2008). "Endogenous or exogenous oligodendrocytes for remyelination." J Neurol Sci **265**(1-2): 43-46.

Boullerne, A. I. (2016). "The history of myelin." Exp Neurol **283**(Pt B): 431-445.

Bramow, S., J. M. Frischer, H. Lassmann, N. Koch-Henriksen, C. F. Lucchinetti, P. S. Sorensen and H. Laursen (2010). "Demyelination versus remyelination in progressive multiple sclerosis." Brain **133**(10): 2983-2998.

Brana, C., M. J. Frossard, R. Pescini Gobert, N. Martinier, U. Boschert and T. J. Seabrook (2014). "Immunohistochemical detection of sphingosine-1-phosphate receptor 1 and 5 in human multiple sclerosis lesions." Neuropathol Appl Neurobiol **40**(5): 564-578.

Brown, J. W. L., A. Coles, D. Horakova, E. Havrdova, G. Izquierdo, A. Prat, M. Girard, P. Duquette, M. Trojano, A. Lugaresi, R. Bergamaschi, P. Grammond, R. Alroughani, R. Hupperts, P. McCombe, V. Van Pesch, P. Sola, D. Ferraro, F. Grand'Maison, M. Terzi, J. Lechner-Scott, S. Flechter, M. Slee, V. Shaygannejad, E. Pucci, F. Granella, V. Jokubaitis, M. Willis, C. Rice, N. Scolding, A. Wilkins, O. R. Pearson, T. Ziemssen, M. Hutchinson, K. Harding, J. Jones, C. McGuigan, H. Butzkueven, T. Kalincik, N. Robertson and M. S. S. Group (2019). "Association of Initial Disease-Modifying Therapy With Later Conversion to Secondary Progressive Multiple Sclerosis." JAMA **321**(2): 175-187.

Bruck, W., R. Pfortner, T. Pham, J. Zhang, L. Hayardeny, V. Piryatinsky, U. K. Hanisch, T. Regen, D. van Rossum, L. Brakelmann, K. Hagemeier, T. Kuhlmann, C. Stadelmann, G. R. John, N. Kramann and C. Wegner (2012). "Reduced astrocytic NF-kappaB activation by laquinimod protects from cuprizone-induced demyelination." Acta Neuropathol **124**(3): 411-424.

Bø, L., C. A. Vedeler, H. I. Nyland, B. D. Trapp and S. J. Mork (2003). "Subpial demyelination in the cerebral cortex of multiple sclerosis patients." J Neuropathol Exp Neurol **62**(7): 723-732.

Calabresi, P. A., E. W. Radue, D. Goodin, D. Jeffery, K. W. Rammohan, A. T. Reder, T. Vollmer, M. A. Agius, L. Kappos, T. Stites, B. Li, L. Cappiello, P. von Rosenstiel and F. D. Lublin (2014). "Safety and efficacy of fingolimod in patients with relapsing-remitting multiple sclerosis (FREEDOMS II): a double-blind, randomised, placebo-controlled, phase 3 trial." Lancet Neurol **13**(6): 545-556.

Camu, W., P. Lehert, C. Pierrot-Deseilligny, P. Hautecoeur, A. Besserve, A. S. Jean Deleglise, M. Payet, E. Thouvenot and J. C. Souberbielle (2019). "Cholecalciferol in relapsing-remitting MS: A randomized clinical trial (CHOLINE)." Neurol Neuroimmunol Neuroinflamm **6**(5).

Canto, E. and J. R. Oksenberg (2018). "Multiple sclerosis genetics." Mult Scler **24**(1): 75-79.

Cantorna, M. T., C. E. Hayes and H. F. DeLuca (1996). "1,25-Dihydroxyvitamin D3 reversibly blocks the progression of relapsing encephalomyelitis, a model of multiple sclerosis." Proc Natl Acad Sci U S A **93**(15): 7861-7864.

Carlton, W. W. (1966). "Response of mice to the chelating agents sodium diethyldithiocarbamate, alpha-benzoinoxime, and biscyclohexanone oxaldihydrazone." Toxicol Appl Pharmacol **8**(3): 512-521.

Carlton, W. W. (1967). "Studies on the induction of hydrocephalus and spongy degeneration by cuprizone feeding and attempts to antidote the toxicity." Life Sci **6**(1): 11-19.

Carlton, W. W. (1969). "Spongiform encephalopathy induced in rats and guinea pigs by cuprizone." Exp Mol Pathol **10**(3): 274-287.

Chabas, J. F., D. Stephan, T. Marqueste, S. Garcia, M. N. Lavaut, C. Nguyen, R. Legre, M. Khrestchatisky, P. Decherchi and F. Feron (2013). "Cholecalciferol (vitamin D(3)) improves myelination and recovery after nerve injury." PLoS One **8**(5): e65034.

Chaudhry, B. Z., J. A. Cohen and D. S. Conway (2017). "Sphingosine 1-Phosphate Receptor Modulators for the Treatment of Multiple Sclerosis." Neurotherapeutics **14**(4): 859-873.

Christakos, S., S. Li, J. De La Cruz and D. D. Bikle (2019). "New developments in our understanding of vitamin metabolism, action and treatment." Metabolism **98**: 112-120.

Chun, J. and H. P. Hartung (2010). "Mechanism of action of oral fingolimod (FTY720) in multiple sclerosis." Clin Neuropharmacol **33**(2): 91-101.

Cohen, J. A., F. Barkhof, G. Comi, H. P. Hartung, B. O. Khatri, X. Montalban, J. Pelletier, R. Capra, P. Gallo, G. Izquierdo, K. Tiel-Wilck, A. de Vera, J. Jin, T. Stites, S. Wu, S. Aradhye, L. Kappos and T. S. Group (2010). "Oral fingolimod or intramuscular interferon for relapsing multiple sclerosis." N Engl J Med **362**(5): 402-415.

Collaborators, G. B. D. M. S. (2019). "Global, regional, and national burden of multiple sclerosis 1990-2016: a systematic analysis for the Global Burden of Disease Study 2016." Lancet Neurol **18**(3): 269-285.

Compston, A. and A. Coles (2002). "Multiple sclerosis." Lancet **359**(9313): 1221-1231.

Compston, A. and A. Coles (2008). "Multiple sclerosis." Lancet **372**(9648): 1502-1517.

Compston, A., H. Lassmann and I. McDonald (2006). The story of multiple sclerosis. McAlpine's Multiple Sclerosis. A. Compston, C. Confavreux, H. Lassmann et al. Edinburgh, Churchill Livingstone**:** 3-68.

Crawford, D. K., M. Mangiardi, X. Xia, H. E. Lopez-Valdes and S. K. Tiwari-Woodruff (2009). "Functional recovery of callosal axons following demyelination: a critical window." Neuroscience **164**(4): 1407-1421.

de la Fuente, A. G., O. Errea, P. van Wijngaarden, G. A. Gonzalez, C. Kerninon, A. A. Jarjour, H. J. Lewis, C. A. Jones, B. Nait-Oumesmar, C. Zhao, J. K. Huang, C. ffrench-Constant and R. J. Franklin (2015). "Vitamin D receptor-retinoid X receptor heterodimer signaling regulates oligodendrocyte progenitor cell differentiation." J Cell Biol **211**(5): 975-985.

Deshmukh, V. A., V. Tardif, C. A. Lyssiotis, C. C. Green, B. Kerman, H. J. Kim, K. Padmanabhan, J. G. Swoboda, I. Ahmad, T. Kondo, F. H. Gage, A. N. Theofilopoulos, B. R. Lawson, P. G. Schultz and L. L. Lairson (2013). "A regenerative approach to the treatment of multiple sclerosis." Nature **502**(7471): 327-332.

Disanto, G., C. Barro, P. Benkert, Y. Naegelin, S. Schadelin, A. Giardiello, C. Zecca, K. Blennow, H. Zetterberg, D. Leppert, L. Kappos, C. Gobbi, J. Kuhle and G. Swiss Multiple Sclerosis Cohort Study (2017). "Serum Neurofilament light: A biomarker of neuronal damage in multiple sclerosis." Ann Neurol **81**(6): 857-870.

Disanto, G., U. Meier, G. Giovannoni and S. V. Ramagopalan (2011). "Vitamin D: a link between Epstein-Barr virus and multiple sclerosis development?" Expert Rev Neurother **11**(9): 1221-1224.

Dobson, R. and G. Giovannoni (2019). "Multiple sclerosis - a review." Eur J Neurol **26**(1): 27-40.

Dorr, J., P. Backer-Koduah, K. D. Wernecke, E. Becker, F. Hoffmann, J. Faiss, B. Brockmeier, O. Hoffmann, K. Anvari, J. Wuerfel, S. K. Piper, J. Bellmann-Strobl, A. U. Brandt and F. Paul (2020). "High-dose vitamin D supplementation in multiple sclerosis -

results from the randomized EVIDIMS (efficacy of vitamin D supplementation in multiple sclerosis) trial." Mult Scler J Exp Transl Clin **6**(1): 2055217320903474.

Duncan, I. D., A. B. Radcliff, M. Heidari, G. Kidd, B. K. August and L. A. Wierenga (2018). "The adult oligodendrocyte can participate in remyelination." Proc Natl Acad Sci U S A **115**(50): E11807-E11816.

Eyles, D. W., S. Smith, R. Kinobe, M. Hewison and J. J. McGrath (2005). "Distribution of the vitamin D receptor and 1 alpha-hydroxylase in human brain." J Chem Neuroanat **29**(1): 21-30.

Fard, M. K., F. van der Meer, P. Sanchez, L. Cantuti-Castelvetri, S. Mandad, S. Jakel, E. F. Fornasiero, S. Schmitt, M. Ehrlich, L. Starost, T. Kuhlmann, C. Sergiou, V. Schultz, C. Wrzos, W. Bruck, H. Urlaub, L. Dimou, C. Stadelmann and M. Simons (2017). "BCAS1 expression defines a population of early myelinating oligodendrocytes in multiple sclerosis lesions." Sci Transl Med **9**(419).

Foster, C. A., L. M. Howard, A. Schweitzer, E. Persohn, P. C. Hiestand, B. Balatoni, R. Reuschel, C. Beerli, M. Schwartz and A. Billich (2007). "Brain penetration of the oral immunomodulatory drug FTY720 and its phosphorylation in the central nervous system during experimental autoimmune encephalomyelitis: consequences for mode of action in multiple sclerosis." J Pharmacol Exp Ther **323**(2): 469-475.

Franklin, R. J. and C. Ffrench-Constant (2008). "Remyelination in the CNS: from biology to therapy." Nat Rev Neurosci **9**(11): 839-855.

Franklin, R. J. and S. A. Goldman (2015). "Glia Disease and Repair-Remyelination." Cold Spring Harb Perspect Biol **7**(7): a020594.

Franklin, R. J. and M. R. Kotter (2008). "The biology of CNS remyelination: the key to therapeutic advances." J Neurol **255 Suppl 1**: 19-25.

Franklin, R. J. M. and C. Ffrench-Constant (2017). "Regenerating CNS myelin - from mechanisms to experimental medicines." Nat Rev Neurosci **18**(12): 753-769.

Frischer, J. M., S. Bramow, A. Dal-Bianco, C. F. Lucchinetti, H. Rauschka, M. Schmidbauer, H. Laursen, P. S. Sorensen and H. Lassmann (2009). "The relation between

inflammation and neurodegeneration in multiple sclerosis brains." Brain **132**(Pt 5): 1175-1189.

Frischer, J. M., S. D. Weigand, Y. Guo, N. Kale, J. E. Parisi, I. Pirko, J. Mandrekar, S. Bramow, I. Metz, W. Bruck, H. Lassmann and C. F. Lucchinetti (2015). "Clinical and pathological insights into the dynamic nature of the white matter multiple sclerosis plaque." Ann Neurol **78**(5): 710-721.

Garcion, E., N. Wion-Barbot, C. N. Montero-Menei, F. Berger and D. Wion (2002). "New clues about vitamin D functions in the nervous system." Trends Endocrinol Metab **13**(3): 100-105.

Goldberg, J., T. Clarner, C. Beyer and M. Kipp (2015). "Anatomical Distribution of Cuprizone-Induced Lesions in C57BL6 Mice." J Mol Neurosci **57**(2): 166-175.

Goldberg, P. (2007). "Multiple sclerosis: vitamin D and calcium as environmental determinants of prevalence." International Journal of Environmental Studies **6**(1): 19-27.

Goldberg, P., M. C. Fleming and E. H. Picard (1986). "Multiple sclerosis: decreased relapse rate through dietary supplementation with calcium, magnesium and vitamin D." Med Hypotheses **21**(2): 193-200.

Goldschmidt, T., J. Antel, F. B. Konig, W. Bruck and T. Kuhlmann (2009). "Remyelination capacity of the MS brain decreases with disease chronicity." Neurology **72**(22): 1914-1921.

Gomez-Pinedo, U., J. A. Cuevas, M. S. Benito-Martin, L. Moreno-Jimenez, N. Esteban-Garcia, L. Torre-Fuentes, J. A. Matias-Guiu, V. Pytel, P. Montero and J. Matias-Guiu (2020). "Vitamin D increases remyelination by promoting oligodendrocyte lineage differentiation." Brain Behav **10**(1): e01498.

Goudarzvand, M., M. Javan, J. Mirnajafi-Zadeh, S. Mozafari and T. Tiraihi (2010). "Vitamins E and D3 attenuate demyelination and potentiate remyelination processes of hippocampal formation of rats following local injection of ethidium bromide." Cell Mol Neurobiol **30**(2): 289-299.

Groebe, A., T. Clarner, W. Baumgartner, J. Dang, C. Beyer and M. Kipp (2009). "Cuprizone treatment induces distinct demyelination, astrocytosis, and microglia cell invasion or proliferation in the mouse cerebellum." Cerebellum **8**(3): 163-174.

Groves, A., Y. Kihara and J. Chun (2013). "Fingolimod: direct CNS effects of sphingosine 1-phosphate (S1P) receptor modulation and implications in multiple sclerosis therapy." J Neurol Sci **328**(1-2): 9-18.

Grytten, N., O. Torkildsen and K. M. Myhr (2015). "Time trends in the incidence and prevalence of multiple sclerosis in Norway during eight decades." Acta Neurol Scand **132**(199): 29-36.

Gudi, V., S. Gingele, T. Skripuletz and M. Stangel (2014). "Glial response during cuprizone-induced de- and remyelination in the CNS: lessons learned." Front Cell Neurosci **8**: 73.

Gueye, Y., T. Marqueste, F. Maurel, M. Khrestchatisky, P. Decherchi and F. Feron (2015). "Cholecalciferol (vitamin D(3)) improves functional recovery when delivered during the acute phase after a spinal cord trauma." J Steroid Biochem Mol Biol **154**: 23-31.

Hall, S. M. (1972). "The effect of injections of lysophosphatidyl choline into white matter of the adult mouse spinal cord." J Cell Sci **10**(2): 535-546.

Hiremath, M. M., Y. Saito, G. W. Knapp, J. P. Ting, K. Suzuki and G. K. Matsushima (1998). "Microglial/macrophage accumulation during cuprizone-induced demyelination in C57BL/6 mice." J Neuroimmunol **92**(1-2): 38-49.

Holick, M. F. (2007). "Vitamin D deficiency." N Engl J Med **357**(3): 266-281.

Holmoy, T. (2008). "Vitamin D status modulates the immune response to Epstein Barr virus: Synergistic effect of risk factors in multiple sclerosis." Med Hypotheses **70**(1): 66-69.

Hu, Y., X. Lee, B. Ji, K. Guckian, D. Apicco, R. B. Pepinsky, R. H. Miller and S. Mi (2011). "Sphingosine 1-phosphate receptor modulator fingolimod (FTY720) does not promote remyelination in vivo." Mol Cell Neurosci **48**(1): 72-81.

Hunter, S. F., J. D. Bowen and A. T. Reder (2016). "The Direct Effects of Fingolimod in the Central Nervous System: Implications for Relapsing Multiple Sclerosis." CNS Drugs **30**(2): 135-147.

Hupperts, R., J. Smolders, R. Vieth, T. Holmoy, K. Marhardt, M. Schluep, J. Killestein, F. Barkhof, M. Beelke, L. M. E. Grimaldi and S. S. Group (2019). "Randomized trial of daily high-dose vitamin D3 in patients with RRMS receiving subcutaneous interferon beta-1a." Neurology **93**(20): e1906-e1916.

Irvine, K. A. and W. F. Blakemore (2008). "Remyelination protects axons from demyelination-associated axon degeneration." Brain **131**(Pt 6): 1464-1477.

Jackson, S. J., G. Giovannoni and D. Baker (2011). "Fingolimod modulates microglial activation to augment markers of remyelination." J Neuroinflammation **8**(76): 76.

Jagannath, V. A., G. Filippini, C. Di Pietrantonj, G. V. Asokan, E. W. Robak, L. Whamond and S. A. Robinson (2018). "Vitamin D for the management of multiple sclerosis." Cochrane Database Syst Rev **9**: CD008422.

Jaillard, C., S. Harrison, B. Stankoff, M. S. Aigrot, A. R. Calver, G. Duddy, F. S. Walsh, M. N. Pangalos, N. Arimura, K. Kaibuchi, B. Zalc and C. Lubetzki (2005). "Edg8/S1P5: an oligodendroglial receptor with dual function on process retraction and cell survival." J Neurosci **25**(6): 1459-1469.

Jurevics, H., C. Largent, J. Hostettler, D. W. Sammond, G. K. Matsushima, A. Kleindienst, A. D. Toews and P. Morell (2002). "Alterations in metabolism and gene expression in brain regions during cuprizone-induced demyelination and remyelination." J Neurochem **82**(1): 126-136.

Kamen, D. L. and V. Tangpricha (2010). "Vitamin D and molecular actions on the immune system: modulation of innate and autoimmunity." J Mol Med (Berl) **88**(5): 441-450.

Kappos, L., A. Bar-Or, B. A. C. Cree, R. J. Fox, G. Giovannoni, R. Gold, P. Vermersch, D. L. Arnold, S. Arnould, T. Scherz, C. Wolf, E. Wallstrom, F. Dahlke and E. C. Investigators (2018). "Siponimod versus placebo in secondary progressive multiple sclerosis (EXPAND): a double-blind, randomised, phase 3 study." Lancet **391**(10127): 1263-1273.

Kappos, L., E. W. Radue, P. O'Connor, C. Polman, R. Hohlfeld, P. Calabresi, K. Selmaj, C. Agoropoulou, M. Leyk, L. Zhang-Auberson, P. Burtin and F. S. Group (2010). "A placebo-controlled trial of oral fingolimod in relapsing multiple sclerosis." N Engl J Med **362**(5): 387-401.

Kataoka, H., K. Sugahara, K. Shimano, K. Teshima, M. Koyama, A. Fukunari and K. Chiba (2005). "FTY720, sphingosine 1-phosphate receptor modulator, ameliorates experimental autoimmune encephalomyelitis by inhibition of T cell infiltration." Cell Mol Immunol **2**(6): 439-448.

Kim, H. J., V. E. Miron, D. Dukala, R. L. Proia, S. K. Ludwin, M. Traka, J. P. Antel and B. Soliven (2011). "Neurobiological effects of sphingosine 1-phosphate receptor modulation in the cuprizone model." FASEB J **25**(5): 1509-1518.

Kim, S., J. Bielawski, H. Yang, Y. Kong, B. Zhou and J. Li (2018). "Functional antagonism of sphingosine-1-phosphate receptor 1 prevents cuprizone-induced demyelination." Glia **66**(3): 654-669.

Kimball, S. M., M. R. Ursell, P. O'Connor and R. Vieth (2007). "Safety of vitamin D3 in adults with multiple sclerosis." Am J Clin Nutr **86**(3): 645-651.

Kipp, M., T. Clarner, J. Dang, S. Copray and C. Beyer (2009). "The cuprizone animal model: new insights into an old story." Acta Neuropathol **118**(6): 723-736.

Kipp, M., B. van der Star, D. Y. Vogel, F. Puentes, P. van der Valk, D. Baker and S. Amor (2012). "Experimental in vivo and in vitro models of multiple sclerosis: EAE and beyond." Mult Scler Relat Disord **1**(1): 15-28.

Klaver, R., V. Popescu, P. Voorn, Y. Galis-de Graaf, P. van der Valk, H. E. de Vries, G. J. Schenk and J. J. Geurts (2015). "Neuronal and axonal loss in normal-appearing gray matter and subpial lesions in multiple sclerosis." J Neuropathol Exp Neurol **74**(5): 453-458.

Koch-Henriksen, N. and P. S. Sorensen (2010). "The changing demographic pattern of multiple sclerosis epidemiology." Lancet Neurol **9**(5): 520-532.

Kuhlmann, T., S. Ludwin, A. Prat, J. Antel, W. Bruck and H. Lassmann (2017). "An updated histological classification system for multiple sclerosis lesions." Acta Neuropathol **133**(1): 13-24.

Kuhlmann, T., L. Remington, B. Maruschak, T. Owens and W. Bruck (2007). "Nogo-A is a reliable oligodendroglial marker in adult human and mouse CNS and in demyelinated lesions." J Neuropathol Exp Neurol **66**(3): 238-246.

Kulakowska, A., M. Zendzian-Piotrowska, M. Baranowski, T. Kononczuk, W. Drozdowski, J. Gorski and R. Bucki (2010). "Intrathecal increase of sphingosine 1-phosphate at early stage multiple sclerosis." Neurosci Lett **477**(3): 149-152.

Kutzelnigg, A. and H. Lassmann (2014). Chapter 2 - Pathology of multiple sclerosis and related inflammatory demyelinating diseases. Handbook of Clinical Neurology. D. S. Goodin, Elsevier. **122:** 15-58.

Lassmann, H. (2011). "Review: the architecture of inflammatory demyelinating lesions: implications for studies on pathogenesis." Neuropathol Appl Neurobiol **37**(7): 698-710.

Lassmann, H. (2018). "Multiple Sclerosis Pathology." Cold Spring Harb Perspect Med **8**(3).

Lassmann, H. (2019). "The changing concepts in the neuropathology of acquired demyelinating central nervous system disorders." Curr Opin Neurol **32**(3): 313-319.

Lemire, J. M. and D. C. Archer (1991). "1,25-dihydroxyvitamin D3 prevents the in vivo induction of murine experimental autoimmune encephalomyelitis." J Clin Invest **87**(3): 1103-1107.

Levin, L. I., K. L. Munger, M. V. Rubertone, C. A. Peck, E. T. Lennette, D. Spiegelman and A. Ascherio (2005). "Temporal relationship between elevation of epstein-barr virus antibody titers and initial onset of neurological symptoms in multiple sclerosis." JAMA **293**(20): 2496-2500.

Lindner, M., J. Fokuhl, F. Linsmeier, C. Trebst and M. Stangel (2009). "Chronic toxic demyelination in the central nervous system leads to axonal damage despite remyelination." Neurosci Lett **453**(2): 120-125.

Lindner, M., S. Heine, K. Haastert, N. Garde, J. Fokuhl, F. Linsmeier, C. Grothe, W. Baumgartner and M. Stangel (2008). "Sequential myelin protein expression during remyelination reveals fast and efficient repair after central nervous system demyelination." Neuropathol Appl Neurobiol **34**(1): 105-114.

Lloyd, A. F. and V. E. Miron (2019). "The pro-remyelination properties of microglia in the central nervous system." Nat Rev Neurol **15**(8): 447-458.

Lublin, F., D. H. Miller, M. S. Freedman, B. A. C. Cree, J. S. Wolinsky, H. Weiner, C. Lubetzki, H. P. Hartung, X. Montalban, B. M. J. Uitdehaag, M. Merschhemke, B. Li, N. Putzki, F. C. Liu, D. A. Haring, L. Kappos and I. s. investigators (2016). "Oral fingolimod in primary progressive multiple sclerosis (INFORMS): a phase 3, randomised, double-blind, placebo-controlled trial." Lancet **387**(10023): 1075-1084.

Lublin, F. D. and S. C. Reingold (1996). "Defining the clinical course of multiple sclerosis: results of an international survey. National Multiple Sclerosis Society (USA) Advisory Committee on Clinical Trials of New Agents in Multiple Sclerosis." Neurology **46**(4): 907-911.

Lublin, F. D., S. C. Reingold, J. A. Cohen, G. R. Cutter, P. S. Sorensen, A. J. Thompson, J. S. Wolinsky, L. J. Balcer, B. Banwell, F. Barkhof, B. Bebo, Jr., P. A. Calabresi, M. Clanet, G. Comi, R. J. Fox, M. S. Freedman, A. D. Goodman, M. Inglese, L. Kappos, B. C. Kieseier, J. A. Lincoln, C. Lubetzki, A. E. Miller, X. Montalban, P. W. O'Connor, J. Petkau, C. Pozzilli, R. A. Rudick, M. P. Sormani, O. Stuve, E. Waubant and C. H. Polman (2014). "Defining the clinical course of multiple sclerosis: the 2013 revisions." Neurology **83**(3): 278-286.

Lucchinetti, C., W. Bruck, J. Parisi, B. Scheithauer, M. Rodriguez and H. Lassmann (2000). "Heterogeneity of multiple sclerosis lesions: implications for the pathogenesis of demyelination." Ann Neurol **47**(6): 707-717.

Ludwin, S. K. (1978). "Central nervous system demyelination and remyelination in the mouse: an ultrastructural study of cuprizone toxicity." Lab Invest **39**(6): 597-612.

Lycke, J. N., J. E. Karlsson, O. Andersen and L. E. Rosengren (1998). "Neurofilament protein in cerebrospinal fluid: a potential marker of activity in multiple sclerosis." J Neurol Neurosurg Psychiatry **64**(3): 402-404.

Magyari, M. and P. S. Sorensen (2019). "The changing course of multiple sclerosis: rising incidence, change in geographic distribution, disease course, and prognosis." Curr Opin Neurol **32**(3): 320-326.

Mannioui, A., Q. Vauzanges, J. B. Fini, E. Henriet, S. Sekizar, L. Azoyan, J. L. Thomas, D. D. Pasquier, C. Giovannangeli, B. Demeneix, C. Lubetzki and B. Zalc (2018). "The Xenopus

tadpole: An in vivo model to screen drugs favoring remyelination." Mult Scler **24**(11): 1421-1432.

Manrique-Hoyos, N., T. Jurgens, M. Gronborg, M. Kreutzfeldt, M. Schedensack, T. Kuhlmann, C. Schrick, W. Bruck, H. Urlaub, M. Simons and D. Merkler (2012). "Late motor decline after accomplished remyelination: impact for progressive multiple sclerosis." Ann Neurol **71**(2): 227-244.

Martin, E. U., B. Beerli, C. Stankoff, B. Lubetzki, C. Bigaud, M. Zalc, B. (2019). Siponimod (BAF312) is a potent promyelinating agent: preclinical mechanistic observations. ECTRIMS 2019.

Mashayekhi, F. and Z. Salehi (2016). "Administration of vitamin D3 induces CNPase and myelin oligodendrocyte glycoprotein expression in the cerebral cortex of the murine model of cuprizone-induced demyelination." Folia Neuropathol **54**(3): 259-264.

Matsushima, G. K. and P. Morell (2001). "The neurotoxicant, cuprizone, as a model to study demyelination and remyelination in the central nervous system." Brain Pathol **11**(1): 107-116.

Metz, I., S. D. Weigand, B. F. Popescu, J. M. Frischer, J. E. Parisi, Y. Guo, H. Lassmann, W. Bruck and C. F. Lucchinetti (2014). "Pathologic heterogeneity persists in early active multiple sclerosis lesions." Ann Neurol **75**(5): 728-738.

Miller, D. M., B. Weinstock-Guttman, F. Bethoux, J. C. Lee, G. Beck, V. Block, L. Durelli, L. LaMantia, D. Barnes, F. Sellebjerg and R. A. Rudick (2000). "A meta-analysis of methylprednisolone in recovery from multiple sclerosis exacerbations." Mult Scler **6**(4): 267-273.

Miron, V. E. and R. J. Franklin (2014). "Macrophages and CNS remyelination." J Neurochem **130**(2): 165-171.

Miron, V. E., J. A. Hall, T. E. Kennedy, B. Soliven and J. P. Antel (2008). "Cyclical and dose-dependent responses of adult human mature oligodendrocytes to fingolimod." Am J Pathol **173**(4): 1143-1152.

Miron, V. E., C. G. Jung, H. J. Kim, T. E. Kennedy, B. Soliven and J. P. Antel (2008). "FTY720 modulates human oligodendrocyte progenitor process extension and survival." Ann Neurol **63**(1): 61-71.

Miron, V. E., S. K. Ludwin, P. J. Darlington, A. A. Jarjour, B. Soliven, T. E. Kennedy and J. P. Antel (2010). "Fingolimod (FTY720) enhances remyelination following demyelination of organotypic cerebellar slices." Am J Pathol **176**(6): 2682-2694.

Mokry, L. E., S. Ross, O. S. Ahmad, V. Forgetta, G. D. Smith, D. Goltzman, A. Leong, C. M. Greenwood, G. Thanassoulis and J. B. Richards (2015). "Vitamin D and Risk of Multiple Sclerosis: A Mendelian Randomization Study." PLoS Med **12**(8): e1001866.

Molina-Gonzalez, I. and V. E. Miron (2019). "Astrocytes in myelination and remyelination." Neurosci Lett **713**: 134532.

Morell, P., C. V. Barrett, J. L. Mason, A. D. Toews, J. D. Hostettler, G. W. Knapp and G. K. Matsushima (1998). "Gene expression in brain during cuprizone-induced demyelination and remyelination." Mol Cell Neurosci **12**(4-5): 220-227.

Munger, K. L., L. I. Levin, B. W. Hollis, N. S. Howard and A. Ascherio (2006). "Serum 25-hydroxyvitamin D levels and risk of multiple sclerosis." JAMA **296**(23): 2832-2838.

Munger, K. L., L. I. Levin, E. J. O'Reilly, K. I. Falk and A. Ascherio (2011). "Anti-Epstein-Barr virus antibodies as serological markers of multiple sclerosis: a prospective study among United States military personnel." Mult Scler **17**(10): 1185-1193.

Munger, K. L., S. M. Zhang, E. O'Reilly, M. A. Hernan, M. J. Olek, W. C. Willett and A. Ascherio (2004). "Vitamin D intake and incidence of multiple sclerosis." Neurology **62**(1): 60-65.

Murray, T. J. (2009). "The history of multiple sclerosis: the changing frame of the disease over the centuries." J Neurol Sci **277 Suppl 1**: S3-8.

Nair, A., T. J. Frederick and S. D. Miller (2008). "Astrocytes in multiple sclerosis: a product of their environment." Cell Mol Life Sci **65**(17): 2702-2720.

Nave, K. A. and H. B. Werner (2014). "Myelination of the nervous system: mechanisms and functions." Annu Rev Cell Dev Biol **30**: 503-533.

Neumann, B., M. Segel, K. J. Chalut and R. J. Franklin (2019). "Remyelination and ageing: Reversing the ravages of time." Mult Scler **25**(14): 1835-1841.

Newsome, S. D., P. J. Aliotta, J. Bainbridge, S. E. Bennett, G. Cutter, K. Fenton, F. Lublin, D. Northrop, D. Rintell, B. D. Walker, M. Weigel, K. Zackowski and D. E. Jones (2017). "A Framework of Care in Multiple Sclerosis, Part 2: Symptomatic Care and Beyond." Int J MS Care **19**(1): 42-56.

Nishimura, H., T. Akiyama, I. Irei, S. Hamazaki and Y. Sadahira (2010). "Cellular localization of sphingosine-1-phosphate receptor 1 expression in the human central nervous system." J Histochem Cytochem **58**(9): 847-856.

Nystad, A. E., S. Wergeland, L. Aksnes, K. M. Myhr, L. Bo and O. Torkildsen (2014). "Effect of high-dose 1.25 dihydroxyvitamin D3 on remyelination in the cuprizone model." APMIS **122**(12): 1178-1186.

Ouda, L., R. Druga and J. Syka (2012). "Distribution of SMI-32-immunoreactive neurons in the central auditory system of the rat." Brain Struct Funct **217**(1): 19-36.

Oveland, E., A. Nystad, F. Berven, K. M. Myhr, O. Torkildsen and S. Wergeland (2018). "1,25-Dihydroxyvitamin-D3 induces brain proteomic changes in cuprizone mice during remyelination involving calcium proteins." Neurochem Int **112**: 267-277.

Pappireddi, N., L. Martin and M. Wuhr (2019). "A Review on Quantitative Multiplexed Proteomics." Chembiochem **20**(10): 1210-1224.

Partridge, M. A., S. Gopinath, S. J. Myers and J. R. Coorssen (2016). "An initial top-down proteomic analysis of the standard cuprizone mouse model of multiple sclerosis." J Chem Biol **9**(1): 9-18.

Patani, R., M. Balaratnam, A. Vora and R. Reynolds (2007). "Remyelination can be extensive in multiple sclerosis despite a long disease course." Neuropathol Appl Neurobiol **33**(3): 277-287.

Patrikios, P., C. Stadelmann, A. Kutzelnigg, H. Rauschka, M. Schmidbauer, H. Laursen, P. S. Sorensen, W. Bruck, C. Lucchinetti and H. Lassmann (2006). "Remyelination is extensive in a subset of multiple sclerosis patients." Brain **129**(Pt 12): 3165-3172.

Patsopoulos, N. A. (2018). "Genetics of Multiple Sclerosis: An Overview and New Directions." Cold Spring Harb Perspect Med **8**(7).

Pebay, A., M. Toutant, J. Premont, C. F. Calvo, L. Venance, J. Cordier, J. Glowinski and M. Tence (2001). "Sphingosine-1-phosphate induces proliferation of astrocytes: regulation by intracellular signalling cascades." Eur J Neurosci **13**(12): 2067-2076.

Peterson, J. W., L. Bo, S. Mork, A. Chang and B. D. Trapp (2001). "Transected neurites, apoptotic neurons, and reduced inflammation in cortical multiple sclerosis lesions." Ann Neurol **50**(3): 389-400.

Plemel, J. R., W. Q. Liu and V. W. Yong (2017). "Remyelination therapies: a new direction and challenge in multiple sclerosis." Nat Rev Drug Discov **16**(9): 617-634.

Popescu, B. F. and C. F. Lucchinetti (2012). "Meningeal and cortical grey matter pathology in multiple sclerosis." BMC Neurol **12**: 11.

Popescu, B. F., I. Pirko and C. F. Lucchinetti (2013). "Pathology of multiple sclerosis: where do we stand?" Continuum (Minneap Minn) **19**(4 Multiple Sclerosis): 901-921.

Praet, J., C. Guglielmetti, Z. Berneman, A. Van der Linden and P. Ponsaerts (2014). "Cellular and molecular neuropathology of the cuprizone mouse model: clinical relevance for multiple sclerosis." Neurosci Biobehav Rev **47**: 485-505.

Prineas, J. W. and F. Connell (1979). "Remyelination in multiple sclerosis." Ann Neurol **5**(1): 22-31.

Prineas, J. W., E. E. Kwon, E. S. Cho and L. R. Sharer (1984). "Continual breakdown and regeneration of myelin in progressive multiple sclerosis plaques." Ann N Y Acad Sci **436**: 11-32.

Rahmanzadeh, R., W. Bruck, A. Minagar and M. A. Sahraian (2018). "Multiple sclerosis pathogenesis: missing pieces of an old puzzle." Rev Neurosci **30**(1): 67-83.

Rasband, W. (2012). "Image J." from imagej.nih.gov/ij/.

Rhead, B., M. Baarnhielm, M. Gianfrancesco, A. Mok, X. Shao, H. Quach, L. Shen, C. Schaefer, J. Link, A. Gyllenberg, A. K. Hedstrom, T. Olsson, J. Hillert, I. Kockum, M. M.

Glymour, L. Alfredsson and L. F. Barcellos (2016). "Mendelian randomization shows a causal effect of low vitamin D on multiple sclerosis risk." Neurol Genet **2**(5): e97.

Rivers, T. M. and F. F. Schwentker (1935). "Encephalomyelitis Accompanied by Myelin Destruction Experimentally Produced in Monkeys." J Exp Med **61**(5): 689-702.

Rosjo, E., A. Lossius, N. Abdelmagid, J. C. Lindstrom, M. T. Kampman, L. Jorgensen, P. Sundstrom, T. Olsson, L. H. Steffensen, O. Torkildsen and T. Holmoy (2017). "Effect of high-dose vitamin D3 supplementation on antibody responses against Epstein-Barr virus in relapsing-remitting multiple sclerosis." Mult Scler **23**(3): 395-402.

Rossi, L., M. F. Lombardo, M. R. Ciriolo and G. Rotilio (2004). "Mitochondrial dysfunction in neurodegenerative diseases associated with copper imbalance." Neurochem Res **29**(3): 493-504.

Rosso, M. and T. Chitnis (2019). "Association Between Cigarette Smoking and Multiple Sclerosis: A Review." JAMA Neurol.

Rotstein, D. L., H. Chen, A. S. Wilton, J. C. Kwong, R. A. Marrie, P. Gozdyra, K. M. Krysko, A. Kopp, R. Copes and K. Tu (2018). "Temporal trends in multiple sclerosis prevalence and incidence in a large population." Neurology **90**(16): e1435-e1441.

Rotstein, D. L., B. C. Healy, M. T. Malik, R. L. Carruthers, A. J. Musallam, P. Kivisakk, H. L. Weiner, B. Glanz and T. Chitnis (2015). "Effect of vitamin D on MS activity by disease-modifying therapy class." Neurol Neuroimmunol Neuroinflamm **2**(6): e167.

Salzer, J., M. Nystrom, G. Hallmans, H. Stenlund, G. Wadell and P. Sundstrom (2013). "Epstein-Barr virus antibodies and vitamin D in prospective multiple sclerosis biobank samples." Mult Scler **19**(12): 1587-1591.

Sen, M. K., D. A. Mahns, J. R. Coorssen and P. J. Shortland (2019). "Behavioural phenotypes in the cuprizone model of central nervous system demyelination." Neurosci Biobehav Rev **107**: 23-46.

Shirazi, H. A., J. Rasouli, B. Ciric, A. Rostami and G. X. Zhang (2015). "1,25-Dihydroxyvitamin D3 enhances neural stem cell proliferation and oligodendrocyte differentiation." Exp Mol Pathol **98**(2): 240-245.

Shirazi, H. A., J. Rasouli, B. Ciric, D. Wei, A. Rostami and G. X. Zhang (2017). "1,25-Dihydroxyvitamin D3 suppressed experimental autoimmune encephalomyelitis through both immunomodulation and oligodendrocyte maturation." Exp Mol Pathol **102**(3): 515-521.

Simpson, S., Jr., B. Taylor, L. Blizzard, A. L. Ponsonby, F. Pittas, H. Tremlett, T. Dwyer, P. Gies and I. van der Mei (2010). "Higher 25-hydroxyvitamin D is associated with lower relapse risk in multiple sclerosis." Ann Neurol **68**(2): 193-203.

Skripuletz, T., J. H. Bussmann, V. Gudi, P. N. Koutsoudaki, R. Pul, D. Moharregh-Khiabani, M. Lindner and M. Stangel (2010). "Cerebellar cortical demyelination in the murine cuprizone model." Brain Pathol **20**(2): 301-312.

Skripuletz, T., V. Gudi, D. Hackstette and M. Stangel (2011). "De- and remyelination in the CNS white and grey matter induced by cuprizone: the old, the new, and the unexpected." Histol Histopathol **26**(12): 1585-1597.

Skripuletz, T., D. Hackstette, K. Bauer, V. Gudi, R. Pul, E. Voss, K. Berger, M. Kipp, W. Baumgartner and M. Stangel (2013). "Astrocytes regulate myelin clearance through recruitment of microglia during cuprizone-induced demyelination." Brain **136**(Pt 1): 147-167.

Skripuletz, T., M. Lindner, A. Kotsiari, N. Garde, J. Fokuhl, F. Linsmeier, C. Trebst and M. Stangel (2008). "Cortical demyelination is prominent in the murine cuprizone model and is strain-dependent." Am J Pathol **172**(4): 1053-1061.

Sloka, S., S. Zhornitsky, C. Silva, L. M. Metz and V. W. Yong (2015). "1,25-Dihydroxyvitamin D3 Protects against Immune-Mediated Killing of Neurons in Culture and in Experimental Autoimmune Encephalomyelitis." PLoS One **10**(12): e0144084.

Slowik, A., T. Schmidt, C. Beyer, S. Amor, T. Clarner and M. Kipp (2015). "The sphingosine 1-phosphate receptor agonist FTY720 is neuroprotective after cuprizone-induced CNS demyelination." Br J Pharmacol **172**(1): 80-92.

Smith, C. M., E. Cooksey and I. D. Duncan (2013). "Myelin loss does not lead to axonal degeneration in a long-lived model of chronic demyelination." J Neurosci **33**(6): 2718-2727.

Smolders, J., O. Torkildsen, W. Camu and T. Holmoy (2019). "An Update on Vitamin D and Disease Activity in Multiple Sclerosis." CNS Drugs **33**(12): 1187-1199.

Stein, M. S., Y. Liu, O. M. Gray, J. E. Baker, S. C. Kolbe, M. R. Ditchfield, G. F. Egan, P. J. Mitchell, L. C. Harrison, H. Butzkueven and T. J. Kilpatrick (2011). "A randomized trial of high-dose vitamin D2 in relapsing-remitting multiple sclerosis." Neurology **77**(17): 1611-1618.

Stidworthy, M. F., S. Genoud, U. Suter, N. Mantei and R. J. Franklin (2003). "Quantifying the early stages of remyelination following cuprizone-induced demyelination." Brain Pathol **13**(3): 329-339.

Strijbis, E. M. M., E. J. Kooi, P. van der Valk and J. J. G. Geurts (2017). "Cortical Remyelination Is Heterogeneous in Multiple Sclerosis." J Neuropathol Exp Neurol **76**(5): 390-401.

Subei, A. M. and J. A. Cohen (2015). "Sphingosine 1-phosphate receptor modulators in multiple sclerosis." CNS Drugs **29**(7): 565-575.

Suzuki, K. and Y. Kikkawa (1969). "Status spongiosus of CNS and hepatic changes induced by cuprizone (biscyclohexanone oxalyldihydrazone)." Am J Pathol **54**(2): 307-325.

Taylor, L. C., W. Gilmore, J. P. Ting and G. K. Matsushima (2010). "Cuprizone induces similar demyelination in male and female C57BL/6 mice and results in disruption of the estrous cycle." J Neurosci Res **88**(2): 391-402.

Tedeholm, H., J. Lycke, B. Skoog, V. Lisovskaja, J. Hillert, C. Dahle, J. Fagius, S. Fredrikson, A. M. Landtblom, C. Malmestrom, C. Martin, F. Piehl, B. Runmarker, L. Stawiarz, M. Vrethem, O. Nerman and O. Andersen (2013). "Time to secondary progression in patients with multiple sclerosis who were treated with first generation immunomodulating drugs." Mult Scler **19**(6): 765-774.

Thacker, E. L., F. Mirzaei and A. Ascherio (2006). "Infectious mononucleosis and risk for multiple sclerosis: a meta-analysis." Ann Neurol **59**(3): 499-503.

Theiler, M. (1934). "Spontaneous Encephalomyelitis of Mice--a New Virus Disease." Science **80**(2066): 122.

Thompson, A. J., B. L. Banwell, F. Barkhof, W. M. Carroll, T. Coetzee, G. Comi, J. Correale, F. Fazekas, M. Filippi, M. S. Freedman, K. Fujihara, S. L. Galetta, H. P. Hartung, L. Kappos, F. D. Lublin, R. A. Marrie, A. E. Miller, D. H. Miller, X. Montalban, E. M. Mowry, P. S. Sorensen, M. Tintore, A. L. Traboulsee, M. Trojano, B. M. J. Uitdehaag, S. Vukusic, E. Waubant, B. G. Weinshenker, S. C. Reingold and J. A. Cohen (2018). "Diagnosis of multiple sclerosis: 2017 revisions of the McDonald criteria." Lancet Neurol **17**(2): 162-173.

Torkildsen, O., L. A. Brunborg, K. M. Myhr and L. Bo (2008). "The cuprizone model for demyelination." Acta Neurol Scand Suppl **188**: 72-76.

Torkildsen, O., L. A. Brunborg, F. Thorsen, S. J. Mork, M. Stangel, K. M. Myhr and L. Bo (2009). "Effects of dietary intervention on MRI activity, de- and remyelination in the cuprizone model for demyelination." Exp Neurol **215**(1): 160-166.

Trapp, B. D., A. Nishiyama, D. Cheng and W. Macklin (1997). "Differentiation and death of premyelinating oligodendrocytes in developing rodent brain." J Cell Biol **137**(2): 459-468.

Trapp, B. D., J. Peterson, R. M. Ransohoff, R. Rudick, S. Mork and L. Bo (1998). "Axonal transection in the lesions of multiple sclerosis." N Engl J Med **338**(5): 278-285.

Vega-Riquer, J. M., G. Mendez-Victoriano, R. A. Morales-Luckie and O. Gonzalez-Perez (2019). "Five Decades of Cuprizone, an Updated Model to Replicate Demyelinating Diseases." Curr Neuropharmacol **17**(2): 129-141.

Venturini, G. (1973). "Enzymic activities and sodium, potassium and copper concentrations in mouse brain and liver after cuprizone treatment in vivo." J Neurochem **21**(5): 1147-1151.

Wang, T. J., F. Zhang, J. B. Richards, B. Kestenbaum, J. B. van Meurs, D. Berry, D. P. Kiel, E. A. Streeten, C. Ohlsson, D. L. Koller, L. Peltonen, J. D. Cooper, P. F. O'Reilly, D. K. Houston, N. L. Glazer, L. Vandenput, M. Peacock, J. Shi, F. Rivadeneira, M. I. McCarthy, P. Anneli, I. H. de Boer, M. Mangino, B. Kato, D. J. Smyth, S. L. Booth, P. F. Jacques, G. L. Burke, M. Goodarzi, C. L. Cheung, M. Wolf, K. Rice, D. Goltzman, N. Hidiroglou, M. Ladouceur, N. J. Wareham, L. J. Hocking, D. Hart, N. K. Arden, C. Cooper, S. Malik, W. D. Fraser, A. L. Hartikainen, G. Zhai, H. M. Macdonald, N. G. Forouhi, R. J. Loos, D. M. Reid, A. Hakim, E. Dennison, Y. Liu, C. Power, H. E. Stevens, L. Jaana, R. S. Vasan, N. Soranzo, J. Bojunga, B. M. Psaty, M. Lorentzon, T. Foroud, T. B. Harris, A. Hofman, J. O. Jansson, J.

A. Cauley, A. G. Uitterlinden, Q. Gibson, M. R. Jarvelin, D. Karasik, D. S. Siscovick, M. J. Econs, S. B. Kritchevsky, J. C. Florez, J. A. Todd, J. Dupuis, E. Hypponen and T. D. Spector (2010). "Common genetic determinants of vitamin D insufficiency: a genome-wide association study." Lancet **376**(9736): 180-188.

Weinshenker, B. G., B. Bass, G. P. Rice, J. Noseworthy, W. Carriere, J. Baskerville and G. C. Ebers (1989). "The natural history of multiple sclerosis: a geographically based study. I. Clinical course and disability." Brain **112 (Pt 1)**: 133-146.

Wergeland, S., K. M. Myhr, K. I. Loken-Amsrud, A. G. Beiske, K. S. Bjerve, H. Hovdal, R. Midgard, S. S. Kvistad, T. Holmoy, T. Riise and O. Torkildsen (2016). "Vitamin D, HLA-DRB1 and Epstein-Barr virus antibody levels in a prospective cohort of multiple sclerosis patients." Eur J Neurol **23**(6): 1064-1070.

Wergeland, S., O. Torkildsen, K. M. Myhr, L. Aksnes, S. J. Mork and L. Bo (2011). "Dietary vitamin D3 supplements reduce demyelination in the cuprizone model." PLoS One **6**(10): e26262.

Wergeland, S., O. Torkildsen, K. M. Myhr, S. J. Mork and L. Bo (2012). "The cuprizone model: regional heterogeneity of pathology." APMIS **120**(8): 648-657.

Werner, S. R., J. K. Saha, C. L. Broderick, E. Y. Zhen, R. E. Higgs, K. L. Duffin and R. C. Smith (2010). "Proteomic analysis of demyelinated and remyelinating brain tissue following dietary cuprizone administration." J Mol Neurosci **42**(2): 210-225.

Wesnes, K., T. Riise, I. Casetta, J. Drulovic, E. Granieri, T. Holmoy, M. T. Kampman, A. M. Landtblom, K. Lauer, A. Lossius, S. Magalhaes, T. Pekmezovic, K. Bjornevik, C. Wolfson, M. Pugliatti and K. M. Myhr (2015). "Body size and the risk of multiple sclerosis in Norway and Italy: the EnvIMS study." Mult Scler **21**(4): 388-395.

Wheeler, D., V. V. Bandaru, P. A. Calabresi, A. Nath and N. J. Haughey (2008). "A defect of sphingolipid metabolism modifies the properties of normal appearing white matter in multiple sclerosis." Brain **131**(Pt 11): 3092-3102.

Yajima, K. and K. Suzuki (1979). "Demyelination and remyelination in the rat central nervous system following ethidium bromide injection." Lab Invest **41**(5): 385-392.

Yamafuji, K. and Y. Matsuki (1989). "Kinin formation from T-kininogen by spleen acid kininogenases." Adv Exp Med Biol **247B**(1): 97-102.

Yazdi, A., H. Baharvand and M. Javan (2015). "Enhanced remyelination following lysolecithin-induced demyelination in mice under treatment with fingolimod (FTY720)." Neuroscience **311**: 34-44.

Yazdi, A., M. Ghasemi-Kasman and M. Javan (2020). "Possible regenerative effects of fingolimod (FTY720) in multiple sclerosis disease: An overview on remyelination process." J Neurosci Res **98**(3): 524-536.

Yenamandra, S. P., U. Hellman, B. Kempkes, S. D. Darekar, S. Petermann, T. Sculley, G. Klein and E. Kashuba (2010). "Epstein-Barr virus encoded EBNA-3 binds to vitamin D receptor and blocks activation of its target genes." Cell Mol Life Sci **67**(24): 4249-4256.

Yeung, M. S. Y., M. Djelloul, E. Steiner, S. Bernard, M. Salehpour, G. Possnert, L. Brundin and J. Frisen (2019). "Dynamics of oligodendrocyte generation in multiple sclerosis." Nature **566**(7745): 538-542.

Zendedel, A., C. Beyer and M. Kipp (2013). "Cuprizone-induced demyelination as a tool to study remyelination and axonal protection." J Mol Neurosci **51**(2): 567-572.

Zhang, J., Z. G. Zhang, Y. Li, X. Ding, X. Shang, M. Lu, S. B. Elias and M. Chopp (2015). "Fingolimod treatment promotes proliferation and differentiation of oligodendrocyte progenitor cells in mice with experimental autoimmune encephalomyelitis." Neurobiol Dis **76**: 57-66.

Aarseth, J. H., T. Smedal, A. B. Skår and S. Wergeland. (2018). "Norwegian Multiple Sclerosis register and biobank annual report 2018." from https://www.kvalitetsregistre.no/sites/default/files/21_arsrapport_2018_norsk_ms_register_biobank.pdf.

9 Appendix

DYREAVDELINGEN
UNIVERSITETET i BERGEN
55973788/94

Dyreavdelingen - VIVARIUM
UNIVERSITETET I BERGEN
Haukeland sykehus
5021 BERGEN

Tel.veterinær: 55973794 Fax: 55973797
E-mail: post@viv.uib.no

Til Øivind Torkildsen
Haukelnad sykeshus

5021 Bergen

Tillatelse til å drive forsøk med dyr.

Jeg har mottatt, behandlet og godkjent søknaden din om å drive forsøk med dyr ved Vivarium, Universitetet i Bergen.Tillatelsen er gitt i henhold til Dyrevelferds-loven §13 og Forskrift om forsøk med dyr §8. Kopi av søknaden er sendt FDU i FOTS
Merk: Følgende betingelser gjelder for dette prosjektet

Godkjent dato:	04-mai-12		
Gyldig til:	31-des-13	Antall og art	Mus
Prosjektnummer	**20124421**		48

Før prosjektet kan starte skal det avholdes prosjektoppstartsmøte. Vennligst ta med utfylt " Sjekkliste til prosjektoppstartmøter"

For prosjektoppstartsmøte ber vi deg ta kontakt med helen.otteraa@ffhs.uib.no (mus) eller ashild.asebo@ffhs.uib.no (rotte, gris) cc: Gry.Bernes@ffhs.uib.no for avtale.

Oppstart forutsetter ledig kapasitet på dyrestallen. I perioder med begrenset kapasitet vil UiB prioritere prosjekter med institusjonell tilknytning til UiB. Videre vil prosjekter prioriteres i følgende rekkefølge: 1: EU prosjekter, 2: NFR prosjekter 3) prosjekter med andre finansieringskilder

Prosjektnummeret skal alltid oppgis ved bestilling av dyr. Dette gjelder og for dyr som er avlet ved institusjonen. For bestilling av dyr, rekvirering legemidler, adgangskort og generelle retningslinjer for bruk av dyreavdelingen se http://www.uib.no/dyreavdelingen/forskning/brukerinformasjon. Alle som er involvert i forsøk med dyr må ha godkjent kurs i forsøksdyrlære.

Alle avvik og endringer fra den godkjent protokoll må alltid meddelses skriftlig og klareres med undertegnede på forhånd. Dette gjelder også ved behov for flere dyr eller forlengelse i tid.

Bergen 04-mai-12

Vennlig hilsen

AURORA M. BRØNSTAD

Aurora Brønstad
Veterinær, ansvarshavende

DYREAVDELINGEN
UNIVERSITETET i BERGEN
55973788/94

Dyreavdelingen - VIVARIUM
UNIVERSITETET I BERGEN
Haukeland sykehus
5021 BERGEN

Tel.veterinær: 55973794 Fax: 55973797
E-mail: post@viv.uib.no

Til Øivind Torkildsen
Haukelnad sykeshus

5021 Bergen

Tillatelse til å drive forsøk med dyr.

Jeg har mottatt, behandlet og godkjent søknaden din om å drive forsøk med dyr ved Vivarium, Universitetet i Bergen.Tillatelsen er gitt i henhold til Dyrevelferds-loven §13 og Forskrift om forsøk med dyr §8. Kopi av søknaden er sendt FDU i FOTS
Merk: Følgende betingelser gjelder for dette prosjektet

Godkjent dato:	11-sep-13		
Gyldig til:	31-des-13	Antall og art	Mus
Prosjektnummer	**20135682**		48

Før prosjektet kan starte skal det avholdes prosjektoppstartsmøte.

For prosjektoppstartsmøte ber vi deg ta kontakt med gry.bernes@k1.uib.no (mus) eller ashild.asebo@k1.uib.no (rotte, gris) cc: gry.bernes@k1.uib.no for avtale og tilsending av dokumentasjon som må fylles ut før møtet.
Oppstart forutsetter ledig kapasitet på dyrestallen. I perioder med begrenset kapasitet vil UiB prioritere prosjekter med institusjonell tilknytning til UiB. Videre vil prosjekter prioriteres i følgende rekkefølge: 1: EU prosjekter, 2: NFR prosjekter 3) prosjekter med andre finansieringskilder. "Vi gjør oppmerksom på at Dyreavdelingen nå er inne i en periode med høy aktivitet og kapasiten er begrenset. En må derfor forvente ventelister for oppstart av forsøk. Det er viktig at det avholdes et prosjektoppstartsmøte for å avklare hvor stort forsøkets ressursbehov er før en kan si noe om oppstartstidspunkt."

Prosjektnummeret skal alltid oppgis ved bestilling av dyr. Dette gjelder og for dyr som er avlet ved institusjonen. For bestilling av dyr, rekvirering legemidler, adgangskort og generelle retningslinjer for bruk av dyreavdelingen se http://www.uib.no/dyreavdelingen/forskning/brukerinformasjon. Alle som er involvert i forsøk med dyr, må ha godkjent kurs i forsøksdyrlære.

Alle avvik og endringer fra den godkjent protokoll må alltid meddelses skriftlig og klareres med undertegnede på forhånd. Dette gjelder også ved behov for flere dyr eller forlengelse i tid.

Bergen: 11-sep-13

Vennlig hilsen

AURORA M. BRØNSTAD

Aurora Brønstad
Veterinær, ansvarshavende

10 Errata

Paper I:

Histopathology. Sentence six: Paraformaldehyde = formaldehyde.

Paper II:

Section 2.2.2. *Remyelination experiment.* Typos, sentence five: 2 microgram corrected to 0.2 microgram calcitriol.

Supplementary table 2. *3) 2µg calcitriol cuprizone and 4) 2µg placebo cuprizone.*

Table legend corrected to 3) 0.2µg calcitriol cuprizone and 4) placebo cuprizone.

Section 2.3. *Histopathology.* Sentence five: Paraformaldehyde = formaldehyde.

Paper III

Section 2.2. *Study design, cuprizone administration and fingolimod treatment.* Last sentence: Paraformaldehyde = formaldehyde.

11 Paper I-IV

I

APMIS
ACTA PATHOLOGICA, MICROBIOLOGICA
ET IMMUNOLOGICA SCANDINAVICA

APMIS 122: 1178–1186

DOI 10.1111/apm.12281

Effect of high-dose 1.25 dihydroxyvitamin D_3 on remyelination in the cuprizone model

AGNES E. NYSTAD,[1,2] STIG WERGELAND,[1,2] LAGE AKSNES,[3,4] KJELL-MORTEN MYHR,[1,2] LARS BØ[1,2] and ØIVIND TORKILDSEN[1,2]

[1]Department of Neurology, Norwegian Multiple Sclerosis Competence Centre, Haukeland University Hospital, Bergen; [2]Kristian Gerhard Jebsen MS Research Centre, Department of Clinical Medicine, University of Bergen, Bergen; [3]Department of Clinical Science, University of Bergen, Bergen; and [4]Department of Pediatrics, Haukeland University Hospital, Bergen, Norway

Nystad AE, Wergeland S, Aksnes L, Myhr KM, Bø L, Torkildsen Ø. Effect of high-dose 1.25 dihydroxyvitamin D_3 on remyelination in the cuprizone model. APMIS 2014; 122: 1178–1186.

Vitamin D supplementation is increasingly recommended to patients with multiple sclerosis (MS). To study the effect of high-dose vitamin D on remyelination, female C57Bl/6 mice were demyelinated with dietary 0.2% cuprizone for 7 weeks. The mice received intraperitoneal injections of 1.25-dihydroxyvitamin D_3 (calcitriol) or placebo (vehicle) injections twice a week, from week 6, throughout week 9. Mice that received calcitriol had initially increased demyelination ($p = 0.021$), astrocytosis ($p = 0.043$), and microglia activation. However, levels of astrocytosis and microglia activation dropped below those of the placebo group during the remyelination phase. There was a significant increase in myelination in the calcitriol group throughout the remyelination phase ($p = 0.041$), while the remyelination in the placebo group was not significant ($p = 0.317$). After 3 weeks of remyelination, the calcitriol group had more myelin than the placebo group ($p = 0.001$). The calcitriol group had a higher density of NOGO-A positive cells throughout the remyelination phase, and the number of NOGO-A positive cells was significantly higher in the calcitriol group at one week of remyelination ($p = 0.019$). There were no significant differences in extent of T-lymphocyte infiltration. High-dose calcitriol seems to be safe regarding remyelination. Our results indicate that this treatment could actually promote the repair process, possibly through a stimulating effect on oligodendrocyte maturation and astrocyte activation. The potential of calcitriol to stimulate the remyelination process should be investigated further in functional studies.

Key words: Multiple sclerosis; cuprizone; calcitriol; vitamin D; remyelination.

Correspondence: Øivind Torkildsen, Department of Neurology, Haukeland University Hospital, N-5021 Bergen, Norway. e-mail: oivind.torkildsen@gmail.com

Multiple Sclerosis (MS) is an immune-mediated disease of the central nervous system (CNS). The cause of the disease is unknown, but it seems to evolve as a result of a complex interplay between genetic and environmental risk factors (1, 2). Vitamin D deficiency is emerging as one of the most promising environmental risk factor candidates (3). Studies have repeatedly found associations between vitamin D levels and disease activity (4, 5), and several authors have suggested that supplementation of vitamin D should be recommended to MS patients (6–8). It has, however, been found that high-dose vitamin D supplements does not have any therapeutic advantages compared with low-dose supplements, and that high-dose vitamin D treatment might even have negative effects (9, 10).

The cuprizone model is a toxic non-T cell-dependent model of CNS demyelination in mice. The copper chelator cuprizone mainly targets mature oligodendrocytes. Oligodendrocyte precursor cells and other glial cells are not or only marginally affected (11). Cuprizone induces oligodendrocyte death with subsequent myelin disruption, and microglia- and macrophage activation. Astroglial activation occurs in the early stages of demyelination (12, 13). The model demonstrates acute demyelination with subsequent spontaneous remyelination within days after termination of cuprizone exposure (14–16).

We have previously used the cuprizone model to study how vitamin D_3 affects demyelination (17).

Received 25 October 2013. Accepted 10 March 2014

Our earlier findings suggested that although vitamin D seemed to have a protective effect on demyelination, the mice exposed to high-dose vitamin D had less initial remyelination. As high-dose vitamin D supplementation is increasingly recommended to MS patients, it is of crucial importance to determine any possibly adverse effect of this treatment (18). The present study aimed to determine the safety of high doses of the active vitamin D metabolite calcitriol on remyelination in the cuprizone model.

MATERIALS AND METHODS

Animals

Forty-eight five-week-old female C57Bl/6 mice (Tacomic, Tornbjerg, Denmark) were used for this experiment. Mean weight was 19.6 g ± SD 1.5. The mice were acclimatized for 12 days prior to the experiment. They were housed six together in GreenLine type II cages with open top, (Scanbur, Karlslunde, Denmark), in standard laboratory conditions. Cage maintenance was performed once a week and the animals were handled by the same individuals throughout the experimental period. Food and tap water was available *ad libitum* throughout the acclimatization and experimental period. The experiment was carried out in accordance with the European Laboratory Animal Science Associations recommendations, and the protocol was approved by the Norwegian Animal Research Authority (permit # 2012–4421).

Study design, cuprizone administration, and high-dose calcitriol injections

After acclimatization, 36 mice were randomized to injections of either 0.2 μg calcitriol (n = 18) or placebo (vehicle) (n = 18). In addition, 6 mice served as healthy controls (no cuprizone or ip. injections) and six mice served as cuprizone controls (cuprizone exposure for 6 weeks without any injections). To induce demyelination, 0.2% cuprizone (bis-cyclohexanone-oxaldihydrazone, Sigma-Aldrich, St. Louis, MO, USA) was added to milled mouse chow. Cuprizone exposure was discontinued after seven weeks. The mice received ip. injections of calcitriol or placebo (vehicle) twice weekly, from week 6 throughout week 9 (Table 1).

Histopathology

The animals were anesthetized with midazolam (Dormicum 'Roche') in combination with fentanyl/fluanisone (Hypnorm 'VetaPharma') and sacrificed at four different time points (start of week 6, 7, 8, and 10). Sacrifice and serum collection were conducted by cardiac puncture. Brains were removed and post-fixed in 4% paraformaldehyde (PFA) for at least 7 days before paraffin embedding. Analyses were performed on 7 ± 1 μm sections from the bregma ± 1 mm (19). Sections were stained with Luxol Fast Blue (LFB) and hematoxylin. For immunohistochemistry, the sections were dewaxed, rehydrated, and microwaved for antigen retrieval. Demasking was performed by boiling (microwaving) sections in either citrate or TRIS-EDTA buffer at 900 W for 10 min and 450 W for 15 min. Sections were then immunostained for oligodendrocytes Neurite Outgrowth Inhibitor Protein A (NOGO-A), astrocytes Glial Fibrillary Acidic Protein (GFAP), microglia (Mac3), and T-lymphocytes (CD3). Buffer, dilution, incubation time and temperature for the primary antibodies are specified in (Table S1). Sections were blocked with peroxidase blocking solution (DAKO, Glostrup, Denmark) and visualized with EnVision 3.3. – diaminobenzidine (1:50); 2 × 3 min at room temperature (RT); (DAKO), then counterstained with hematoxylin. For LFB, GFAP, NOGO-A, and Mac-3 normal brain tissue from healthy controls served as positive controls. For CD-3, sections

Table 1. Overview of experimental groups, cuprizone exposure, intra-peritoneal (Ip.) injections and euthanasia through the experimental period

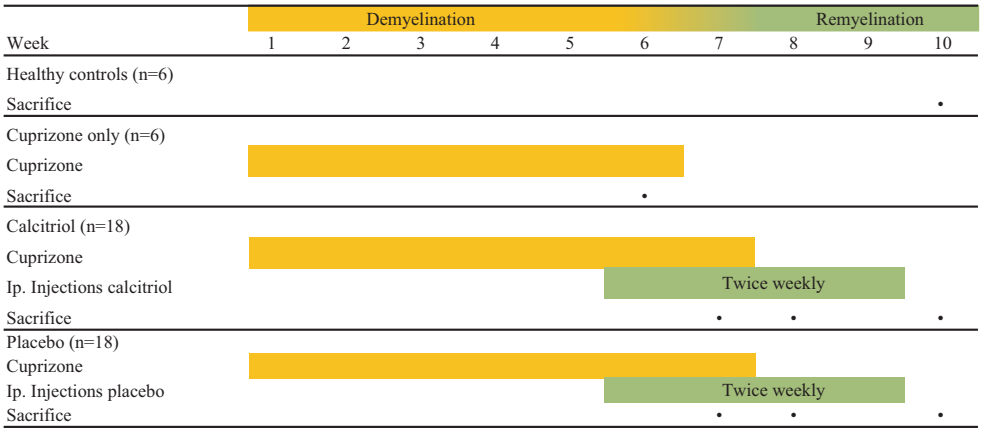

from tonsil tissue served as positive controls. Omission of the primary antibodies served as negative controls.

Characterization of brain tissue

Sections were scored in a blinded manner by two observers, using light microscopy (Zeiss, Axio Imager A2, 40x, Oberkochen, Germany) . For quantification of myelin loss, we used a semi-quantitative scoring system: no (0), minimal (0. 5), <33% (1), 33–66% (2) and >66% (3) demyelination. As astrocyte reactivity is characterized both by an increase in the number of astrocytes, hypertrophy, hyperplasia and an increased GFAP immunoreactivity in astrocyte processes(20), astrocytosis was evaluated semi-quantitatively: no (0), minimal (1), moderate (2) or severe (3) reactive astrocytosis (21). The density of mature oligodendrocytes (NOGO-A immunopositive cells) was determined; microglia Mac-3 and T-cells (CD3) were counted in an area of 0.0625 mm^2 at 40x, using an ocular morphometric grid. All sections were scored in the midline area of corpus callosum, from the bregma ± 1 mm.

Analyses of vitamin D_3 metabolites and calcium

Serum was collected at two time points during the experimental period; from the healthy control group at the start point of the study, and from all mice when sacrificed. The 25(OH)-vitamin D_3 and 24.25$(OH)_2$ vitamin D_3 analysis were performed in accordance with a modified version of a method previously described (22). 25 µl serum samples were spiked with 26.27 dexadeuterium-25-OH-Vitamin D_3 (Syntetica AS, Oslo, Norway) as internal standard and extracted with methanol and n-hexane. The n-hexane phase was collected, evaporated to dryness and injected into a reverse-phase high-performance liquid chromatography system. Elution of the vitamin D-metabolites was performed with methanol/water (88:12, v/v, with 0.1 formic acid) and the eluate was monitored by a LC/MSMS – detector (G6410A, Agilent Technology Inc., Santa Clara, CA, USA) equipped with an ESI ion-source. 25(OH)-vitamin D_3 was monitored at 401.5 m/z and 383.5 m/z as precursor- and production- ions, respectively (401.5/383.5 m/z). 24.25(OH)2-vitamin D_3 was monitored at 417.5/381.5 m/z and the internal standard at 407.5/389.5 m/z. mSerum calcium was analyzed using Calcium AS FS (DiaSys Diagnostic System GmbH, Holtzheim, Germany) (23).

Weight and RotaRod test

Weight measurements were conducted twice weekly (Figure S1). The mice's motor performance was tested twice a week throughout the experimental period using the LE8200 Accelerating RotaRod for five mice, Panlab, (Figure S2), which previously has been reported to assess motor coordination and balance in cuprizone-exposed mice (24). The test was administrated within the 12-h light cycle in an isolated restricted-access room. To test the performance, the mice were placed on the rotating rod, which accelerated to a maximum speed over 200 s. Time to the mice fell off the rotating cylinder was registered, and averaged over three consecutive experiments at each time point. All groups were tested; up to three mice were evaluated at the same time.

Statistical methods

One-way analysis of variance (ANOVA) was used to analyze parametric data, followed by Fisher's least significant difference (LSD) for post hoc analysis, where applicable. The Mann–Whitney test was used to analyzing non-parametric data. For non-parametric-related data, Wilcoxon's signed rank test was performed. All calculations were carried out using SPSS 20.0 (IBM; 2011). Differences were considered significant at $p < 0.05$.

RESULTS

Effects on de- and remyelination

Significant loss of myelin, as evaluated by LFB staining, was evident in all cuprizone-exposed mice after 6 and 7 weeks, compared with the healthy controls ($p < 0.005$). After 7 weeks of cuprizone exposure, mice in the calcitriol group that had been receiving calcitriol for only one week had significantly lower LFB-score than the placebo group ($p = 0.021$, Fig. 1A–B). After one week of remyelination (week 8), the difference was no longer significant ($p = 0.593$) and after three weeks of remyelination, the calcitriol group had more myelin than the placebo group ($p = 0.001$). There was a gain of myelin in the calcitriol group during the three weeks after ending cuprizone exposure ($p = 0.041$). Although remyelination also occurred in the placebo group in this period, the increase of myelin was not significant ($p = 0.317$).

Effects on NOGO-A-positive oligodendrocytes

An extensive loss of NOGO-A-positive cells was observed in all cuprizone-treated groups compared with healthy controls ($p < 0.005$). At all measured points, the number of mature oligodendrocytes was higher in the calcitriol than in the placebo group (Fig. 2A–B). There was a non-significant trend of a higher number of NOGO-A-positive oligodendrocytes in the calcitriol group after discontinuation of the cuprizone diet ($p = 0.055$, Table S2). There was a significant difference between the groups with regard to the number of mature oligodendrocytes after one week of remyelination ($p = 0.019$). After three weeks of remyelination, there were no significant differences between the groups.

Astrocyte activation

At the end of cuprizone exposure, increased astrocyte activity, as measured by GFAP-positivity, was observed in all cuprizone-exposed groups compared with the controls ($p < 0.0001$). After seven weeks of cuprizone exposure, mice that received calcitriol had an increased astrocytosis compared with the placebo group ($p = 0.043$, Fig. 3). One week after

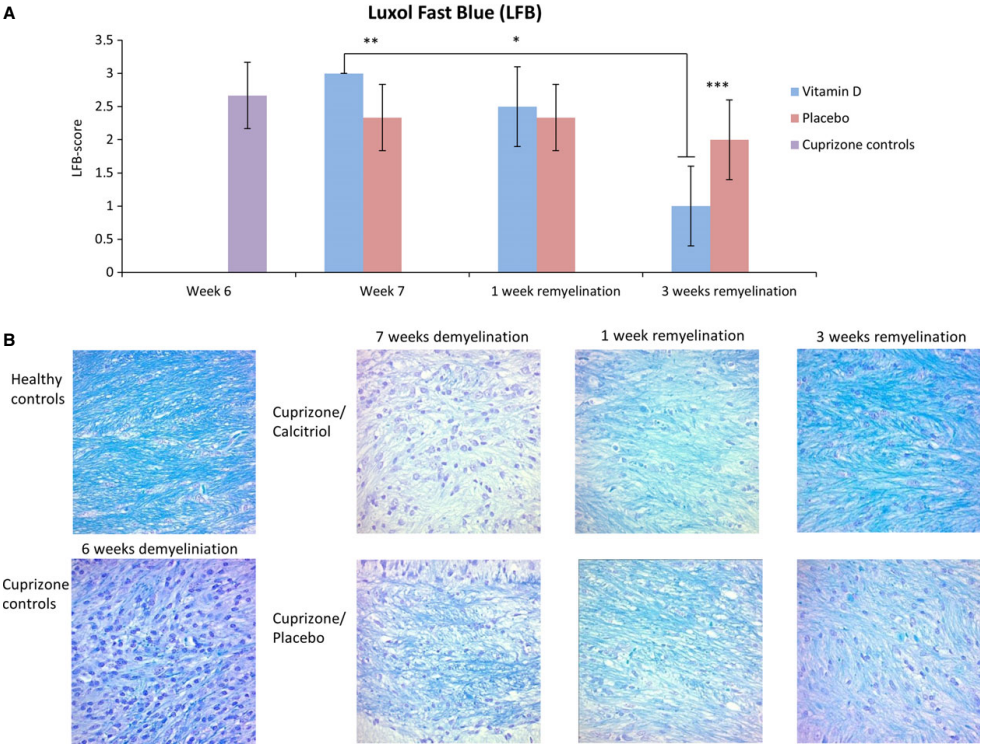

Fig. 1. Myelin status in the midline of corpus callosum after 7 weeks of demyelination, 1 and 3 weeks of remyelination. (A) There was significant remyelination in the calcitriol group from week 7 until three weeks of remyelination (*; $p = 0.041$). Mice given calcitriol had less myelin remaining at week 7, than the placebo group (**; $p = 0.021$). The remaining myelin in the placebo group had, however, a more unstructured pattern typical for damaged myelin. After three weeks of remyelination, the calcitriol group had more myelin than the mice that received placebo (***; $p = 0.001$). Scale: no (0), minimal (0. 5), <33% (1), 33–66% (2) and >66% demyelination. (B) Sections stained with Luxol Fast Blue and hematoxylin. Error bars: 1 SEM. All images at 40x.

ending cuprizone exposure, there was a non-significant increase in astrocytosis in the placebo group ($p = 0.109$), while the astrocyte activity decreased in the calcitriol group.

Macrophage/microglia activation and T-lymphocyte infiltration during remyelination

After 6 weeks of cuprizone exposure, increased microglia activation was observed in cuprizone-exposed mice, compared with the controls ($p < 0.0001$). After ending cuprizone exposure, microglia activation was more prominent in the calcitriol group, compared with the placebo group, and then fell gradually (Fig. 4). Placebo- treated mice had an equally extensive, but delayed microglia activation compared with the calcitriol-treated mice. After one week of remyelination, the density of Mac-3 cells in the placebo group was higher than in the calcitriol group ($p = 0.019$, Table S2). One to five CD-3 positive lymphocytes were observed per area counted in the cuprizone-exposed mice, none in the controls (Table S2). There was no significant difference between the calcitriol or placebo group.

Serum levels

Serum calcium (s-ca) levels were normal in both calcitriol and placebo-treated mice, and there was no significant difference between the groups at any time points. Thus, the mice who received high-dose calcitriol had normal s-ca levels at all time points (Table S3). As calcitriol has a short half-life and there is a reciprocal relationship between

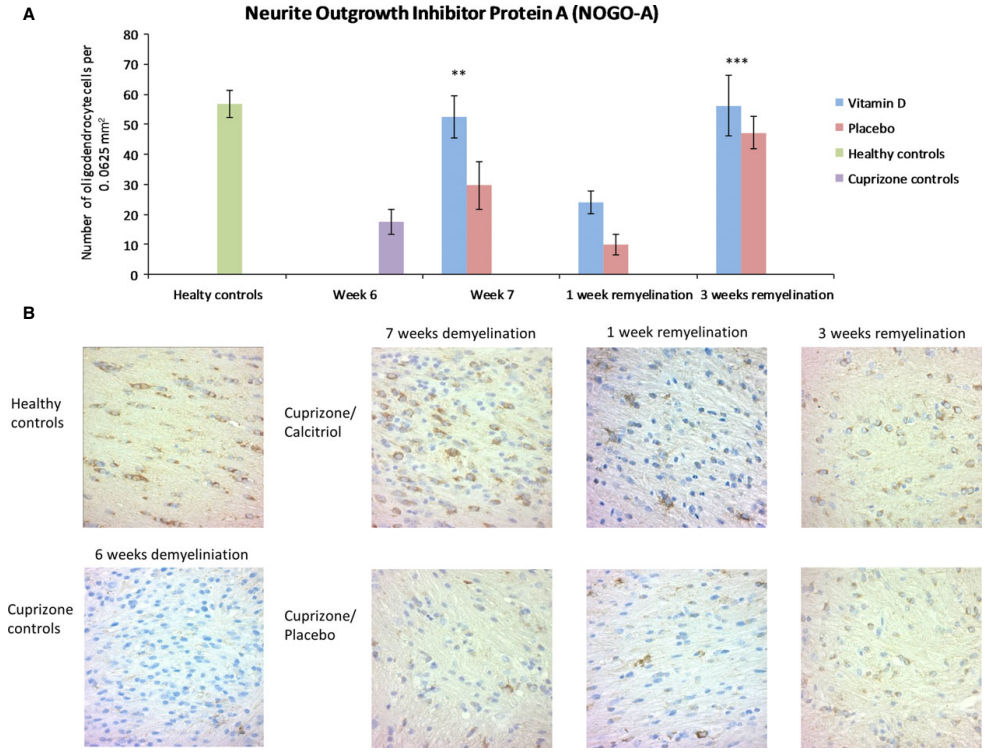

Fig. 2. Mature oligodendrocyte cells in the midline of corpus callosum after 7 weeks of demyelination, 1 and 3 weeks of remyelination. (A) After 7 weeks of demyelination, there was a difference in oligodendrocyte density, but this was not significant. (**; $p = 0.055$). The calcitriol group had a higher number of mature oligodendrocytes after one week of remyelination (***; $p = 0.019$). After 3 weeks of remyeliniation, there was no longer a significant difference between the groups. Cell counts are provided as mean (±SEM) number of cells per 0.0625 mm^2, midline corpus callosum, bregma ± 1 mm. (B) Sections stained for Neurite Outgrowth Inhibitor Protein A and hematoxylin. Error bars: 1 SEM. All images at 40x.

self-production of calcitriol and 24.25-$(OH)_2$-vitamin D_3, we used the metabolite 24.25-$(OH)_2$-vitamin D_3 as an indirect measure of levels of calcitriol. The mice who received calcitriol had significant lower levels of 24.25-$(OH)_2$-vitamin D_3 than mice that received placebo injections (week 7, 9, and 10, $p < 0.014$). The calcitriol group also had significantly lower levels of 25-OH-D_3 at all time points measured ($p < 0.033$, Table S3).

Weight and RotaRod test

Cuprizone exposure led to weight loss in the cuprizone-exposed mice compared with the mice receiving a standard diet. At the endpoint of the study, the cuprizone-exposed mice regained almost all of the weight loss, and had a mean weight of 21.6 ± 1.5 g. vs. 23.4 ± 1.6 g in the controls (Figure S1). Mice exposed to cuprizone had an increased motor performance compared with the control group, as measured with the RotaRod test. Over time, the motor performance fell in the cuprizone-exposed mice (Figure S2). There were no significant differences in RotaRod performances between mice given calcitriol or placebo supplementation.

DISCUSSION

In this study, we aimed to determine the safety of high-dose vitamin D_3 on the remyelination process in a T cell-independent model for de- and remyelination. We have shown that high-dose injections of calcitriol have no negative effects on remyelination,

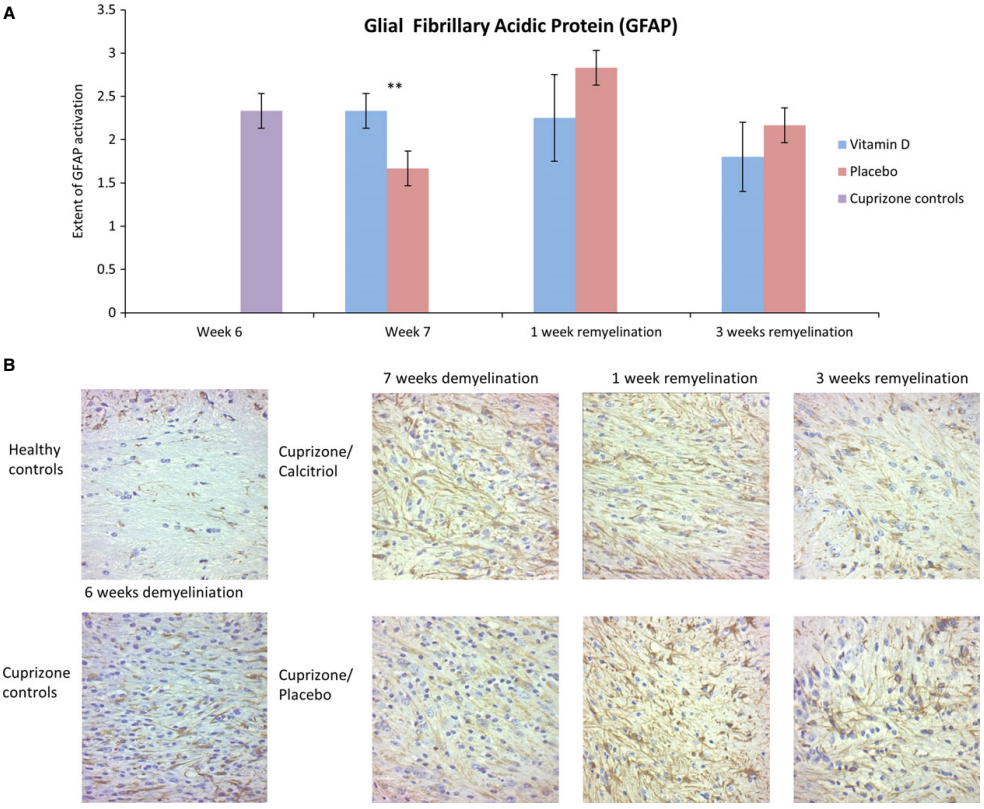

Fig. 3. Astrocytosis in the midline of corpus callosum after 7 weeks of demyelination, 1 and 3 weeks of remyelination. (A) Mice that received calcitriol had an increased GFAP immunopositivity at week 7 of demyelination, compared with the placebo group (**; $p = 0.043$). In the placebo group, there was a non-significant increase in astrocytosis after one week of remyelination ($p = 0.109$). The astrocyte activity decreased steadily in the calcitriol group. Scale: no (0), minimal (1), moderate (2) or severe (3) reactive astrocytosis. Sections were scored in the midline area of corpus callosum, from the bregma ± 1 mm. (B) Sections stained for Glial Fibrillary Acidic Protein and hematoxylin. Error bars: 1 SEM. All images at 40x.

as measured with LFB staining, but could actually have a potential in promoting oligodendrocyte maturation and myelin regeneration. Most effects of vitamin D are mediated by 1.25-$(OH)_2$D binding to the vitamin D receptor (VDR). The VDR is abundantly expressed on T cells, and much of the effect of vitamin D in autoimmune diseases has been suggested to be mediated through an immunomodulatory effect on these cells (25). Immunohistochemical studies have demonstrated that the VDR is also present in gray matter neurons and astrocytes (26). Recently, it has been found nuclear staining for VDR in oligodendrocyte-like cells, astrocytes and microglia, implicating that vitamin D also has a regulatory function in these cells (27). Our experimental findings, in a T cell-independent model of de- and remyelination, confer that vitamin D may have a functional role in the CNS not only in regulating T-cell function but also in myelin regeneration. The activation of microglia is a physiological response to CNS injury; its role is to support and protect neurons (28). It has been suggested that astrocytes may play a key role in regulation of demyelinating diseases in the CNS (29). Astrocytes have been demonstrated to provide an environment that forms the basis for recruitment of microglia. The removal of myelin debris by microglia is required for subsequent remyelination and delayed removal

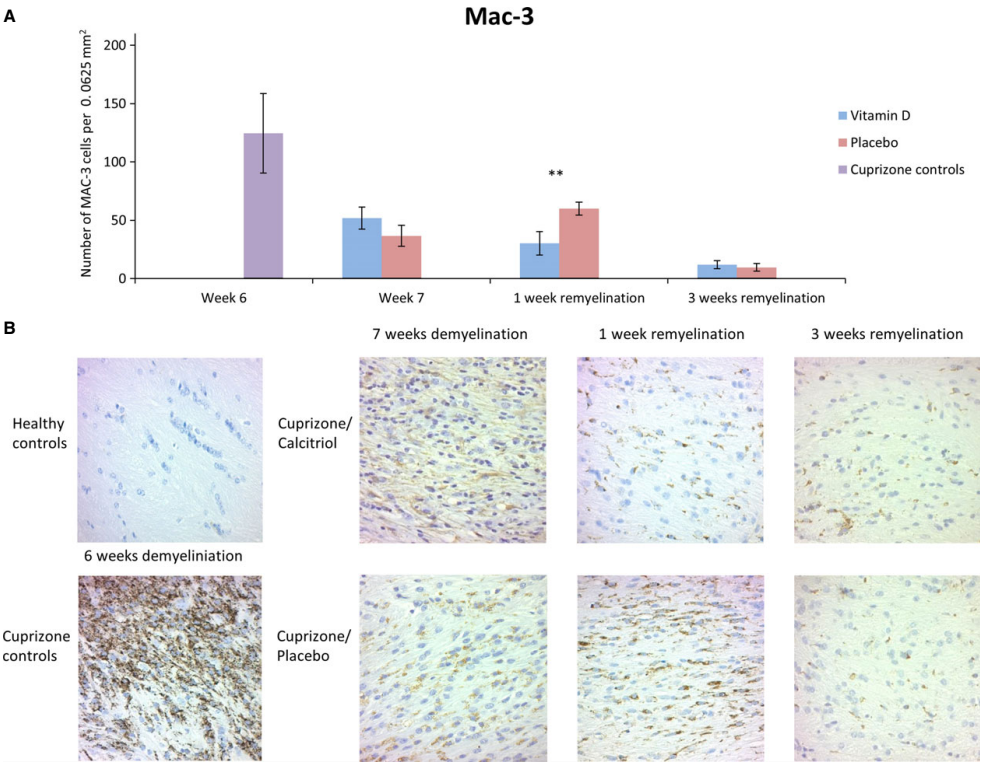

Fig. 4. Microglia activation in the midline of corpus callosum after 7 weeks of demyelination, 1 and 3 weeks of remyelination. (A) After 7 weeks of demyelination, microglia activation was most prominent in the calcitriol group, compared with the placebo group. The activation fell gradually. After 1 week of remyelination, there was a significant increase in the number of MAC-3 cells in the placebo group (**; $p = 0.019$). Cell counts are provided as mean (±SEM) number of cells per 0.0625 mm^2, midline area of corpus callosum, from the bregma ± 1 mm. **(B)** Sections stained for MAC-3 and hematoxylin. Error bars: 1 SEM. All images at 40x.

of damaged myelin will prevent the early remyelination (30). The mice receiving calcitriol had an initially increased astrocyte activation, microglia recruitment and clearance of damaged myelin. The stimulating effects on remyelination could partly have been caused by increased clearance of damaged myelin, through stimulation of astrocytes and microglia, which were initially more activated in the calcitriol group. In addition, we detected an increased number of oligodendrocytes in the calcitriol group compared with the placebo group.

There are no animal models that fully describe the complexity of the mechanisms underlying MS. Yet, the cuprizone model has been proved to be particularly suitable for studying the repair process after demyelination, this without interference of infiltrating immune cells, such as T cells (30). (16, 31). When cuprizone is administered for 6 weeks, remyelination usually starts after about 5 weeks of cuprizone exposure and is usually almost complete after 3 weeks of remyelination (16). We chose to give cuprizone administration for 7 weeks to achieve a high serum level of calcitriol throughout the remyelination phase. This seems to have resulted in a slower remyelination in both groups than what has been observed in studies using a shorter period of cuprizone exposure. It has been demonstrated that mice exposed to cuprizone for longer periods have a prolonged remyelination phase (31). Still, the mice given high-dose calcitriol had a significantly higher degree of remyelination and oligodendrocyte maturation than the placebo group. The main limitation to our experiment was that we were not able to conduct functional studies on exactly how vitamin D

affects astrocytes, microglia and oligodendrocytes. This is an important question, which should be addressed in future studies.

By our knowledge, this is the first study that examines the effect of high-dose calcitriol on remyelination in the cuprizone model. We have previously demonstrated that 25-OH-vitamin D_3 has a protective effect against demyelination and oligodendrocyte loss in the same model (17). We have now investigated vitamin D in both de- and remyelination by using the cuprizone model. Our findings may have implications in the understanding of the role of vitamin D in the remyelination of the brain. The results indicate that it is not harmful to give high doses of calcitriol. Our findings suggest that vitamin D could have a positive effect not only in decreasing inflammation but also in enhancing the repair process. Several randomized trials of vitamin D intervention in MS are currently being conducted (32, 33), and our findings could have implications for the future interpretation of these studies.

In conclusion, we demonstrate that high-dose treatment with calcitriol has no negative effects on remyelination in a T cell-independent animal model for demyelination. Contrary, our results suggest that calcitriol could have a positive effect on the remyelination process, possibly through a stimulating effect on oligodendrocyte maturation and astrocyte activation. The potential of calcitriol to stimulate oligodendrocyte maturation and remyelination should be investigated further, with functional data to clarify the exact mechanism for this effect.

CONFLICT OF INTEREST

The authors report no conflicts of interest.

The authors thank Edith Fick for excellent technical assistance and Dr. Charalampos Tzoulis for providing the RotaRod machine.

REFERENCES

1. Compston A, Coles A. Multiple sclerosis. Lancet 2008;372:1502–17.
2. Pugliatti M, Casetta I, Drulovic J, Granieri E, Holmoy T, Kampman MT, et al. A questionnaire for multinational case-control studies of environmental risk factors in multiple sclerosis (EnvIMS-Q). Acta Neurol Scand Suppl 2012;195:43–50.
3. Simon KC, Munger KL, Ascherio A. Vitamin D and multiple sclerosis: epidemiology, immunology, and genetics. Curr Opin Neurol 2012;25:246–51.
4. Løken-Amsrud KI, Holmøy T, Bakke SJ, Beiske AG, Bjerve KS, Bjørnara BT, et al. Vitamin D and disease activity in multiple sclerosis before and during interferon-beta treatment. Neurology 2012;79:267–73.
5. Simpson S Jr, Taylor B, Blizzard L, Ponsonby AL, Pittas F, Tremlett H, et al. Higher 25-hydroxyvitamin D is associated with lower relapse risk in multiple sclerosis. Annals of neurology 2010;68:193–203.
6. Myhr KM. Vitamin D treatment in multiple sclerosis. J Neurol Sci 2009;286:104–8.
7. Hewer S, Lucas R, van der Mei I, Taylor BV. Vitamin D and multiple sclerosis. Journal of clinical neuroscience. official journal of the Neurosurgical Society of Australasia. 2013;20:634–41.
8. Soilu-Hanninen M, Aivo J, Lindstrom BM, Elovaara I, Sumelahti ML, Farkkila M, et al. A randomised, double blind, placebo controlled trial with vitamin D3 as an add on treatment to interferon beta-1b in patients with multiple sclerosis. J Neurol Neurosurg Psychiatry 2012;83:565–71.
9. Stein MS, Liu Y, Gray OM, Baker JE, Kolbe SC, Ditchfield MR, et al. A randomized trial of high-dose vitamin D2 in relapsing-remitting multiple sclerosis. Neurology 2011;77:1611–8.
10. Kampman MT, Steffensen LH, Mellgren SI, Jørgensen L. Effect of vitamin D3 supplementation on relapses, disease progression, and measures of function in persons with multiple sclerosis: exploratory outcomes from a double-blind randomised controlled trial. Mult scler 2012;18:1144–51.
11. Benardais K, Kotsiari A, Skuljec J, Koutsoudaki PN, Gudi V, Singh V, et al. Cuprizone [Bis(Cyclohexylidenehydrazide)] is selectively toxic for mature oligodendrocytes. Neurotox Res 2013;24:244–50.
12. Buschmann JP, Berger K, Awad H, Clarner T, Beyer C, Kipp M. Inflammatory response and chemokine expression in the white matter corpus callosum and gray matter cortex region during cuprizone-induced demyelination. Journal of molecular neuroscience: MN 2012;48:66–76.
13. Hiremath MM, Saito Y, Knapp GW, Ting JPY, Suzuki K, Matsushima GK. Microglial/macrophage accumulation during cuprizone-induced demyelination in C57BL/6 mice. J Neuroimmunol 1998;92:38–49.
14. Kipp M, Clarner T, Dang J, Copray S, Beyer C. The cuprizone animal model: new insights into an old story. Acta Neuropathol 2009;118:723–36.
15. Matsushima GK, Morell P. The neurotoxicant, cuprizone, as a model to study demyelination and remyelination in the central nervous system. Brain Pathol 2001;11:107–16.
16. Lindner M, Heine S, Haastert K, Garde N, Fokuhl J, Linsmeier F, et al. Sequential myelin protein expression during remyelination reveals fast and efficient repair after central nervous system demyelination. Neuropathol Appl Neurobiol 2008;34:105–14.
17. Wergeland S, Torkildsen Ø, Myhr KM, Aksnes L, Mørk SJ, Bø L. Dietary vitamin D3 supplements reduce demyelination in the cuprizone model. PLoS ONE. 2011;6:e26262.
18. Holmøy T, Kampman MT, Smolders J. Vitamin D in multiple sclerosis: implications for assessment and treatment. Expert Rev Neurother 2012;12:1101–12.

19. Paxinos GF, Keith B.J. The mouse brain in stereotaxic coordinates. Amsterdam; London: Elsevier Academic Press, 2008.
20. Duchen LW. In: Adams JH CJ, Duchen LWeditors. Greenfield's neuropathology: General pathology of neurons and glia. New York, USA: Wiley, 1984: 1–52.
21. Bruck W, Pfortner R, Pham T, Zhang J, Hayardeny L, Piryatinsky V, et al. Reduced astrocytic NF-kappaB activation by laquinimod protects from cuprizone-induced demyelination. Acta Neuropathol 2012;124:411–24.
22. Aksnes L. Simultaneous determination of retinol, alpha-tocopherol, and 25-hydroxyvitamin D in human serum by high-performance liquid chromatography. J Pediatr Gastroenterol Nutr 1994;18:339–43.
23. Michaylova V, Ilkova P. Photometric determination of micro amounts of calcium with arsenazo III. Anal Chim Acta 1971;53:194–8.
24. Franco-Pons N, Torrente M, Colomina MT, Vilella E. Behavioral deficits in the cuprizone-induced murine model of demyelination/remyelination. Toxicol Lett 2007;169:205–13.
25. Smolders J, Damoiseaux J, Menheere P, Hupperts R. Vitamin D as an immune modulator in multiple sclerosis, a review. J Neuroimmunol 2008;194:7–17.
26. Eyles DW, Smith S, Kinobe R, Hewison M, McGrath JJ. Distribution of the vitamin D receptor and 1 alpha-hydroxylase in human brain. J Chem Neuroanat 2005;29:21–30.
27. Smolders J, Schuurman KG, van Strien ME, Melief J, Hendrickx D, Hol EM, et al. Expression of vitamin D receptor and metabolizing enzymes in multiple sclerosis-affected brain tissue. J Neuropathol Exp Neurol 2013;72:91–105.
28. Streit WJ. Microglia as neuroprotective, immunocompetent cells of the CNS. Glia 2002;40:133–9.
29. Nair A, Frederick TJ, Miller SD. Astrocytes in multiple sclerosis: a product of their environment. Cell Mol Life Sci 2008;65:2702–20.
30. Skripuletz T, Gudi V, Hackstette D, Stangel M. De- and remyelination in the CNS white and grey matter induced by cuprizone: the old, the new, and the unexpected. Histol Histopathol 2011;26:1585–97.
31. Lindner M, Fokuhl J, Linsmeier F, Trebst C, Stangel M. Chronic toxic demyelination in the central nervous system leads to axonal damage despite remyelination. Neurosci Lett 2009;453:120–5.
32. Dorr J, Ohlraun S, Skarabis H, Paul F. Efficacy of Vitamin D supplementation in multiple sclerosis (EVIDIMS Trial): study protocol for a randomized controlled trial. Trials.2012;13:15.
33. Smolders J, Hupperts R, Barkhof F, Grimaldi LME, Holmoy T, Killestein J, et al. Efficacy of vitamin D-3 as add-on therapy in patients with relapsing-remitting multiple sclerosis receiving subcutaneous interferon beta-1a:a Phase II, multicenter, double-blind, randomized, placebo-controlled trial. J Neurol Sci 2011; 311:44–9.

SUPPORTING INFORMATION

Additional Supporting Information may be found in the online version of this article:

Table S1. Antibodies used for immunohistochemistry

Table S2. Density of NOGO-A immunopositive mature oligodendrocytes, Mac-3 immunopositive microglia and macrophages and CD3 immunopositive t-lymphocytes, midline corpus callosum. Cell counts are provided as mean (±SD) number of cells per 0.0625 mm^2.

Table S3. Serum Ca (S-Ca) levels were normal in both groups and there was no significant difference between the placebo and vitamin D groups at any time points. We used the metabolite 24.25 D_3 as an indirect measure of levels of 1.25-dihydroxy-vitamin D_3. The mice who received 1.25-dihydroxy-vitamin D_3 had significantly lower levels of 24.25 D_3 than mice that received placebo injections (weeks 7,9, and 10) ($p < 0.014$). The vitamin D group had also a lower level of 25-OH-D_3 at all measured points ($p < 0.033$).

Fig. S1. Weight changes (in grams) for all days. The cuprizone mice had an initial weight loss and then stabilized at a lower level than the controls. When the cuprizone diet was terminated, the weight increased again to 21.6 ± 1.5 g, control mice weight stabilized at 23.4 ± 1.6 g.

Fig. S2. The mice's motor behavior was tested twice a week using the Rotarod apparatus. The average time of three experiments was measured. All groups were tested throughout the experimental period; three mice were evaluated at the same time. Mice exposed to cuprizone mice had an increased activity level compared with the control group. There was no significant difference in the results of tests between mice given calcitriol or placebo supplementation.

Target antigen	Species/ isotype	Working dilution	Incubation time/ Temperature	Antigen/ demasking*	Source
Neurite Outgrowth Inhibitor Protein A (NOGO-A)	Rabbit polyclonal	1:1000	1h/RT	Citrate	Chemicon, Temecula (CA), USA
MAC-3	Rat IgG1, κ	1:200	24h/RT	Citrate	BD Biosciences
CD3	Rabbit polyclonal	1:500	½h/RT	Tris-EDTA	Dako
Glial Fibrillary Acidic Protein (GFAP)	Rabbit, IgG1	1:2000	½h/ RT	Tris-EDTA	Dako

Supplementary table 1.

	Controls		Only Cuprizone		Calcitriol or placebo treated					
			Demyelination				Remyelination			
Week			6		7		8		10	
	M	SD	M	SD	M	SD	M	SD	M	SD
NOGO-A	56.7	(10.90)	17.5	(9.90)						
Calcitriol					52.4	(9.90)	24	(7.40)	56.2	(22.80)
Placebo					29.7	(19.50)	10	(4.40)	47.2	(12.40)
Mac-3	0	(0.00)	124	(76.55)						
Calcitriol					51.8	(21.30)	30.25	(20.00)	12	(7.80)
Placebo					36.67	(22.30)	60	(13.70)	9.7	(8.00)
CD3	0	(0.00)	0.5	(0.80)						
Calcitriol					1.6	(0.80)	2.25	(0.50)	2.2	(1.90)
Placebo					1.6	(2.00)	2.2	(1.70)	1.4	(1.10)

Supplementary table 2. Density of NOGO-A immunopositve mature oligodendrocytes, Mac-3 immunopositive microglia and macrophages and CD3 immunopositive t-lymphocytes, midline corpus callosum. Cell counts are provided as mean (±SD) number of cells per 0.0625 mm^2

	Controls		Only Cuprizone		Calcitriol or placebo treated					
			Demyelination				Remyelination			
Week			6		7		8		10	
	M	SD	M	SD	M	SD	M	SD	M	SD
s-calcium	2.3	(0.20)	2.4	(0.30)						
Calcitriol					2.7	(0.17)	2.8	(0.60)	2.6	(0.60)
Placebo					2.3	(0.10)	2.1	(0.20)	2.4	(0.20)
24.25 D3	40.8	(5.30)	37	(8.90)						
Calcitriol					19.9	(4.70)	22.85	(11.10)	21.9	(2.90)
Placebo					35.5	(5.00)	32.3	(2.90)	37.1	(9.20)
25-OH-D3	12.1	(1.30)	10.5	(4.20)						
Calcitriol					2	(0.40)	2.85	(0.40)	1.74	(0.60)
Placebo					7.5	(0.80)	9.1	(1.40)	7.7	(3.60)

Supplementary table 3. Serum Ca (S-Ca) levels were normal in both groups and there was no significant difference between the placebo and vitamin D groups at any time points. We used the metabolite 24.25 D_3 as an indirect measure of levels of 1.25-dihydroxy-vitamin D_3. The mice who received 1.25-dihydroxy-vitamin D_3 had significantly lower levels of 24.25 D_3, than mice that received placebo injections (week 7,9 and 10) ($p's<0.014$). The vitamin D group had also a lower level of 25-OH-D_3 at all measured points ($p's<0.033$).

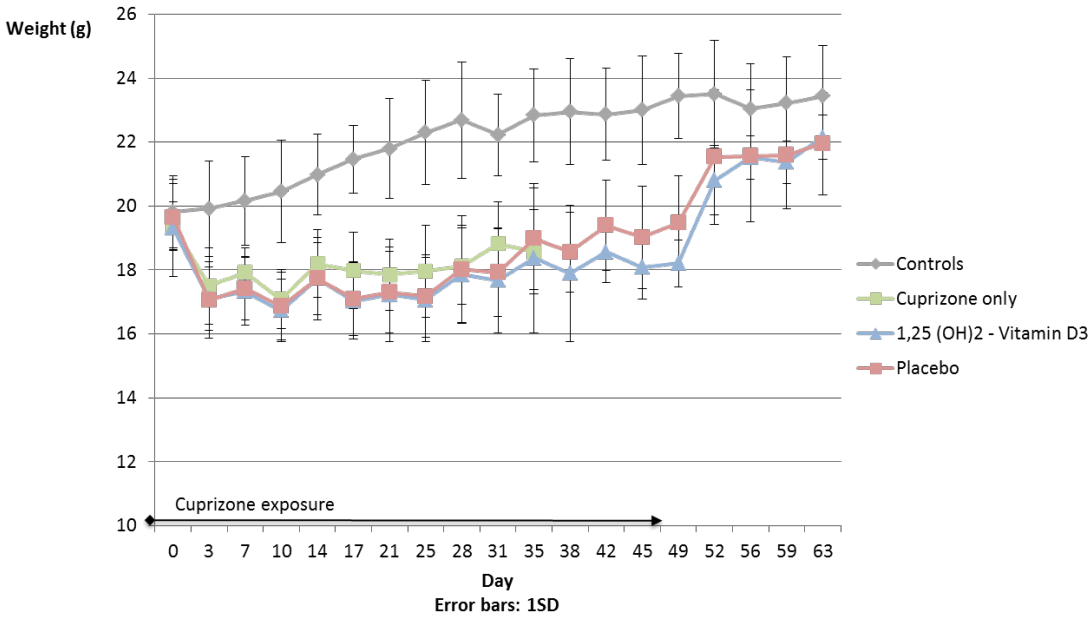

Supplemental figure 1. Weight changes (in grams) for all days. The cuprizone mice had a initially weight loss and then stabilized at a lower level than the controls. When the cuprizone diet was terminated the weight increased again to 21.6±1.5g, control mice weight stabilized at 23.4±1.6g.

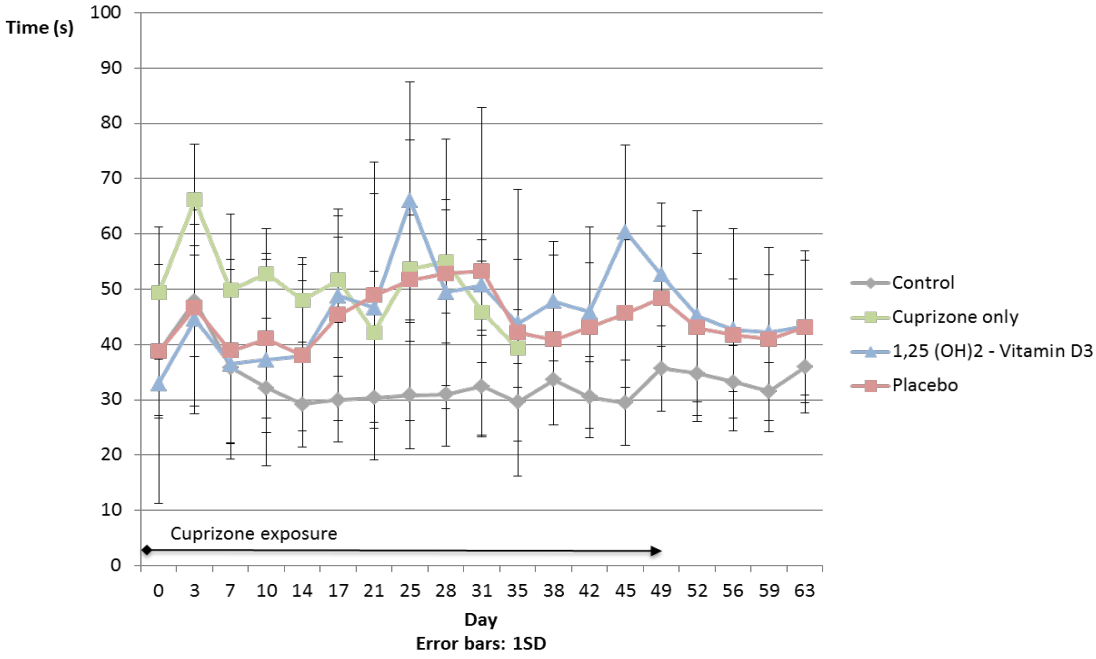

Supplemental figure 2. The mice's motor behavior was tested twice a week using the Rotarod apparatus. The average time of three experiments was measured. All groups were tested throughout the experimental period; three mice were evaluated at the same time.

Mice exposed to cuprizone mice had an increased activity level compared with the control group. There was no significant difference in the results of tests between mice given calcitriol or placebo supplementation.

II

Journal of Neuroimmunology 321 (2018) 61–65

Contents lists available at ScienceDirect

Journal of Neuroimmunology

journal homepage: www.elsevier.com/locate/jneuroim

Effects of vitamin D on axonal damage during de- and remyelination in the cuprizone model

Agnes E. Nystad[a,b,*], Øivind Torkildsen[a,b], Stig Wergeland[a]

[a] Norwegian Multiple Sclerosis Competence Centre, Department of Neurology, Haukeland University Hospital, Bergen, Norway
[b] Department of Clinical Medicine, University of Bergen, Bergen, Norway

ARTICLE INFO

Keywords:
Multiple sclerosis
Cuprizone
Demyelination
Remyelination
Vitamin D
Axonal damage

ABSTRACT

Vitamin D deficiency is a risk factor for multiple sclerosis and associated with higher disease activity. The aim of this study was to investigate the effects of cholecalciferol and calcitriol on axonal damage during de- and remyelination in the cuprizone model. We found significantly less reduction of neurofilament immunopositive axons in the high vs. low cholecalciferol group, while high dose calcitriol, given during remyelination, did not influence axonal regeneration. Our results indicate that high dose vitamin D could protect against axonal loss in an experimental model for demyelination, if given before and during the demyelination.

1. Introduction

Multiple sclerosis (MS) is a chronic neurological disease characterized by inflammation, demyelination and axonal damage in the central nervous system (CNS). Axonal injury is suggested to be associated with inflammation in all lesions and disease stages of the disease (Frischer et al., 2009; Dutta and Trapp, 2011). Axonal conduction block, due to inflammation and demyelination, leads to neurological disability during the acute relapses in MS, while axonal transection and subsequent loss of neurons is the cause of permanent neurological deficits (Trapp et al., 1999; Trapp and Nave, 2008). To study neuronal and axonal protective strategies is of high importance to prevent disease progression.

Vitamin D deficiency is an environmental factor that has been shown to increase both risk and disease activity of MS (Holmøy et al., 2012; Holmøy and Torkildsen, 2016; Smolders et al., 2016; Shoemaker and Mowry, 2018). It is unclear how vitamin D affects axonal damage in an MS affected brain.

We have previously studied the effect of vitamin D, cholecalciferol, on experimental demyelination, using the cuprizone model for de- and remyelination. The results suggested that cholecalciferol had a protective effect against demyelination (Wergeland et al., 2011). Further, we used the model for investigating the impact of high dose calcitriol on remyelination, and the results indicated that calcitriol could promote the repair process, probably by stimulating oligodendrocyte maturation and astrocyte activation (Nystad et al., 2014). Early remyelination seems to provide a protective effect against axonal damage (Irvine and Blakemore, 2008; Lindner et al., 2009). In another animal model for MS, experimental autoimmune encephalomyelitis (EAE), calcitriol treatment diminished the level of clinical disability and reduced the loss of axons, when initiated at peak disease severity (Sloka et al., 2015).

Here, we investigate the effects of high dose cholecalciferol and calcitriol on axonal damage in the cuprizone model respectively during de- and remyelination. We hypothesized that vitamin D could have a protective effect against axonal damage, leading to less axonal loss in cuprizone mice receiving vitamin D than in the control group.

2. Materials and methods

2.1. Mice

Five-week-old female c57Bl/6 mice, $n = 72$, (Taconic, Tornbjerg, Denmark), with a mean weight of 20.4 g ± SD 1.0, were used for the demyelination experiment. For the remyelination experiment, we used five-week-old female c57Bl/6 mice, $n = 48$. Mean weight was 19.6 g ± SD 1.5. The mice were housed six together in GreenLine type II individually ventilated cages (Scanbur, Karlslunde, Denmark), in standard laboratory conditions. Maintenance was performed once a week, and the same individuals handled the animals throughout the experimental period. They were weighed twice a week. Food and tap water were available ad libitum throughout the acclimatization and trial period. We have previously published serum levels of vitamin D and calcium for both experiments (Wergeland et al., 2011; Nystad et al., 2014). The experiments were carried out following the European

* Corresponding author at: Norwegian Multiple Sclerosis Competence Centre, Department of Neurology, Haukeland University Hospital, Jonas Lies Road 65, 5021 Bergen, Norway.
E-mail addresses: agnes.elisabeth.nystad@helse-bergen.no (A.E. Nystad), oivind.torkildsen@helse-bergen.no (Ø. Torkildsen), stig.wergeland@helse-bergen.no (S. Wergeland).

https://doi.org/10.1016/j.jneuroim.2018.05.016
Received 25 April 2018; Received in revised form 29 May 2018; Accepted 30 May 2018

Laboratory Animal Science Associations recommendations, and the Norwegian Animal Research Authority approved the protocols (permits #2009-1767 and #2012-4421).

2.2. Study design, vitamin D-diet, high dose calcitriol injections and cuprizone administration

2.2.1. Demyelination experiment

After one week of acclimatization the animals ($n = 72$) were randomized to one of four experimental diets ($n = 18$ per diet group). Two weeks later, 2/3 ($n = 12$) of the mice in each diet group were randomized to cuprizone exposure. To induce demyelination, 0.2% cuprizone (bis-cyclohexanone-oxaldihydrazone, Sigma-Aldrich, St. Louis, MO, USA) was added to milled mouse chow (Altromin GmbH, Lage, Germany) for six weeks. The remaining 1/3 ($n = 6$) served as healthy controls for each diet group (Table S1). The differing vitamin D content for the groups was 1) < 50 IU/kg, 2) 500 IU/kg, 3) 6200 IU/kg and 4) 12500 IU/kg. The content was verified by high-performance liquid chromatography (HPLC) in an independent laboratory (Norwegian Institute for Nutrition and Seafood Research, Bergen, Norway). An assumed intake of 5 g chow each day gave human equivalent doses ranging from < 76 IU/day to 19,003 IU/day, as described before (Wergeland et al., 2011; Farinotti et al., 2012). The animals were euthanized after 9 and 11 weeks (Table S1).

2.2.2. Remyelination experiment

After 12 days of acclimatization, the mice ($n = 48$) were randomized into one of four groups. One group served as healthy controls ($n = 6$) and one as cuprizone-exposed controls (n = 6). The remaining mice ($n = 36$) were randomized to either intraperitoneal (ip.) injections of 2 μg calcitriol or placebo, twice weekly, from week 6 throughout week 9 (Table S2). We have previously shown that it takes weeks to obtain steady-state serum concentration with cholecalciferol treatment (Wergeland et al., 2011). Thus, we used calcitriol injections, instead of cholecalciferol supplements to achieve a faster serum increase. In this way, we also avoided that the serum increase came after the majority of the remyelination was over. To induce demyelination, 0.2% cuprizone was added to milled mouse chow, the cuprizone exposure was discontinued after six weeks in the cuprizone control group, and after seven weeks in the remaining groups to achieve a high serum level of calcitriol throughout the remyelination phase. The animals were euthanized after 6, 7, 8 and 10 weeks (Table S2).

2.3. Histopathology

The animals were euthanized by CO_2 asphyxiation or by exsanguination under anaesthesia by midazolam (Dormicum "Roche") in combination with fentanyl/fuanisone (Hypnorm "VetaPharma") and sacrificed by exsanguination at different time points (Tables S1 and S2). Brains were removed and post-fixed in 4% paraformaldehyde for at least 7 days before paraffin embedding. Analyses were performed on 7 ± 1 μm coronal sections from the bregma ± 1 mm (Paxinos, 2008). For immunohistochemistry (IHC), the sections were deparaffinised in xylene and rehydrated in serial dilutions of ethanol. Antigen retrieval was performed by microwaving sections in either citrate (pH 6.1) or TRIS-EDTA (pH 9.0) buffer. Sections were then immunostained for amyloid precursor protein A4 (APP), non-phosphorylated neurofilament H (SMI-32) and pan-phosphorylated neurofilament light antibody (NFL). Species, buffer, dilution, incubation time, temperature, target and source for the primary antibodies are specified in Table S3. Sections were blocked with peroxidase blocking solution (DAKO, Glostrup, Denmark) and visualized with EnVision 3.3. – diaminobenzidine (1:50); 2 × 3 minutes at room temperature (DAKO, Glostrup, Denmark), then counterstained with hematoxylin. For each antibody normal brain tissue from healthy mice served as controls.

2.4. Assessment of brain tissue

Axonal transection was quantified as the density of APP-immunopositive bulbs in the midline of the corpus callosum, using an ocular morphometric grid. Immunopositivity for NFL and SMI-32 were quantified using digital densitometry. The midline of the corpus callosum was photographed with identical exposure settings at 40× magnifications (Zeiss, Axio Imager A2 with AxioCam ERc5 digital camera). Greyscale images were thresholded to ameliorate background staining (ImageJ ver 1.41, Research Services Branch, National Institute of Mental Health, Bethesda, Maryland, USA). Immunopositivity was expressed as the relative (%) area of immunopositivity to the total image area.

2.5. Statistical methods

All calculations were performed using SPSS (IBM Corp. Released 2011. IBM SPSS Statistics for Windows, Version 20.0. Armonk, NY: IBM Corp). Shapiro-Wilk and Kolmogorov-Smirnov test tested normal distribution. For statistical analyses, the Mann-Whitney U test was used due to non-normality in the dataset. Differences were considered significant at $p < .05$.

3. Results

3.1. Effects of cholecalciferol on axonal loss and damage during demyelination

After six weeks of cuprizone exposure, the two groups receiving the diets with the highest vitamin D_3 content (6200 and 12,500 IU/kg) had less axonal loss in the corpus callosum, than the groups receiving a diet low or deficient of vitamin D (< 50 IU/kg, or 500 IU/kg), as measured by the relative area of NFL immunopositivity, 78.5% ± SD 9.3 (high dose) vs. 50.3% ± SD 26.6 (low dose, $p = .006$, Fig. 1, Table 1). There were no differences in the density of damaged axons, as measured by the relative area of SMI-32 immunopositivity, 49.1% ± SD 27.7 (high dose) vs. 36.0% ± SD 20.1 (low dose) $p = .24$ (Fig. 1, Table 1). As assessed by immunohistochemical staining for APP, the density of transected axons was lower in the high diet groups than in the low-diet groups, but this difference did not reach statistical significance, 74.9 APP^+ bulbs/0.0625mm^2 ± SD 57.2 (high dose) vs. 109.7 ± SD 38.9 (low dose) $p = .064$ (Fig. 1, Table 1).

3.2. Effects of calcitriol on axonal loss and damage during remyelination

There were no differences between the calcitriol and the placebo group after 3 weeks of remyelination, as measured by the relative area of NFL immunopositivity 81.8% ± SD 12.2 (calcitriol) vs. 80.8% ± SD 7.0 (placebo), $p = .69$. Positively stained axons, as measured by the relative area of SMI-32 immunopositivity, could be observed from week 5 in the remyelination experiment. There was no difference between the groups at 3 weeks of remyelination 5.0% ± SD 6.3 (calcitriol) vs. 3.3% ± SD 3.5 (placebo), $p = .54$ (Fig. 2, Table 2). There was no significant difference in APP-immunopositivity between the groups after 3 weeks of remyelination, 23.4 ± SD 8.7 (calcitriol) vs. 25.2 ± SD 4.3 (placebo), $p = .92$ (Fig. 2, Table 2). The axonal transection diminished throughout the remyelination period in both the calcitriol and placebo group (data not shown).

4. Discussion

Our results indicate that cholecalciferol given before and during demyelination may mitigate axonal loss. The results are consistent with previous data. Chabas et al. have found that higher levels of cholecalciferol protect against axonal damage, as well as improve myelination and recovery after nerve injury, probably by modifying expression

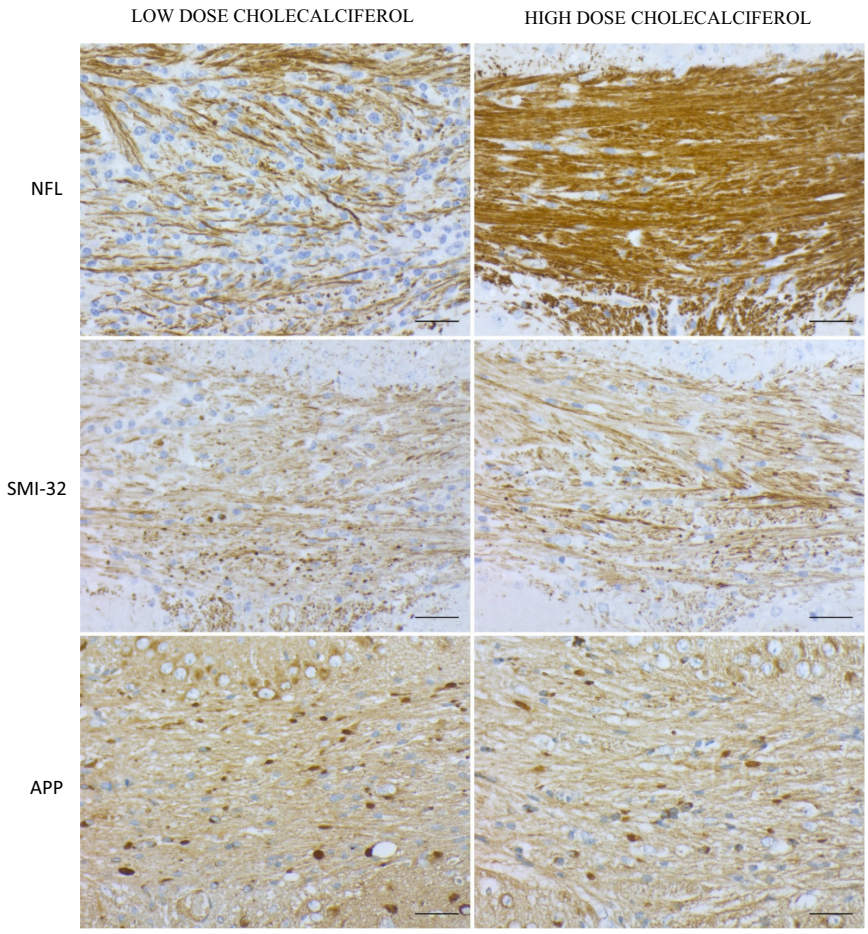

Fig. 1. Demyelination.
NFL, SMI-32 and APP immunostaining in the midline of corpus callosum after six weeks of cuprizone exposure in the low and high vitamin D diet groups. The mice receiving a high vitamin D diet (6200 IU/kg or 12,500 IU/kg) had less axonal loss vs. mice on a low diet (< 50 IU/kg or 500 IU/kg) ($p = .006$). All images at 40×. Scale bar = 20 μm.

Table 1
Demyelination – 6 weeks cuprizone exposure.

	Low cholecalciferol		High cholecalciferol		*p*
	Mean	(SD)	Mean	(SD)	
NFL area	50.3	(26.6)	78.5	(9.3)	0.006
SMI-32 area	36.0	(20.1)	49.1	(27.7)	0.235
APP density	109.7	(38.9)	74.9	(57.2)	0.064

Mean and standard deviation (SD) quantified by NFL and SMI-32 staining in % area and APP density, area after 6 weeks of cuprizone exposure (week 9).

of genes involved in axogenesis and myelination (Chabas et al., 2013). In a study of rats subjected to nerve damage, cholecalciferol was able to improve movement, breath, and spasticity, probably due to improved myelination or increased number of preserved or newly formed axons. The same study showed that vitamin D had to be given as soon as possible after the damage, to promote effective repair (Gueye et al., 2015). The possibly protective mechanism could be mediated by increased vitamin D receptor mRNA expression providing neuroprotection against excitotoxicity of glutamate (Taniura et al., 2006). Pretreatment with calcitriol, but not co-treatment, has also been suggested to protect dopaminergic neurons against cytotoxicity caused by glutamate and dopaminergic toxins, through reduction of oxidative stress (Ibi et al., 2001). Another study reported that calcitriol had a neuroprotective effect in a primary neuron culture from rats, as dopamine neurons increased due to upregulation of the gene expression of glial-derived neurotrophic factor (Orme et al., 2013).

The NFL is a CSF marker of axonal degradation in the CNS and is increased in the CSF of patients with relapsing-remitting MS (Lycke et al., 1998). High vitamin D levels are associated with lower levels of CSF-NFL (Sandberg et al., 2015). Our results also indicate less neurofilament loss in mice brain, after receiving cholecalciferol before and during demyelination. Calcitriol, given after demyelination seems not to have the same effect. SMI-32 is a marker for the non-phosphorylated epitope of the heavy and medium neurofilament subunits. The reaction is masked when the epitope is phosphorylated. SMI-32 antibodies do therefore not stain neurofilaments in myelinated axons. Thus, SMI-32

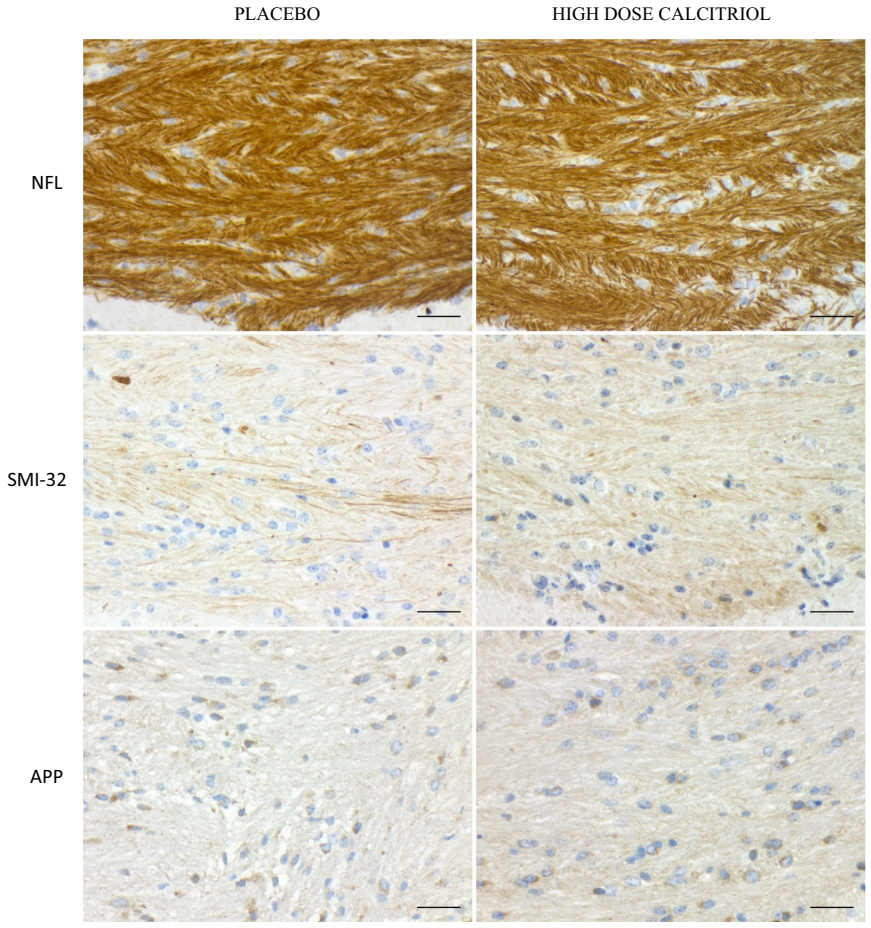

Fig. 2. Remyelination.
NFL, SMI-32 and APP immunostaining in the midline of corpus callosum after three weeks of remyelination in mice receiving intraperitoneal injections of 2 μg calcitriol vs. placebo. There were no significant differences between the calcitriol- and placebo-treated mice. All images at 40×. Scale bar = 20 μm.

Table 2
Remyelination – 3 weeks of remyelination.

	Placebo		Calcitriol		*p*
	Mean	(SD)	Mean	(SD)	
NFL area	80.8	(7.0)	81.8	(12.2)	0.690
SMI-32 area	3.3	(3.5)	5.0	(6.3)	0.537
APP density	25.2	(4.3)	23.4	(8.7)	0.916

Mean and standard deviation (SD) quantified by NFL and SMI-32 staining in % area and APP density, area after 3 weeks of remyelination (week 10).

immunoreactivity provides a sensitive marker for demyelination or axonal injury (Trapp et al., 1998; Ouda et al., 2012). In the cuprizone model SMI-32 has been observed after long-term demyelination (after 8 weeks) as punctuations, ovoids and continuous lines (Lindner et al., 2009). In the present study, as expected, few SMI-32 positive axons were detected after cuprizone exposure, and there were no significant group differences. We have not examined the effect of vitamin D on chronic demyelination (Armstrong et al., 2006) and during remyelination, over a prolonged period. Axonal damage is postulated to happen over time when the brain no longer can compensate for further axonal loss (Dutta and Trapp, 2011). The duration of cuprizone exposure may have been too short to evaluate the extent of, and group differences in SMI-32 immunopositivity.

The APP is a membrane glycoprotein, present in neuronal cells. In damaged axons, APP accumulates locally but is redistributed if axonal transport is restored, or if the axon degenerates (Lavi and Constantinescu, 2005; Lindner et al., 2009). Few have studied the effect of vitamin D on APP. In a mice model for Alzheimer disease, Durk et al. demonstrated that long-term calcitriol treatment decreased the levels of soluble and insoluble amyloid beta (Aβ), particularly in the hippocampus (Durk et al., 2014). Calcitriol has also been shown to increase the clearance of Aβ and decrease Aβ in the hippocampus of aged rats (Briones and Darwish, 2012) In our study, there were fewer transected axons in the high cholecalciferol diet groups than in the low diet groups, the difference was not significant. Our group assessed APP in the corpus callosum of mice, and the results cannot be directly compared to the previous findings in the hippocampus.

Failure of remyelination after cuprizone-induced demyelination

results in an increase in demyelination-associated axonal degeneration, and remyelination may protect axons and increase axonal survival (Irvine and Blakemore, 2008). Previously, we have found that mice given calcitriol are less demyelinated after three weeks of remyelination than mice receiving placebo (Nystad et al., 2014). However, calcitriol given during remyelination seemed not to diminish axonal loss or promote axonal repair in the current study despite more efficient remyelination. Continuous axonal damage despite sufficient remyelination has been described after chronic cuprizone-induced demyelination (Lindner et al., 2009). Despite remyelination, axonal degeneration continues at a low level and accumulates over time (Manrique-Hoyos et al., 2012; Zendedel et al., 2013). This could indicate that vitamin D should be given before, or at least at the same time as demyelination occurs, to affect axonal damage and loss.

A limitation of the present study was that we did not perform functional studies on the pathophysiological mechanisms underlying the effects of cholecalciferol on the axonal injury during demyelination. Several research groups have used the cuprizone model to study demyelination, remyelination and axonal damage, but the model does not directly mimic human MS pathology (Kipp et al., 2009; Zendedel et al., 2013).

5. Conclusion

High dose cholecalciferol, given before and during cuprizone exposure, appears to have a protective effect on axonal loss, while high dose calcitriol, given after the demyelination phase, seems not to influence axonal regeneration. In the future, clinical trials are necessary to gain a deeper insight into vitamin D's effects on axonal loss and damage.

Disclosure

Agnes E. Nystad received unrestricted grants from Novartis.
Stig Wergeland received speaker honorary from Biogen, Sanofi-Aventis, and Novartis.
Øivind Torkildsen received speaker honorary from and served on the scientific advisory board of Biogen, Sanofi-Aventis, and Merck and received speaker honorary from Novartis.

Funding

This research did not receive any specific grant from funding agencies in the public, commercial, or not-for-profit sectors.

References

Armstrong, R.C., Le, T.Q., Flint, N.C., Vana, A.C., Zhou, Y.X., 2006. Endogenous cell repair of chronic demyelination. J. Neuropathol. Exp. Neurol. 65 (3), 245–256.
Briones, T.L., Darwish, H., 2012. Vitamin D mitigates age-related cognitive decline through the modulation of pro-inflammatory state and decrease in amyloid burden. J. Neuroinflammation 9.
Chabas, J.F., Stephan, D., Marqueste, T., Garcia, S., Lavaut, M.N., Nguyen, C., Legre, R., Khrestchatisky, M., Decherchi, P., Feron, F., 2013. Cholecalciferol (vitamin D(3)) improves myelination and recovery after nerve injury. PLoS One 8 (5), e65034.
Durk, M.R., Han, K., Chow, E.C., Ahrens, R., Henderson, J.T., Fraser, P.E., Pang, K.S., 2014. 1alpha,25-Dihydroxyvitamin D3 reduces cerebral amyloid-beta accumulation and improves cognition in mouse models of Alzheimer's disease. J. Neurosci. 34 (21), 7091–7101.
Dutta, R., Trapp, B.D., 2011. Mechanisms of neuronal dysfunction and degeneration in multiple sclerosis. Prog. Neurobiol. 93 (1), 1–12.
Farinotti, M., Vacchi, L., Simi, S., Di Pietrantonj, C., Brait, L., Filippini, G., 2012. Dietary interventions for multiple sclerosis. Cochrane Database Syst. Rev. 12, CD004192.
Frischer, J.M., Bramow, S., Dal-Bianco, A., Lucchinetti, C.F., Rauschka, H., Schmidbauer, M., Laursen, H., Sorensen, P.S., Lassmann, H., 2009. The relation between inflammation and neurodegeneration in multiple sclerosis brains. Brain 132 (Pt 5), 1175–1189.
Gueye, Y., Marqueste, T., Maurel, F., Khrestchatisky, M., Decherchi, P., Feron, F., 2015. Cholecalciferol (vitamin D(3)) improves functional recovery when delivered during the acute phase after a spinal cord trauma. J. Steroid Biochem. Mol. Biol. 154, 23–31.
Holmøy, T., Torkildsen, Ø., 2016. Can vitamin D reduce inflammation in relapsing-remitting multiple sclerosis? Expert. Rev. Neurother. 16 (3), 233–235.
Holmøy, T., Torkildsen, Ø., Myhr, K.M., Løken-Amsrud, K.I., 2012. Vitamin D supplementation and monitoring in multiple sclerosis: who, when and wherefore. Acta Neurol. Scand. Suppl. 126, 63–69.
Ibi, M., Sawada, H., Nakanishi, M., Kume, T., Katsuki, H., Kaneko, S., Shimohama, S., Akaike, A., 2001. Protective effects of 1 alpha,25-(OH)(2)D(3) against the neurotoxicity of glutamate and reactive oxygen species in mesencephalic culture. Neuropharmacology 40 (6), 761–771.
Irvine, K.A., Blakemore, W.F., 2008. Remyelination protects axons from demyelination-associated axon degeneration. Brain 131 (Pt 6), 1464–1477.
Kipp, M., Clarner, T., Dang, J., Copray, S., Beyer, C., 2009. The cuprizone animal model: new insights into an old story. Acta Neuropathol. 118 (6), 723–736.
Lavi, E., Constantinescu, C.S., 2005. Experimental Models of Multiple Sclerosis. from. https://books.google.no/books?id=CCnt_ulPMgUC&lpg=PA138&dq=APP%20accumulates%20locally%20in%20a%20damaged%20axon%2C&hl=no&pg=PA138#v=onepage&q&f=false.
Lindner, M., Fokuhl, J., Linsmeier, F., Trebst, C., Stangel, M., 2009. Chronic toxic demyelination in the central nervous system leads to axonal damage despite remyelination. Neurosci. Lett. 453 (2), 120–125.
Lycke, J.N., Karlsson, J.E., Andersen, O., Rosengren, L.E., 1998. Neurofilament protein in cerebrospinal fluid: a potential marker of activity in multiple sclerosis. J. Neurol. Neurosurg. Psychiatry 64 (3), 402–404.
Manrique-Hoyos, N., Jurgens, T., Gronborg, M., Kreutzfeldt, M., Schedensack, M., Kuhlmann, T., Schrick, C., Bruck, W., Urlaub, H., Simons, M., Merkler, D., 2012. Late motor decline after accomplished remyelination: impact for progressive multiple sclerosis. Ann. Neurol. 71 (2), 227–244.
Nystad, A.E., Wergeland, S., Aksnes, L., Myhr, K.M., Bø, L., Torkildsen, Ø., 2014. Effect of high-dose 1.25 dihydroxyvitamin D3 on remyelination in the cuprizone model. APMIS 122 (12), 1178–1186.
Orme, R.P., Bhangal, M.S., Fricker, R.A., 2013. Calcitriol imparts neuroprotection in vitro to midbrain dopaminergic neurons by upregulating GDNF expression. PLoS One 8 (4), e62040.
Ouda, L., Druga, R., Syka, J., 2012. Distribution of SMI-32-immunoreactive neurons in the central auditory system of the rat. Brain Struct. Funct. 217 (1), 19–36.
Paxinos, G., 2008. In: Franklin, Keith B.J., Paxinos, George (Eds.), The Mouse Brain in Stereotaxic Coordinates. Elsevier Academic Press, Amsterdam; London (2008).
Sandberg, L., Bistrom, M., Salzer, J., Vagberg, M., Svenningsson, A., Sundstrom, P., 2015. Vitamin D and axonal injury in multiple sclerosis. Mult. Scler. 22, 1027–1031.
Shoemaker, T.J., Mowry, E.M., 2018. A review of vitamin D supplementation as disease-modifying therapy. Mult. Scler. 24 (1), 6–11.
Sloka, S., Zhornitsky, S., Silva, C., Metz, L.M., Yong, V.W., 2015. 1,25-Dihydroxyvitamin D-3 protects against immune-mediated killing of neurons in culture and in experimental autoimmune encephalomyelitis. PLoS One 10 (12).
Smolders, J., Hupperts, R., Vieth, R., Holmøy, T., Marhardt, K., Schluep, M., Killestein, J., Barkhof, F., Grimaldi, L.M., Beelke, M., 2016. High Dose Cholecalciferol (Vitamin D3) Oil as Add-on Therapy in Subjects with Relapsing-remitting. ECTRIMS.
Taniura, H., Ito, M., Sanada, N., Kuramoto, N., Ohno, Y., Nakamichi, N., Yoneda, Y., 2006. Chronic vitamin D3 treatment protects against neurotoxicity by glutamate in association with upregulation of vitamin D receptor mRNA expression in cultured rat cortical neurons. J. Neurosci. Res. 83 (7), 1179–1189.
Trapp, B.D., Nave, K.A., 2008. Multiple sclerosis: an immune or neurodegenerative disorder? Annu. Rev. Neurosci. 31, 247–269.
Trapp, B.D., Peterson, J., Ransohoff, R.M., Rudick, R., Mørk, S., Bø, L., 1998. Axonal transection in the lesions of multiple sclerosis. N. Engl. J. Med. 338 (5), 278–285.
Trapp, B.D., Ransohoff, R., Rudick, R., 1999. Axonal pathology in multiple sclerosis: relationship to neurologic disability. Curr. Opin. Neurol. 12 (3), 295–302.
Wergeland, S., Torkildsen, O., Myhr, K.M., Aksnes, L., Mork, S.J., Bo, L., 2011. Dietary vitamin D3 supplements reduce demyelination in the cuprizone model. PLoS One 6 (10), e26262.
Zendedel, A., Beyer, C., Kipp, M., 2013. Cuprizone-induced demyelination as a tool to study remyelination and axonal protection. J. Mol. Neurosci. 51 (2), 567–572.

Supplementary table 1 (Table S1) Demyelination

			Demyelination						Remyelination		
Week	1	2	3	4	5	6	7	8	9	10	11
Cuprizone (n = 12 x 4)											
Vitamin D diets											
Cuprizone											
Euthanasia									•		•
Controls (n = 6 x 4)											
Vitamin D diets											
Cuprizone											
Euthanasia											•

Overview of experimental groups, cuprizone exposure, vitamin D-diet and euthanasia through the experimental period. 72 mice were randomized to one of four groups, 1) <50 IU/kg, 2) 500 IU/kg, 3) 6200 IU/kg and 4) 12500 IU/kg. After two weeks 48 mice were randomized to 6 weeks cuprizone exposure. The animals were euthanized after 9 and 11 weeks. Published results for week 9 (6 weeks cuprizone exposure).

Supplementary table 2 (Table S2) Remyelination

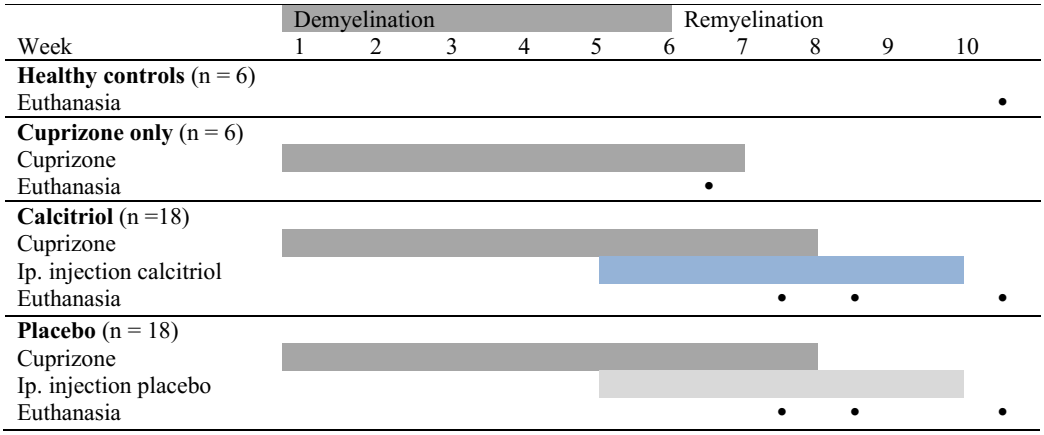

Overview of experimental groups, cuprizone exposure, intra-peritoneal (ip.) injections twice weekly and euthanasia through the experimental period. 48 mice were randomized to one of four groups, 1) healthy controls, 2) cuprizone only, 3) 2µg calcitriol cuprizone and 4) 2µg placebo cuprizone. After two weeks 42 mice were exposed to cuprizone. The animals were euthanized after 6, 7, 8 and 10 weeks. Published results from week 10 (3 weeks remyelination).

Supplementary table 3 (Table S3)

Antigen	Species/isotype	Antigen retrieval	Working dilution	Incubation time and room temperature (RT)	Target	Source
NFL[1]	Mouse IgG1, mAb	Tris-EDTA	1:1600	1h/RT	Phosphorylated neurofilament chain L	Millipore
SMI-32[2]	Mouse IgG1, mAb	Citrate	1:2000	1h/RT	Non-Phosfoylated chain H	Millipore
APP[3]	Mouse IgG1, mAb	Citrate	1:2000	24h/RT	APP: protein A4	Millipore

Antibodies used for immunohistochemistry specified.

mAb = monoclonal antibody.

[1]Anti-Neurofilament 70 kDa antibody, clone DA2, MAB1615.

[2]Anti-Neurofilament H Non-Phosphorylated.

[3]Anti-Alzheimer Precursor Protein A4, clone 22C11.

III

Journal of Neuroimmunology 285 (2015) 180–186

Contents lists available at ScienceDirect

Journal of Neuroimmunology

journal homepage: www.elsevier.com/locate/jneuroim

Fingolimod does not enhance cerebellar remyelination in the cuprizone model

Maria Nordheim Alme [a,*], Agnes E. Nystad [b,c], Lars Bø [a,b,c], Kjell-Morten Myhr [a,b,c], Christian A. Vedeler [a,c,d], Stig Wergeland [b,c], Øivind Torkildsen [a,b,c]

[a] Department of Clinical Medicine, University of Bergen, Pb 7804, 5020 Bergen, Norway
[b] Norwegian Multiple Sclerosis Competence Centre, Department of Neurology, Haukeland University Hospital, Haukelandsveien 22, 5021 Bergen, Norway
[c] Kristian Gerhard Jebsen MS Research Centre, Department of Clinical Medicine, University of Bergen, Pb 7804, 5020 Bergen, Norway
[d] Department of Neurology, Haukeland University Hospital, Haukelandsveien 22, 5021 Bergen, Norway

ARTICLE INFO

Article history:
Received 1 April 2015
Received in revised form 8 June 2015
Accepted 10 June 2015

Keywords:
FTY720
Fingolimod
Cuprizone
Cerebellum
Demyelination
Remyelination

ABSTRACT

Fingolimod (FTY720) is approved for treatment of relapsing–remitting multiple sclerosis. In vitro studies have found that fingolimod stimulates remyelination in cerebellar slices, but in vivo animal studies have not detected any positive effect on cerebral remyelination. The discrepant findings could be a result of different mechanisms underlying cerebral and cerebellar remyelination. The cuprizone model for de- and remyelination was used to evaluate whether fingolimod had an impact on cerebellar remyelination in vivo. We found that fingolimod did not have any effect on cerebellar remyelination, number of mature oligodendrocytes, microglia or astrocytes when fed after cuprizone exposure.

1. Introduction

Fingolimod (FTY720) is a non-selective sphingosine 1-phosphate (S1P) receptor modulator that regulates lymphocyte trafficking and retains lymphocytes within the lymph node. It is widely used for the treatment of relapsing–remitting multiple sclerosis (RRMS). S1P receptors are also expressed on neuroglia and fingolimod could therefore have a role in neuroprotection and remyelination independent on its role on peripheral lymphocytes (Brinkmann et al., 2010; Groves et al., 2013; Sobel et al., 2015). It has been demonstrated that fingolimod enhances oligodendrocyte survival (Miron et al., 2008a,b), as well as remyelination in organotypic cerebellar slices in vitro (Miron et al., 2010). However, fingolimod is not able to promote remyelination in the corpus callosum (Hu et al., 2011; Kim et al., 2011; Slowik et al., 2015) or cerebral cortex (Slowik et al., 2015) of mice after experimentally induced demyelination. Different mechanisms seem to underlay cortical and white matter remyelination (Gudi et al., 2009), as well as cerebellar remyelination (Skripuletz et al., 2010), suggesting that the discrepant findings could have resulted from comparisons of different brain areas.

The cuprizone model is a T cell independent experimental model of toxic CNS demyelination. The copper chelator *bis*-cyclohexanone oxaldihydrazone (cuprizone) induces apoptosis of mature oligodendrocytes with subsequent myelin disruption, microglia activation, astrogliosis and infiltration of blood monocytes (macrophages) (Blakemore, 1973a; Torkildsen et al., 2008; Praet et al., 2014). The model demonstrates acute, selective demyelination with subsequent spontaneous remyelination after five weeks of cuprizone exposure (Blakemore, 1973b; Skripuletz et al., 2011; Wergeland et al., 2012). Although most studies using this model have focused on corpus callosum demyelination, demyelination and remyelination in the cerebellum have been well-studied and described (Groebe et al., 2009; Skripuletz et al., 2010), making it an ideal model to study the effects of fingolimod on cerebellar remyelination in vivo.

2. Methods

2.1. Mice

Five-week-old female c57Bl/6 mice (total n = 32) were purchased from Tacomic, Tornbjerg, Denmark. Mean weight was 18.5 g +/− SD

Abbreviations: S1P, sphingosine 1-phosphate; Wr, weeks of recovery; β-APP, amyloid β precursor protein; IHC, immunohistochemistry; PL, Purkinje layer; GL, granule layer.

* Corresponding author.
E-mail addresses: maria.alme@uib.no (M.N. Alme), Agnes.elisabeth.nystad@helse-bergen.no (A.E. Nystad), lars.bo@helse-bergen.no (L. Bø), kjell-morten.myhr@helse-bergen.no (K.-M. Myhr), christian.alexander.vedeler@helse-bergen.no (C.A. Vedeler), stig.wergeland@helse-bergen.no (S. Wergeland), oivind.torkildsen@helse-bergen.no (Ø. Torkildsen).

http://dx.doi.org/10.1016/j.jneuroim.2015.06.006

1.1. The mice were acclimatized for 12 days prior to the experiment. They were housed by six together in GreenLine type II cages with open top (Scanbur, Karlslunde, Denmark), in standard laboratory conditions. Cage maintenance was performed once a week and the animals were handled by the same individuals throughout the experimental period. Food and tap water were available ad libitum throughout the acclimatization and experimental period. The experiment was carried out in accordance with the European Laboratory Animal Science Associations recommendations, and the protocol was approved by the Norwegian Animal Research Authority (permit 2013*5682).

2.2. Study design, cuprizone administration and fingolimod treatment

To induce demyelination, all mice were fed with 0.2% cuprizone (Sigma, St. Louis, MO, USA) mixed into ground mouse chow for six weeks. Cuprizone exposure was then discontinued. Control group (no demyelination) got normal mouse chow for the entire period. To study the effect on cerebellar remyelination, fingolimod was reconstituted in distilled water and given orally 1×/d by gavage at 1 mg/kg (Hu et al., 2011; Kim et al., 2011; Deshmukh et al., 2013) body weight from week five. Cuprizone exposure and fingolimod treatment overlapped with one week to make sure that the drug was taken up and phosphorylated to its active compound while cuprizone was still present. For comparison, animals in the cuprizone control group (maximal demyelination) were given the same volume of water (vehicle) by gavage. To study the dynamic effect of fingolimod on remyelination, animals in each group ($n = 4$) were sacrificed at weeks 5, 6 (1 wr), 7 (2 wr) and 9 (4 wr) as illustrated in Fig. 1. The animals were anesthetized with midazolam (Dormicum; F. Hoffmann-La Roche AG, Basel, Switzerland) in combination with fentanyl/fluanisone (Hypnorm, VetaPharma Ltd., UK) and sacrificed by cardiac puncture. Cerebelli were removed, post-fixed in 4% paraformaldehyde (PFA) and cryo-preserved.

2.3. Immunohistochemsitry

Sagittal 8 μm sections were cut on a Leica CM1960 cryostat. Antigen retrieval was performed using the 2100 Retriever and Diva decloaker buffer as described by the manufacturer (Dako, Glostrup, Denmark), unless otherwise specified. Antibodies used: Iba1 (1:1000, Wako chemicals 019-19741), GFAP (1:1000, Sigma G3893), NOGO-A (1:500, Millipore AB5664P), β-APP (1:1000, Abcam ab32136), PLP1 (1:1000, AbD Serotec MCA839G), MBP (1:500, without antigen retrieval, Abcam ab24567), and neurofilament (1:1000, Millipore MAB1615). Secondary antibodies were Alexa Fluor 488 and 594 anti-mouse or anti-rabbit. Pictures were taken with a Nikon TE2000, with a 10× or 40× objective, or a Leica Confocal SP2 with 40× or 63× objective. Myelin was analysed by visual scoring of demyelination on a scale from 0 (no demyelination) to 3 (total demyelination), as previously described (Skripuletz et al., 2010; Wergeland et al., 2011). Results are given as a mean between the score for PLP1 and MBP. For cell number analysis, numbers are given as a mean from 2 pictures within the subcortical region and 2 pictures from the cerebellar cortex (Fig. 1b). β-APP was measured by counting particles in the range of 10–600 pixels using the FIJI software. 2–4 sections were analysed for each animal per antibody. All analyses were done blinded.

2.4. Statistics

One-way analysis of variance (ANOVA) was used to analyse parametric data, followed by Fisher's least significant difference (LSD) for post-hoc analysis when applicable. Kruskal–Wallis H-test was used to analyse non-parametric data. Statistical analyses were done using IBM SPSS statistics 22.

3. Results

3.1. Mice

After five weeks of cuprizone exposure, cuprizone-exposed mice had a mean weight 18.5 g +/− 1.1 (SD) compared to 22.1 +/− 1.2 (SD) in healthy controls ($p < 0.0001$). There were no significant differences between mice randomized to fingolimod or vehicle treatment ($p = 0.23$). After ending cuprizone exposure, no significant weight difference between fingolimod and vehicle treated mice was observed at any time points (data not shown). One mouse died of unknown cause.

3.2. Remyelination

To evaluate cerebellar de- and remyelination, PLP1- and MBP- staining was scored in the subcortex and two areas of rostral parts of cerebellar cortex as shown in Fig. 1b. The myelin scores are provided as the mean of PLP1 and MBP scores. Subcortical demyelination of the cerebellum was robust and significant in animals exposed to cuprizone ($p < 0.0005$) (Fig. 2). After 2 weeks of recovery, there was a mild and significant subcortical remyelination for both placebo ($p < 0.0005$) and fingolimod ($p = 0.05$). After 4 weeks of recovery, remyelination was clearer ($p < 0.0005$ for both placebo and fingolimod compared to the cuprizone control group), although not complete (significant demyelination for both groups compared to the control group, $p < 0.0005$). Cuprizone exposure led to mild demyelination of the cerebellar cortex that did not reach significance on group level ($p = 0.054$). Single comparison between the control group and cuprizone control group showed significant demyelination. Similar single comparison showed significant remyelination after 4 weeks (both placebo and fingolimod) compared to the cuprizone control group. There were no significant effects of fingolimod at any time points, neither in the cerebellar subcortex nor in the cerebellar cortex (Fig. 2).

3.3. Axonal damage

Accumulation of β-APP was measured to study acute axonal damage. Cuprizone exposure led to a significant increase in β-APP positive

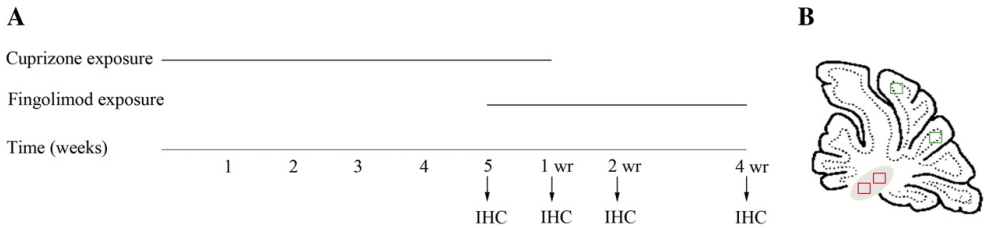

Fig. 1. Study design. Mice were fed with cuprizone for 6 weeks. From week 5, either fingolimod or placebo (vehicle) was given by gauge. Mice were sacrificed and cerebellum taken for IHC at 5 weeks cuprizone exposure (cuprizone control), 1 wr, 2 wr, and 4 wr (A). Mouse cerebellum with rectangles showing the regions examined with IHC, red; subcortical region, green; Purkinje cell and internal granule layer (B). Wr: weeks of recovery. IHC: immunohistochemistry.

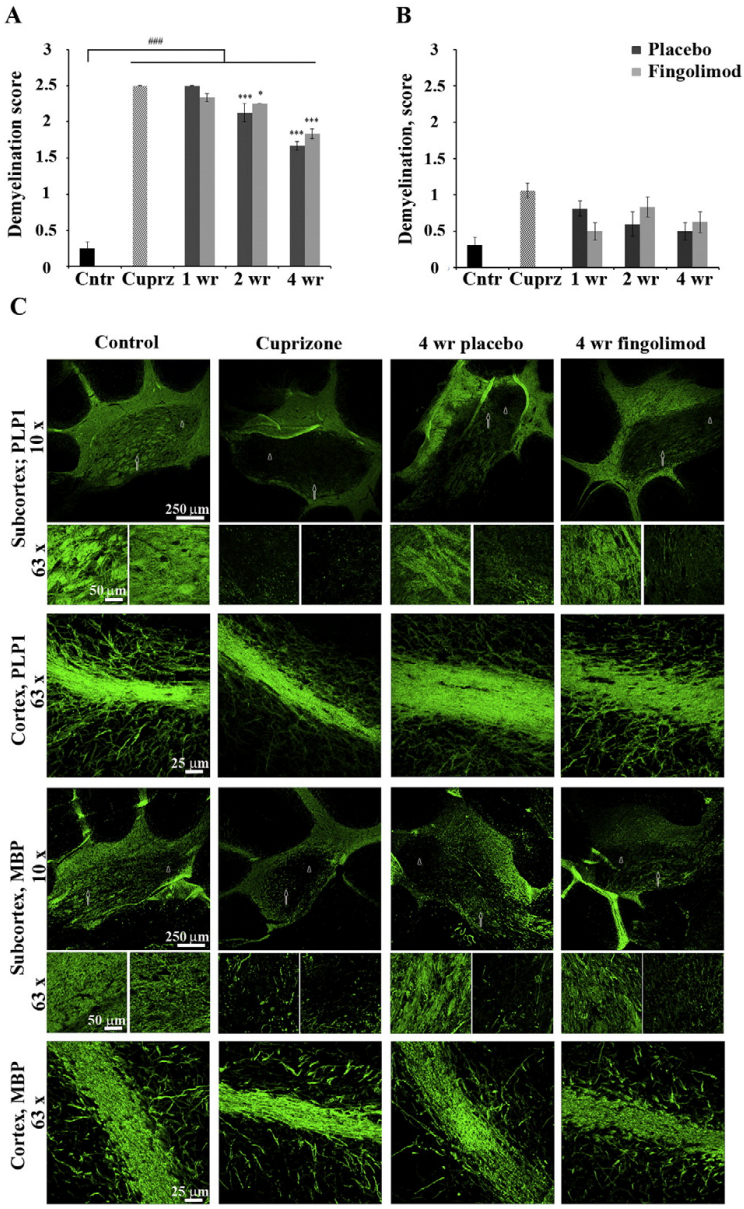

Fig. 2. Effect of fingolimod on remyelination in cerebellum of cuprizone-exposed mice. Robust subcortical demyelination was apparent after 5 weeks of cuprizone exposure compared to untreated controls. After 2 weeks of recovery, both placebo and fingolimod groups were significantly remyelinated and remyelination proceeded throughout the recovery period (A). Cuprizone exposure led to a mild, but not significant, demyelination of the cerebellar cortex (B). Representative pictures show myelination (PLP1 and MBP) in the subcortex and cortex of mouse cerebellum for control, 5 weeks of cuprizone exposure and after 4 weeks of fingolimod/placebo treatment. For subcortex, higher magnification pictures (63×) of the region with highest degree of myelination (arrow) and lowest degree of myelination (arrow head) are given (C). 2–4 sections were analysed per animal ($n = 3–4$). $^{###}p < 0.001$ to control group. $^{***}p < 0.001$, $^{*}p < 0.5$ to cuprizone group. Scale bars: 250 µm for subcortex (10×), 25 µm for subcortex (63×) and 50 µm cortex (63×).

axons in the subcortical region ($p < 0.0005$) (Fig. 3a). There was no loss of neurofilament positive axons after cuprizone treatment (Fig. 3b). After 1 week of recovery β-APP positive axons were almost not detectable, and the levels remained low and close to baseline in the recovery period ($p < 0.0005$ for all groups compared to 5 weeks of cuprizone exposure). There were no differences in the number of β-APP positive axons between fingolimod- and placebo treated mice. In cerebellar cortical regions, no β-APP positive axons were detected (results not shown).

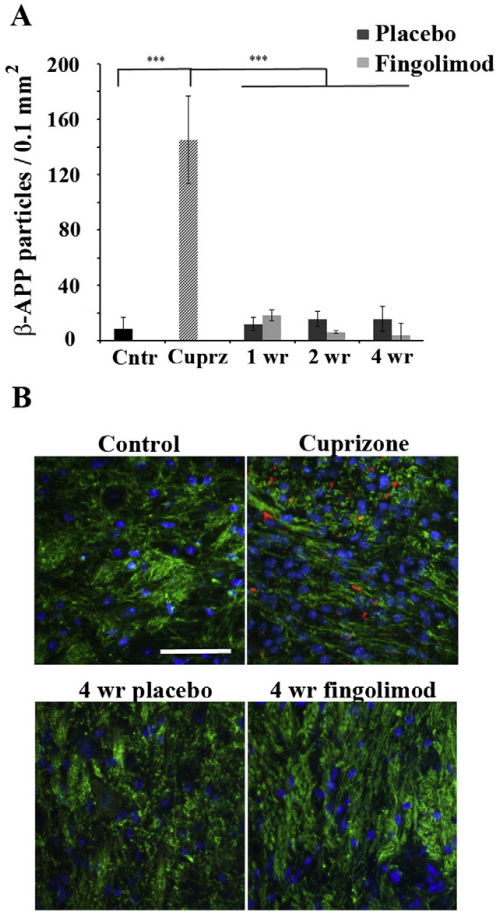

Fig. 3. Effect from fingolimod on accumulation of subcortical β-APP accumulation and neurofilment integrity. Five weeks of cuprizone exposure led to an increased subcortical accumulation of β-APP with no change of neurofilament integrity. After 1 week of recovery β-APP positive axons were hardly detected. Fingolimod did not affect the accumulation of β-APP particles throughout the recovery period (A). Subcortical β-APP (red) and neurofilament (green) staining of control, after 5 weeks of cuprizone exposure and after 4 weeks of recovery (B). 2–4 sections were analysed per animal (n = 3–4). β-APP: amyloid β precursor protein. ***p < 0.001. Scale bar 25 μm.

3.4. Mature oligodendrocytes, astrocytes and microglia

Cuprizone exposure led to a significant subcortical and cortical loss of NOGO-A positive mature oligodendrocytes ($p = 0.003$ and $p = 0.001$). In both regions, the number of NOGO-A positive oligodendrocytes increased during the recovery period, reaching normal levels by 4 weeks of recovery. Fingolimod did not have any significant effect on NOGO-A positive (mature) oligodendrocytes (Fig. 4a and b).

There was a subcortical increase in GFAP-positive astrocytes after 5 weeks of cuprizone treatment (>4-fold, $p < 0.0005$) (Fig. 4 c). During remyelination, the number of GFAP-positive astrocytes remained high in both placebo- and fingolimod-groups, with no significant differences at any time points. In the cerebellar cortex, there were no changes in number of GFAP-immunopositive astrocytes at any time points.

In line with previous studies (Groebe et al., 2009; Ingwersen et al., 2012), 5 weeks of cuprizone exposure led to a robust subcortical increase in Iba1-positive microglia/macrophages (12-fold, $p < 0.0005$) (Fig. 5a). It has previously been found that cuprizone-induced microgliosis is a combination of strong local proliferation of brain resident microglia and infiltration of blood-derived monocytes (macrophages) (Praet et al., 2014). In this study, microglia and infiltrated macrophages were not distinguished and are referred to as microglia. During the recovery phase, the number of microglia steadily decreased, although not to normal levels. In the cerebellar cortex, there was no significant microgliosis (Fig. 5b). Fingolimod did not have any effect on microglia numbers at any time points.

4. Discussion

The aim of this study was to investigate the possible effect of fingolimod on cerebellar remyelination in vivo by using the cuprizone model. We analysed three time points during the recovery phase without detecting any effect of fingolimod on cerebellar remyelination. We did not detect any effect of fingolimod on maturation of oligodendrocytes, microglia numbers or GFAP positive astrocytes in the recovery period after cuprizone induced demyelination.

The cuprizone mouse model is a highly reproducible and well described animal model used to study mechanisms underlying de- and remyelination (Torkildsen et al., 2008; Wergeland et al., 2012; Praet et al., 2014). Previous work from our group has shown that a vitamin D rich diet can reduce demyelination (Torkildsen et al., 2009; Wergeland et al., 2011) and promote remyelination (Nystad et al., 2014) in the corpus callosum of cuprizone-exposed mice.

In line with previous studies (Groebe et al., 2009; Skripuletz et al., 2010), cuprizone exposure induced cerebellar demyelination. Subcortical regions were severely demyelinated, while demyelination was minor in the cerebellar cortex after five weeks of cuprizone exposure. We did not detect remyelination after the first week of recovery, suggesting that cerebellar remyelination is delayed compared to the rapid remyelination seen in the corpus callosum (Skripuletz et al., 2008; Wergeland et al., 2012). Remyelination is known to be initiated by proliferation and migration of oligodendrocyte precursor cells towards the lesion site where they mature into myelin forming mature oligodendrocytes in a process that is dependent on a plethora of growth factors and signalling molecules (Praet et al., 2014). S1P is considered a survival factor for mature oligodendrocytes (Jaillard et al., 2005) and when fingolimod is given together with cuprizone, it protects mature oligodendrocytes from apoptosis (Kim et al., 2011). In our study, fingolimod was given after cuprizone-induced remyelination, at a time point where hardly any mature oligodendrocytes were present in the demyelinated area. The number of NOGO-A positive mature oligodendrocytes steadily increased during the recovery phase, corresponding to subcortical remyelination, without any influence from fingolimod.

It has been shown that fingolimod may have neuroprotective properties, reducing axonal damage in the corpus callosum after acute and chronic cuprizone-induced demyelination (Slowik et al., 2015). However, we did not detect any effect of fingolimod on axonal damage in the cerebellum, as subcortical β-APP positive axons were almost at baseline levels after one week of remyelination and there were no differences in neurofilament levels or number of APP-positive axons between placebo and fingolimod groups throughout the recovery phase.

Cuprizone exposure resulted in sustained subcortical astrogliosis throughout the remyelination period. This is in line with previous studies (Groebe et al., 2009; Hibbits et al., 2012), and has been suggested that astrocytes promote remyelination by supporting oligodendrocyte differentiation and recruitment of microglia/macrophages to lesion sites (Nair et al., 2008; Praet et al., 2014; Tanaka and Yoshida, 2014). Five weeks of cuprizone exposure induced extensive subcortical microgliosis, which declined during the recovery phase independent of fingolimod treatment. This is in line with recent results from the corpus callosum

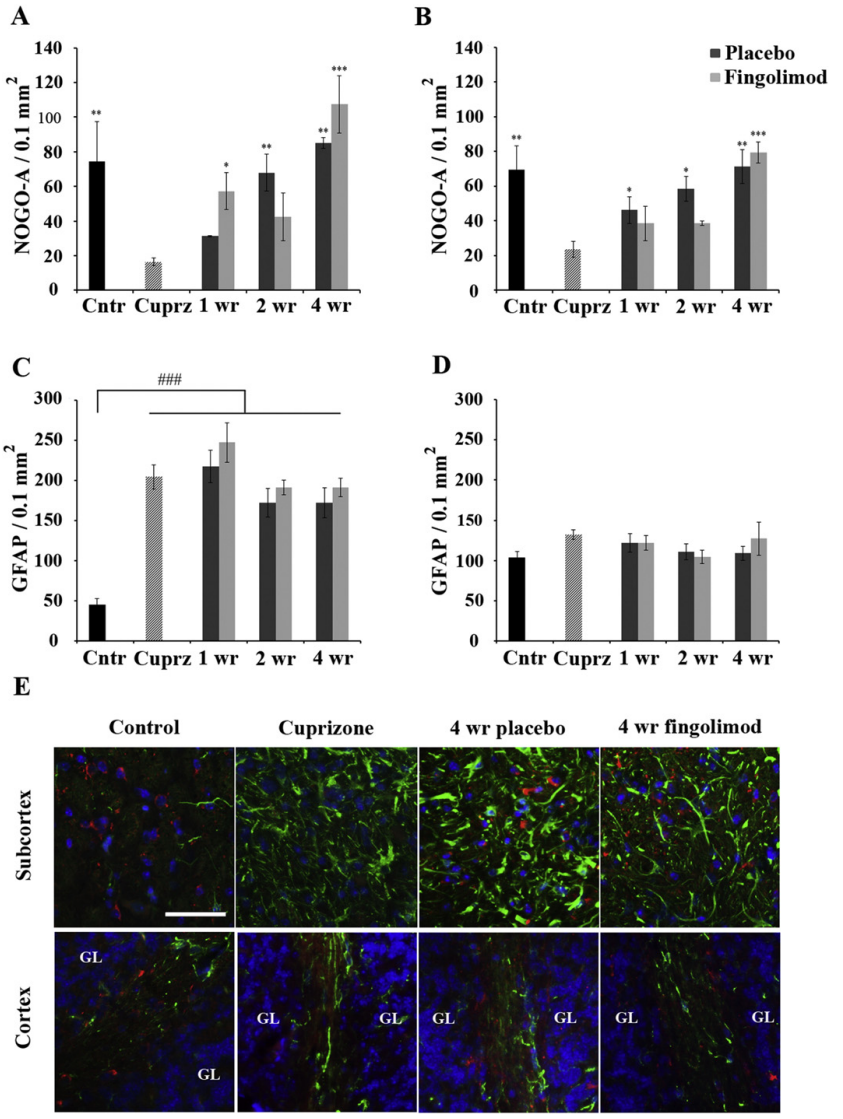

Fig. 4. Effect from fingolimod on mature oligodendrocytes and astrocytes in mouse cerebellum after cuprizone exposure. Numbers of NOGO-A positive oligodendrocytes were significantly reduced in the subcortex (A) and cortex (B) after 5 weeks of cuprizone exposure. During the recovery period, there was a steady increase in NOGO-A positive oligodendrocytes in both regions, reaching normal levels after 4 weeks of recovery (A and B). Cuprizone exposure led to robust subcortical astrogliosis that sustained during the recovery phase (C). No astrogliosis was seen in the cerebellar cortex (D). NOGO-A positive mature oligodendrocytes (red) and GFAP-expressing astrocytes (green) in subcortex and cortex in control, 5 weeks of cuprizone exposure and after 4 weeks of recovery (E). 3–4 sections were analysed per animal ($n = 3–4$). $^{***}p < 0.001$, $^{**}p < 0.01$,$^{*}p < 0.05$ to cuprizone, $^{###}p < 0.001$ to control group, GL: granule layer. Scale bar 25 μm.

(Slowik et al., 2015). Whether fingolimod has any clinical significant effect on microglia is debated (Groves et al., 2013). The use of different experimental model systems, inducing CNS damage with different aetiologies, could be a plausible explanation for the discrepant findings. Regenerative functions of microglia depend on their phenotype. Microglia in a pro-inflammatory state are considered inhibitory to remyelination while microglia in an anti-inflammatory state could promote remyelination by phagocytosis of myelin debris and secretion of cytokines and growth factors (Miron and Franklin, 2014). In this study we analysed the total number of microglia without distinguishing between different functional phenotypes and it is therefore possible that fingolimod has functional effects on microglia that we did not detect. However, regardless of any effects on microglia functions, we did not find that fingolimod promotes remyelination in the cuprizone model.

Fingolimod is effective in preventing acute attacks in RRMS by internalising T cells in the lymph nodes (Brinkmann et al., 2010; Ingwersen et al., 2012). From murine models it has been found that fingolimod is distributed to and phosphorylated to its active form

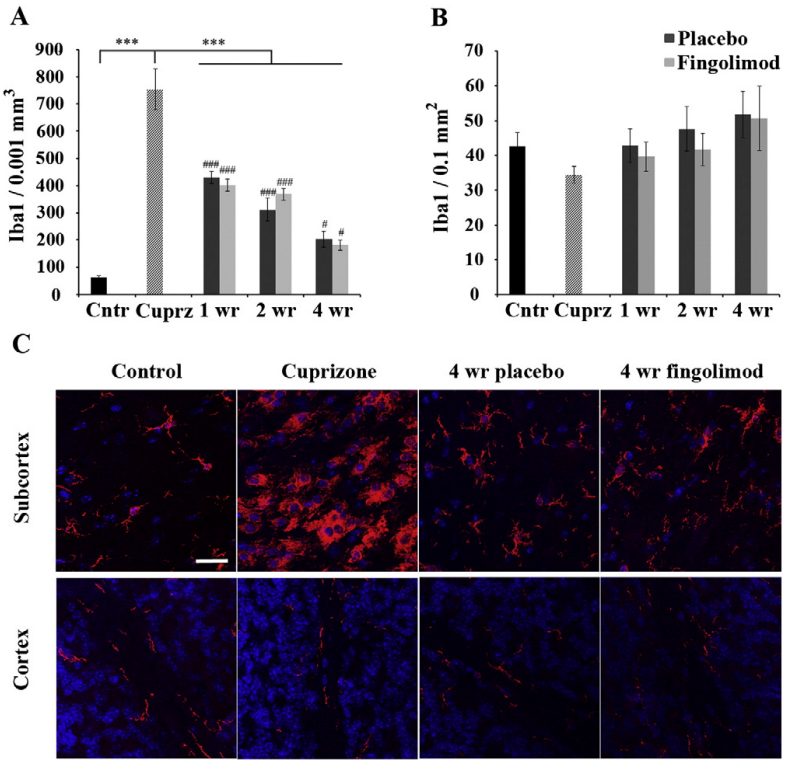

Fig. 5. Effect from fingolimod on microglia in mouse cerebellum after cuprizone exposure. There was extensive subcortical microgliosis (Iba1) after 5 weeks of cuprizone exposure which steadily decreased during the recovery period. There were no differences between fingolimod and placebo groups (A). No microgliosis was detected in cerebellar cortex after 5 weeks of cuprizone exposure (B). Representative pictures show microglia in the subcortex and cortex in control, 5 weeks of cuprizone exposure and after 4 weeks of recovery (C). 3–4 sections were analysed per animal (n = 3–4). ***$p < 0.001$ to cuprizone. #$p < 0.05$, ###$p < 0.001$ to control group. PL: Purkinje layer. GL: granule layer. Scale bar 25 μm.

within the brain (Meno-Tetang et al., 2006). It has therefore been suggested that fingolimod could modulate immune responses and promote CNS regeneration by targeting neurons and neuroglia (Miron et al., 2008c; Groves et al., 2013). As S1P is involved in immune cell trafficking, vascular homeostasis and cell communication in the CNS, it has been suggested that S1P can mediate activation and proliferation of neuroglia during inflammatory responses (Brinkmann, 2007). Results from the present study show that there is no effect of fingolimod on maturation of oligodendrocytes, astrogliosis or microgliosis in the cerebellum after cuprizone exposure. This indicates that modulating neuroglial S1P receptors by fingolimod does not have any clear regenerative effects although it has been found to have some neuroprotective effects during cuprizone induced CNS damage (Kim et al., 2011).

5. Conclusions

We show that fingolimod does not affect cerebellar remyelination, number of mature oligodendrocytes, microglia or astrocytes in the recovery phase after cuprizone-induced demyelination. This suggests that fingolimod does not have any effect on cerebellar remyelination in vivo. Our conclusions are in line with the previous reported in vivo studies on the corpus callosum (Hu et al., 2011; Kim et al., 2011; Slowik et al., 2015), but differ from the in vitro study using organotypic cerebellar slices (Miron et al., 2010). We suggest that the discrepant results are caused by the use of different experimental models and not by different effects from fingolimod on cerebral and cerebellar remyelination.

Conflict of interest

MNA and AEN have received unrestricted grants from Novartis.

SW has received unrestricted grants and honoraria as a speaker from Alexion Pharmaceuticals and Novartis.

LB has participated on scientific advisory boards for Novartis Norway; received funding for travel from Sanofi-Aventis, Novartis, Merck-Serono and Biogen Idec; received speaker honoraria from Bayer, Genzyme, Sanofi-Aventis, Novartis, Merck-Serono and Biogen Idec; and received unrestricted research support from Bayer, Sanofi-Aventis, Novartis, Merck-Serono and Biogen Idec.

KMM has participated on scientific advisory boards for Novartis Norway, Biogen Idec, and Genzyme; received funding for travel from Bayer, Novartis, Merck-Serono and Biogen Idec; received speaker honoraria from Bayer, Genzyme, Sanofi-Aventis, Novartis, Merck-Serono and Biogen Idec; and received unrestricted research support from Bayer, Sanofi-Aventis, Novartis, Merck-Serono, Biogen Idec, Pronova Biocare and Norwegian MS Society.

ØT has participated on a scientific advisory board for Biogen Idec and received speaker honoraria and travel grants from Genzyme, Merck-Serono, Novartis and Biogen-Idec.

Acknowledgements

This study was supported with an unconditional research grant from Novartis. Imaging was performed at the Molecular Imaging Center (MIC) at the University of Bergen.

References

Blakemore, W.F., 1973a. Demyelination of the superior cerebellar peduncle in the mouse induced by cuprizone. J. Neurol. Sci. 20, 63–72.

Blakemore, W.F., 1973b. Remyelination of the superior cerebellar peduncle in the mouse following demyelination induced by feeding cuprizone. J. Neurol. Sci. 20, 73–83.

Brinkmann, V., 2007. Sphingosine 1-phosphate receptors in health and disease: mechanistic insights from gene deletion studies and reverse pharmacology. Pharmacol. Ther. 115, 84–105.

Brinkmann, V., Billich, A., Baumruker, T., Heining, P., Schmouder, R., Francis, G., Aradhye, S., Burtin, P., 2010. Fingolimod (FTY720): discovery and development of an oral drug to treat multiple sclerosis. Nat. Rev. Drug Discov. 9, 883–897.

Deshmukh, V.A., Tardif, V., Lyssiotis, C.A., Green, C.C., Kerman, B., Kim, H.J., Padmanabhan, K., Swoboda, J.G., Ahmad, I., Kondo, T., Gage, F.H., Theofilopoulos, A.N., Lawson, B.R., Schultz, P.G., Lairson, L.L., 2013. A regenerative approach to the treatment of multiple sclerosis. Nature 502, 327–332.

Groebe, A., Clarner, T., Baumgartner, W., Dang, J., Beyer, C., Kipp, M., 2009. Cuprizone treatment induces distinct demyelination, astrocytosis, and microglia cell invasion or proliferation in the mouse cerebellum. Cerebellum 8, 163–174.

Groves, A., Kihara, Y., Chun, J., 2013. Fingolimod: direct CNS effects of sphingosine 1-phosphate (S1P) receptor modulation and implications in multiple sclerosis therapy. J. Neurol. Sci. 328, 9–18.

Gudi, V., Moharregh-Khiabani, D., Skripuletz, T., Koutsoudaki, P.N., Kotsiari, A., Skuljec, J., Trebst, C., Stangel, M., 2009. Regional differences between grey and white matter in cuprizone induced demyelination. Brain Res. 1283, 127–138.

Hibbits, N., Yoshino, J., Le, T.Q., Armstrong, R.C., 2012. Astrogliosis during acute and chronic cuprizone demyelination and implications for remyelination. ASN Neuro 4, 393–408.

Hu, Y., Lee, X., Ji, B., Guckian, K., Apicco, D., Pepinsky, R.B., Miller, R.H., Mi, S., 2011. Sphingosine 1-phosphate receptor modulator fingolimod (FTY720) does not promote remyelination in vivo. Mol. Cell. Neurosci. 48, 72–81.

Ingwersen, J., Aktas, O., Kuery, P., Kieseier, B., Boyko, A., Hartung, H.P., 2012. Fingolimod in multiple sclerosis: mechanisms of action and clinical efficacy. Clin. Immunol. 142, 15–24.

Jaillard, C., Harrison, S., Stankoff, B., Aigrot, M.S., Calver, A.R., Duddy, G., Walsh, F.S., Pangalos, M.N., Arimura, N., Kaibuchi, K., Zalc, B., Lubetzki, C., 2005. Edg8/S1P5: an oligodendroglial receptor with dual function on process retraction and cell survival. J. Neurosci. 25, 1459–1469.

Kim, H.J., Miron, V.E., Dukala, D., Proia, R.L., Ludwin, S.K., Traka, M., Antel, J.P., Soliven, B., 2011. Neurobiological effects of sphingosine 1-phosphate receptor modulation in the cuprizone model. FASEB J. 25, 1509–1518.

Meno-Tetang, G.M., Li, H., Mis, S., Pyszczynski, N., Heining, P., Lowe, P., Jusko, W.J., 2006. Physiologically based pharmacokinetic modeling of FTY720 (2-amino-2[2-(-4-octylphenyl)ethyl]propane-1,3-diol hydrochloride) in rats after oral and intravenous doses. Drug Metab. Dispos. 34, 1480–1487.

Miron, V.E., Franklin, R.J., 2014. Macrophages and CNS remyelination. J. Neurochem. 130, 165–171.

Miron, V.E., Hall, J.A., Kennedy, T.E., Soliven, B., Antel, J.P., 2008a. Cyclical and dose-dependent responses of adult human mature oligodendrocytes to fingolimod. Am. J. Pathol. 173, 1143–1152.

Miron, V.E., Jung, C.G., Kim, H.J., Kennedy, T.E., Soliven, B., Antel, J.P., 2008b. FTY720 modulates human oligodendrocyte progenitor process extension and survival. Ann. Neurol. 63, 61–71.

Miron, V.E., Schubart, A., Antel, J.P., 2008c. Central nervous system-directed effects of FTY720 (fingolimod). J. Neurol. Sci. 274, 13–17.

Miron, V.E., Ludwin, S.K., Darlington, P.J., Jarjour, A.A., Soliven, B., Kennedy, T.E., Antel, J.P., 2010. Fingolimod (FTY720) enhances remyelination following demyelination of organotypic cerebellar slices. Am. J. Pathol. 176, 2682–2694.

Nair, A., Frederick, T.J., Miller, S.D., 2008. Astrocytes in multiple sclerosis: a product of their environment. Cell. Mol. Life Sci. 65, 2702–2720.

Nystad, A.E., Wergeland, S., Aksnes, L., Myhr, K.M., Bo, L., Torkildsen, O., 2014. Effect of high-dose 1.25 dihydroxyvitamin D3 on remyelination in the cuprizone model. APMIS 122, 1178–1186.

Praet, J., Guglielmetti, C., Berneman, Z., Van Der Linden, A., Ponsaerts, P., 2014. Cellular and molecular neuropathology of the cuprizone mouse model: clinical relevance for multiple sclerosis. Neurosci. Biobehav. Rev. 47, 485–505.

Skripuletz, T., Lindner, M., Kotsiari, A., Garde, N., Fokuhl, J., Linsmeier, F., Trebst, C., Stangel, M., 2008. Cortical demyelination is prominent in the murine cuprizone model and is strain-dependent. Am. J. Pathol. 172, 1053–1061.

Skripuletz, T., Bussmann, J.H., Gudi, V., Koutsoudaki, P.N., Pul, R., Moharregh-Khiabani, D., Lindner, M., Stangel, M., 2010. Cerebellar cortical demyelination in the murine cuprizone model. Brain Pathol. 20, 301–312.

Skripuletz, T., Gudi, V., Hackstette, D., Stangel, M., 2011. De- and remyelination in the CNS white and grey matter induced by cuprizone: the old, the new, and the unexpected. Histol. Histopathol. 26, 1585–1597.

Slowik, A., Schmidt, T., Beyer, C., Amor, S., Clarner, T., Kipp, M., 2015. The sphingosine 1-phosphate receptor agonist FTY720 is neuroprotective after cuprizone-induced CNS demyelination. Br. J. Pharmacol. 172, 80–92.

Sobel, K., Monnier, L., Menyhart, K., Bolinger, M., Studer, R., Nayler, O., Gatfield, J., 2015. FTY720-P activates sphingosine-1-phosphate receptor 2 and selectively couples to Galpha12/13/Rho/ROCK to induce myofibroblast contraction. Mol. Pharmacol. 87 (6), 916–927.

Tanaka, T., Yoshida, S., 2014. Mechanisms of remyelination: recent insight from experimental models. Biomol. Concepts 5, 289–298.

Torkildsen, O., Brunborg, L.A., Myhr, K.M., Bo, L., 2008. The cuprizone model for demyelination. Acta Neurol. Scand. Suppl. 188, 72–76.

Torkildsen, O., Brunborg, L.A., Milde, A.M., Mork, S.J., Myhr, K.M., Bo, L., 2009. A salmon based diet protects mice from behavioural changes in the cuprizone model for demyelination. Clin. Nutr. 28, 83–87.

Wergeland, S., Torkildsen, O., Myhr, K.M., Aksnes, L., Mork, S.J., Bo, L., 2011. Dietary vitamin D3 supplements reduce demyelination in the cuprizone model. PLoS One 6, e26262.

Wergeland, S., Torkildsen, O., Myhr, K.M., Mork, S.J., Bo, L., 2012. The cuprizone model: regional heterogeneity of pathology. APMIS 120, 648–657.

IV

Journal of Neuroimmunology 339 (2020) 577091

Contents lists available at ScienceDirect

Journal of Neuroimmunology

journal homepage: www.elsevier.com/locate/jneuroim

Fingolimod downregulates brain sphingosine-1-phosphate receptor 1 levels but does not promote remyelination or neuroprotection in the cuprizone model

Agnes E. Nystad[a,b,*], Ragnhild Reehorst Lereim[c,d], Stig Wergeland[a,b], Eystein Oveland[c], Kjell-Morten Myhr[b,e], Lars Bø[a], Øivind Torkildsen[a,b]

[a] Norwegian Multiple Sclerosis Competence Centre, Department of Neurology, Haukeland University Hospital, Bergen, Norway
[b] Department of Clinical Medicine, University of Bergen, Bergen, Norway
[c] Proteomics Unit at University of Bergen (PROBE), Department of Biomedicine, University of Bergen, Norway
[d] Computational Biology Unit (CBU), Department of Informatics, University of Bergen, Bergen, Norway
[e] Neuro-SysMed, Department of Neurology, Haukeland University Hospital, Bergen, Norway

ARTICLE INFO

Keywords:
Fingolimod
Cuprizone
Remyelination
Multiple sclerosis
Quantitative proteomics
Sphingosine-1-phosphate receptors

ABSTRACT

Fingolimod is used to treat patients with relapsing-remitting multiple sclerosis; it crosses the blood-brain barrier and modulates sphingosine-1-phosphate receptors (S1PRs). Oligodendrocytes, astrocytes, microglia, and neuronal cells express S1PRs, and fingolimod could potentially improve remyelination and be neuroprotective. We used the cuprizone animal model, histo-, immunohistochemistry, and quantitative proteomics to study the effect of fingolimod on remyelination and axonal damage. Fingolimod was functionally active during remyelination by downregulating S1PR1 brain levels, and fingolimod-treated mice had more oligodendrocytes in the secondary motor cortex after three weeks of remyelination. However, there were no differences in remyelination or axonal damage compared to placebo. Thus, fingolimod does not seem to directly promote remyelination or protect against axonal injury or loss when given after cuprizone-induced demyelination.

1. Introduction

Multiple sclerosis (MS) is a chronic immune-mediated disease, characterized by inflammation, demyelination, and axonal degeneration of the central nervous system (CNS) (Lassmann, 2018). Current treatments target the inflammatory aspects of MS but do not directly promote CNS remyelination (Plemel et al., 2017). Pro-remyelinating substances may be an important supplement to immunomodulating therapies to optimize MS therapy. Fingolimod (2-amino-2-[2-(4-octylphenyl)ethyl]propane-1,3-diol) (Kiuchi et al., 1998) is used in the treatment of relapsing-remitting multiple sclerosis (RRMS) (Kappos et al., 2010; Calabresi et al., 2014; Thompson et al., 2018). The medication binds to and modulates sphingosine-1-phosphate receptors (S1PRs), causing sequestration of lymphocytes within lymph nodes by $S1P_1$ downregulation, which reduces lymphocyte infiltration into the CNS parenchyma (Chiba et al., 1998; Brinkmann et al., 2000). A wide range of cell types within the CNS expresses S1PRs, including oligodendrocytes (Jaillard et al., 2005), neurons, astrocytes (Pebay et al., 2001) and microglia (Chun and Hartung, 2010). Fingolimod crosses the blood-brain barrier (Brinkmann, 2007; Chun and Hartung, 2010; Groves et al., 2013) and may have a direct impact on CNS remyelination. However, results from experimental studies on the effects of fingolimod on remyelination are inconsistent. In vitro studies have indicated that fingolimod enhances remyelination in cerebellar slices (Miron et al., 2010) and promotes remyelination in a rat CNS spheroid culture (Jackson et al., 2011). In vivo, fingolimod improved remyelination following lysolecithin-induced demyelination in mice (Yazdi et al., 2015) and promoted the proliferation and differentiation of oligodendrocyte progenitors facilitating remyelination in experimental autoimmune encephalomyelitis (EAE) (Zhang, Zhang et al., 2015). However, other studies have not found that fingolimod improves remyelination (Hu et al., 2011; Kim et al., 2011; Alme et al., 2015; Slowik et al., 2015; Kim et al., 2018). A recent review indicates that fingolimod might have a direct and regulatory role in remyelination and that the dose of fingolimod and the time of administration are crucial to the remyelination process (Yazdi et al., 2019). In the present

Abbreviations: S1P, Sphingosine-1-phosphate; S1PRs, sphingosine-1-phosphate receptors

* Corresponding author at: Department of Neurology, Haukeland University Hospital, Jonas Lies road 65, 5021 Bergen, Norway.
E-mail address: agnes.elisabeth.nystad@helse-bergen.no (A.E. Nystad).

https://doi.org/10.1016/j.jneuroim.2019.577091
Received 20 September 2019; Received in revised form 22 October 2019; Accepted 22 October 2019

study, we aimed to clarify if fingolimod could promote remyelination and possibly diminish axonal damage in the cerebrum of mice in the cuprizone model for de- and remyelination.

2. Materials and methods

Additional information is available in the Supplementary methods.

2.1. Mice

Forty-eight, female, five-week-old c57Bl/6 mice were obtained from Taconic (Tornbjerg, Denmark), mean weight was 18,54 g ± 1,14 (SD). The mice were housed six together in GreenLine type II cages (Scanbur, Karlslunde, Denmark), in standard laboratory conditions. Food and tap water were available ad libitum. Cage maintenance was performed once a week, and the same individuals handled the mice throughout the experimental period. The experiment followed the recommendations of the Federation of European Laboratory Animal Science Associations, and the protocol was approved by the Norwegian Animal Research Authority (permit # 2013-5682).

2.2. Study design, cuprizone, and fingolimod/placebo administration

After 12 days of acclimatization, the mice ($n = 48$) were randomized into four groups: healthy controls ($n = 6$), cuprizone controls (n = 6), cuprizone + fingolimod ($n = 18$) and cuprizone + placebo (n = 18). We added 0.2% cuprizone (bis-cyclohexanone-oxaldihydrazone, Sigma-Aldrich, St. Louis, MO, USA) to milled mouse chow for six weeks, to induce demyelination. Subsequently, mice were fed normal chow. Fingolimod, 1 mg/kg (Hu et al., 2011; Kim et al., 2011; Deshmukh et al., 2013) reconstituted in distilled water or placebo (equivalent volume of water), was administered by oral gavage once daily from week 5. There was a one week overlap in cuprizone exposure and fingolimod treatment to make sure that fingolimod was taken up and phosphorylated to its active compound during the cuprizone exposure (Fig. S1A). For unknown reasons, one mouse died during the experiment resulting in 47 mice for analysis.

2.3. Histopathology and immunohistochemistry

In anesthesia by midazolam (Dormicum “Roche”) and fentanyl/fuanisone (Hypnorm “VetaPharma”), the animals were euthanized by cardiac puncture after five weeks (cuprizone controls), six weeks (DM, maximal demyelination), one week of remyelination (1RM) and after three weeks of remyelination (3RM) (Fig. S1A). Brains were dissected and post-fixed in 4% formaldehyde for at least seven days before paraffin embedding. For analyses, we used 3–7 μm coronal sections from the bregma ± 1 mm (Paxinos, 2008). Sections were histochemically stained with Luxol Fast Blue (LFB) to evaluate myelination. Before immunostaining, paraffin-embedded sections were dewaxed and rehydrated, and antigens were retrieved by microwaving sections in either TRIS-EDTA (pH 9.0) or citrate buffer (pH 6.1) (Nystad et al., 2014). Sections were stained for myelin (anti-Proteolipid Protein, PLP), mature oligodendrocytes (Neurite Outgrowth Inhibitor Protein A, NOGO-A), astrocytes (Glial Fibrillary Acidic Protein, GFAP), macrophages and microglia (MAC-3), T-cells (CD3), axonal transection and loss (respectively, amyloid precursor protein A4, APP, and phosphorylated neurofilament light, NFL). The use of buffers, dilutions, incubation times, and temperatures for the antibodies are specified in Table S1. Sections were blocked with peroxidase blocking solution and visualized with EnVision 3.3. – diaminobenzidine (1:50, 3 min at RT) (DAKO, Glostrup, Denmark). Furthermore, counterstained with hematoxylin, dehydrated, and fixated. Brain tissue from healthy or demyelinated mice controls served as controls for all stainings.

2.4. Analyzes of brain sections

We used light microscopy to analyze the sections (Zeiss Axio Imager.A2, Oberkochen, Germany). Myelin loss (LFB staining) was quantified by two blinded observers, using a semi-quantitative scoring system from no (0) to complete demyelination (3) as described before (Nystad et al., 2014). Reactive astrocytosis (GFAP immunoreactivity) was evaluated by a semi-quantitative scale as no (0), minimal (1), moderate (2) or extensive (3) (Wergeland et al., 2012). To evaluate the density of mature oligodendrocytes (NOGO-A immunopositive cells), activated microglia and macrophages (MAC-3 immunopositive cells), T-cells (CD3 immunopositive cells) and acute axonal damage (APP immunopositive cells), one blinded observer counted immunopositive cells within an area of 0.0625 mm^2 at 40×, using an ocular morphometric grid. Immunopositivity for pan-phosphorylated NFL and PLP was quantified using digital densitometry. The area of interest was photographed with identical exposure settings at 40× magnifications (Zeiss Axio Imager.A2 with AxioCam ERc5 digital camera). Greyscale images were thresholded using ImageJ, v1.41 (Research Services Branch, National Institute of Mental Health, Bethesda, Maryland, USA) to diminish background staining. Immunopositivity was expressed as the area of immunopositivity relative to (%) the total image area. Sections were assessed in the midline of the corpus callosum (CC), the lateral corpus callosum area, the supplemental somatosensory area, the secondary motor cortex (M2) and deep grey matter – striatum (Fig. S1B).

2.5. Statistical methods

We did a priori sample size calculations based on the differences in the myelin content between calicitriol- and placebo-treated mice from (Nystad et al., 2014), a sample size of six animals per experimental group would give a power of 0.7 (mean LFB.score of 2.0 ± SD 0.6 and 1.0 ± SD 0.6 after three weeks of remyelination). Kolmogorov-Smirnov and Shapiro-Wilk tests of normality were used to test the assumption of normally distributed data. We used independent sample *t*-tests to compare parametric data and the Mann-Whitney test for non-parametric data. Differences were considered significant at $p < 0.05$. The calculations were carried out unblinded, using Statistical Package for the Social Sciences (IBM Corp. Released 2017. IBM SPSS Statistics for Windows, Version 25.0. Armonk, NY: IBM Corp).

2.6. Quantitative proteomics

We prepared the samples of mouse brain lysates as previously described (Lereim et al., 2016). Briefly, the individual frontal right hemisphere of mice receiving fingolimod or placebo were lysed in 4% SDS, 100 mM Tris/HCl pH 7.6, 0.1 M DTT, and the protein concentration estimated. Before digestion, the samples were pooled (Table S2), and 50 μg of each pool was digested by the Filter-aided sample preparation (FASP) protocol (Wiśniewski et al., 2009). The samples were tagged by a tandem mass tag (TMT) 10-plex set (Thermo Scientific) that was split in two, enabling simultaneous tagging of 20 samples; 18 sample pools and two identical reference samples enabling combining and comparing the two 10 plexes (Table S2). Each TMT 10 plex experiment was fractioned by mixed-mode reverse phase chromatography as previously described (Lereim et al., 2016). This resulted in 58 fractions each 10 plex that was lyophilized and dissolved in 1% formic acid (FA)/2% acetonitrile (ACN) prior to LC-MS/MS analysis (supplementary methods). Following LC-MS/MS, peptides were identified, quantified, and normalized in Proteome discoverer 2.0 (Thermo Scientific). The samples were analyzed by the statistical software limma (Ritchie et al., 2015) in R. The script used to analyze the samples and create the graphics is available on GitHub (https://github.com/RagnhildRLereim/Fingolimod). We analyzed Gene Ontology Biological process enrichment for the proteins considered to be significantly different in Panther

(Thomas et al., 2006; Mi et al., 2019). The proteomics data is available in the PRIDE database (Vizcaino et al., 2016) under accession PXD012676 (Username: reviewer53224@ebi.ac.uk, Password: VJxAVcfS). For additional information about the quantitative proteomics experiment, see Supplementary methods.

3. Results

3.1. Effects of fingolimod treatment on the brain proteome during remyelination

Using TMT labeling and proteomics, we identified 7949 proteins, of which 7183 were quantified. In total, the same 6386 proteins were identified and quantified in both TMT 10-plexes and formed the basis of our statistical analysis with three mini pools for each condition, where each pool contained equal amounts of two biological replicates (Table S2). Significant proteomic changes were seen in the dataset ($p < 0.01$, $\log_2$ fold change (FC) Fingolimod – Placebo < -0.2, > 0.2) between the fingolimod and the placebo-treated animals, albeit the distribution of mean expression values were narrow (Fig. S2) and comparison analysis showed moderate fold changes (min $\log_2$ FC -1.17, max = 1.7, normal values = 0.4–3.2). A detailed table of the significant proteins from each comparison can be found in Supplementary tables S3–S5. Gene Ontology enrichment analysis of these proteins did not show any significantly overrepresented biological processes at any time point.

3.2. Fingolimod was functionally active during remyelination by downregulating S1PR1 levels

The two proteins, S1PR1, and guanine nucleotide-binding protein gamma 5 (GNG5) were significantly regulated in the samples from the fingolimod-treated mice compared to placebo at all measured time points (Fig. 1). Both S1PR1 and GNG5 were less abundant in samples from fingolimod-treated mice; however, only S1PR1 was significant after false discovery rate (FDR) correction ($q < 0.01$). At one week of remyelination, the protein Lysosomal thioesterase (PPT2) was significantly downregulated in the samples from fingolimod-treated mice after FDR correction.

3.3. Fingolimod did not affect remyelination

3.3.1. Remyelination in the corpus callosum and the cortex

There was a detectable loss of myelin in the midline of the corpus callosum (CC), as measured by LFB score after five weeks in the cuprizone-treated mice (1.5 ± SD 0.5) compared to healthy controls (0.33 ± SD 0.52, $p = 0.036$) (Fig. 2, Table S6A). There was no difference in myelin loss in the CC between the fingolimod group and placebo group after six weeks of demyelination (DM: 1.83 vs. 2.0, $p = 0.38$), one week of remyelination (1RM: 2.2 vs. 2.1, $p = 1.0$) or three weeks of remyelination (3RM: 1.7 vs. 1.25, $p = 0.40$) (Fig. 2, Table S6B–D). Similarly, there were no differences in PLP staining, at any time point (DM: $p = 0.64$, 1RM: $p = 0.96$, 3RM: $p = 0.28$, Fig. 3, Table S6B–D). Fingolimod did not affect the density of mature oligodendrocytes (NOGO-A, DM: $p = 0.58$, 1RM: $p = 0.31$, 3RM: $p = 0.90$, Fig. 4, Table S6B–D). In the secondary motor cortex, there was no difference in the LFB score (DM: $p = 1.0$, 1RM: $p = 0.77$, 3RM: $p = 1.0$.) or PLP immunopositivity (DM: $p = 0.128$, 1RM: $p = 0.481$, 3RM: $p = 0.662$) between the intervention groups. The density of mature oligodendrocytes was increased in fingolimod-treated mice compared to mice in the placebo group after three weeks of remyelination (5.17 ± SD 4.26 vs. 1.6 ± SD 0.55, $p = 0.032$). However, the number of mature oligodendrocytes were not increased in fingolimod mice after six weeks of demyelination ($p = 0.23$) or at one week of remyelination (p = 0.66) compared to placebo mice (Table S7B–D).

3.3.2. Proteomic markers of remyelination

During the remyelination phase, there was a time-dependent increase in proteins involved in myelination (Fig. 5). There were, however, no differences in levels of myelin basic protein (MBP), myelin-associated glycoprotein (MAG), myelin-oligodendrocyte glycoprotein (MOG), oligodendrocyte-myelin glycoprotein (OMG), myelin expression factor 2 (MYEF2), myelin-associated oligodendrocyte basic protein (MOBP), myelin transcription factor 1-like protein (MYT1l) or PLP between the intervention groups at any time points (Fig. 5). Correspondingly, no difference was detected in the protein abundance of NOGO between fingolimod- and placebo-treated mice at any time point (Fig. S3).

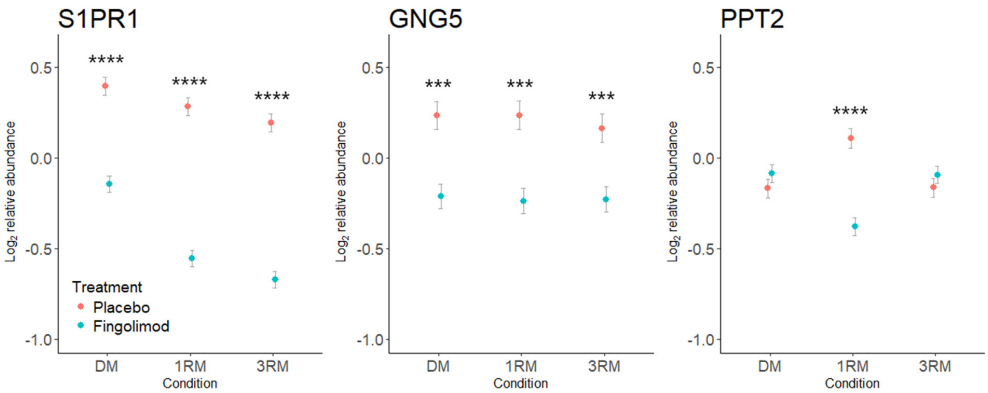

Fig. 1. Protein levels of S1PR1, GNG5 and PPT2 measured by quantitative proteomics.
Sphingosine-1-phosphate receptor-1 (S1PR1) and guanine nucleotide binding protein gamma 5 (GNG5) were significantly less abundant (p-value < 0.01, $\log_2$ FC Fingolimod – Placebo > 0.2, < -0.2) in fingolimod animals after six weeks of demyelination (DM), one week of remyelination (1RM) and 3 weeks of remyelination (3RM). S1PR1 was significantly different in all comparisons after FDR correction (q-value < 0.05). Lysosomal thioesterase (PPT2) was significantly downregulated at 1RM in fingolimod-treated mice after FDR correction. The average $\log_2$ abundance is plotted; the error bars represent the standard deviation based on three sample pools containing two biological replicates each.
*** = p-value $<$ 0.001, **** = p-value $\ll$ 0.0001.

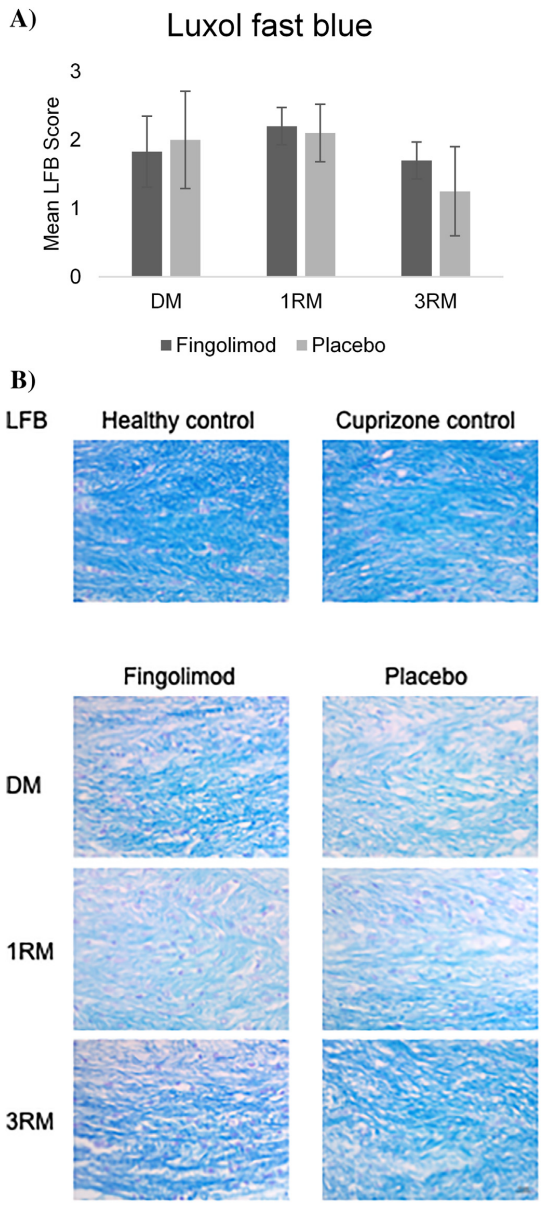

Fig. 2. Myelin loss measured by Luxol fast blue.
A) Myelin loss in the midline of corpus callosum in the placebo and fingolimod group after six weeks of demyelination (DM), one week of remyelination (1RM) and three weeks of remyelination (3RM), as measured by Luxol fast blue. Scale: no (0), minimal (0.5), < 33% (1), 33–66% (2) and > 66% (3) demyelination. Data presented as mean, error bars: ± 1 SD. Number (n) of animals included: DM placebo (n: 6), DM fingolimod (n: 6), 1RM placebo (n: 6), 1RM fingolimod (n: 5), 3RM placebo (n: 5), 3RM fingolimod (n: 5).
B) Luxol Fast Blue (LFB) stained sections. DM = six weeks of demyelination, 1RM = one week of remyelination, 3RM = three weeks of remyelination. All images at 40×. (For interpretation of the references to colour in this figure legend, the reader is referred to the web version of this article.)

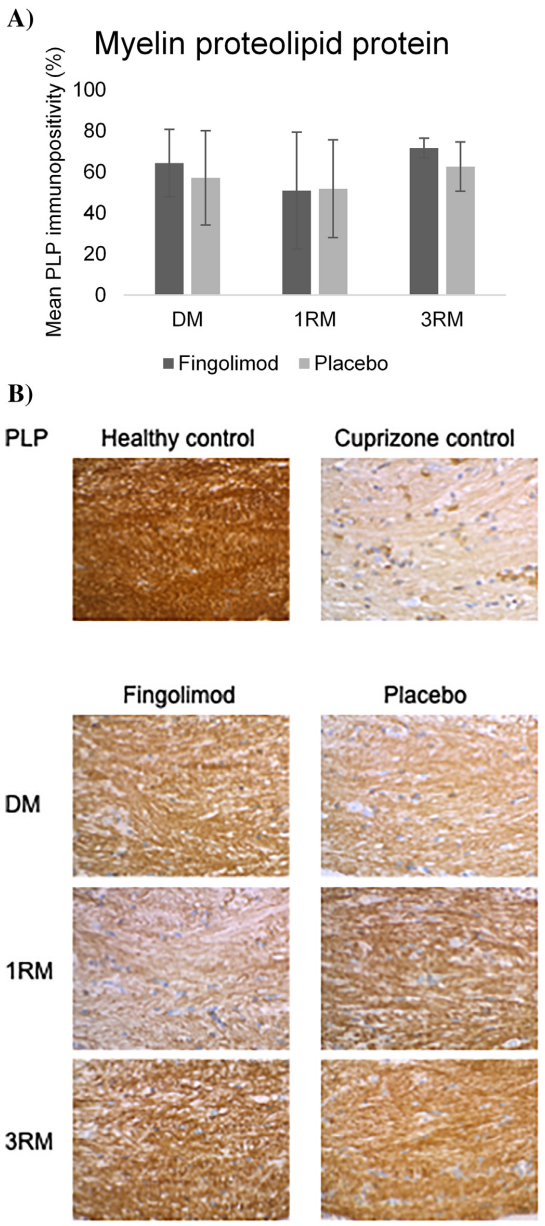

Fig. 3. Myelin loss measured by proteolipid protein immunoreactivity.
A) Immunoreactivity in % for PLP in the fingolimod and placebo group after six weeks of demyelination, one week of remyelination and three weeks of remyelination. There were no differences between the groups at any time point. Sections were scored in the midline of corpus callosum. Data presented as mean, error bars: ± 1 SD. Number (n) of animals included: DM placebo (n: 5), DM fingolimod (n: 5), 1RM placebo (n: 4), 1RM fingolimod (n: 4), 3RM placebo (n: 4), 3RM fingolimod (n: 5).
B) PLP and hematoxylin stained sections. DM = six weeks of demyelination, 1RM = one week of remyelination, 3RM = three weeks of remyelination. All images at 40×.

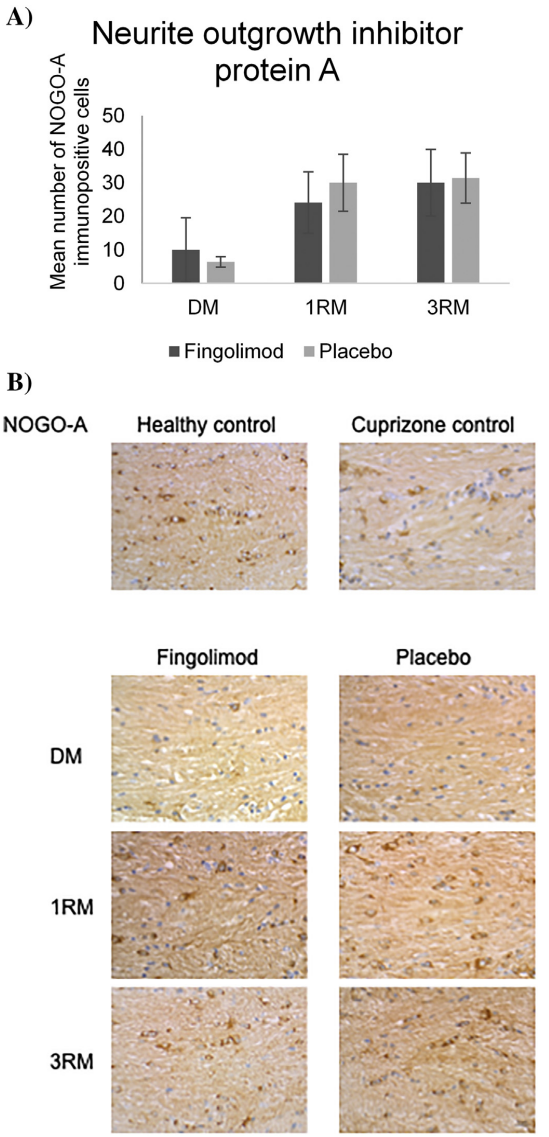

Fig. 4. Mature oligodendrocytes measured by Neurite outgrowth inhibitor protein A immunoreactivity.
A) Number of mature oligodendrocytes in the fingolimod and placebo group after six weeks of demyelination, one week of remyelination and three weeks of remyelination. There were no differences between the fingolimod and the placebo group at any time point. Cell counts are provided as mean number of cells per 0.0625 mm^2, in the midline of the corpus callosum. Error bars: ± 1 SD. Number (n) of animals included: DM placebo (n: 5), DM fingolimod (n: 3), 1RM placebo (n: 6), 1RM fingolimod (n: 5), 3RM placebo (n: 5), 3RM fingolimod (n: 6).
B) NOGO-A and hematoxylin stained sections. DM = six weeks of demyelination, 1RM = one week of remyelination, 3RM = three weeks of remyelination. All images at 40×.

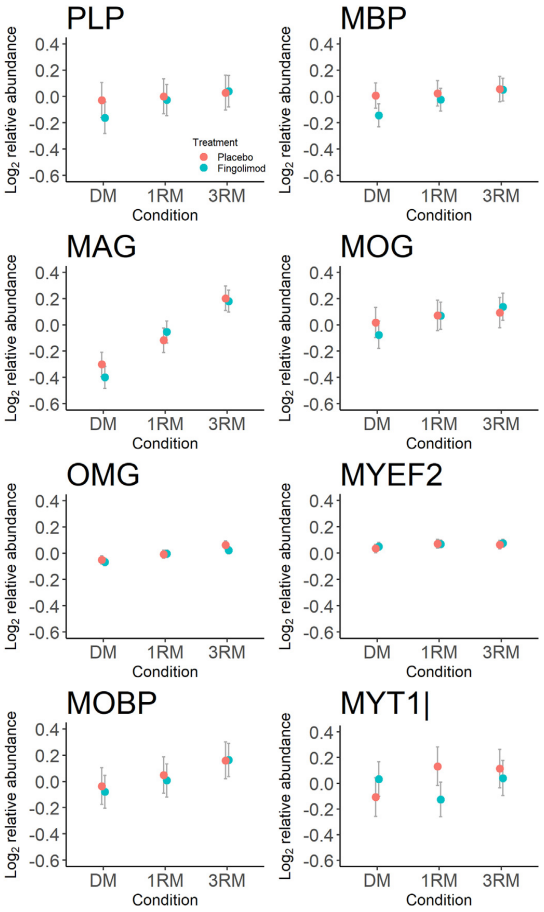

Fig. 5. Myelin protein levels measured by quantitative proteomics.
The average log_2 abundances based on three pools, each containing two biological replicates and their standard deviation. PLP: Myelin Proteolipid Protein, MBP: myelin basic protein, MAG: myelin-associated glycoprotein, MOG: myelin-oligodendrocyte glycoprotein, OMG: oligodendrocyte-myelin glycoprotein, MYEF2: myelin expression factor 2, MOBP: myelin-associated oligodendrocyte basic protein, MYT1l: myelin transcription factor 1-like protein. DM = six weeks of demyelination, 1RM = one week of remyelination, 3RM = three weeks of remyelination.

3.4. Fingolimod did not affect astrocytosis or microglia activation

3.4.1. Astrocytosis and microglia activation in the corpus callosum and the cortex

There was increased GFAP immunopositivity in the CC of cuprizone controls compared to healthy controls (0.7 ± SD 0.27 vs. 1.83 ± SD 0.58, $p = 0.024$, Table S6A). Astrocytosis remained moderate to minimal during remyelination in the fingolimod and placebo groups. No differences in astrocytosis were detected at any time points (DM: $p = 0.93$, 1RM: $p = 0.36$, 3RM: $p = 0.81$, Fig. 6, Table S6B–D). Increased microglia and macrophage activation, as measured by the density of MAC-3 immunopositive cells, was observed in the cuprizone controls compared to healthy controls (0.0 ± SD 0.0 vs. 14 ± SD 6.56, $p = 0.018$, Table S6A). We found no difference in MAC-3 immunopositivity between the fingolimod or placebo exposed mice at any time points (DM: $p = 0.058$, 1RM: $p = 0.42$, 3RM: $p = 0.10$, Fig. 7,

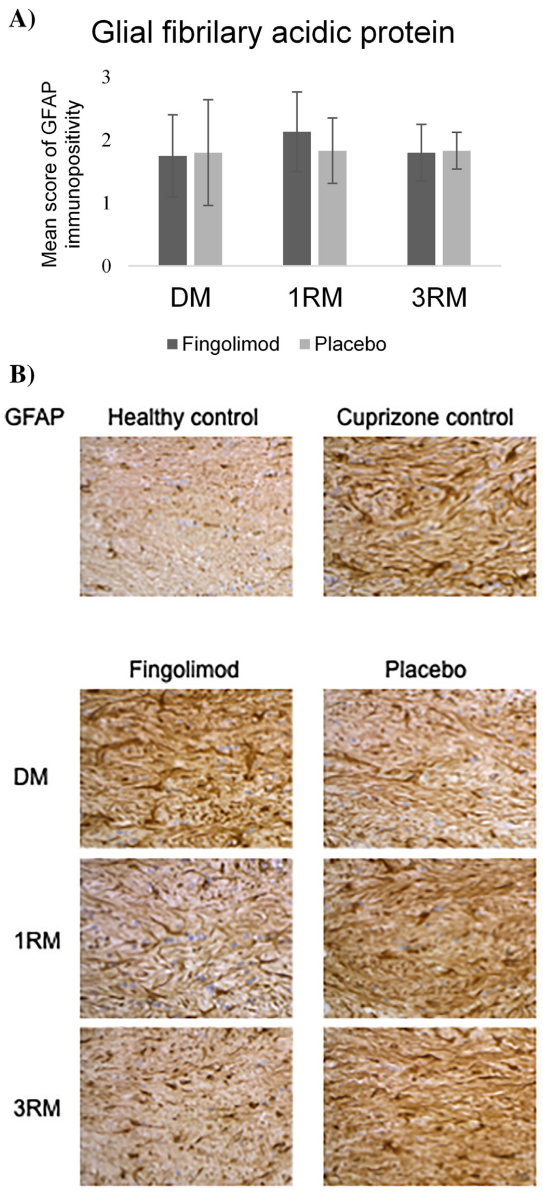

Fig. 6. Astrocytosis measured by Glial fibrillary acidic protein immunoreactivity.
A) Degree of GFAP immunopositivity in the fingolimod and placebo group after six weeks of demyelination, one week of remyelination and three weeks of remyelination. We could not find any difference between the fingolimod and the placebo group at any time point. Scale: no (0), minimal (1), moderate (2), severe (3) astrocytosis. Sections were scored in the midline of corpus callosum. Data presented as mean, error bars: ± 1 SD. Number (n) of animals included: DM placebo (n: 5), DM fingolimod (n: 4), 1RM placebo (n: 6), 1RM fingolimod (n: 6), 3RM placebo (n: 4), 3RM fingolimod (n: 5).
B) GFAP and hematoxylin stained sections. DM = six weeks of demyelination, 1RM = one week of remyelination, 3RM = three weeks of remyelination. All images at 40×.

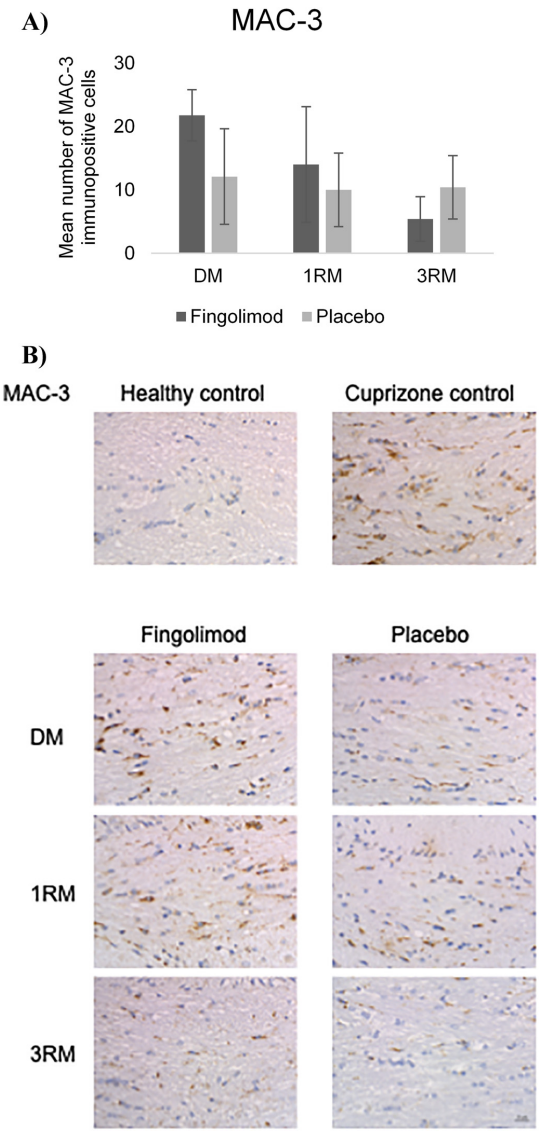

Fig. 7. Microglia/macrophages measured by MAC-3 immunoreactivity.
A) Number of microglia/macrophages (MAC-3 immunopositivity) in the fingolimod and placebo group after six weeks of demyelination, one week of remyelination and three weeks of remyelination. There were no significant differences between the fingolimod and the placebo group at any time point. Cell counts are provided as mean number of cells per 0.0625 mm^2, in the midline of the corpus callosum. Error bars: ± 1 SD. Number (n) of animals included: DM placebo (n: 5), DM fingolimod (n: 4), 1RM placebo (n: 6), 1RM fingolimod (n: 4), 3RM placebo (n: 5), 3RM fingolimod (n: 5).
B) MAC-3 and hematoxylin stained sections. DM = six weeks of demyelination, 1RM = one week of remyelination, 3RM = three weeks of remyelination. All images at 40×.

Table S6B–D). As expected, (Matsushima and Morell, 2001; Wergeland et al., 2012) we only observed 0–3 CD3 immunopositive lymphocytes per counted area and no differences between the groups (Fig. S4, Table S6A–D). In the secondary motor cortex,there was no difference in astrocytosis (DM: $p = 0.16$, 1RM: $p = 0.17$, 3RM: $p = 0.64$) or MAC-3 immunopositivity (DM: $p = 0.95$, 1RM: $p = 0.65$, 3RM: $p = 0.78$, Table S7B–D) between the fingolimod and placebo exposed mice at any time points.

3.4.2. Proteomic markers of astrocytosis and microglia activation

There was a reduction in the average $\log_2$ abundances of GFAP in both intervention groups from six weeks of demyelination throughout the remyelination phase (Fig. S3). After one week of remyelination, the fingolimod-treated mice had increased proteomic expression of MAC-3 ($p < 0.01$). The difference was not considered significant under our criteria as the fold change was < 20% compared to placebo. Thus, there were no differences ($p < 0.01$, $\log_2$ FC > ± 0.2) between the fingolimod-treated and placebo-treated animals (Fig. S3).

3.5. Fingolimod did not lead to less axonal loss

3.5.1. Axonal damage in corpus callosum and the cortex

Cuprizone exposure led to an increased density of APP-positive bulbs in the CC (0.0 cells/0.0625mm^2 ± SD 0.0 vs. 29.0 ± SD 28.5, $p = 0.002$, Table S6A). Treatment with fingolimod caused no difference in acute axonal damage compared to placebo at the different time points (DM: $p = 0.80$, 1RM: $p = 0.25$, 3RM: $p = 0.35$, Fig. 8, Table S6B–D). In the lateral CC, the fingolimod-treated mice had significantly more APP-positive bulbs after 3RM compared to placebo (11.0 ± SD 4.2 vs. 3.4 ± SD 2.51, $p = 0.006$).

The cuprizone exposed mice had less NFL immunopositivity than the healthy controls (90.87 ± SD 2.55 vs. 63.2 ± SD 24.89, $p = 0.041$, Table S6A). There were, however, no differences in NFL loss between the fingolimod-treated and placebo-treated mice (DM: $p = 0.81$, 1RM: $p = 0.30$, 3RM: $p = 0.26$, Fig. 9, Table S6B–D). In the secondary motor cortex,we found no APP-positive bulbs in the fingolimod or placebo group. The fingolimod group had less NFL immunopositivity after six weeks of demyelination (9.37 ± SD 4.25 vs. 19.9 ± SD 5.19, $p = 0.005$, Table S7B). However, there were no differences between the groups at later time points (Table S7C–D).

3.5.2. Proteomic markers of axonal damage

There were no differences ($p < 0.01$, $\log_2$ FC > ± 0.2) between the fingolimod- and placebo-treated mice in the proteomic expression of APP or NFL (Fig. S3).

4. Discussion

Fingolimod downregulated S1PR1 in the cerebrum of cuprizone-treated mice at all time points investigated. When examining the corpus callosum and the secondary motor cortex in cuprizone mice, at three different time points, we found that fingolimod given after cuprizone-induced demyelination did not enhance remyelination, as supported by our earlier experiments in the cerebellum (Alme et al., 2015) and by other groups (Hu et al., 2011; Kim et al., 2011; Slowik et al., 2015; Kim et al., 2018). In our study, fingolimod increased the number of mature oligodendrocytes in the secondary motor cortex after three weeks of remyelination but did not improve remyelination. There could be several explanations for this discrepancy. Gudi et al. found that the density of oligodendrocytes is lower in the cortex compared to the corpus callosum. Moreover, oligodendrocytes may not be capable of driving the remyelination process in the cortex as in the corpus callosum. They hypothesized that the demyelination process in the cortex may be delayed compared to corpus callosum or that signals that drive the remyelination process in corpus callosum are deficient in the cortex. Further, they speculated that few mature oligodendrocytes might not

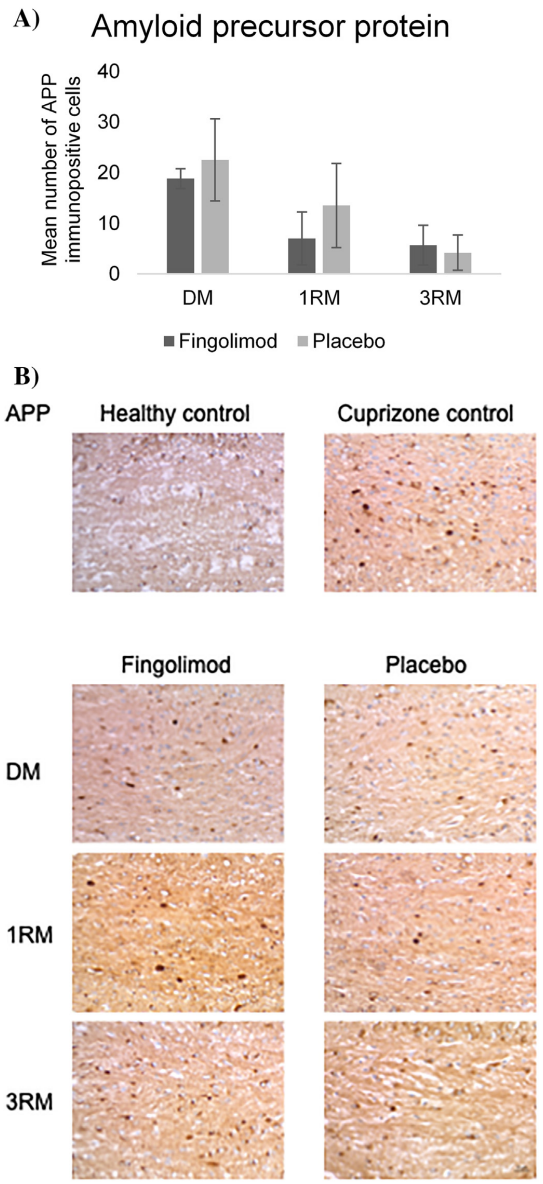

Fig. 8. Acute axonal damage measured by Amyloid precursor protein immunoreactivity.
A) Number of APP immunopositive bulbs in the fingolimod and placebo group after six weeks of demyelination, one week of remyelination and three weeks of remyelination. There was no difference between the fingolimod and the placebo group at any time point. Cell counts are provided as mean number of cells per 0.0625 mm^2, in the midline of the corpus callosum. Error bars: ± 1 SD. Number (n) of animals included: DM placebo (n: 6), DM fingolimod (n: 6), 1RM placebo (n: 6), 1RM fingolimod (n: 5), 3RM placebo (n: 5), 3RM fingolimod (n: 6).
B) APP and hematoxylin stained sections. DM = six weeks of demyelination, 1RM = one week of remyelination, 3RM = three weeks of remyelination. All images at 40×.

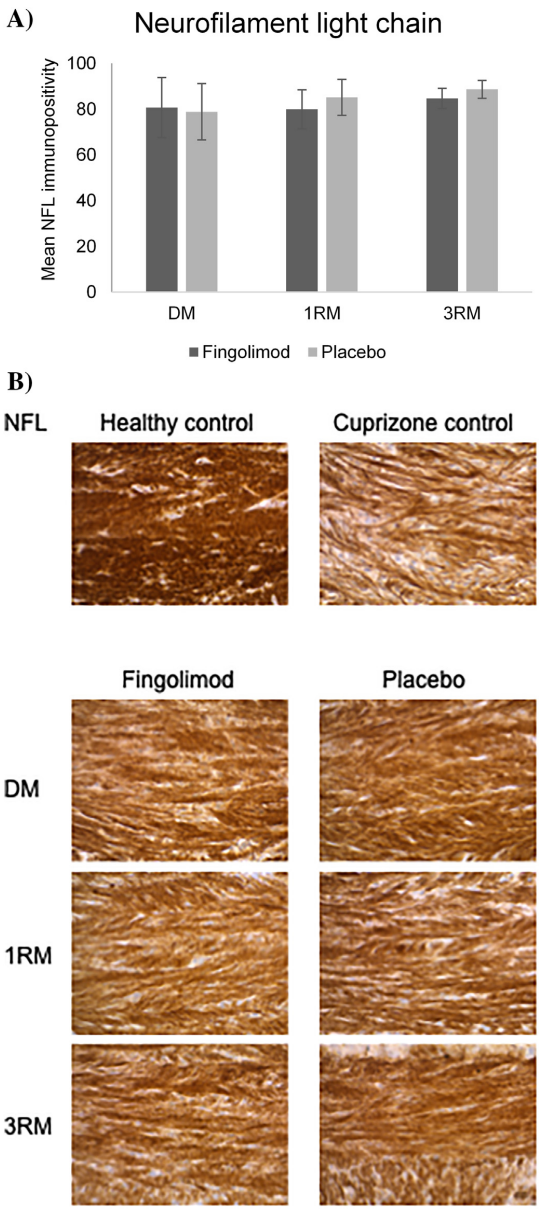

Fig. 9. Axonal loss measured by Neurofilament light chain immunoreactivity. A) Immunoreactivity in % for NFL in the fingolimod and placebo group after six weeks of demyelination, one week of remyelination and three weeks of remyelination. There were no differences between the groups at any time point. Sections were scored in the midline of corpus callosum. Data presented as mean, error bars: ± 1 SD. Number (n) of animals included: DM placebo (n: 6), DM fingolimod (n: 6), 1RM placebo (n: 6), 1RM fingolimod (n: 6), 3RM placebo (n: 3), 3RM fingolimod (n: 6).

B) NFL and hematoxylin stained sections. DM = six weeks of demyelination, 1RM = one week of remyelination, 3RM = three weeks of remyelination. All images at 40×.

have the capacity to drive detectable remyelination (Gudi et al., 2009). Another possibility is that fingolimod stimulates the recruitment and differentiation of oligodendrocytes in the cortex yet fails to increase remyelination of the axons. Electron microscopy (EM) is considered the gold standard for assessing remyelination but was not used to assess remyelination in this experiment. However, Lindner et al. have demonstrated that EM correlates well with LFB myelin staining (Lindner et al., 2008) and Wergeland et al. have found that PLP staining detect myelin-regeneration after one week of cuprizone withdrawal (Wergeland et al., 2012).

The cuprizone model is a well-described and reliable animal model (Matsushima and Morell, 2001; Torkildsen et al., 2008; Kipp et al., 2009; Wergeland et al., 2012). Through our IHC and proteomic analyses, we demonstrate the well-established time-dependent changes in remyelination (Matsushima and Morell, 2001; Lindner et al., 2008; Kipp et al., 2009; Werner et al., 2010) in both fingolimod- and placebo-treated cuprizone mice. After six weeks of cuprizone-induced demyelination, myelin proteins are reduced with a subsequent increase during recovery in cuprizone mice compared to controls. Furthermore, the protein abundance of GFAP is increased after six weeks, and gradually returns to control levels during remyelination (Werner et al., 2010). Correspondingly, we show downregulation of myelin and upregulation of GFAP protein levels after six weeks of demyelination. As expected, the myelin protein levels increased, and GFAP levels decreased throughout the remyelination phase. Proteomics appeared to have a higher sensitivity than IHC for monitoring the time-dependent changes in GFAP. This difference may be due to variations in the areas that were analyzed. Although the cuprizone model does not directly mimic MS pathology, robust de- and remyelination in the absence of adaptive immune responses makes this model well suited to study remyelination (Kipp and Amor, 2012). It is not possible to generalize results directly from the model to humans, yet findings can indicate effects on remyelination and the mechanisms involved.

To our knowledge, the present study is the first to apply proteomics to elucidate the mechanisms of action of fingolimod on remyelination and axonal damage after cuprizone exposure. Fingolimod treatment caused downregulation of the total level of S1PR1in the mouse brain. Healthy control mice treated with fingolimod would have strengthened our study. Nevertheless, the difference in the S1PR1 abundance between the fingolimod and placebo group is reliable, as S1PR1 was significantly downregulated after FDR correction ($q < 0.01$).

S1P levels decrease during cuprizone exposure but recover during remyelination after cuprizone withdrawal (Kim et al., 2012). The level of S1P also decreases in cuprizone exposed mice cotreated with fingolimod (Kim et al., 2018). In healthy CBA/CaHArc mice, S1PR1 is upregulated after two months of intraperitoneal treatment with fingolimod (7.5 mg/kg/week) compared to vehicle control (Gupta et al., 2017). Fingolimod regulates S1PRs in cuprizone mice but does not prevent a cuprizone-induced S1P drop (Kim et al., 2018). In cuprizone exposed mice, the expression of S1PR1 was moderately increased, and S1PR3 and -5 significantly increased compared to controls. However, only the protein level of S1PR1 was downregulated by fingolimod cotreatment (Kim et al., 2018). Unlike us, Kim et al. did not investigate S1PRs protein levels during remyelination after fingolimod rescue treatment.

In the proteomics experiment, we analyzed the right frontal brain section; thus, the quantified proteins represent the bulk of proteins originating from different cell types in this particular section. Therefore, we cannot rule out that S1PR1 and other proteins could be more down- or upregulated in some cell types than others or be differently regulated in other parts of the CNS. Both S1PR1 and GNG5 were less abundant in samples from fingolimod-treated mice than placebo-treated mice. After one week of remyelination, the protein PPT2 was downregulated in fingolimod-treated mice. The aforementioned proteins are, to our knowledge, not known to be involved in the remyelination process. The GNG5 is a G-protein and an interactor with

S1PR1 (Huttlin et al., 2017). Therefore, both S1PR1 and GNG5 could be downregulated because of a refractory phase of signaling occurring after prolonged activation of the S1PR1 pathway. Such a non-responsive phase of signaling might occur as a negative feedback mechanism set to play by internalization of receptor complexes by endocytosis followed by degradation by the lysosomal pathway (Reeves et al., 2016). PPT2 is a lysosomal enzyme involved in removing thioester-linked fatty acyl groups from various substrates, including G-proteins, during lysosomal degradation processes (Soyombo and Hofmann, 1997). However, its role in S1PR1 signaling is not clear (Reeves et al., 2016). Myelin proteins (MOG, MAG, MBP, MOBP, PLP) (Han et al., 2013) and proteins reflecting axonal damage and loss (APP, NFL) (Teunissen et al., 2005) were not regulated between the fingolimod-treated and placebo-treated groups. Thus, the results support that fingolimod does not promote the remyelination process or mitigate axonal loss.

In our experiment, principal component analysis of the $\log_2$ relative protein abundances showed an apparent batch effect between the two TMT experiments, likely introduced by technical variance. In unbalanced experiments, especially when the sample sizes are small, a technical variance can overshadow biological variance and induce differences between groups. Attempts were made to reduce the technical variance observed by applying a normalization strategy for combining TMT experiments (Plubell et al., 2017), though without improvement (data not shown). Several methods to tackle batch effects exist (Leek et al., 2010; Nygaard et al., 2016), limma (Ritchie et al., 2015) was selected due to the unbalanced nature of the study and the small number of biological replicates in each group. A linear model was created, taking the batch effect into account, prior to empirical Bayes statistics for differential Expression and Benjamini Hochberg FDR correction. After FDR correction, the downregulation of the S1PR1 receptor was identified.

In the lysolecithin model, force-feeding fingolimod (0,3 mg/kg and 1 mg/kg) before lysophosphatidylcholine (LPC) exposure decreased inflammation and the extent of demyelination; and the low dose of fingolimod increased oligodendrocyte precursor cells recruitment, oligodendrogenesis, and remyelination (Yazdi et al., 2015). However, inflammatory cytokines may cause cell death and prevent oligodendrocyte precursor cell differentiation (Feldhaus et al., 2004); the enhanced myelination may thus have been caused by a reduced inflammation with subsequent less demyelination (Yazdi et al., 2015). Oral fingolimod did not promote remyelination after LPC injection or after cuprizone exposure (Hu et al., 2011). At a late disease stage, where the axonal loss is prominent, there is less capacity to compensate for nerve damage and further nerve loss; this will consequently increase functional impairment. In line with our results, Hu et al. concluded that patients treated with fingolimod might benefit from add-on therapy to promote remyelination.

Prophylactic treatment with fingolimod (0.4 mg/kg) in EAE Dark Agouti (DA) rats prevents the onset and development of EAE symptoms. Rescue therapy with fingolimod reversed EAE symptoms and restored the nerve conductance in rats with fully established EAE. The fingolimod and the control group had comparable levels of remyelination. The authors speculated that fingolimod could exert a centralized effect in the CNS through interaction with S1PRs on glial cells, yet, they did not exclude that the effect of fingolimod is due to its known anti-inflammatory effect (Balatoni et al., 2007). During relapsing EAE early intervention with fingolimod inhibited subsequent relapses and neurodegeneration, yet late initiated, long-term treatment could not impede the disease deterioration in progressive EAE (Al-Izki et al., 2011). Fingolimod (0.3 mg/kg) initiated at EAE symptom onset, promoted proliferation and differentiation of oligodendrocyte precursor cell in mice, and increased the MBP levels (Zhang et al., 2015). The findings could be a consequence of attenuated inflammation and myelin protection, rather than remyelination through direct CNS effects, as the same group found that fingolimod (0.3 mg/kg) alone failed to enhance remyelination in the secondary progressive (SP) stage of EAE (Zhang et al., 2017). Due to the interference of and indirect effects by the systemic immune cell responses, it is challenging to monitor remyelination separately in the EAE model.

Fingolimod may enhance the MBP expression and remyelination at low doses (< 5 nM in vitro and 0.3 mg/kg/day in vivo). However, fingolimod seems to cause oligodendrocyte death at higher concentrations (Zhang et al., 2017). In humans, oligodendrocyte precursor cells and mature oligodendrocytes may show dose-dependent, cell-type-specific, and differing cytoskeletal responses to fingolimod. Miron et al. indicated that disparities in human- and rat oligodendrocyte-responses make it challenging to transfer interpretations from rodent in vitro studies to human cells (Miron et al., 2008a). In another study, fingolimod had dose- and time-dependent effects on process extension, differentiation, and survival in oligodendrocyte precursor cells (Miron et al., 2008b). Moreover, a low dose (100 pmol/L) fingolimod could enhance remyelination and affect oligodendrocyte precursor cells in organotypic cerebellar slices after LPC-induced demyelination (Miron et al., 2010). In the rat telencephalon reaggregate spheroid cell culture system, 1 and 10 nM fingolimod did not affect remyelination when given before LPC-induced demyelination (Jackson et al., 2011). Slowik et al. gave mice a low dose (0.3 mg/kg) of fingolimod after cuprizone-induced demyelination, yet there was no difference in remyelination between the fingolimod and placebo after acute or chronic demyelination. However, fingolimod seemed to decrease axonal damage (Slowik et al., 2015).

In the present study, we used 1 mg/kg/day fingolimod, as used in several other studies (Kataoka et al., 2005; Al-Izki et al., 2011; Hu et al., 2011; Kim et al., 2011; Kim et al., 2018). We found that fingolimod does not decrease acute axonal injury or axonal loss after acute cuprizone demyelination, as fingolimod-treated mice compared to placebo had increased acute axonal injury (APP immunoreactivity) after three weeks of remyelination. However, this was not confirmed by proteomic analyses, as we found no difference in axonal damage or loss between the intervention groups. We cannot exclude that a lower dose of fingolimod could have a beneficial effect. Kim et al. found that fingolimod given during cuprizone exposure led to diminished injury to oligodendrocytes, myelin, and axons (Kim et al., 2011) and suppressed astrocytosis and microgliosis (Kim et al., 2018). Nonetheless, fingolimod (1 mg or 5 mg/kg) did not reduce inflammation, oligodendrocytes loss, or enhance remyelination if given after the occurrence of oligodendrocyte apoptosis and myelin damage (Kim et al., 2018). Thus, whether fingolimod is administrated before or during cuprizone exposure would affect the degree of de- and remyelination. The discrepant findings between our results and other studies could be due to the chosen animal model, degree and capacity of de- and remyelination, experimental settings, the time point for fingolimod initiation, doses, duration of treatment, and different brain regions analyzed.

Our data give a new insight into the mechanisms of action behind fingolimod during remyelination. Based on the current research, the hypothetical direct effect of fingolimod on S1PRs in the brain does not appear to have any significant influence on remyelination. The INFORMS study, a phase three, randomized controlled trial (RCT), did not find any advantages of fingolimod in primary progressive MS patients, as they found no effect on brain volume loss and disability progression (Lublin et al., 2016). This supports that fingolimod has to be given at an early disease stage, before damage has occurred, to exert neuroprotective effects. Another RCT (EXPAND), investigated the impact of the selective $S1P_1$ and $S1P_5$ modulator, siponimod, on patients with secondary progressive MS. The results showed that siponimod, to some extent, reduced the risk of disability progression and could be used to treat patients with secondary progressive MS (Kappos et al., 2018). In the future, well-designed clinical trials are necessary to determine to what extent fingolimod and other substances may affect myelin repair and axonal loss in MS patients.

5. Conclusion

Fingolimod was functionally active during remyelination by downregulating S1PR1 brain levels in fingolimod-treated cuprizone mice. We detected more oligodendrocytes in the secondary motor cortex after three weeks of remyelination in the fingolimod compared to placebo-exposed mice. However, HC, IHC, and proteomic analyses detected no differences in the degree of remyelination, axonal damage or loss in fingolimod-treated mice compared to placebo. In conclusion, fingolimod does not seem to directly promote remyelination or protect against axonal injury or loss when given after cuprizone-induced demyelination.

Acknowledgments

We thank Edith Fick for excellent technical assistance and Håvard Nyhagen Henriksen for proofreading of the manuscript. Neuro-SysMed is jointly hosted by Haukeland University Hospital and University of Bergen, and supported as a Centre for Clinical Treatment Research (FKB) by grants from The Research Council of Norway, project number 288164.

Funding

This work was funded by the University of Bergen K1, Kristian Gerhard Jebsen Foundation, and grants from Novartis, Norway AS. Fingolimod was provided by Material Transfer Management, NIBR Operational Alliances, Fabrikstrasse 28-Z1.28.1, Novartis Campus, CH-4056 Basel, Switzerland.

Author contributions

Conceptualization, Ø.T., S.W. and L.B.; *Methodology*, Ø.T., S.W., E.O., and L.B; *Investigation*, A.E.N., R.R.L., E.O. and S.W.; *Formal Analysis*, A.E.N., R.R.L., E.O. and S.W.; *Writing – Original Draft*, A.E.N.; *Writing – Review & Editing*, All authors; *Visualization*, A.E.N., S.W.; *Supervision*, Ø.T, E.O. and S.W.; *Funding Acquisition*, Ø.T., S.W., K.M. and L.B.

Declaration of competing interest

Agnes E. Nystad has received an unrestricted research grant from Novartis.

Ragnhild Reehorst Lereim: none.

Stig Wergeland has received speaker honoraria from Biogen and Novartis.

Eystein Oveland: none.

Kjell-Morten Myhr has received unrestricted research grants to his institution and/or scientific advisory board or speakers honoraria from Almirall, Biogen,

Genzyme, Merck, Novartis, Roche and Teva; and has participated in clinical trials organized by Biogen, Merck, Novartis, and Roche.

Lars Bø has received unrestricted research grants to his institution and/or scientific advisory board or speakers honoraria from Almirall, Biogen, Genzyme, Merck, Novartis, Roche and Teva; and has participated in clinical trials organized by Biogen, Merck, Novartis, Roche, and Genzyme.

Øivind Torkildsen has received speaker honoraria from and served on scientific advisory boards for Biogen, Sanofi-Aventis, Merck, and Novartis.

Appendix A. Supplementary data

Supplementary data to this article can be found online at https://doi.org/10.1016/j.jneuroim.2019.577091.

References

Al-Izki, S., Pryce, G., Jackson, S.J., Giovannoni, G., Baker, D., 2011. Immunosuppression with FTY720 is insufficient to prevent secondary progressive neurodegeneration in experimental autoimmune encephalomyelitis. Mult. Scler. J. 17 (8), 939–948.

Alme, M.N., Nystad, A.E., Bo, L., Myhr, K.M., Vedeler, C.A., Wergeland, S., Torkildsen, O., 2015. Fingolimod does not enhance cerebellar remyelination in the cuprizone model. J. Neuroimmunol. 285, 180–186.

Balatoni, B., Storch, M.K., Swoboda, E.M., Schonborn, V., Koziel, A., Lambrou, G.N., Hiestand, P.C., Weissert, R., Foster, C.A., 2007. FTY720 sustains and restores neuronal function in the DA rat model of MOG-induced experimental autoimmune encephalomyelitis. Brain Res. Bull. 74 (5), 307–316.

Brinkmann, V., 2007. Sphingosine 1-phosphate receptors in health and disease: mechanistic insights from gene deletion studies and reverse pharmacology. Pharmacol. Ther. 115 (1), 84–105.

Brinkmann, V., Pinschewer, D., Chiba, K., Feng, L., 2000. FTY720: a novel transplantation drug that modulates lymphocyte traffic rather than activation. Trends Pharmacol. Sci. 21 (2), 49–52.

Calabresi, P.A., Radue, E.W., Goodin, D., Jeffery, D., Rammohan, K.W., Reder, A.T., Vollmer, T., Agius, M.A., Kappos, L., Stites, T., Li, B., Cappiello, L., von Rosenstiel, P., Lublin, F.D., 2014. Safety and efficacy of fingolimod in patients with relapsing-remitting multiple sclerosis (FREEDOMS II): a double-blind, randomised, placebo-controlled, phase 3 trial. Lancet Neurol. 13 (6), 545–556.

Chiba, K., Yanagawa, Y., Masubuchi, Y., Kataoka, H., Kawaguchi, T., Ohtsuki, M., Hoshino, Y., 1998. FTY720, a novel immunosuppressant, induces sequestration of circulating mature lymphocytes by acceleration of lymphocyte homing in rats. I. FTY720 selectively decreases the number of circulating mature lymphocytes by acceleration of lymphocyte homing. J. Immunol. 160 (10), 5037–5044.

Chun, J., Hartung, H.P., 2010. Mechanism of action of oral fingolimod (FTY720) in multiple sclerosis. Clin. Neuropharmacol. 33 (2), 91–101.

Deshmukh, V.A., Tardif, V., Lyssiotis, C.A., Green, C.C., Kerman, B., Kim, H.J., Padmanabhan, K., Swoboda, J.G., Ahmad, I., Kondo, T., Gage, F.H., Theofilopoulos, A.N., Lawson, B.R., Schultz, P.G., Lairson, L.L., 2013. A regenerative approach to the treatment of multiple sclerosis. Nature 502 (7471), 327–332.

Feldhaus, B., Dietzel, I.D., Heumann, R., Berger, R., 2004. Effects of interferon-gamma and tumor necrosis factor-alpha on survival and differentiation of oligodendrocyte progenitors. J. Soc. Gynecol. Investig. 11 (2), 89–96.

Groves, A., Kihara, Y., Chun, J., 2013. Fingolimod: direct CNS effects of sphingosine 1-phosphate (S1P) receptor modulation and implications in multiple sclerosis therapy. J. Neurol. Sci. 328 (0), 9–18.

Gudi, V., Moharregh-Khiabani, D., Skripuletz, T., Koutsoudaki, P.N., Kotsiari, A., Skuljec, J., Trebst, C., Stangel, M., 2009. Regional differences between grey and white matter in cuprizone induced demyelination. Brain Res. 1283, 127–138.

Gupta, V.K., M, M., Klistorner, A., Graham, S., 2017. Mapping proteomics changes induced by fingolimod in different regions of the brain and retina. Mult. Scler. J. 23 (3_suppl), 680–975.

Han, H., Myllykoski, M., Ruskamo, S., Wang, C., Kursula, P., 2013. Myelin-specific proteins: a structurally diverse group of membrane-interacting molecules. Biofactors 39 (3), 233–241.

Hu, Y.H., Lee, X.H., Ji, B.X., Guckian, K., Apicco, D., Pepinsky, R.B., Miller, R.H., Mi, S., 2011. Sphingosine 1-phosphate receptor modulator fingolimod (FTY720) does not promote remyelination in vivo. Mol. Cell. Neurosci. 48 (1), 72–81.

Huttlin, E.L., Bruckner, R.J., Paulo, J.A., Cannon, J.R., Ting, L., Baltier, K., Colby, G., Gebreab, F., Gygi, M.P., Parzen, H., Szpyt, J., Tam, S., Zarraga, G., Pontano-Vaites, L., Swarup, S., White, A.E., Schweppe, D.K., Rad, R., Erickson, B.K., Obar, R.A., Guruharsha, K.G., Li, K., Artavanis-Tsakonas, S., Gygi, S.P., Harper, J.W., 2017. Architecture of the human interactome defines protein communities and disease networks. Nature 545 (7655), 505–509.

Jackson, S.J., Giovannoni, G., Baker, D., 2011. Fingolimod modulates microglial activation to augment markers of remyelination. J. Neuroinflammation 8 (76), 1742–2094.

Jaillard, C., Harrison, S., Stankoff, B., Aigrot, M.S., Calver, A.R., Duddy, G., Walsh, F.S., Pangalos, M.N., Arimura, N., Kaibuchi, K., Zalc, B., Lubetzki, C., 2005. Edg8/S1P5: an oligodendroglial receptor with dual function on process retraction and cell survival. J. Neurosci. 25 (6), 1459–1469.

Kappos, L., E. W. Radue, P. O'Connor, C. Polman, R. Hohlfeld, P. Calabresi, K. Selmaj, C. Agoropoulou, M. Leyk, L. Zhang-Auberson, P. Burtin and F. S. Group, 2010. A placebo-controlled trial of oral fingolimod in relapsing multiple sclerosis. N. Engl. J. Med. 362 (5), 387–401.

Kappos, L., Bar-Or, A., Cree, B.A.C., Fox, R.J., Giovannoni, G., Gold, R., Vermersch, P., Arnold, D.L., Arnould, S., Scherz, T., Wolf, C., Wallstrom, E., Dahlke, F., Investigators, E.C., 2018. Siponimod versus placebo in secondary progressive multiple sclerosis (EXPAND): a double-blind, randomised, phase 3 study. Lancet 391 (10127), 1263–1273.

Kataoka, H., Sugahara, K., Shimano, K., Teshima, K., Koyama, M., Fukunari, A., Chiba, K., 2005. FTY720, sphingosine 1-phosphate receptor modulator, ameliorates experimental autoimmune encephalomyelitis by inhibition of T cell infiltration. Cell. Mol. Immunol. 2 (6), 439–448.

Kim, H.J., Miron, V.E., Dukala, D., Proia, R.L., Ludwin, S.K., Traka, M., Antel, J.P., Soliven, B., 2011. Neurobiological effects of sphingosine 1-phosphate receptor modulation in the cuprizone model. FASEB J. 25 (5), 1509–1518.

Kim, S., Steelman, A.J., Zhang, Y., Kinney, H.C., Li, J., 2012. Aberrant upregulation of astroglial ceramide potentiates oligodendrocyte injury. Brain Pathol. 22 (1), 41–57.

Kim, S., Bielawski, J., Yang, H., Kong, Y., Zhou, B., Li, J., 2018. Functional antagonism of sphingosine-1-phosphate receptor 1 prevents cuprizone-induced demyelination. Glia 66 (3), 654–669.

Kipp, M., Amor, S., 2012. FTY720 on the way from the base camp to the summit of the mountain: relevance for remyelination. Mult. Scler. 18 (3), 258–263.
Kipp, M., Clarner, T., Dang, J., Copray, S., Beyer, C., 2009. The cuprizone animal model: new insights into an old story. Acta Neuropathol. 118 (6), 723–736.
Kiuchi, M., Adachi, K., Kohara, T., Teshima, K., Masubuchi, Y., Mishina, T., Fujita, T., 1998. Synthesis and biological evaluation of 2,2-disubstituted 2-aminoethanols: analogues of FTY720. Bioorg. Med. Chem. Lett. 8 (1), 101–106.
Lassmann, H., 2018. Multiple sclerosis pathology. Cold Spring Harb. Perspect. Med. 8 (3).
Leek, J.T., Scharpf, R.B., Bravo, H.C., Simcha, D., Langmead, B., Johnson, W.E., Geman, D., Baggerly, K., Irizarry, R.A., 2010. Tackling the widespread and critical impact of batch effects in high-throughput data. Nat. Rev. Genet. 11 (10), 733–739.
Lereim, R.R., Oveland, E., Xiao, Y., Torkildsen, O., Wergeland, S., Myhr, K.M., Sun, S.C., Berven, F.S., 2016. The brain proteome of the ubiquitin ligase Peli1 knock-out mouse during experimental autoimmune encephalomyelitis. J. Proteomics Bioinform. 9 (9), 209–219.
Lindner, M., Heine, S., Haastert, K., Garde, N., Fokuhl, J., Linsmeier, F., Grothe, C., Baumgartner, W., Stangel, M., 2008. Sequential myelin protein expression during remyelination reveals fast and efficient repair after central nervous system demyelination. Neuropathol. Appl. Neurobiol. 34 (1), 105–114.
Lublin, F., Miller, D.H., Freedman, M.S., Cree, B.A., Wolinsky, J.S., Weiner, H., Lubetzki, C., Hartung, H.P., Montalban, X., Uitdehaag, B.M., Merschhemke, M., Li, B., Putzki, N., Liu, F.C., Haring, D.A., Kappos, L., 2016. Oral fingolimod in primary progressive multiple sclerosis (INFORMS): a phase 3, randomised, double-blind, placebo-controlled trial. Lancet 387 (10023), 1075–1084.
Matsushima, G.K., Morell, P., 2001. The neurotoxicant, cuprizone, as a model to study demyelination and remyelination in the central nervous system. Brain Pathol. 11 (1), 107–116.
Mi, H., Muruganujan, A., Ebert, D., Huang, X., Thomas, P.D., 2019. PANTHER version 14: more genomes, a new PANTHER GO-slim and improvements in enrichment analysis tools. Nucleic Acids Res. 47 (D1), D419–D426.
Miron, V.E., Hall, J.A., Kennedy, T.E., Soliven, B., Antel, J.P., 2008a. Cyclical and dose-dependent responses of adult human mature oligodendrocytes to fingolimod. Am. J. Pathol. 173 (4), 1143–1152.
Miron, V.E., Jung, C.G., Kim, H.J., Kennedy, T.E., Soliven, B., Antel, J.P., 2008b. FTY720 modulates human oligodendrocyte progenitor process extension and survival. Ann. Neurol. 63 (1), 61–71.
Miron, V.E., Ludwin, S.K., Darlington, P.J., Jarjour, A.A., Soliven, B., Kennedy, T.E., Antel, J.P., 2010. Fingolimod (FTY720) enhances remyelination following demyelination of organotypic cerebellar slices. Am. J. Pathol. 176 (6), 2682–2694.
Nygaard, V., Rodland, E.A., Hovig, E., 2016. Methods that remove batch effects while retaining group differences may lead to exaggerated confidence in downstream analyses. Biostatistics 17 (1), 29–39.
Nystad, A.E., Wergeland, S., Aksnes, L., Myhr, K.M., Bø, L., Torkildsen, Ø., 2014. Effect of high-dose 1.25 dihydroxyvitamin D3 on remyelination in the cuprizone model. APMIS 122 (12), 1178–1186.
Paxinos, G., 2008. In: Franklin, Keith B.J., Paxinos, George (Eds.), The Mouse Brain in Stereotaxic Coordinates. Elsevier Academic Press, 2008, Amsterdam; London.
Pebay, A., Toutant, M., Premont, J., Calvo, C.F., Venance, L., Cordier, J., Glowinski, J., Tence, M., 2001. Sphingosine-1-phosphate induces proliferation of astrocytes: regulation by intracellular signalling cascades. Eur. J. Neurosci. 13 (12), 2067–2076.
Plemel, J.R., Liu, W.Q., Yong, V.W., 2017. Remyelination therapies: a new direction and challenge in multiple sclerosis. Nat. Rev. Drug Discov. 16 (9), 617–634.
Plubell, D.L., Wilmarth, P.A., Zhao, Y., Fenton, A.M., Minnier, J., Reddy, A.P., Klimek, J., Yang, X., David, L.L., Pamir, N., 2017. Extended multiplexing of tandem mass tags (TMT) labeling reveals age and high fat diet specific proteome changes in mouse epididymal adipose tissue. Mol. Cell. Proteomics 16 (5), 873–890.
Reeves, P.M., Kang, Y.L., Kirchhausen, T., 2016. Endocytosis of ligand-activated sphingosine 1-phosphate receptor 1 mediated by the clathrin-pathway. Traffic 17 (1), 40–52.
Ritchie, M.E., Phipson, B., Wu, D., Hu, Y., Law, C.W., Shi, W., Smyth, G.K., 2015. limma powers differential expression analyses for RNA-sequencing and microarray studies. Nucleic Acids Res. 43 (7), e47.
Slowik, A., Schmidt, T., Beyer, C., Amor, S., Clarner, T., Kipp, M., 2015. The sphingosine 1-phosphate receptor agonist FTY720 is neuroprotective after cuprizone-induced CNS demyelination. Br. J. Pharmacol. 172 (1), 80–92.
Soyombo, A.A., Hofmann, S.L., 1997. Molecular cloning and expression of palmitoyl-protein thioesterase 2 (PPT2), a homolog of lysosomal palmitoyl-protein thioesterase with a distinct substrate specificity. J. Biol. Chem. 272 (43), 27456–27463.
Teunissen, C.E., Dijkstra, C., Polman, C., 2005. Biological markers in CSF and blood for axonal degeneration in multiple sclerosis. Lancet Neurol. 4 (1), 32–41.
Thomas, P.D., Kejariwal, A., Guo, N., Mi, H., Campbell, M.J., Muruganujan, A., Lazareva-Ulitsky, B., 2006. Applications for protein sequence-function evolution data: mRNA/protein expression analysis and coding SNP scoring tools. Nucleic Acids Res. 34 (Web Server issue), W645–W650.
Thompson, A.J., Baranzini, S.E., Geurts, J., Hemmer, B., Ciccarelli, O., 2018. Multiple sclerosis. Lancet 391 (10130), 1622–1636.
Torkildsen, O., Brunborg, L.A., Myhr, K.M., Bo, L., 2008. The cuprizone model for demyelination. Acta Neurol. Scand. Suppl. 188, 72–76.
Vizcaino, J.A., Csordas, A., Del-Toro, N., Dianes, J.A., Griss, J., Lavidas, I., Mayer, G., Perez-Riverol, Y., Reisinger, F., Ternent, T., Xu, Q.W., Wang, R., Hermjakob, H., 2016. 2016 update of the PRIDE database and its related tools. Nucleic Acids Res. 44 (22), 11033.
Wergeland, S., Torkildsen, O., Myhr, K.M., Mork, S.J., Bo, L., 2012. The cuprizone model: regional heterogeneity of pathology. APMIS 120 (8), 648–657.
Werner, S.R., Saha, J.K., Broderick, C.L., Zhen, E.Y., Higgs, R.E., Duffin, K.L., Smith, R.C., 2010. Proteomic analysis of demyelinated and remyelinating brain tissue following dietary cuprizone administration. J. Mol. Neurosci. 42 (2), 210–225.
Wiśniewski, J.R., A, Z., Nagaraj, N., Mann, M., 2009. Universal sample preparation method for proteome analysis. Nat. Methods 6 (5), 359–362.
Yazdi, A., Baharvand, H., Javan, M., 2015. Enhanced remyelination following lysolecithin-induced demyelination in mice under treatment with fingolimod (FTY720). Neuroscience 311, 34–44.
Yazdi, A., Ghasemi-Kasman, M., Javan, M., 2019. Possible regenerative effects of fingolimod (FTY720) in multiple sclerosis disease: an overview on remyelination process. J. Neurosci. Res. 00, 1–13.
Zhang, J., Zhang, Z.G., Li, Y., Ding, X., Shang, X., Lu, M., Elias, S.B., Chopp, M., 2015. Fingolimod treatment promotes proliferation and differentiation of oligodendrocyte progenitor cells in mice with experimental autoimmune encephalomyelitis. Neurobiol. Dis. 76, 57–66.
Zhang, Y., Li, X., Ciric, B., Ma, C.G., Gran, B., Rostami, A., Zhang, G.X., 2017. Effect of fingolimod on neural stem cells: a novel mechanism and broadened application for neural repair. Mol. Ther. 25 (2), 401–415.

Supplementary figures

Figure S1A

Study design.

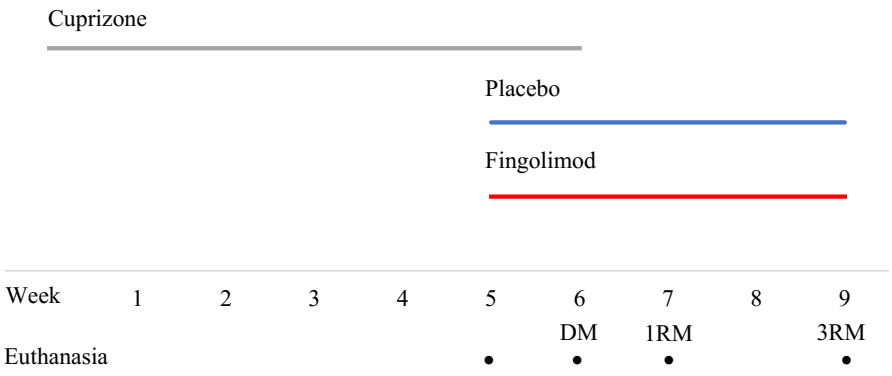

Supplementary figure 1.

The figure shows the timeline for the experiment, including cuprizone exposure. Fingolimod or placebo was given by gavage daily from week five until euthanasia. Cuprizone controls and healthy controls were euthanized after 5 and 9 weeks, respectively. Brain samples for cuprizone mice treated with fingolimod or placebo were prepared for immunohistochemistry and proteomics at three different time points, 6 weeks of demyelination (DM), 1 week of remyelination (1RM) and 3 weeks of remyelination (3RM).

Figure S1B

Regional sampling sites for histochemistry and immunohistochemistry in the mouse brain.

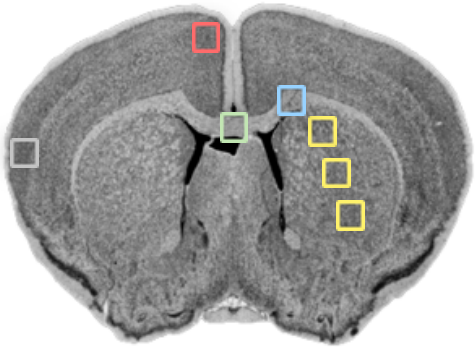

Red: Supplementary motor cortex (M2), green: Medial corpus callosum (cc), blue: Lateral corpus callosum (cingulum, cg), yellow: Deep gray matter –striatum (CPu), grey: 2nd somatosensory cortex (S2).

Figure S2

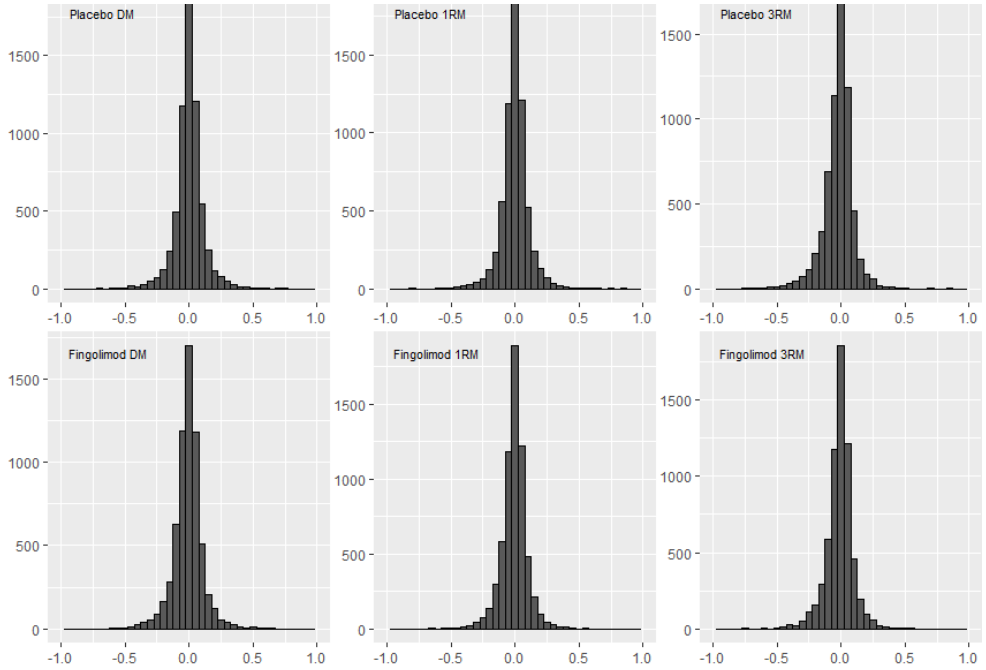

Supplementary figure 2: Distribution of the average protein $\log_2$ abundances prior to statistical analysis in limma. The averages are based on three pools, each containing two biological replicates. DM= six weeks of demyelination, 1RM= one week of remyelination, 3RM = three weeks of remyelination.

Figure S3

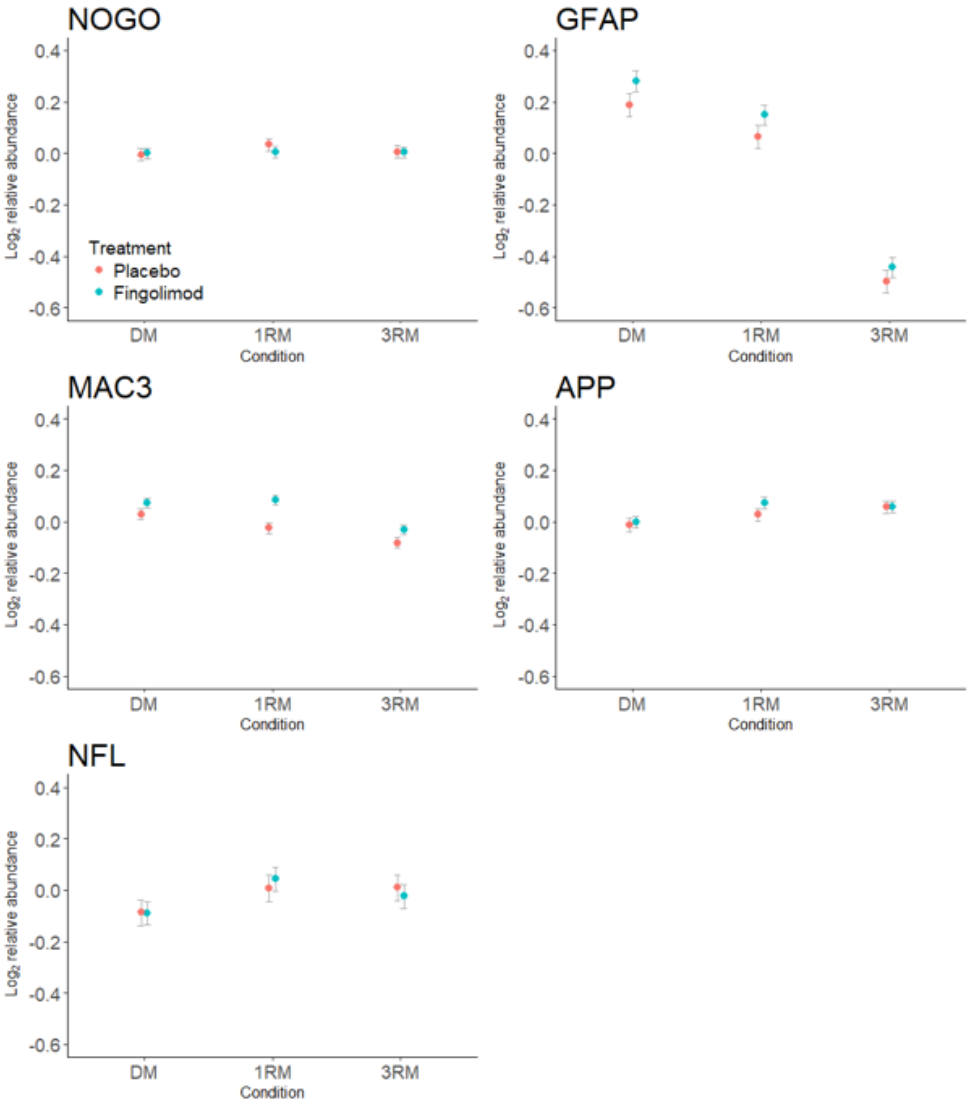

Supplementary figure 3: The average log_2 abundances based on three pools, each containing two biological replicates and their standard deviation. NOGO-A: Neurite Outgrowth Inhibitor Protein A, GFAP: Glial Fibrillary Acidic Protein, MAC-3: macrophages and microglia, APP: amyloid precursor

protein A4, NFL: phosphorylated neurofilament light. DM= six weeks of demyelination, 1RM= one week of remyelination, 3RM= three weeks of remyelination.

Figure S4. CD3 immunopositivity

A)

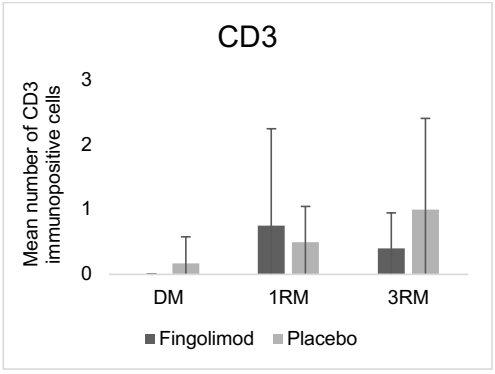

B)

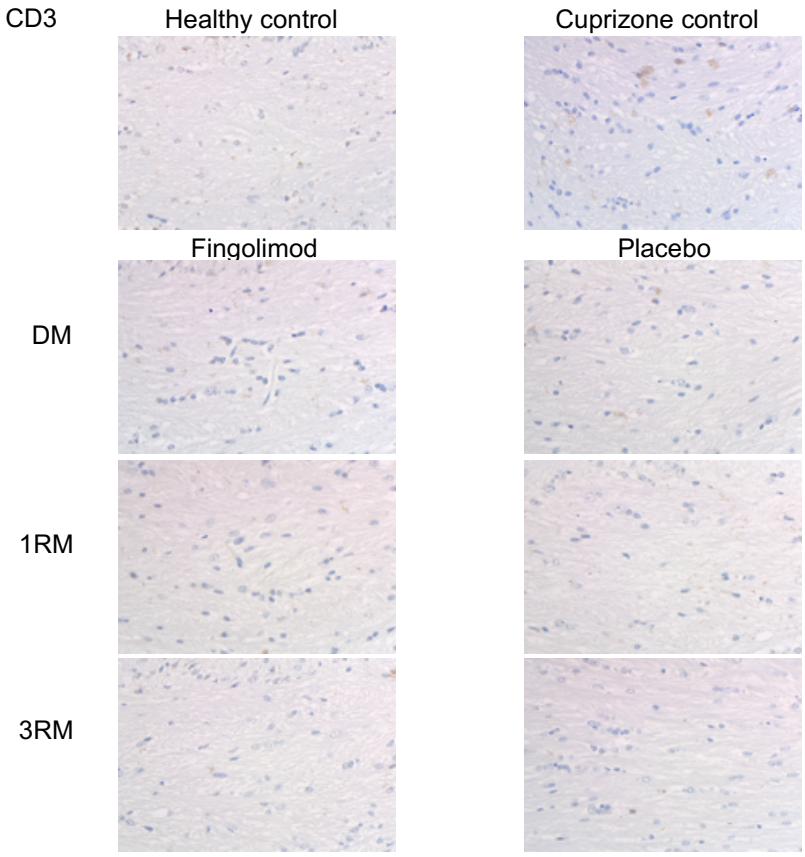
CD3
Healthy control
Cuprizone control
Fingolimod
Placebo
DM
1RM
3RM

Figure S4. CD3 immunoreactivity

A) Number of CD3 immunopositive cells in the fingolimod and placebo group after 6 weeks of demyelination, 1 week of remyelination and 3 weeks of remyelination. We did not find a difference between the fingolimod and the placebo group at any time point. Cell counts are provided as mean number of cells per 0.0625 mm^2, in the midline of the corpus callosum. Error bars: ±1 SD.

B) CD3 and hematoxyline stained sections. DM= six weeks of demyelination, 1RM= one week of remyelination, 3RM= three weeks of remyelination. All images at 40x.

Supplementary methods

LC-MS analysis of TMT-labeled samples

About 0.5 µg tryptic peptides were injected into an Ultimate 3000 RSLC system (Thermo Scientific, Sunnyvale, California, USA) connected to a Q-Exactive HF equipped with a nanospray Flex ion source (Thermo Scientific, Bremen, Germany). The sample was loaded and on a pre-column Acclaim PepMap 100, 2cm x 75µm i.d. nanoViper column, packed with 3µm C18 beads at a flow rate of 3µl/min for 5 min with 0.1% TFA (trifluoroacetic acid, vol/vol). Peptides were separated during a biphasic ACN gradient from two nanoflow UPLC pumps (flow rate of 0.250 µl/min) on a 25 cm analytical column (Easy-Spray 802, 25cm x 75µm i.d. PepMap RSLC column, packed with 2µm C18 beads (Thermo Scientific). Solvent A was 0.1% FA (vol/vol) in water, and solvent B was 100% ACN. The fractions were applied different LC-methods depending on their elution from the mixed mode column.

LC-gradients for the TMT-labeled fractions in the LC-MS analysis

The mixed mode fractions were applied different LC-gradients depending on their elution from the mixed mode column, solvent A was 0.1% FA (vol/vol) in water and solvent B was 100% ACN. Fraction 1-6 had a gradient of 5 % B 0-5 min, then 5-12 % B 5-65 min, 12-30 % B from 65-87 min, 30-90 % B from 87-92 min, 90 % B from 92-102 min, 90-5 % B from 102-105 min and held at 5% B until the end. Fractions 7-36 had a gradient of 5 % B from 0-5 min, 5-7 % B from 5-5,5 min, 7-22 % B from 5.5-65 min, 22-35% B from 65-87 min, 35-90 % B from 87-92 min, 90 % B from 92-102 min, 90-5 % B from 102-105 min, 5 % B from 108-120. Fractions 37-60 had a gradient of 5 % B 0-5 min, 5-7 % B from 5-5,5 min, 7-40 % B from 5,5-87 min, 40-90 % B from 87-92 min, 90 % B from 92-102 min, 90-5 % B from 102-105 min, and 5% from 105-120 min.

Mass spectrometer settings

The mass spectrometer was operated in the data-dependent-acquisition mode to automatically switch between full scan MS^1 and MS^2 acquisition. The instrument was controlled through Q-Excative HF Tune 2.4 and Xcalibur 3.0. MS^1 spectra were acquired to detect precursors in the scan range 375-1500 m/z with resolution R = 60,000 at 200 m/z. The automatic gain control (AGC) had an ion target of 3e6 and a maximum injection time (IT) of 50 milliseconds (ms). The 15 most intense precursors with charge states 2 or higher and above intensity threshold 5e4 were sequentially isolated. The target AGC value for MS^2 was 1e5, aquired at R = 30,000. The ions were collected with IT 45 ms and fragmented with a normalized collision energy of 32 %. The precursor isolation window was 1.6 m/z, and with isolation offset of 0.3 Da. A dynamic exclusion of 30 seconds was used to prevent precursor re-sampling and to maximize the number of sampled precursors. Lock-mass internal calibration was used, and isotype exclusion was on.

Quantification of TMT data in Proteome Discoverer

Following LC-MS analysis, data from the two TMT-10 plex experiments were collected and analyzed in Proteome Discoverer 2.0 (Thermo Scientific), using Sequest HT, and MS Amanda (version 1.4.4.2822) and the SwissProt *Mus musculus* downloaded 15.10.2015 (canonical sequences not including isoforms) and the cRAP contaminants database from 30.01.2015 (ftp://ftp.thegpm.org/fasta/cRAP/). The following settings were used for both search engines. Trypsin was set as the enzyme, and maximum two missed cleavages were allowed. TMT tagging of N-terminals and lysines were established as a fixed modification, in addition to carbamidomethylation of cysteine. Oxidation of methionine was set as a variable modification. The fragment mass tolerance was set to 0.01 Da for MS Amanda and 0.02 for Sequest HT. The identification deviance was set to 10 ppm for MS1 precursors**.** The PSM validation from all search engines was performed using Percolator, with a strict and relaxed target FDR of 0.01 and 0.05, respectively. TMT 10-plex was set as the quantification method with the integration tolerance 20 ppm and the integration method most

confident centroid. All samples were normalized to the reference sample within each TMT 10-plex using Proteome Discoverer. Unique peptides were used for quantification.

The two 10-plexes were merged globally by search engine type, and PSMs with low confidence were discarded. The reporter ion isotopic distribution provided with the TMT kit was used to minimize cross-contamination in the TMT channels. The co-isolation threshold was set to 50%. The reporter abundance was based on a signal to noise values when available, if not intensities were used. The average signal to noise threshold was set to 10 s/n. Only proteins identified with unambiguously identified high confidence peptides (FDR <1%) were used. The datasets were normalized to the total peptide amount. The resulting quantified proteins were filtered so that only master proteins were exported for analysis.

Statistical analysis in R

Prior to data upload to R, contaminants and proteins containing missing values were removed.

The dataset was analyzed by the statistical software limma (Ritchie et al., 2015), where the batch effect was taken into account. Specifically, a linear model with the function abundance = condition+batch (condition = Placebo DM, Placebo 1RM, Placebo 3RM, Fingolimod DM, Fingolimod 1RM, Fingolimod 3RM) (batch = 0 or 1 depending on the TMT experiment) was generated before empirical Bayes statistics (Smyth, 2004) on the resulting values for condition. Proteins with a p-value <0.01 and a $\log_2$ FC >0.2 or <-0.2 was considered significant. Benjamini Hochberg correction was used to adjust the p-values for multiple comparisons (q-value <0.05). The graphics package ggplot2 (H. Wickham. ggplot2: Elegant Graphics for Data Analysis. Springer-Verlag New York, 2009) was used to generate figures. Gene Ontology Biological process enrichment analysis was carried out for the proteins considered to be significantly different in Panther (Mi, Muruganujan, Ebert, Huang, & Thomas, 2019; Thomas et al., 2006). The R script used for statistical analysis and graphics is publicly available at https://github.com/RagnhildRLereim/Fingolimod.

Refrences

Mi, H., Muruganujan, A., Ebert, D., Huang, X., & Thomas, P. D. (2019). PANTHER version 14: more genomes, a new PANTHER GO-slim and improvements in enrichment analysis tools. *Nucleic Acids Res, 47*(D1), D419-D426. Retrieved from https://www.ncbi.nlm.nih.gov/pubmed/30407594 https://www.ncbi.nlm.nih.gov/pmc/articles/PMC6323939/pdf/gky1038.pdf. doi:10.1093/nar/gky1038

Ritchie, M. E., Phipson, B., Wu, D., Hu, Y., Law, C. W., Shi, W., & Smyth, G. K. (2015). limma powers differential expression analyses for RNA-sequencing and microarray studies. *Nucleic Acids Res, 43*(7), e47. Retrieved from https://www.ncbi.nlm.nih.gov/pubmed/25605792 https://www.ncbi.nlm.nih.gov/pmc/articles/PMC4402510/pdf/gkv007.pdf. doi:10.1093/nar/gkv007

Smyth, G. K. (2004). Linear models and empirical bayes methods for assessing differential expression in microarray experiments. *Stat Appl Genet Mol Biol, 3*, Article3. Retrieved from https://www.ncbi.nlm.nih.gov/pubmed/16646809 https://www.degruyter.com/view/j/sagmb.2004.3.issue-1/sagmb.2004.3.1.1027/sagmb.2004.3.1.1027.xml. doi:10.2202/1544-6115.1027

Thomas, P. D., Kejariwal, A., Guo, N., Mi, H., Campbell, M. J., Muruganujan, A., & Lazareva-Ulitsky, B. (2006). Applications for protein sequence-function evolution data: mRNA/protein expression analysis and coding SNP scoring tools. *Nucleic Acids Res, 34*(Web Server issue), W645-650. Retrieved from https://www.ncbi.nlm.nih.gov/pubmed/16912992 https://www.ncbi.nlm.nih.gov/pmc/articles/PMC1538848/pdf/gkl229.pdf.

Supplementary tables

Table S1. **Antibodies used for immunohistochemistry specified.**

Target antigen	Species, type	Working dilution	Incubation time/ Temperature	Demasking	Provider
PLP	Mouse, monoclonal	1:1000	24h/4°C	Citrate	Serotec
GFAP	Rabbit, monoclonal	1:2000	½h/ RT	Tris-EDTA	Dako (Agilent)
NOGO-A	Rabbit, polyclonal	1:1000	1h/RT	Citrate	Chemicon, Temecula
MAC-3	Rat, monoclonal	1:200	24h/RT	Citrate	BD Biosciences
CD3	Rabbit, polyclonal	1:500	½h/RT	Tris-EDTA	Dako
APP	Mouse, monoclonal	1:2000	24h/4°C	Citrate	Merck
NFL	Mouse, monoclonal	1:1600	1h/RT	Tris-EDTA	Merck

RT = room temperature

PLP: anti-Proteolipid Protein

GFAP: anti-Glial Fibrillary Acidic Protein

NOGO-A: anti-Neurite Outgrowth Inhibitor Protein A

CD3: cluster of differentiation 3

APP: anti-Alzheimer Precursor Protein A4, clone 22C11

NFL: anti-phosphorylated Neurofilament light

Table S2.
Pooling strategy for the proteomics experiment.

Fingolimod			Placebo			Reference
DM	**1RM**	**3RM**	**DM**	**1RM**	**3RM**	
2 biological samples TMT 126	2 biological samples TMT 127N	2 biological samples TMT 128N	2 biological samples TMT 129N	2 biological samples TMT 130C	2 biological samples TMT 130N	36 samples TMT 131
2 biological samples TMT 127C	2 biological samples TMT 128C	2 biological samples TMT 129C	2 biological samples TMT 128C	2 biological samples TMT 129C	2 biological samples TMT 130C	36 samples TMT131
2 biological samples TMT 126	2 biological samples TMT 127C	2 biological samples TMT 127N	2 biological samples TMT 128N	2 biological samples TMT 129N	2 biological samples TMT 130N	

The brain samples (n=6 in each condition) were randomized and divided into 3 mini-pools. Each condition was represented in both TMT 10 plex experiment 1 (White) and 2 (Blue). One reference pool containing equal amounts of each brain lysate was included in each TMT 10-plex to enable comparison in the post analysis.

Table S3.
Proteins significantly different ($p<0.01$ log_2 FC Fingolimod - Placebo >20%) after 6 weeks of demyelination.

Accession	Description	Gene short	log_2 FC	p-value
O08530	Sphingosine 1-phosphate receptor 1	S1pr1	-0.54	0.0000005
Q7M6Z0	Reticulon-4 receptor-like 2	Rtn4rl2	0.21	0.0002
Q80SZ7	Guanine nucleotide-binding protein G(I)/G(S)/G(O) subunit gamma-5	Gng5	-0.45	0.0003
Q8CJ61	CKLF-like MARVEL transmembrane domain-containing protein 4	Cmtm4	-0.29	0.0003
Q6PGG6	Guanine nucleotide-binding protein-like 3-like protein	Gnl3l	-0.43	0.0005
Q8BUV8	Protein GPR107	Gpr107	-0.47	0.001
Q922W5	Pyrroline-5-carboxylate reductase 1, mitochondrial	Pycr1	-0.35	0.001

Q8K209	G-protein coupled receptor 56	Gpr56	-0.39	0.002
E9Q5K9	YTH domain-containing protein 1	Ythdc1	-0.26	0.002
Q810B8	SLIT and NTRK-like protein 4	Slitrk4	-0.22	0.003
Q9CX11	rRNA-processing protein UTP23 homolog	Utp23	-0.29	0.003
O89020	Afamin	Afm	-0.68	0.003
P46662	Merlin	Nf2	-0.32	0.003
Q3UHF7	Transcription factor HIVEP2	Hivep2	-0.23	0.004
Q8BHR8	UPF0705 protein C11orf49 homolog	1 SV=1	-0.26	0.004
Q5RJH6	Protein SMG7	Smg7	-0.34	0.006
Q6PDY0	Coiled-coil domain-containing protein 85B	Ccdc85b	0.22	0.007
Q62313	Trans-Golgi network integral membrane protein 1	Tgoln1	-0.22	0.008
Q8CI11	Guanine nucleotide-binding protein-like 3	Gnl3	-0.23	0.009
Q91W92	Cdc42 effector protein 1	Cdc42ep1	-0.46	0.009
A2AV25	Fibrinogen C domain-containing protein 1	Fibcd1	-0.32	0.010

Table S4.
Proteins significantly different ($p<0.01$, $\log_2$ FC Fingolimod – Placebo >20%) after 1 week of remyelination.

Accession	Description	Gene short	$\log_2$ FC	p-value
O08530	Sphingosine 1-phosphate receptor 1	S1pr1	-0.84	0.000000003
O35448	Lysosomal thioesterase PPT2	Ppt2	-0.49	0.000004
Q80SZ7	Guanine nucleotide-binding protein G(I)/G(S)/G(O) subunit gamma-5	Gng5	-0.47	0.0001
O55236	mRNA-capping enzyme	Rngtt	-0.21	0.002
Q8BHK1	Magnesium transporter NIPA1	Nipa1	-0.21	0.002
Q9QXN3	Activating signal cointegrator 1	Trip4	0.28	0.003
Q9D1G2	Phosphomevalonate kinase	Pmvk	-0.33	0.004
Q9CR24	Nucleoside diphosphate-linked moiety X motif 8, mitochondrial	Nudt8	0.28	0.004

Q3TRM8	Hexokinase-3	Hk3	-0.38	0.004
Q9WTQ8	Mitochondrial import inner membrane translocase subunit Tim23	Timm23	0.22	0.005
Q9DC04	Regulator of G-protein signaling 3	Rgs3	0.22	0.005
Q8BNA6	Protocadherin Fat 3	Fat3	0.25	0.005
Q69ZN7	Myoferlin	Myof	-0.28	0.006
Q00623	Apolipoprotein A-I	Apoa1	-0.24	0.007
Q8CFJ9	WD repeat-containing protein 24	Wdr24	-0.23	0.009
Q8BGS7	Choline/ethanolaminephosphotransferase 1	Cept1	0.20	0.009

Table S5.
Proteins significantly different ($p<0.01$, $\log_2$ FC Fingolimod – Placebo >20%) after 3 weeks of remyelination.

Accession	Description	Gene short	$\log_2$ FC	p-value
O08530	Sphingosine 1-phosphate receptor 1	S1pr1	-0.87	0.000000002
Q9WVA4	Transgelin-2	Tagln2	0.21	0.0005
Q9JHK5	Pleckstrin	Plek	0.21	0.001
Q80SZ7	Guanine nucleotide-binding protein G(I)/G(S)/G(O) subunit gamma-5	Gng5	-0.39	0.001
P08207	Protein S100-A10	S100a10	0.58	0.001
O88878	AN1-type zinc finger protein 5	Zfand5	0.43	0.001
Q8CAM5	Ras-related protein Rab-36	Rab36	0.49	0.002
Q9CX11	rRNA-processing protein UTP23 homolog	Utp23	0.31	0.002
Q9JJR9	Nuclear receptor-interacting protein 3	Nrip3	0.26	0.002
Q8BWU8	Ethanolamine-phosphate phospho-lyase	Etnppl	0.27	0.002
Q8VCM7	Fibrinogen gamma chain	Fgg	0.28	0.002
P97433	Rho guanine nucleotide exchange factor 28	Arhgef28	-0.40	0.002
P31649	Sodium- and chloride-dependent GABA transporter 2	Slc6a13	0.44	0.003
Q8BFR6	AN1-type zinc finger protein 1	Zfand1	-0.30	0.003
Q9QXE0	2-hydroxyacyl-CoA lyase 1	Hacl1	-0.26	0.003

Q8R5F3	O-acetyl-ADP-ribose deacetylase 1	Oard1	0.24	0.003
Q08091	Calponin-1	Cnn1	0.62	0.003
Q9CQ28	Diphthine--ammonia ligase	Dph6	0.31	0.004
Q63959	Potassium voltage-gated channel subfamily C member 3	Kcnc3	0.21	0.004
Q8VC16	Leucine-rich repeat-containing protein 14	Lrrc14	0.20	0.004
Q64339	Ubiquitin-like protein ISG15	Isg15	-0.23	0.005
Q9D658	Protein tyrosine phosphatase type IVA 3	Ptp4a3	-0.29	0.006
Q64345	Interferon-induced protein with tetratricopeptide repeats 3	Ifit3	-0.25	0.006
Q9EP71	Ankycorbin	Rai14	0.23	0.006
P28653	Biglycan	Bgn	0.46	0.006
Q8K353	Cysteine-rich and transmembrane domain-containing protein 1	Cystm1	0.27	0.007
Q9CZE3	Ras-related protein Rab-32	Rab32	0.40	0.008
P37804	Transgelin	Tagln	0.71	0.009
Q8BHG9	CGG triplet repeat-binding protein 1	Cggbp1	0.22	0.009
Q9ES52	Phosphatidylinositol 3,4,5-trisphosphate 5-phosphatase 1	Inpp5d	-0.27	0.009

Table S6A
Histochemistry and immunohistochemistry data from the midline of corpus callosum.

Controls

	Healthy Control			Cuprizone Control			
	Mean and Median		SD	Mean and Median		SD	*p*
LFB	0.3	0.0	0.5	1.5	1.5	0.5	**0.036**
PLP	90.2	91.9	5.5	71.3	64.1	13.7	0.13
GFAP	0.7	0.5	0.3	1.8	1.5	0.6	**0.024**
MAC-3	0.0	0.0	0.0	14.0	15.0	6.6	**0.018**
NOGO-A	29.8	29.5	16.4	15.5	15.5	12.0	0.21
NFL	90.9	91.0	2.6	63.2	64.9	24.9	**0.041**
APP	0.0	0.0	0.0	29.0	28.5	17.1	**0.002**
CD3	0.5	0.0	1.2	1.0	1.0	1.0	0.46

p = Sig. (2-tailed), Exact. Sig. (2-tailed) when Mann-Whitney is used.

Table S6B
Histochemistry and immunohistochemistry data from the midline of corpus callosum.

6 weeks of cuprizone exposure

	Fingolimod			Placebo			
	Mean and Median		SD	Mean and Median		SD	*p*
LFB	1.8	2.0	0.5	2.0	2.5	0.7	0.38
PLP	64.3	66.7	16.4	57.1	65.2	22.9	0.64
GFAP	1.8	1.8	0.7	1.8	2.0	0.8	0.93
MAC-3	21.8	22.0	4.0	12.1	10.0	7.3	0.058
NOGO-A	10.0	5.0	9.5	6.4	7.0	1.5	0.58
NFL	80.7	84.4	13.1	78.9	82.2	12.4	0.81
APP	18.8	18.5	1.9	22.5	20.5	8.1	0.80
CD3	0.0	0.0	0.0	0.2	0.0	0.4	1.00

p = Sig. (2-tailed), Exact. Sig. (2-tailed) when Mann-Whitney is used.

Table S6C
Histochemistry and immunohistochemistry data from the midline of corpus callosum.

1 week of remyelination

	Fingolimod			Placebo			
	Mean and Median		SD	Mean and Median		SD	*p*
LFB	2.2	2.0	0.3	2.1	2.0	0.4	1.00
PLP	50.8	39.5	28.4	51.8	54.8	23.8	0.96
GFAP	2.1	2.0	0.6	1.8	2.0	0.5	0.36
MAC-3	14.0	12.5	9.1	10.0	9.0	5.8	0.42
NOGO-A	24.2	22.0	9.2	30.0	29.0	8.5	0.31
NFL	79.9	81.6	8.5	85.1	85.2	7.9	0.30
APP	7.0	5.0	5.2	13.5	15.5	8.3	0.25
CD3	0.8	0.0	1.5	0.5	0.5	0.6	0.79

p = Sig. (2-tailed), Exact. Sig. (2-tailed) when Mann-Whitney is used.

Table S6D
Histochemistry and immunohistochemistry data from the midline of corpus callosum.

3 weeks of remyelination

	Fingolimod			Placebo			
	Mean and Median		SD	Mean and Median		SD	*p*
LFB	1.7	1.5	0.3	1.3	1.3	0.7	0.40
PLP	71.6	70.9	4.8	62.6	57.6	12.0	0.28
GFAP	1.8	1.5	0.5	1.8	2.0	0.3	0.81
MAC-3	5.4	5.0	3.5	10.4	9.0	5.0	0.10
NOGO-A	30.0	32.5	9.9	31.4	29.0	7.5	0.90
NFL	84.7	85.5	4.4	88.6	90.9	4.0	0.26
APP	5.7	5.0	3.9	4.2	2.0	3.5	0.35
CD3	0.4	0.0	0.6	1.0	0.5	1.4	0.76

p = Sig. (2-tailed), Exact. Sig. (2-tailed) when Mann-Whitney is used.

Table S7A
Histochemistry and immunohistochemistry data from the secondary motor cortex

Controls

	Healthy Control			Cuprizone Control			
	Mean and Median		(SD)	Mean and Median		(SD)	*p*
LFB	1.4	1.5	1.3	3.0	3.0	0.0	0.15
PLP	7.9	7.3	5.9	0.9	1.1	0.4	**0.053**
GFAP	0.0	0.0	0.0	2.0	2.0	0.0	**0.008**
MAC-3	0.0	0.0	0.0	14.0	5.0	6.6	**0.018**
NOGO-A	10.3	9.0	4.3	4.5	4.5	6.4	**0.004**
NFL	16.2	5.5	16.0	13.1	12.6	9.6	0.697

p = Sig. (2-tailed), Exact. Sig. (2-tailed) when Mann-Whitney is used.

Table S7B

6 weeks of cuprizone exposure

	Fingolimod			Placebo			
	Mean and Median		(SD)	Mean and Median		(SD)	*p*
LFB	3.0	3.0	0.0	2.9	3.0	0.2	1.0
PLP	1.0	1.0	0.3	2.9	1.8	2.7	0.128
GFAP	2.4	2.5	0.6	1.7	1.5	0.8	0.160
MAC-3	21.8	5.5	4.0	12.2	4.0	7.5	0.530
NOGO-A	0.7	0.0	1.2	7.2	8.0	5.8	0.084
NFL	9.4	8.7	4.3	19.9	19.2	5.2	**0.005**

p = Sig. (2-tailed), Exact. Sig. (2-tailed) when Mann-Whitney is used.

Table S7C

1 week of remyelination

	Fingolimod			Placebo			
	Mean and Median		(SD)	Mean and Median		(SD)	*p*
LFB	2.5	3.0	0.9	2.8	3.0	0.3	0.773
PLP	2.1	2.3	0.8	4.7	4.9	3.7	0.481
GFAP	1.6	1.5	0.3	1.9	2.0	0.5	0.171
MAC-3	14.0	4.5	9.1	10.0	2.5	5.8	0.065
NOGO-A	4.2	3.0	2.7	4.5	4.5	2.6	0.749
NFL	21.1	19.7	12.0	16.1	16.9	8.2	0.419

p = Sig. (2-tailed), Exact. Sig. (2-tailed) when Mann-Whitney is used.

Table S7D

3 weeks of remyelination

	Fingolimod			Placebo			
	Mean and Median		(SD)	Mean and Median		(SD)	*p*
LFB	2.4	2.5	0.7	2.5	2.5	0.6	1.0
PLP	3.3	2.0	3.2	3.8	2.6	2.6	0.662
GFAP	1.2	1.0	0.3	1.0	1.0	0.5	0.643
MAC-3	5.4	1.0	3.5	10.4	0.0	5.0	0.784
NOGO-A	5.2	3.5	4.3	1.6	2.0	0.6	**0.032**
NFL	14.0	13.4	7.1	12.9	13.7	3.8	0.824

p = Sig. (2-tailed), Exact. Sig. (2-tailed) when Mann-Whitney is used.

Graphic design: Communication Division, UiB / Print: Skipnes Kommunikasjon AS

uib.no

ISBN: 9788230840993 (print)
9788230868966 (PDF)